

2010

Extracellular matrix based substrates for propagation of human pluripotent stem cells

Sheena Abraham

Virginia Commonwealth University

Follow this and additional works at: <http://scholarscompass.vcu.edu/etd>

 Part of the [Chemical Engineering Commons](#)

© The Author

Downloaded from

<http://scholarscompass.vcu.edu/etd/92>

This Dissertation is brought to you for free and open access by the Graduate School at VCU Scholars Compass. It has been accepted for inclusion in Theses and Dissertations by an authorized administrator of VCU Scholars Compass. For more information, please contact libcompass@vcu.edu.

© Sheena Abraham, 2010

All Rights Reserved

*To my Parents
and Prashant*

***EXTRACELLULAR MATRIX-BASED SUBSTRATES FOR PROPAGATION OF
HUMAN PLURIPOTENT STEM CELLS***

A dissertation submitted in partial fulfillment of the requirements for the degree of Ph.D
in Chemical and Life Science Engineering at Virginia Commonwealth University.

by

SHEENA ABRAHAM
M.S, Virginia Commonwealth University, 2005
B.E University of Mumbai, India, 2001

Director: RAJ R. RAO
ASSISTANT PROFESSOR, CHEMICAL AND LIFE SCIENCE ENGINEERING

Virginia Commonwealth University
Richmond, Virginia
February, 2010

ACKNOWLEDGMENTS

First I would like to express my genuine appreciation to Dr. Raj R. Rao “my academic father” for my professional development fostered by his dedicated guidance. His patience and encouragement were integral to my academic success. His quiet demeanor and optimism helped me throughout the graduate school experience.

There are no words to express my gratitude for the love, friendship and support that I have received from Cindy. I will always cherish the time we spent together. Joe’s friendship and laughter will always be a part of me. He has taught me to be a critical thinker and for which I am extremely grateful. I admire Nikolai’s enthusiasm towards science, his free spirit and sharp mind has always kept me on my toes. Big thanks to my fellow cellmates, Venkat, Rick, Ena, Rukmani, Wendy and Kamyia.

I appreciate the help and guidance that I have received from Dr. Kordula, Katherine, and Sandeep for use of their facilities. I am extremely thankful to Dr. Valerie’s generous donation of cells that have been extensively used in this work.

I am honoured to have Drs. McGee, Fong, Bowlin and Peters on my committee. Their input and encouragement has been invaluable in the progress of my work.

Last, but not least, my heartfelt love and thanks to my parents Abraham and Leelamma, family Prashant, Shiny, Mathew and friends Amy, Preeti, Kavita and Nitu, without them I would not be who I am today.

Table of Contents

	Page
Acknowledgements	ii
List of Tables	vi
List of Figures	vii
Chapter	
1 Background and Literature Review	1
Summary	1
Introduction	2
Substrates for pluripotent stem cell self-renewal	4
Feeder layer dependent propagation systems	5
Feeder layer independent propagation systems	8
Natural biopolymers for pluripotent stem cell self renewal	9
Synthetic biomaterials for pluripotent stem cell self-renewal	11
Substrates for pluripotent stem cell differentiation	20
Endodermal differentiation	21
Mesodermal differentiation	23
Ectodermal differentiation	28
Rationale for study	32

2	Stable propagation of human embryonic and induced pluripotent stem cells on decellularized human substrates	35
	Abstract	35
	Introduction	36
	Materials and Methods	38
	Results	44
	Discussion	62
3	Characterization and application of human fibroblast-derived extracellular matrix for human pluripotent stem cell propagation.....	66
	Abstract	66
	Introduction	67
	Materials and Methods	69
	Results	78
	Discussion	100
	Conclusion.....	103
4	Propagation of human embryonic and induced pluripotent stem cells in an indirect co-culture system.....	106
	Abstract	106
	Introduction	107
	Materials and Methods	109

Results	116
Discussion	130
Conclusions	136
5 Conclusions and Future Directions.....	137
Conclusions	137
Future Directions.....	139
References.....	142
Appendices.....	
A Additional images for Chapter 2.....	185
B Proteomic data for acellular substrates	189
C Protocols	237
D Preliminary data for microwell experiments.....	244

List of Tables

	Page
Table 1 : Summary of substrates used for propagation of human and mouse pluripotent stem cells.....	19
Table 2 : Substrates used to induce differentiation in mouse and human pluripotent stem cells.	31
Table 3 : List of primers used for determination of relative gene expression.	42
Table 4 : Increase in gene expression of germ layer specific markers in embryoid bodies.	58
Table 5 : List of proteins in the three acellular substrates pertaining to cellular compartment identified using LC-MS/MS.	83
Table 6 : Proteins of interest that might contribute to the maintenance of self renewal in hPSCs.....	84
Table 7 : A tabulated summary of the different ECM combination tested and hPSC response to these substrate with respect to adhesion, differentiation and pluripotency markers.....	99
Table 8 : R ² correlation coefficients between expression profiles of different culture conditions.....	125
Table 9 : 14 transcriptional regulators examined in the enrichment analysis.....	127
Table 10 : TF-targets and GO categories enriched in sets of genes differentially expressed.....	129

List of Figures

	Page
Figure 1: Schematic of the transfer of non-human carbohydrate moiety	6
Figure 2: Components of the cellular microenvironment in vitro need to mimic in vivo conditions.....	13
Figure 3: Schematic of the preparation of acellular substrates for hPSC propagation	45
Figure 4: hPSCs maintain embryonic characteristics on acellular substrates.....	47
Figure 5: hPSCs maintain embryonic characteristics on cellular substrates.....	48
Figure 6: Differentiation seen in hPSC maintained on Matrigel	50
Figure 7: Pluripotent markers expressed in hPSCs maintained on acellular substrates	51
Figure 8: Decellularization causes loss of nuclear material.....	52
Figure 9: Normalized gene expression of undifferentiated markers.....	54
Figure 10: Normalized gene expression of <i>germ layer specific markers</i>	57
Figure 11: QPCR analysis of undifferentiated hPSCs and differentiated EBs derived from hPSCs using expression index	59
Figure 12: Histologic evidence of tri-lineage differentiation in embryoid bodies generated from hPSCs	60
Figure 13: Cytogenetic analysis on 20 metaphase spreads was performed on WA09	61
Figure 14: Functional biological and cellular profiles of the proteins identified in the three acellular substrates	79

Figure 15: Distribution of proteins identified in the three acellular substrates.....	82
Figure 16: Immunocytochemical validation of the presence of major constituents of the extracellular matrix in cellular and acellular HFFs and HDFs	85
Figure 17: Immunocytochemical validation of the presence of major constituents of the extracellular matrix in cellular and acellular MEFs.....	86
Figure 18: Phase contrast images of human pluripotent stem cells	89
Figure 19: Percentage of Alkaline Phosphatase positive colonies within different combinatorial-ECM substrates.....	90
Figure 20: Progressive differentiation of hPSCs propagated on fibronectin substrates	91
Figure 21: Immunofluorescence staining of hPSCs for pluripotency markers.....	93
Figure 22: Quantitative expression of pluripotency markers using cytopsin	94
Figure 23: Normalized gene expression of undifferentiated markers in WA09.....	96
Figure 24: QPCR analysis of undifferentiated hPSCs and differentiated EBs derived from hPSCs using expression index	98
Figure 25: Schematic of the potential synergistic adhesion and signaling pathway interactions.....	105
Figure 26: Schematic of a Microporous Membrane-based indirect co-culture system ...	111
Figure 27: Scanning electron micrograph of WA09 hESCs.....	117
Figure 28: Morphology and pluripotency markers on hPSCs grown within the millicell culture system	120

Figure 29: Quantitative real time polymerase chain reaction (QPCR) analysis of undifferentiated hPSCs and differentiated EBs derived from hPSCs	121
Figure 30: Histologic Evidence of Tri-Lineage Differentiation in embryoid bodies generated from hPSCs.....	122
Figure 31: Agglomerative hierarchical clustering by average distance, using the Pearson correlation coefficient as the distance measure	124
Figure 32: Venn diagrams indicating the overlap between the sets of genes	126
Figure 33: Relationships between the five cell types analyzed in the global gene expression studies	135

Abstract

EXTRACELLULAR MATRIX-BASED SUBSTRATES FOR PROPAGATION OF HUMAN PLURIPOTENT STEM CELLS

By Sheena Abraham, M.S.

A dissertation submitted in partial fulfillment of the requirements for the degree of Doctor of Philosophy at Virginia Commonwealth University.

Virginia Commonwealth University, 2010

Major Director: Raj R. Rao
Assistant Professor, Chemical and Life Science Engineering

In human pluripotent stem cell (hPSC) research and applications, the need for a culture system devoid of non-human components is crucial. Such a system should exhibit characteristics observed in conventional culture systems that have used mouse embryonic fibroblast feeders for hPSC self renewal without the requirement of excessive supplementation with growth factors. To achieve this, we focused on the identification and characterization of extracellular matrix (ECM) substrates for hPSC propagation. ECM substrates derived from mouse and human fibroblasts were assessed for their ability to support self-renewal of hPSCs. Characterization of hPSCs on ECM-based substrates

demonstrated maintenance of pluripotent characteristics based on a) high nuclear-cytoplasmic ratio b) immunocytochemical analyses for pluripotent markers (Alkaline phosphatase, AP, Octamer Binding Transcription Factor-4, OCT4 and Specific surface embryonic antigen-4, SSEA4) c) in vitro differentiation potential by embryoid body formation d) Real time RT-PCR analysis for pluripotent and germ-layer specific markers and e) karyotype analysis for chromosome number. Compositional characterization of the ECM substrates using proteomic analysis identified some of the major constituents of the matrix that might contribute to hPSC self-renewal. Based on results from the proteomic analysis, combinatorial ECM substrates were formulated using commercially available proteins and evaluated for applicability in hPSC propagation. Extensive characterization of hPSC propagated on the ECM substrates suggest that a combination of heparan sulfate proteoglycan and fibronectin was sufficient for the promoting hPSC self-renewal. Finally, an in-direct co-culture system utilizing microporous membranes coated with acellular substrates and a physically separated feeder layer was developed as a microenvironment for hPSC propagation. Real time conditioning of the growth medium and an ECM-based substrate for hPSC adhesion provides a synergy of the biochemical and biophysical cues necessary for hPSC self-renewal. hPSCs cultured in this system demonstrated equivalent pluripotent characteristics as those propagated in conventional culture systems, and provided opportunities for scale up without cell mixing. Overall, these studies could prove to be useful in the development of humanized propagation systems for the production of stable hPSCs and its derivatives for research and therapeutic applications.

CHAPTER 1: Background and literature review

Summary

Human pluripotent stem cells that include embryonic and induced pluripotent stem cells hold enormous potential for the treatment of many diseases, due of their ability to generate cell types useful for therapeutic applications. Currently, many stem cell culture propagation and differentiation systems incorporate animal-derived components for promoting self-renewal and differentiation. However, use of these components are labor intensive, carry the risk of xenogenic contamination and yield compromised experimental results that are difficult to duplicate. From a biomaterials perspective, the generation of an animal-free and cell-free bio-mimetic microenvironment that provides the appropriate physical and chemical cues for stem cell self-renewal or differentiation into specialized cell types would be ideal. This chapter presents the use of natural and synthetic polymers that support propagation and differentiation of stem cells, in an attempt to obtain a clear understanding of the factors responsible for the determination of stem cell fate.

Introduction

Over the last decade, human pluripotent stem cells (hPSCs) that include human embryonic stem cells (hESCs) [1, 2] and more recently, induced pluripotent stem cells (iPSCs) [3-5] have garnered a lot of attention due to their inherent self renewal and pluripotent capabilities. The pluripotent nature of these cells i.e., the ability to differentiate into all somatic cell types, have opened avenues for potential stem cell based regenerative therapies, development of drug discovery platforms and as unique *in vitro* models for the study of early human development. To meet specific needs for cell-based therapies, some of the key research questions that need to be addressed include a) the elucidation of molecular mechanisms that determine the stem cell fates of self-renewal, differentiation, apoptosis and quiescence; and (b) bioprocessing strategies to generate bankable and uniform populations of undifferentiated cells. The key variables in the development of bioprocessing strategies for propagation of pluripotent stem cells involve medium formulations and biomaterials as substrates. In this chapter, we present an overview of the potential for different biomaterials in determining pluripotent stem cell fate (mouse and human) relating to self-renewal and differentiation.

Mouse embryonic stem cells (mESCs) were one of the first ES cell types derived from the inner cell mass (ICM) of pre-implantation blastocysts, and cultured in direct contact with mitotically inactivated mouse embryonic fibroblasts (MEF) feeder layers [6]. This culture methodology was primarily adopted to provide the cells with the appropriate conditions conducive for self-renewal rather than differentiation and has since been

employed by many laboratories for the isolation and maintenance of pluripotent stem cells of different species. In primates, ES cells were first isolated from rhesus monkeys and subsequently from humans, and maintained for extended periods without undergoing differentiation in direct co-culture with MEFs. The removal of MEF feeders in the culture system triggered spontaneous differentiation into many somatic cell types [2, 7].

From a cell-based regenerative therapy perspective, the use of MEFs for the propagation of hPSCs is recognized as a potential hurdle by many researchers. It is widely acknowledged that mice carry pathogenic parasites, bacteria, and viruses as well as endogenous retroviruses in their genome. Some endogenous retroviruses have the capability to infect foreign species and have been shown to cause diseases like leukemia in immuno-suppressed primates [8]. Researchers in the stem cell community are thus presented with the challenge of developing of hPSC propagation systems that do not involve the use of other species-derived feeders.

Biomaterials have been investigated extensively as substrates for cell propagation, scaffolds for tissue engineering and as delivery vehicles in many regenerative biomedical paradigms. One of the key benefits of using biomaterials for pluripotent stem cell propagation is the elimination of direct co-culture with a feeder layer. This removes the risk of contamination with xenogenic pathogens and reduces variability in experimental outcomes due to feeder layer contribution. Additionally, specialized biomaterials that include appropriate chemical (incorporation of growth factors) and physical (topographic features) modifications, have contributed to successful differentiation of ES cells to multiple cell types.

Biomaterials such as hydrogels have been used in mammalian cell culture for over 30 years, because of its high water absorbability and tissue-like texture. Poly methylmethacrylate (PMMA) and Poly lactic glycolic acid (PLGA) are examples of a few biocompatible materials used in various tissue culture based applications [9, 10]. In ES cell research, polymeric substrates have largely been used as carrier systems for lineage specific differentiated cells. Instances of the use of polymeric-based biomaterials employed in hPSC self renewal maintenance are few in number. The use of a polymer-based substrate that can be synthesized with "off-the shelf" constituents for hPSC culture has several advantages, as a) economic feasibility b) reduction in the labor involved to maintain an additional cell line as feeders and c) elimination of the source of potential xenogenic contamination. It is expected that advances in biomaterial-based approaches will immensely contribute to standardization of culture methodologies, leading to development of bioprocesses for hPSC propagation and differentiation. Here, we attempt to present the knowledge acquired from the integration of biomaterial engineering and pluripotent stem cell biology to chalk out standardized routes for stem cell self-renewal and/or directed differentiation.

Substrates for pluripotent stem cell self-renewal

The need for an unlimited supply of starting hPSC populations for current research and future therapeutic applications fuels this area of research. In this section, we address the application of different substrates that are both feeder-dependent and feeder-

independent systems and have contributed to successful long term propagation of pluripotent stem cells in their undifferentiated state.

Feeder-layer dependent propagation systems

Mitotically inactivated mouse embryonic fibroblasts (MEFs) have been the traditional ‘feeder-layer’ of choice since the isolation and propagation of mESCs [6]. They have served as ideal substrates as they provide appropriate physical and chemical cues conducive for the maintenance of self-renewal in pluripotent stem cell populations. In a few cases, such as those involving rat ES cells and American mink ES cell propagation, it was demonstrated that the best feeder-layer were fibroblasts derived from the host animal [11, 12]. However, the isolation and propagation of several rodent, non-rodent ES [13-15] and non-human primate ES cells [7, 16] required MEFs as feeders for long term propagation. MEFs have also been used as the feeder of choice for culture systems that were initially developed for propagating hESCs and were shown to be capable of maintaining hESCs in their undifferentiated state for > 250 population doublings [1, 2]. The successful long term maintenance of ESCs on MEFs has been attributed to unidentified physical cues provided by the cellular layer or chemical cues based on nutrients released into the growth medium that create an environment suitable for proliferation and self-renewal. However, the use of animal cells as a substrate poses risks of xenogenic contamination by animal pathogens, which in turn could be transmitted to patients. Recent findings have revealed the presence of a non-human carbohydrate moiety on the surface of hESCs with the potential of eliciting an immune reaction from humans [17] Figure 1.

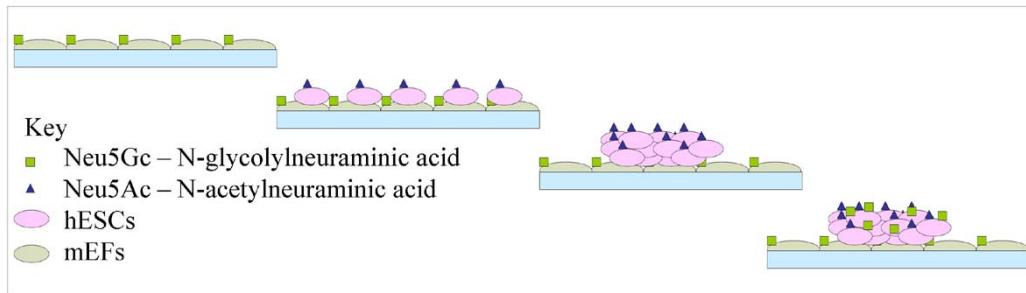


Figure 1

Schematic of the transfer of non-human carbohydrate moiety from mouse feeder layers onto the cell surface of human pluripotent stem cells. Contamination of hESCs with a non-human sialic acid, N-glycolylneuraminic (Neu5Gc) due to its metabolic uptake acid from MEFs, animal-based serum and other products in the growth medium. In humans, a precursor to Neu5Gc; N-acetylneuraminic acid (Neu5Ac) and circulating antibodies for this foreign sugar are present, which might lead to the rejection of specialized cells derived from such hESCs

Extensive research to propagate hPSCs in culture conditions with reduced or zero animal-derived products is being actively pursued. One of the earliest advances towards a xeno-free environment was the elimination of serum, specifically fetal bovine serum in hESC cultures. Fetal bovine serum has been extensively used in mammalian cell cultures; however, the composition of serum is not entirely known and different batches vary in their capabilities to support undifferentiated proliferation. A serum replacement, Knockout Serum Replacement (KSR) [18] optimized for mESC cultures, was successfully introduced in hPSC cultures [19], and is now routinely used as a serum-substitute in many laboratories to propagate hPSCs [20, 21]. In attempts to make the hPSC culture conditions animal-free, several human fibroblast cell lines have been tested and proven to be suitable feeders. Propagation conditions involving human foreskin fibroblasts as feeders in KSR-supplemented growth medium have been used to maintain hESCs for 70 passages [22], and in the derivation of new hESC lines [21]. An advantage to using human foreskin fibroblasts as a feeder layer lies in its ability to be continuously cultured for about 42 passages unlike MEFs which senesce in 5-7 passages. There was no significant difference found in the hESCs propagated on different lines of foreskin fibroblasts obtained from several newborns leading to the conclusion that the source of the foreskin fibroblasts does not affect the undifferentiated propagation of hESCs [23, 24].

Other human fibroblast feeders tested include fetal skin and muscle cells, adult fallopian tubal epithelial cells, adult skin, muscle, glandular and stromal endometrial cells, and commercially available fetal skin, lung and neonatal foreskin cell lines. One general observation made by the investigators was that fetal lines were more supportive of long

term hESC propagation compared to adult lines [25, 26]. Other examples of human feeders tested were human marrow stromal cells[27], human adult uterine endometrial cells, human adult breast parenchymal cells, embryonic fibroblasts[28], and human placental fibroblasts[29, 30]. To test the efficiency of hESC derived fibroblasts (hES-dF) as possible feeders, two different hESC lines (NCLI and H1) were grown on their autogenic as well as allogeneic fibroblast derivatives. These studies demonstrated that hESC derived feeders were capable of maintaining self renewal in both the parent as well as a foreign hESC line [31]. Cynomolgus monkey ES cells grown on human placental feeder layers; amniotic epithelial plate cells or chorionic plate cells, remained pluripotent for at least 18 passages[32]. These studies demonstrated that regardless of the source of the feeder layer, certain cell types are more capable of maintaining self-renewal capabilities of pluripotent stem cells. Detailed analyses of the similarities and differences between such feeders will provide valuable insights on key factors that maintain self-renewal capabilities and prevent differentiation of pluripotent stem cells.

Feeder-layer independent propagation systems

A few groups have demonstrated that hESCs can be maintained without feeders or feeder-conditioned medium, relying on growth medium supplementation with high concentrations of basic-fibroblast growth factor (bFGF). Many of these studies helped ascertain the molecular mechanisms involved in hESC self-renewal, such as the central role played by inhibition of components of the BMP signaling pathway[33, 34]. In this section we have focused on the role of natural biopolymers such as Gelatin, Matrigel™, naturally derived polymers such as alginate, agarose, and hyaluronic acid and several

synthetic polymers that allow controlled modifications and incorporation of physical, chemical and mechanical cues for the maintenance of pluripotent stem cells.

Natural biopolymers for pluripotent stem cell self renewal

Gelatin is thermally denatured collagen derived from animal skin and bones, and has long been used as a promoter of cell adhesion and proliferation in various cell lines [35-37]. mESCs, in the absence of a feeder layer have been maintained on gelatin coated dishes and growth medium supplemented with interleukin-6 family member cytokine Leukemia Inhibitory Factor (LIF) for extended periods [38-40]. The binding of LIF receptor β /gp130 heterodimer and the activation of the JAK/STAT3 signaling pathway has been implicated in mESC self-renewal [41]. As a cost-effective alternative to periodic LIF supplementation; LIF immobilized photoreactive gelatin demonstrated that mESCs maintained pluripotent characteristics after six days of culture [42]. The cells grown on gelatin-coated polyamide nanofibers electrospun onto glass coverslips demonstrate enhanced proliferation and self-renewal capabilities when compared to cells directly grown on gelatin-coated glass coverslips. These effects were correlated to an increase in the expression of NANOG, activation of the small GTPase Rac, and the activation of the phosphoinositide 3-kinase (PI3K) pathway. The relationship between the PI3K pathway and regulation of STAT3 and ERK make it likely that microenvironmental cues are a major factor in control of mESC self-renewal [43, 44].

In an attempt to move away from MEF-based feeder layers in human pluripotent stem cell cultures, an extracellular (ECM) -based substrate, Matrigel™ has been used to support hESC cultures. Matrigel™ is an ECM protein based gel derived from the basement

membrane of Engelberth-Holm-Swarm (EHS) mouse sarcoma. Matrigel™ has been found to be rich in collagen, laminin, heparin sulfate proteoglycans and growth factors such as transforming growth factor β (TGF β), epidermal growth factor (EGF), fibroblast growth factor (FGF) [45-47]. Extensive studies on the efficacy of Matrigel™ and the individual components of Matrigel™; such as laminin, collagen IV and fibronectin have been investigated for hESC propagation. Collagen IV and fibronectin individually did not support hESC propagation whereas laminin was successful in maintaining long-term undifferentiated hESC cultures. However, all of these hESCs were propagated in mouse embryonic fibroblast conditioned medium (MEF-CM), with the absence of MEF-CM leading to extensive spontaneous differentiation of the hESCs [48]. Another study demonstrated the successful maintenance of hESC cultures in growth medium containing KSR supplemented with high concentrations of bFGF, TGF β 1 and LIF, on a fibronectin matrix [20]. The premise for the use of these factors was that (a) bFGF is routinely used to maintain hESC cultures [19]; (b) TGF β 1 was found in Matrigel™ [48]; (c) fibronectin promotes cell adhesion [49] and (d) leukemia inhibitory factor (LIF) activates the JAK/Stat3 pathway and is sufficient for the self-renewal of mESCs [38-40, 50] and might elicit the same response in hESCs. However, it was found that neither the addition of LIF nor the activation of Stat3 pathway contributed to self-renewal in hESCs [2, 51].

Apart from the use of Matrigel™, very few studies have demonstrated the use of ECM based substrates for hESC maintenance, with one study reporting the use of human serum as a substrate to maintain hESCs for over 27 passages [52]. A recent study that is extremely promising has focused on the usefulness of hyaluronic acid (HA) based

hydrogels for propagation of hESCs [53]. HA is a nonsulfated linear polysaccharide of (1- β -4) D-glucuronic acid and (1- β -3) N-acetyl-D-glucosamine found largely in the ECM of undifferentiated cells during early embryogenesis and shows reduced expression on differentiation [54]. Hyaluronic acid (HA) is also present in the body as a major constituent in ECM in connective, neural and epithelial tissue. Large scale microbial production of HA has allowed for the use of this polymer in different therapeutic applications. Such naturally derived polysaccharides also considered as synthetic ECM hydrogels can substitute natural ECM. The premise for the use of ECM based protein hydrogels is to create a microenvironment that mimics the physiological milieu of the inner cell mass (ICM), by acting as a host that provides the resident cells with 3-dimensional architecture and mechanical support for structured organization and easy diffusibility for nutrients and metabolites [55-57]. HESCs that were encapsulated within the HA construct in MEF conditioned medium maintained their undifferentiated state for 20 days. The cells were released from the hydrogel by treating the constructs with hyaluronidase to digest the HA hydrogel, cells showed no adverse effects to extended exposure (24 hours) to the enzyme. Although natural biopolymers such as polysaccharides, ECM-based substrates and other hydrogels hold great promise as biomaterials for pluripotent stem cell propagation and presenting cells with familiar microenvironments, new strategies are required for greater control to promote uniform proliferation of stem cells in their undifferentiated state.

Synthetic Biomaterials for pluripotent stem cell self-renewal

Replacing natural materials with synthetic polymers allows for controlled modifications; such as addition of embryologically relevant growth factors. It is useful to note that

mammalian cell culture propagation have traditionally been conducted on flat, rigid substrates. However, the three-dimensional microenvironments that the cells encounter in the body have a combination of physical, chemical and mechanical cues [58, 59] (Figure 2). Consequently, the ease with which polymers can be engineered into complex 3D structures is a key benefit of using polymers instead of feeder cells in pluripotent propagation systems. Poly (α -hydroxy esters), and polyurethane are few examples of synthetic polymers that have been used as part of pluripotent stem cell propagation systems. Poly(α -hydroxy esters) with enhanced surface hydrophilicity and roughness properties [60], and fluorinated hydroxyapatites have been identified as substrates that can maintain mESCs as colonies[61]. Poly (hydroxyethyl methacrylate) p(HEMA), a widely used non-degradable biomaterial is another synthetic polymer that supports mESC proliferation[62, 63]. mESCs were maintained in their undifferentiated state for a limited time period of 4 days, which was confirmed by replating the cells extracted from the hydrogel slabs onto gelatin-coated dishes. Cells that were allowed to proliferate for longer periods in the p(HEMA) slabs, formed large clusters (6-8 days) and showed reduced expression of pluripotent markers when replated on gelatin-coated dishes compared to the 4-day cultures. mESCs grown on non-woven polyester fabrics from polyethylene terephthalate (PET) initially exhibited high expression of pluripotent markers alkaline phosphatase (AP) and Stage-specific embryonic antigen (SSEA-1)[64]. However, reduced expression of SSEA-1 was seen in mESCs after 72-96 hours, indicating that PET substrates did not facilitate long-term undifferentiated propagation and would be best suited for differentiation studies rather than for maintaining self renewal.

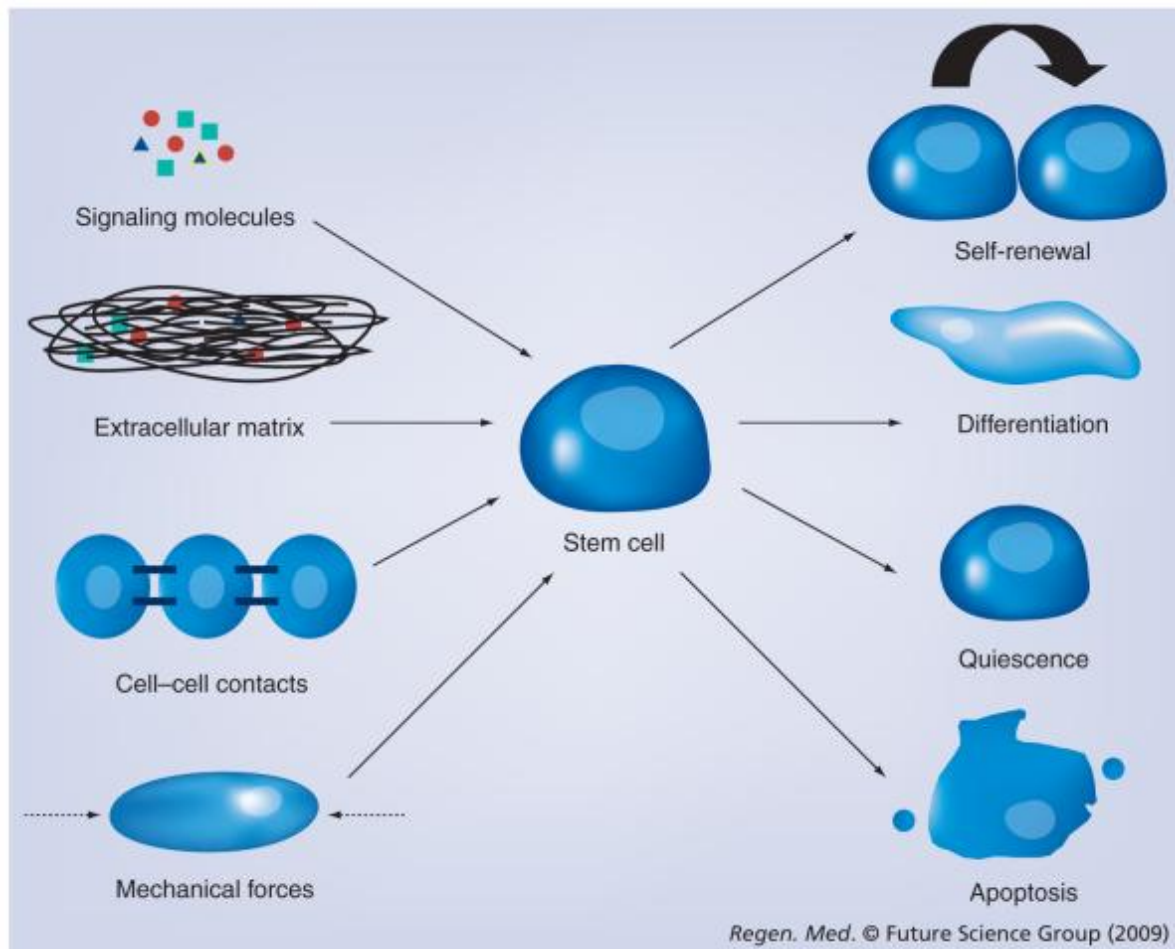


Figure 2:

Components of the cellular microenvironment in vitro need to mimic in vivo conditions: Synergy of biochemical cues such as signaling molecules and growth factors; biophysical cues such as substrates; mechanical cues such as hemodynamic forces, shear forces and periodic strains; and cell-cell interactions are required for determination of fate of pluripotent stem cells

However, another study involving fibrous PET matrices was shown to sustain long-term growth of mESCs [65], where matrices with pores 30-60 μm wide caused more rapid cell growth than in pores of 60-130 μm in width. This was attributed to greater contact between the cells and PET fibers within smaller pores leading to increased attachment and better support. Large pores allowed cells to aggregate more easily, which induced mESC differentiation. Gelatin coating of the polymers did not improve mESC proliferation and self-renewal, though such effects could be due to blocking and partial destruction of the pore structure of the PET matrices. One drawback of such a 3D fibrous matrix construct for ESC culture is poor oxygen supply at high cell densities. The effects of poor oxygen transfer could be seen when cell proliferation slowed and cellular death was seen at or near day 14. Thus comparative studies of superporous polymers with varying pore sizes, surface charges and hydrophobicity characteristics show that substrates with smaller pores sizes in the range of 30 μm wide supported proliferation of mESC better than pores of larger dimensions(100 μm). Neutral or cationic substrates as compared to a negatively charged substrate and hydrophobic surfaces compared to a hydrophilic allowed for greater mESCs adhesion and aggregation for colony formation [62, 63] The effect of surface roughness on mESC culture on poly(α -hydroxy esters) substrates demonstrated that within a certain range increase in roughness with a corresponding reduction in hydrophilicity enhanced mESC attachment and proliferation[60]. These informative studies demonstrate that surface texture modifications can play a role in influencing the self-renewal properties of stem cells

Studies have demonstrated that presentation of various cell adhesion ligands, introduction of roughness and patterned features can influence stem cell fate by stimulating cell attachment, proliferation and differentiation [66, 67]. Patterned surfaces of hyaluronan and poly-L-Lysine (PLL) were shown to maintain mESC in their undifferentiated state within a spatially controlled culture system with fibroblasts. In these studies, Hyaluronan was lithographically patterned on glass surfaces to create parallel strips alternating with glass; fibronectin was selectively deposited on the glass, with poly-L-Lysine on hyaluronan permitting differential cell adhesion on the two surfaces. Fibroblasts were grown on glass surfaces treated with fibronectin and mESC on PLL surfaces. Such systems have a potential advantage over random co-culture where mixing of feeder cells with ESC is unavoidable [68].

A three-dimensional porous polymer scaffold of elastomer, poly-(glycerolsebacate)-acrylate (PGSA) support undifferentiated hESC culture for one week [69]. PGSA is an elastic hydrogel that is known to elicit low inflammation in response to *in vivo* transplantation [70, 71] and allows for future applications as a biocompatible and biodegradable scaffold. Polyurethane microwells coated with Matrigel™ demonstrated the ability to maintain hESCs in for three weeks without the need for routine passaging. The cells grown in these conditions maintained their pluripotency and differentiated into the three germ layers when cultured in suspension. The use of mouse-derived Matrigel™ as a substrate indicated that an ECM modification of the synthetic polymer was essential for propagating hESCs [72]. A synthetic 3-D ECM based semi-interpenetrating polymer network of poly(N-isopropyl acrylamide-co-acrylic acid) was reported to support short

term hESC self-renewal. Modification of the hydrogel polymer with the incorporation of synthetic RGD peptides to present the cells with adhesion sites improved cell attachment, allowed the formation of colonies and maintained pluripotency for a limited period of five days [73]. Recent studies have also investigated the feasibility of culturing hESCs on microcarriers in feeder-free, 3-dimensional suspension culture[74, 75]. These studies suggest that suspension-based propagation of hESCs on microcarriers may provide unique opportunities for bulk hESC production and storage.

Combinatorial and microarray approaches have been adopted recently in high-throughput screening of materials to control ESC fate on polymer surfaces. Such high-throughput approaches also hold much promise in 3-D screening of libraries of biofunctional groups such as morphogenetic proteins incorporated within synthetic 3-D materials. A vast number of possible combinations of polymers, surface treatments, surface-bound ligands, and other substrate modifications need to be investigated in ES cell propagation systems. A recent study has demonstrated the potential of high-throughput arrays in studying biomaterial- ES cell interactions and provided insights on the role of specific polymers in promoting cell attachment, proliferation and differentiation [76]. Another combinatorial approach focused on the effects of eighteen different laminin-derived peptides on proliferation and self-renewal of hESCs. Self assembled monolayers (SAMs) were designed which allowed the formation of array elements of well-defined shapes and sizes. Five out of the eighteen peptides tested were effective in maintaining the undifferentiated state of hESCs for 5-7 days. Further characterization of the five peptides with a nanofibers based peptide (RNIAEIIKDI)- amphiphile containing 3D- hydrogel

demonstrated their potential in promoting proliferation and maintaining undifferentiated hESCs [77].

Recent developments involving transductions of somatic cells to induce pluripotency has been heralded as one of the major breakthroughs in stem cell research; primarily due to its potential to advance customized cell-based therapies and the evasion of embryo-related ethical debates [3-5]. Although the use of synthetic materials for promoting iPSC fate from somatic cells has not been explored, the use of synthetic polymers as gene or protein delivery vehicles for inducing pluripotency is a definite possibility. Recent studies have demonstrated the potential of poly (amino esters) based biodegradable nanoparticulate vectors for gene delivery to efficiently transfect ESCs with low cytotoxicity [78, 79]. These methodologies have significant implications in the generation of iPSC lines that are free of exogenous viral additions to the genome. Ultimately, the development of a completely synthetic substrate to maintain hESC cultures or in the induction of pluripotency from somatic cells would present the ideal feeder-free and animal-free culture environments for long term undifferentiated and stable hESC propagation.

The culture of pluripotent stem cells on polymeric surfaces with or without immobilized proteins opens up avenues for identification of synthetic microenvironments that can be easily synthesized and modified to form scaffolds that support the differentiation of ES cells into highly ordered 3D structures. In ES-cell studies, biomaterials have been frequently used to direct differentiation to specific lineages, in the presence of appropriate growth factors. However, maintenance of its undifferentiated state has proven

to be a challenge. The use of native and synthetic polymers in promoting ES cell self-renewal is still in its nascent phase and has great potential as demonstrated by the various studies conducted to date (summarized in Table 1).

Table 1

Summary of substrates used for propagation of human and mouse pluripotent stem cells

Substrate Type	Cell Source	Substrate	Time line of study	References
Feeder layer based	hESCs	Human foreskin fibroblasts	> 70 passages	[80] [23, 81]
		Fetal skin cells	20 passages	[82, 83]
		Fetal muscle cells	> 50 passages	
		Adult skin fibroblasts	> 30 passages	
		Adult muscle fibroblasts	> 30 passages	
		Commercially available fetal skin fibroblasts	> 25 passages	
		Adult Fallopian tubal epithelial fibroblasts	> 20 passages	
		Adult marrow cells	13 passages	[84]
		human adult uterine endometrial cells (hUECs),	90 passages	[85]
		Human adult breast parenchymal cells (hBPCs), Human embryonic fibroblasts (hEFs)	50 passages 80 passages	
		Human placental fibroblasts	> 25 passages	[86, 87]
		HESC derived fibroblasts	44 passages 30-52 passages	[88],[89]
Natural substrates	mESCs	LIF immobilized on gelatin	6 days	[90]
		Gelatin-coated polyamide nanofibers	3 days	[43]
	hESCs	Matrigel	~130 passages	[91]
		Human Serum	> 27 passages	[52]
		Mouse embryonic fibroblasts ECM	> 30 passages	[92]
		Hyaluronic Acid	20 days	[93]
Synthetic substrates	mESCs	Hydroxyapatites polymers	48 hours (time required for colonization)	[94], [95]
		Poly(hydroxyethyl Methacrylate)	4 days	[62]
		LIF immobilized PET fibers	72-96 hours	[64]
		Gelatin immobilized PET fibers	15 days	[96]
	hESCs	Poly - (glycerolcoesebacate)-acrylate (PGSA)	1 Week	[97]
		Polyurethane micro-wells	> 21 days	[98]
		Poly(N-isopropyl acrylamide-co-acrylic acid) sIPN	5 days	[73]

Substrates for pluripotent stem cell differentiation

The excitement in the biomedical community with regard to pluripotent stem cells centers on their ability to differentiate into any somatic cell type. This unique property makes it possible to derive rare tissue types in unlimited quantities, which would be of immense use in areas such as *in vitro* drug screening and regenerative medicine. Differentiation of ESCs occurs spontaneously either in prolonged cultures or in the absence of feeder layers, leading to populations consisting of multiple cell types from many different lineages. Directed differentiation involves either a) exposure of ES cells to growth factors that mimic natural pathways in embryonic development b) co-culture with suitable cytokines secreting feeders or c) replating enriched populations derived from EBs. A more commonly used method to induce differentiation is the formation of embryoid bodies (EB), which are three-dimensional ES cell aggregates grown in suspension or in an environment that does not support cell adhesion [99]. Heterogeneous subpopulations are enriched for a cell type of interest, isolated and replated [100-105], with induction of differentiation by the addition of growth factors to the medium [106, 107]. Cell types that have been derived through use of EB include those of chondrogenic, adipogenic, neurogenic, cardiogenic, hematopoietic and myogenic lineages. However, thus far, the resulting populations have been largely random in their phenotype and organization. Consequently, there exists a need for protocols that can differentiate ES cells to highly specific derivatives with increased reproducibility and capacity for scale-up. The challenges in directed differentiation protocols are a direct result of the basic lack of

understanding of the mechanisms involved in lineage specification. In this section we briefly describe feeder-dependent and feeder-free (natural and synthetic polymers) approaches to differentiation of ES cells into multiple cell types from the three different germ layers (ectoderm, endoderm and mesoderm).

Endodermal Differentiation

Of the several cell types that originate from the endoderm, differentiation strategies for hepatic and pancreatic cell types have been extensively studied. Induction of hepatic and pancreatic differentiation from ESCs has garnered a lot of attention due to possible therapeutic applications for diseases such as liver damage and diabetes. Studies of the differentiation of ESCs into the pancreatic lineage largely involve formation of EBs followed by a sequential and elaborate exposure to endodermal lineage promoting growth factors and extracellular matrix proteins [108, 109]. Currently, there are no reports that points of the use of polymeric substrates for induction of pancreatic differentiation in mouse or human ES cells. However, there have been published reports on the use of both feeder layers and polymers in the differentiation towards the hepatic lineage. Co-culture of mESCs with primary adult rat hepatocytes has been shown to induce hepatocyte differentiation, with enhancement upon addition of hepatotrophic growth factors [110]. Additional studies for hepatic differentiation have focused on the use of natural polymers such as collagen and alginate [111]. Alginate is a biocompatible hydrophilic viscous gum derived from algae and has been used in various biomedical applications due to its hydrogel and ECM gel-like properties[112, 113]. The use of alginate beads for EB formation allows for scale up of hepatocyte derivation and act as a source of cells for a

bioartificial liver system [114]. Naturally derived alginate beads were used to form EBs from mESCs followed by replating of the dissociated cells in medium supplemented with appropriate growth factors to induce hepatocyte differentiation.

Synthetic polymers such as polyurethane have also been used to promote hepatogenesis. For example, a polyurethane foam (PUF) as part of a hepatocyte culture system was presented as a hybrid artificial liver [115], with subsequent replacement of hepatocytes with ES cells as a cell source within this module. When mESCs were placed in the porous PUF, they aggregated into spherical multicellular structures, on further exposure to a cocktail of growth factors, differentiated into mature hepatocytes [116]. An improvement to this culture system was later introduced by the same group of researchers that included a bioreactor consisting of a PUF block with capillaries to aid growth medium flow to effect hepatic lineage induction in mouse and cynomolgus monkey ES cells [117, 118].

Hepatocytes have commonly been derived from hESCs by either replating cells from EBs or by sequential exposure to different growth factors [119-121]. Similar to mESCs, natural ECM-based polymers have been used in hepatic differentiation of hESCs. A comparative study between 2D and 3D culture systems that utilized collagen demonstrated that 3-D collagen scaffolds induced specification in 5 day old EBs. Further, addition of exogenous growth factors to 3-D collagen scaffold allowed for better hepatocyte differentiation than collagen coated 2-D dishes [122]. Unlike mESCs, no reported studies of synthetic polymers as substrates in hESC hepatogenesis have been identified.

Mesodermal Differentiation

Derivatives of the mesoderm that have been successfully differentiated from ESC cultures include cardiomyocytes, cells of hematopoietic lineage, endothelial cells, and germ line cells [123-129]. The utilization of biomaterials as part of differentiation strategies for specialized cells from the mesodermal lineages: hematopoietic, osteogenic, chondrogenic and adipogenic, have been extensively studied.

Feeder dependent and feeder free systems have been extensively used in hematopoietic differentiation of mESCs. Cells of the hematopoietic lineage were the first reported cell types derived by direct differentiation of mESCs using a bone marrow stromal cell based feeder layers, OP9 cells [130] and RP010 [131], in growth medium conditioned by fetal liver stromal cells and supplemented with interleukin 6 (IL-6).

Natural polymers such as MatrigelTM, fibrin, dextran and collagen have been used as substrates for differentiation of mESCs to both the hematopoietic and endothelial lineage. Researchers achieved hematopoietic differentiation of mESCs by culture on collagen type IV, through a chain of intermediate differentiation steps, with mESCs first forming cells from the proximal lateral mesoderm, followed by formation of hemangiogenic progenitors, differentiation into hematopoietic precursors and ultimately mature blood cells. This study also identified the progression of lineage commitment for hematopoietic precursor cells and it was noted that hemangiogenic progenitor constituted a critical stage for the divergence of the endothelial and hematopoietic lineage [132, 133]. Differentiation of mESCs on Collagen IV substrate was later adapted to generate a pure

endothelial progenitor population [134, 135]. However, collagen-based substrates were found to be inefficient in differentiating rhesus monkey ES cells to endothelial cells [136].

Endothelial and hematopoietic differentiation of ES cells have also been demonstrated within three-dimensional fibrin constructs [137]. Researchers demonstrated that fibrin polymers reinforced with poly(ethylene glycol) (PEG), promoted a high expression of VE(vascular endothelial)-cadherin in encapsulated mESC-derived EBs formed within the construct. It has been postulated that PEGylation of fibrin blocks antigens, resulting in a reduction of cell-matrix interactions as fibrin gels have the capacity to engage cell-adhesion molecules [138], this reduced cell-matrix interaction might be involved in promoting differentiation of the ES cells [139]. 3D dextran constructs modified with bioactive ECM molecules have also been used to generate EBs from mESCs. Addition of vascular endothelial growth factor (VEGF) within the dextran constructs yielded cells with increased expression of endothelial markers KDR/Flk-1 and decreased expression of ectodermal and endodermal markers. These cells also showed lower ectodermal (Nestin) and endodermal (α -fetoprotein) marker expression, indicating a preference for mesodermal differentiation of ESCs within the VEGF - dextran culture environment. Further specification was achieved by removing the cells from the hydrogels and propagating on gelatin-coated dishes in endothelial differentiation medium [140]. Another study which further highlighted the importance of ECM components in the differentiation of mESC-derived EBs involved the used of 3D constructs that consisted of a collagen-based semi-interpenetrating polymer networks (SIPNs) with varying concentrations of fibronectin (FN) and laminin (LM) [141]. EBs differentiating within the

FN-loaded SIPNs formed cord-like structures indicative of endothelial differentiation, while LM-loaded SIPNs produced beating cells that provided evidence of increased differentiation towards cardiomyocytes.

Synthetic polymers have also been used to direct differentiation of ES cells to hematopoietic cells based on use of Cytomatrix®, a porous tantalum-based scaffold synthesized using chemical vapor deposition of metals onto an open pore carbon scaffold, creating a mechanically strong and highly porous scaffold. EBs generated in this scaffold produced hematopoietic progenitor cells with a greater efficiency than EBs generated from traditional 2D culture dishes, and exhibited a greater propensity to produce dendritic cell-like myeloid cells. Dynamic culture conditions using spinner flask technology increased the efficiency of hematopoietic differentiation within the scaffolds, EBs within the scaffolds were less likely to aggregate when covered with an ECM coating.

These studies demonstrated that differentiation within 3-D microenvironment enhanced ECM production, which in turn increased cell-cell and cell-substrate interactions and contributed to more efficient hematopoietic differentiation [137, 142].

Recent studies that have focused on differentiation of hESCs to hematopoietic cells have utilized human feeders and other natural polymers. Direct co-culture of hESCs with stromal cells from mouse hematopoietic tissue, bone marrow cells line S17, or a yolk sac endothelial line C166 induced differentiation into the hematopoietic lineage [143]. An example of the application of natural polymers in mesodermal differentiation involved a study that compared three models for differentiation: 2D culture conditions, EBs formed within a polymeric (alginate) scaffold and a slow turning lateral vessel bioreactor.

Undifferentiated hESCs seeded into the porous scaffolds formed EBs similar to those produced by a slow-turning lateral vessel bioreactor, in that they were well-rounded and did not form aggregates. However, alginate scaffolds induced vascular differentiation to a greater extent than the 2D culture plates and the bioreactor [144]. Unlike mESCs, no reported studies of synthetic polymers as substrates in hESC differentiation to hematopoietic and endothelial cells have been identified.

Feeder layers of similar lineage have been shown to support and induce osteogenic differentiation in mESCs and hESCs. For example, fetal murine osteoblasts with mESCs [101] and human periodontal ligament fibroblasts (hPLFs) with hESCs have been used in co-culture systems to enhance osteogenic differentiation [145].

Alginate was initially postulated to support chondrogenic proliferation [146, 147] but studies showed that EBs formed from mESCs encapsulated within an alginate construct with dexamethasone supplementation showed no enhanced chondrogenic potential when compared to intact EBs [148]. Additionally, there was no stimulatory effect of dexamethasone on chondrogenic differentiation. However, this report was one of the first to demonstrate chondrogenic potential of EBs within a 3-D construct. Successful examples of the application of a scaffold for osteogenic differentiation from mESCs include; the use of a 3-dimensional self assembling peptide substrate [149] and alginate beads loaded into a bioreactor fed with osteogenic inducing growth medium [150].

Synthetic polymers such as PEG have been successfully used in a recent study that reported the induction of chondrogenic differentiation in mESCs within a poly-(ethylene glycol) based polymeric 3-D environment. In these studies, 5 -day old EBs prepared in

suspension cultures were encapsulated in a photopolymerizable PEG polymer, with addition of TGF β 1 and glucosamine to the growth medium, enhancing the chondrogenic differentiation capabilities of EBs [151, 152]. Such 3D systems exhibit potential for ES cell delivery to the site of injury circumventing issues that arise with low proliferative capacity of differentiated chondrocytes as well as loss of phenotype during ex-vivo expansion [153]. An inorganic substrate derived from bioactive sol-gel glass initially used for the differentiation and proliferation of human and murine osteoblasts was also used to promote osteogenic differentiation from mESCs. Temporal and dose dependent manipulations of growth factors supplementation further enhanced the positive effect of this sol-gel [154, 155].

For osteogenic and chondrogenic induction of hESCs, researchers have demonstrated that pre-differentiated hESCs (5-day old EBs) replated in the presence of osteogenic supplements induced differentiation. *In vivo* implantation of these pre-differentiated cells within poly-D, L-lactide (PDLA) scaffolds in severely combined immunodeficient (SCID) mice allowed for further differentiation to specialized mineralizing tissue [156].

Substrate based adipogenic differentiation of mESCs have only been demonstrated on polycaprolactone (PCL) synthetic polymer. The study reported the use of nanoscale fibers from electrospun PCL scaffolds to mimic ECM architecture and induce mESC differentiation. mESCs were directly seeded onto the scaffolds and treated with insulin, triiodothyronine (T₃) and retinoic acid (RA) to induce adipogenesis. On comparing cells derived from this 3D culture system to those derived from a 2D system which involved

pre-specification with EB formation, it was noted that optimal results were achieved when the cellular micro-environments closely resembled in-vivo conditions [157].

A high-throughput screening approach utilized microprinting technology to present pluripotent cells with combinations of ECM proteins in a microarray [158] and in a multiwell format [159]. A commercial arrayer was used to deposit mixtures of varying concentrations of collagen I, collagen III, collagen IV, fibronectin, and laminin onto a thin custom-made acrylamide gel pad. The ECM was deposited in a highly controlled manner, and there were no detected instances of cross-contamination between spots. A multiwell format was generated using a slide carrier and gaskets, followed by seeding of mESCs within these wells and presentation of twelve different combinations of four growth factors known to induce cardiac differentiation. A total of 240 ECM and growth factor signaling environments were studied and the results acquired during this expansive run, were consistent with published data on cardiogenesis. The nature of the microenvironment that comprises of specific physical, chemical and mechanical cues need to be taken into account, prior to determining the biomaterial to be used in specific directed differentiation strategies.

Ectodermal differentiation

Ectodermal derivatives are often seen in spontaneously differentiating cultures and are considered as the “default pathway” for differentiation of pluripotent stem cells [160]. Several ectodermal derivatives such as oligodendrocytes, dopaminergic neurons and motor neurons have been produced using a cocktail of growth factors including FGF2, retinoic acid (RA), epidermal growth factor, brain and glial derived neurotrophic factor and sonic

hedgehog (SHH) [52, 161-164]. Direct co-culture of mouse and primate ES cells with PA6 stromal cells induced differentiation into dopaminergic neurons and circumvented the formation of multicellular aggregates (EBs) in the differentiation process. These studies determined that stromal cell- derived inducing activity (SDIA) was responsible for the differentiation, but little was ascertained of its molecular nature or induction mechanism [165, 166]. Naturally derived ECMs and synthetic polymers have both been used to differentiate mESCs into ectodermal derivatives. A comparative study was conducted to determine the effects of 2-D and 3-D fibrin based constructs on neural differentiation of EBs from mESCs. These studies showed that intact EBs encapsulated within the 3D fibrin gel differentiated more readily than those grown on 2D-fibrin gel into mature neurons and astrocytes under specific culture conditions [167]. mESCs cultured in hollow fibers made of cellulose triacetate polymer and ethylene vinyl alcohol copolymer in the presence of stromal cell conditioned medium differentiated into dopaminergic neurons [168]. This study presents a model system for *in-vivo* delivery of mESCs within scaffolds that promote differentiation. Such transplantation strategies might avoid obstacles that arise with rejection of implanted cells by the host with the added advantage of the semi-permeable membrane permitting the influx of nutrients for the survival of the implanted cells and the efflux of dopamine.

Few studies have reported the application of synthetic biomaterials for neural differentiation of hESCs. When pre-differentiated hESCs as 8-day old EBs were dissociated and seeded in a 50/50 blend of poly L-lactic acid) and poly(lactic co-glycolic acid) based biomaterial, multilayered rosette like bodies with epithelial cell-lined narrow

lumen was induced by supplementing the growth medium with retinoic acid. However, in the same construct, mesodermal differentiation was induced by addition of TGF β and endodermal differentiation was induced by addition of Activin A and IGF [169]. Enhanced neural differentiation of hESCs was achieved in the construct by addition of RA, nerve growth factor (NGF) and neurotrophins [170].

As part of a teratoma formation protocol used to investigate pluripotent potential of hESCs, researchers investigated the differentiation potential of hESCs seeded in laminin-coated poly-(lactic-*co*-glycolic acid) (PLGA) scaffolds [171]. Further analysis of the teratomas provided evidence of different cell types that originated from the three germ layers. However, close to 38% of the cells, exhibited increased expression of the neuronal marker, Nestin, thereby indicating that the nature of pre-transplantation treatment, the site of transplantation, and the ECM components in the scaffold could selectively enhance neural phenotypes within the teratoma [172].

The differentiation of mouse and human ES cells into the different lineages and specialized cells using different feeder dependent and independent substrates is summarized in Table 2.

Based on the different self renewal maintenance and differentiation strategies described in this chapter, it is evident that numerous physical, chemical and mechanical factors are at play in determining stem cell fate. Taking this into consideration, we attempt to generate and study in detail a substrate that will allow for undifferentiated propagation of hPSCs.

Table 2

Substrates used to induce differentiation in mouse and human pluripotent stem cells.

Substrate Type	Cell Source	Substrate	Differentiation Lineage	References
Feeder layer based	mESCs	Primary rat hepatocyte	Hepatic	[173]
		Mouse stromal cells OP9 and RP010	Hematopoietic	[130], [131]
		Fetal murine osteoblasts	Osteogenic	[174]
		Stromal cells PA6	Neuronal	[175]
	hESC	Mouse bone marrow cells line S17, yolk sac endothelial line C166	Hematopoietic	[143]
		Human periodontal ligament fibroblasts	Osteogenic	[145]
Natural substrates	mESCs	Collagen coated plates	Hepatic	[111]
		Alginate Beads	Hepatic	[114]
		Collagen type IV	Hematopoietic	[176]
		Fibrin polymers reinforced with poly(ethylene glycol)	Endothelial and Hematopoietic	[177]
		Dextran constructs	Endothelial	[178]
		Semi-interpenetrating polymer networks (SIPNs) with fibronectin (FN) and laminin (LM).	Endothelial and Cardiac	[179]
		Alginate construct	Chondrogenic	[148], [180]
		Self assembling peptide construct	Osteogenic	[181]
		Fibrin polymer construct	Neuronal	[167]
			hESCs	Collagen scaffolds
Alginate scaffolds	Hematopoietic			[144]
Synthetic Substrates	mESCs	Polyurethane foam	Hepatic	[117, 118]
		Cytomatrix	Hematopoietic	[177, 182]
		Poly-(ethylene glycol)	Osteogenic	[183], [184]
		Nanoscale fibers based electrospun polycaprolactone (PCL) scaffolds	Adipogenic	[185]
		Copolymer of cellulose triacetate polymer and ethylene vinyl alcohol	Neuronal	[186]
	hESCs	Poly-D, L-lactide (PDLA) scaffolds	Osteogenic	[187]
		Poly (L-lactic acid) and Poly(lactic co-glycolic acid)		[188]
		+ Retinoic Acid + TGFb + Activin A and IGF	Neuronal Chondrogenic Pancreatic	

Rationale for study

Human pluripotent stem cells (hPSCs) that include human embryonic stem cells (hESCs) and more recently, induced pluripotent stem cells have conventionally been cultured on mouse embryonic fibroblasts (MEFs) as feeder layers [1-5] The use of an additional cell-line as feeders and complex expansion techniques make hPSC culture a labor intensive process. In an attempt to engineer hPSC culture conditions devoid of non-human components, alternative feeders, mostly involving the use of MEF conditioned medium [22-26] or a mouse derived extracellular matrix (ECM)-based substrate: Matrigel™ [48] has been extensively studied. Though these strategies are partially successful in maintaining undifferentiated hPSC cultures, they do not completely eliminate the use of non-human derived products, thus still posing risks of xenogenic contamination.

Taking into consideration that adherent cell lines require extracellular matrix (ECM) for adhesion and proliferation, we hypothesize that the ECM components generated by the feeder layer fibroblasts will be sufficient in maintaining the undifferentiated state of hPSCs. Towards testing this hypothesis, we propose to characterize ECM substrates derived from different fibroblasts and their capability to support self-renewal of hPSCs. Further analysis of the ECM substrates will permit the identification of the major constituents in the matrix deposited by mouse and human fibroblasts that might be responsible for the maintenance of self-renewal of hESCs. The results from this analysis will allow the generation of a protein based substrate.

Our long term goal is the development of feeder-free conditions that utilize the self-renewal sustainability of ECM to engineer substrates that will provide hPSCs with the

appropriate physical and chemical cues required for long term undifferentiated propagation. The core hypothesis is that human ECM in controlled microenvironments provides sufficient physical cues to maintain hPSCs in their undifferentiated state. The experiments outlined under three different specific aims to test the hypothesis will determine the efficacy of acellular (ECM based) substrates, protein combinations (matrix composition based) and in-direct culture systems in supporting the undifferentiated proliferation of hPSCs.

Specific Aim 1) To characterize human fibroblast cell derived ECM as suitable acellular substrates for sustained undifferentiated propagation of hPSCs.

To address this aim, hPSCs will be propagated on two human fibroblasts as feeders.

Characterization of the hPSCs after 15 passages will involve analyzing the expression of key pluripotent markers based on immunocytochemistry and real time PCR. The rationale behind using these fibroblast cell lines is based on their human origin and their capacity for excessive ECM secretion.

Specific Aim 2) To formulate a protein substrate based on the proteomic analysis of the extracellular matrix (ECM) composition of the acellular substrates

Proteomic analysis of the acellular ECM substrates that have demonstrated the capability of maintaining long term undifferentiated propagation of hPSCs will identify proteins that play a role in adhesion and key signaling pathways for self-renewal maintenance. Based on results from the proteomic analysis protein based substrates will be formulated and tested for hPSC propagation. hPSCs cultured on such protein combinations will be characterized for expression of standard pluripotent markers.

Specific Aim 3) To incorporate acellular substrates on microporous membranes in an indirect co-culture system and assess their capability for hPSC propagation.

The use of microporous membranes coated with acellular substrates in addition to the presence of a physically separated feeder layer will allow for synergistic effects of the biochemical and biophysical cues necessary for self renewal maintenance. Such a system will allow for scale up of hPSCs without feeder cell contamination. hPSCs cultured in such controlled microenvironments will be characterized for expression of standard pluripotent markers.

General experimental analyses of a culture system across the three specific aims involve sustained propagation of undifferentiated hPSCs on the substrates for 15 passages, followed by characterization studies. Characterization will involve a) morphological analyses: high nuclear-cytoplasmic ratio for pluripotent cells b) immunocytochemical analyses for pluripotent markers (Alkaline phosphatase, AP, Octamer Binding Transcription Factor-4, OCT4, and Stage specific embryonic antigen-4, SSEA4) c) in vitro differentiation potential by embryoid body formation and test for the presence of germ layer specific markers from all three germ layers (ectoderm, endoderm and mesoderm) from pluripotent hPSCs d) Real time RT-PCR analysis for pluripotent and germ-layer specific markers and e) karyotype analysis for chromosome number

Overall, the studies conducted as part of this dissertation research project are expected to contribute to the development of propagation systems and controlled microenvironments for sustained propagation of undifferentiated and stable hPSCs.

CHAPTER 2: Stable propagation of human embryonic and induced pluripotent stem cells on decellularized human substrates

Abstract

Human pluripotent stem cells (hPSCs) that include human embryonic stem cells (hESCs) and human induced pluripotent stem cells (hiPSCs) have gained enormous interest as potential sources for regenerative biomedical therapies and model systems for studying early development. Traditionally, mouse embryonic fibroblasts (MEFs) have been used as a supportive feeder layer for the sustained propagation of hPSCs. However, the use of non-human derived feeders presents concerns about the possibility of xenogenic contamination, labor intensiveness and variability in experimental results in hPSC cultures. Towards addressing some of these concerns, we report the propagation of three different hPSCs on feeder-free extracellular matrix-based substrates derived from human fibroblasts. hPSCs propagated in this setting were indistinguishable by multiple criteria, including colony morphology, expression of pluripotency protein markers, tri-lineage in-vitro differentiation and gene expression patterns, from hPSCs cultured directly on a fibroblast feeder layer. Further, hPSCs maintained a normal karyotype when analyzed after fifteen passages in this setting. Development of this ECM-based culture system is a significant advance in hPSC propagation methods as it could serve a critical component in the development of

humanized propagation systems for the production of stable hPSCs and its derivatives for research and therapeutic applications.

Introduction

Human embryonic stem cells (hESCs) and more recently human induced pluripotent stem cells (hiPSCs) are primary examples of human pluripotent stem cells (hPSCs) and have garnered a lot of attention in the past decade due to their inherent properties of indefinite self renewal and differentiation into multiple cell types [1, 2, 4, 5]. Since their derivation, the preferred method of hPSC expansion has been the use of mitotically inactivated mouse embryonic fibroblasts (MEF) as feeder layers [2, 189]. The success of MEFs as a feeder layer is largely attributed to the presence of a cellular substrate for stem cell adhesion mimicking physiological milieu and the nutrients released into the medium providing a suitable microenvironment for undifferentiated propagation of hPSCs. However, the use of non-human cells as a substrate poses risks of xenogenic contamination by the possible introduction of animal retroviruses and other pathogens, which could potentially be transmitted to patients when used in biomedical therapies. This possibility is reinforced by the report of the presence a non-human carbohydrate moiety on the surface of hESCs propagated on MEFs, with the potential of eliciting an immune response when used in humans [17]. Additionally, the need to maintain two cell lines simultaneously and the mechanical passaging techniques employed to ensure normal karyotype in hPSCs [190] renders this culture methodology time consuming and labor intensive. The use of a live feeder layer has also presented researchers with challenges concerning feeder contamination of experimental data in downstream analysis [191].

Extensive research has introduced various alternate culture conditions; however the key factors responsible for the maintenance of the hPSC self-renewal capabilities are not evident [48, 192-194]. Studies have implicated the bFGF, Wnt, activin/Nodal pathways in the maintenance of pluripotency [192-194], however the interaction of these pathways with transcription factors that mediate self-renewal (OCT-4, SOX2, NANOG) is not clear [33]. The development of controlled propagation systems to maintain and expand stable hPSC populations is key to creating bankable populations of cells required for future research geared towards regenerative therapies [195].

Apart from MEFs, several human fibroblast cell lines have been tested and proven suitable feeders [22-25, 196]. It is realistic to state that adhesion based culture of hPSCs depend extensively on the extracellular matrices deposited by the feeder cells for their attachment and proliferation. Based on this principle, hPSCs were cultured and successfully propagated on mouse sarcoma derived protein mix: Matrigel™ and human serum deposits [48, 52]. However, such substrates are expensive and also require supplementation by way of MEF-conditioned medium (MEF-CM).

In order to address some of these challenges, our study focused on the potential of extracellular matrix (ECM) based substrates from human fibroblasts in the long-term maintenance of three different hPSCs in their undifferentiated state. In this study, we report the use of two human immortalized fibroblast (foreskin and dermal) lines as sources for the ECM-based substrates, thus avoiding the need for recurrent isolations of primary fibroblasts as is the case with MEFs. Our studies demonstrate the unique potential of these ECM-based substrates in promoting the stable propagation of undifferentiated hPSCs,

based on the assessment of multiple criteria for pluripotency. Additionally, this is the first report of hPSC propagation in a feeder-free, all human setting without the need for conditioned medium of any kind.

Materials & methods

Generation of inactivated feeder layers and extracellular matrix-based substrates. Mouse embryonic fibroblasts (MEFs) were isolated from embryos derived from 13.5d pregnant CF1 mice and maintained in Dulbecco's modified Eagle's medium with 4.5 g/L glucose, 2mM L-Glutamine, 1% Penicillin/Streptomycin and 10% fetal bovine serum. Human foreskin fibroblasts (HFFs) were maintained in Dulbecco's modified Eagle's medium (DMEM) with 4.5 g/L glucose, 2mM L-Glutamine, 1% Penicillin/Streptomycin and 10% cosmic calf serum and 2% Medium 199 (10x) to create a blend of basal medium comprising of M199 and DMEM. Human dermal fibroblasts (HDFs) were maintained in Minimum Essential medium supplemented with 2mM L-Glutamine, 1% Penicillin/Streptomycin, 15% fetal bovine serum, non-essential and essential amino acids, sodium pyruvate and vitamins. Inactivation of the three fibroblast lines was achieved by incubation in 10µg/ml of Mitomycin C, a mitotic inhibitor, for a period of two hours. Post-incubation, the cells were thoroughly washed with PBS 6 times, followed by trypsinization and additional three washes in growth medium to fully remove the mitomycin C. The cells were subsequently plated at a density of 300,000 cells/35mm dish.

Acellular extracellular matrix based substrates were generated by allowing the cultures (HFFs and HDFs) to proliferate 6 to 8 days past 100% confluency. The plates were washed with sterile distilled water to remove traces of growth medium followed by a

short exposure to 20mM NH₃ solution to expose the deposited ECM. The substrates were thoroughly washed with phosphate buffered saline (PBS) to avoid the deleterious effects of the alkaline ammonia solution [197]. For the purposes of application in our different experiments, the acellular HFFs (aHFFs) and acellular HDFs (aHDFs) once generated were stored at 37°C and used within a week.

Long term propagation of hPSCs. Karyotypically normal diploid hESC (WA09, <http://stemcells.nih.gov>) [2] and hiPSC (WiCell Research Institute, Madison, WI) [5] were routinely passaged on MEFs and transferred onto human feeders and acellular matrices in 35mm dishes. A rapidly dividing, karyotypically aneuploid cell line BG01v (Bresagen, Athens, GA) [198, 199] was also routinely passaged on MEFs and transferred onto human feeders and acellular matrices. WA09 and hiPSCs were passaged as colonies by mechanical dissociation while BG01v was enzymatically passaged every 3-4 days at subculturing ratios of 1:4. All the hPSCs were maintained in DMEM/F12 supplemented with 20% knockout serum replacement, 0.1mM β-mercaptoethanol, 1% non-essential amino acids, 100U/ml penicillin, 100mg/ml streptomycin and 4ng/ml basic fibroblast growth factor (bFGF). All reagents were obtained from Invitrogen (Carlsbad, CA) unless otherwise noted.

Alkaline Phosphatase assay. Staining for alkaline phosphatase was performed as per manufacturer instructions (Vector Labs, Burlingame, CA). Briefly, the hPSCs were washed with deionized water to remove traces of growth medium. The final solution was prepared by the addition of the three constituents in 0.2M Tris HCl buffer, pH 8.0. The hPSCs were incubated in the final mixture for 40 minutes in the dark and images were

acquired using a Nikon Coolpix 5000 camera mounted on a Nikon TS100 Microscope (Nikon, Melville, NY).

Antibodies and Immunocytochemical analysis. hPSCs cultured on the acellular substrates were transferred onto 4 chambered glass slides. 4% paraformaldehyde in PBS was used for fixation, permeabilization for intracellular markers was achieved with 0.2% Triton X-100 in PBS and blocked with normal goat serum. Fixed cells were incubated with primary antibodies: OCT4 (Santa Cruz Biotechnology, Santa Cruz, CA) and SSEA-4 (Millipore, Temecula, CA). Goat anti-mouse IgG conjugated to Alexa 488 (Molecular Probes, Eugene, OR) were used as secondary antibodies. Fluorescent images were acquired using a CoolSnap EZ camera (Photometrics, Tucson, AZ) mounted on a Nikon Eclipse TE 2000-S inverted microscope (Nikon, Melville, NY) with attached image analysis software. All image settings were controlled for uniform acquisition between samples. Specifically, uniform exposure time was maintained for images acquired from experimental samples as well as negative controls for background subtraction.

In vitro differentiation of hPSCs and histology of hPSC-derived embryoid bodies. To generate embryoid bodies (EBs), hPSCs were dissociated using collagenase and resuspended in growth medium devoid of bFGF. EB formation was facilitated using suspension culture by a hanging drop method, where cells at a density of 25,000 cells/ml were suspended from a petri-dish lid in 20 μ l droplets. After 5 days, the EBs were transferred to agarose plates at a density of 25 – 30 EBs per 10mls to facilitate further differentiation with media changes every 3-4 days for a total differentiation duration of 15 days. EBs were prepared for morphological analysis by fixation in 3.7% paraformaldehyde

(PFA) in 1.5ml microfuge tubes at approximately 15-25 EBs per tube. Once fixed overnight, EBS were rinsed with PBS to remove PFA, resuspended in 200 μ l melted 4% low melting point agarose (Sigma Aldrich) at 42°C and incubated for 2 hours to allow settling. Final pelleting and agarose solidification was performed with brief room temperature centrifugation at 500g. Agarose embedded samples were removed as single plugs and processed by dehydration with increasing ethanol concentration to 100% followed by xylene and paraffination in a Leica TP1020 tissue processor. Hematoxylin and Eosin (H&E) staining was performed on microscope slide mounted 5 μ m sections in a Leica Autostainer XL workstation (Leica Microsystems, Richmond, IL). Images were acquired using an Olympus BX51 microscope (Olympus, Center Valley, PA) using the default imaging parameters.

RNA isolation, real time reverse transcription polymerase chain reaction and gene expression analysis. RNA was isolated from hPSCs propagated for 15 passages under different conditions and from EBs after 15 days in suspension using Trizol (Invitrogen, Carlsbad, CA) and quantified using BioMate3 UV-VIS Spectrophotometer (Thermo Scientific, Waltham, MA). cDNA was synthesized from 1 μ g of RNA using cDNA reverse transcription kit (Applied Biosystems, Foster City, CA). Expression of pluripotent genes and differentiation markers (Table 3) within undifferentiated and differentiated samples were analyzed using quantitative real time RT-PCR (QPCR). QPCR was performed in an ABI HT7900 system (Applied Biosystems, Foster City, CA) and the data was acquired using Sequence Detection System software (SDS v2.2.1, Applied Biosystems, Foster City, CA).

Table 3

List of primers used for determination of relative gene expression of pluripotency and germ-layer specific genes as part of quantitative real-time PCR analysis

Gene Name	Primer sequence	
	Forward	Reverse
POU5F1/ OCT-4	GAAGGTATTCAGCCAAAC	CTTAATCCAAAAACCCTGG
NANOG	GATCGGGCCCGCCACCATGAGTGTG GATCCAGCTTG	GATCGAGCTCCATCTTCACAC GTCTTCAGGTTG
SOX2	GCGGAAAGCGTTTTCTTTG	TAATCTGACTTCTCCTCCC
Neuro D	<i>GTCCTTCGATAGCCATTAC</i>	<i>CTTTGATCCCCTGTTTCTTCC</i>
IGF2	TCCTCCCTGGACAATCAGAC	AGAAGCACCAGCATCGACTT
AFP	AGAACCTGTCACAAGCTGTG	GACAGCAAGCTGAGGATGTC

Gene expression data (three replicates) were acquired and SDS software was used to estimate differential gene expression using Δ CT quantification methods. Endogenous 18S ribosomal RNA was used for normalization. Relative gene expression for hPSCs propagated on acellular substrates was assessed against hPSCs propagated on MEFs. Relative gene expression of differentiated EBs obtained from different conditions was assessed against hPSCs propagated under the original condition. Expression Index (EI) was used to determine the relative differentiation state of cells [200] and was based on the average CT values from triplicate measurements. An expression ratio of two or more genes was determined using a mathematical model based on the geometric average of assessed genes, previously described in detail [201], given by the following equation:

$$EI = K_{RS} \frac{\sqrt[m]{(1 + E_{gene1m})^{Ct_{gene1m}} \cdot (1 + E_{gene2m})^{Ct_{gene2m}} \dots (1 + E_{genem})^{Ct_{genem}}}}{\sqrt[n]{(1 + E_{gene1n})^{Ct_{gene1n}} \cdot (1 + E_{gene2n})^{Ct_{gene2n}} \dots (1 + E_{genen})^{Ct_{genen}}}}$$

E is the PCR efficiency calculated from dilution series of purified PCR products, CT is the threshold cycle, and m and n are the numbers of genes that are up and down regulated upon differentiation respectively. K_{RS} is the relative sensitivity constant and was not determined as it does not affect relative comparisons between samples.

Preparation of hPSC for karyotype analysis. hPSCs propagated on acellular substrates for > 15 passages were subjected to cytogenetic karyotype analysis as per earlier published protocols [190]. Briefly, hPSCs were incubated with Ethidium Bromide (12 μ g/ml) for 40 min at 37°C, 5% CO₂, followed by 120ng/ml of colcemid (Invitrogen, Carlsbad, CA) treatment for 20 min. The cells were treated with 0.25% trypsin, and dislodged cells were centrifuged at 200g for 8 min at room temperature. The cell pellet was gently resuspended

in 0.075 M KCl solution, and fixed in a solution containing 3:1 of methyl alcohol and glacial acetic acid. Fixed cells were dropped on wet slides, air dried and baked at 90°C for 1 hour. G-banding was performed for visualizing chromosomes using Trypsin-EDTA and Lieshman Stain (Giemsa/Trypsin/Lieshman technique, GTL) by immersing slides in 1X Trypsin-EDTA with 2 drops of 0.4N Sodium Phosphate (Na_2HPO_4) for 20 to 30 seconds, rinsed in distilled water and stained with Lieschman Stain (Sigma) for 1.5 minutes, rinsed in distilled water, and air dried. Twenty metaphases of each sample were examined.

Results

Extracellular matrix based decellularized substrates allows expansion of hPSCs.

Decellularization using ammonia solution lyses the cells leaving behind an extensive ECM-based network that contributes to hPSC adhesion and propagation. A schematic of the procedure for generating extracellular matrix-based substrate is shown in Figure 3. Karyotypically normal hPSCs (WA09 and hiPSC) used in this study were cultured on MEFs for < 60 passages, while the aneuploid BG01v was cultured on MEFs for <75 passages prior to transfer onto acellular substrates. Upon transition of the three hPSCs onto the acellular substrates, minimal spontaneous differentiation was observed during culture condition transition. hPSCs formed both undifferentiated colonies with tight boundaries as well as heterogeneous colonies containing a population of differentiated cells at the colony boundaries and between colonies as seen in earlier studies [20, 48]. However, the transition effect diminished within 2-3 passages and undifferentiated colonies with tight boundaries were observed that continued through subsequent passages. The culture conditions permit

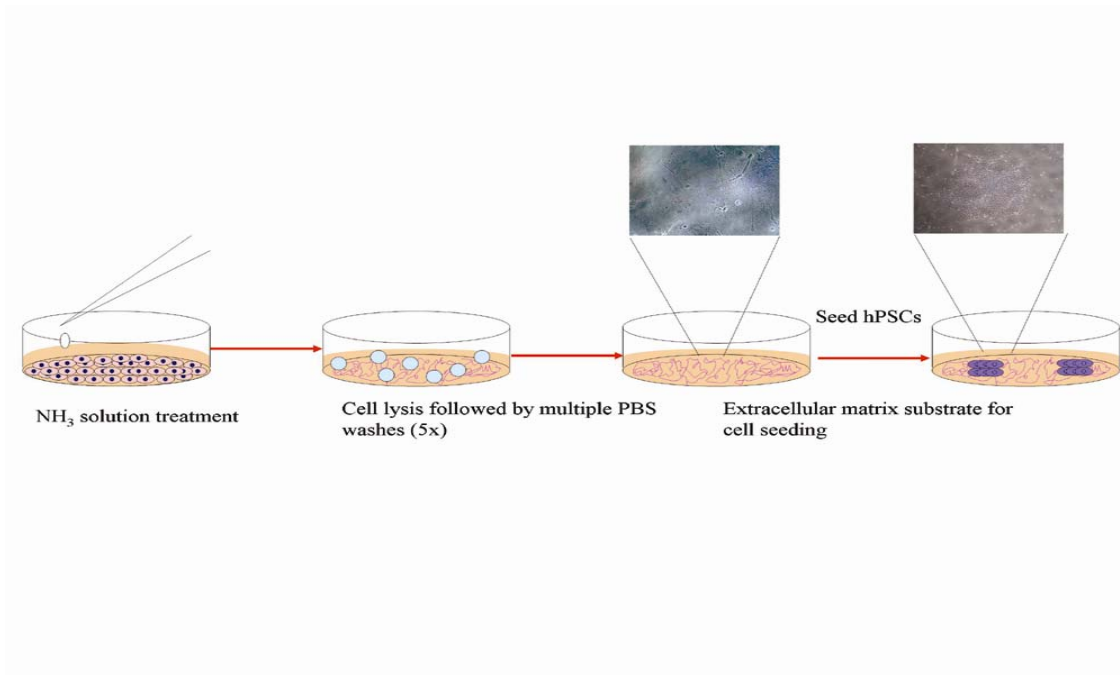


Figure 3:

Schematic of the preparation of acellular substrates for hPSC propagation. Feeder cells are allowed to grow past 100% confluency for ECM deposition. Treatment with 20mM ammonia solution for 5 min lyses the cells to expose the ECM layer onto which hPSCs are seeded

uniform hPSC propagation during subsequent passages, resulting in very few differentiated cells in the later passages. The aneuploid BG01v cultured on acellular substrates did not exhibit typical morphological characteristics as when propagated on MEFs. BG01v formed a continuous layer of spindle shaped or fibroblastic cells on acellular substrates, without losing any of its core pluripotent characteristics (Appendix A). The normal hPSC lines (WA09 and hiPSC) however exhibited similar morphology on acellular substrates when compared to their respective MEF based cultures (Figure 4 a-f). The hPSCs formed colonies with distinct boundaries and demonstrated high nuclear to cytoplasmic ratio. This difference in cell morphology between the two types could be due to the difference in passaging techniques; BG01v cells were enzymatically passaged leading to formation of single cell suspension, whereas the normal lines were maintained as clusters during passaging. It was observed that the hPSC colonies were flat and enlarged compared to those propagated on feeders. The larger size of the colony, while maintaining normal morphology on the acellular substrates, could be attributed to the availability of more surface area for spreading and propagation. hPSCs were successfully cultured on inactivated HFFs and HDFs feeder layers for 15 passages (Figure 5); however, in all our analyses, cultures of the three different hPSCs on MEF feeders were used as controls. Under the passage conditions adopted, the doubling time for the hPSCs passaged on acellular substrates was in the range of 24-30 hours, which is comparable to what was observed in other MEF and feeder-free studies [20, 48, 202].

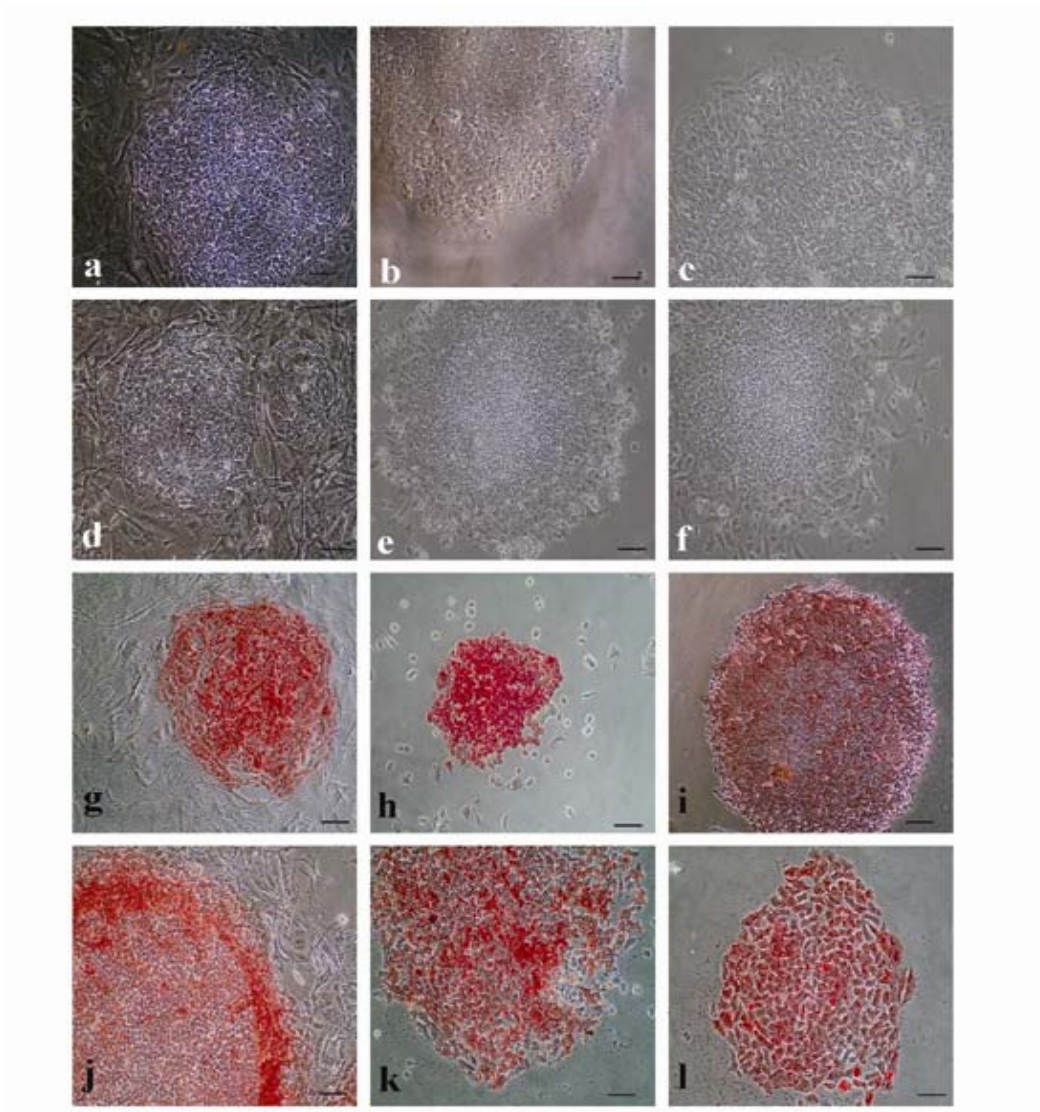


Figure 4:

hPSCs maintain embryonic characteristics on acellular substrates: WA09 hESCs and hiPSCs maintain high nuclear to cytoplasmic ratio and tight boundaries on control, MEFs (a, d) and on acellular HFF (b,e) and HDF substrates (c, f). Positive expression of alkaline phosphatase in WA09 (g, h, i) and hiPSC (j, k, l) propagated for 15 passages on MEF (g,j), aHFF (h,k) and aHDF (i,l) was observed, Scale bar = 100 μ m

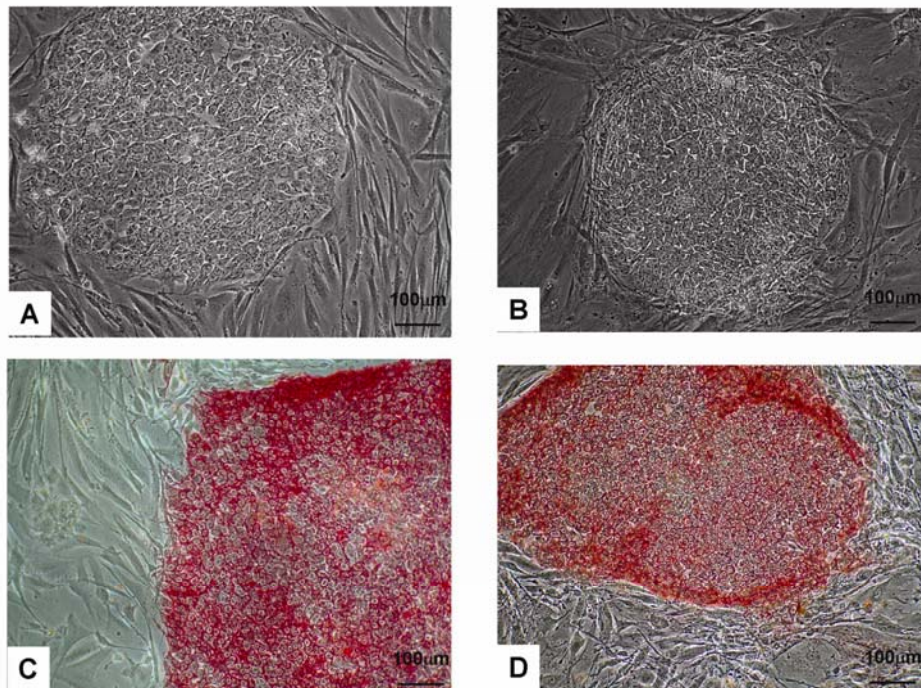


Figure 5:

WA09 hESCs maintain high nuclear to cytoplasmic ratio and tight boundaries on inactivated HFFs (iHFFs) (A) and on inactivated HDFs (iHDFs) (B). Positive expression of alkaline phosphatase in WA09 (C) propagated for 15 passages on iHFFs (C) and iHDF (D) was observed, Scale bar = 100 μm

hPSCs cultured on Matrigel™ (as a negative control) without the additional supplementation of the growth medium led to heterogeneous populations of undifferentiated and differentiated colonies (Figure 6), similar to what has been observed in previous studies [192].

Acellular substrates maintains undifferentiated state of hPSCs

Validation of the acellular substrates for stable undifferentiated hPSC propagation was based on alkaline phosphatase staining and immunocytochemical analysis for expression of transcription factor OCT4 and the cell surface marker SSEA4. hPSCs propagated on different acellular substrates were assessed for their expression at 5, 10 and 15 passages post-transfer from feeders. Positive robust expression of alkaline phosphatase, a reliable marker of pluripotency [203], is indicative of sustained maintenance of the undifferentiated state of hPSCs (Figure 4). At intermittent passages as well as on passage 15, positive expression for pluripotency markers tested was observed (Figure 7). Further, monitoring the expression of the nuclear marker 4',6-diamidino-2-phenylindole (DAPI) under all the acellular conditions served the purpose of staining any nuclear/DNA material left behind from the decellularization process. The absence of additional staining within the substrate was indicative of an efficient lysis and post-decellularization wash procedure (Figure 8).

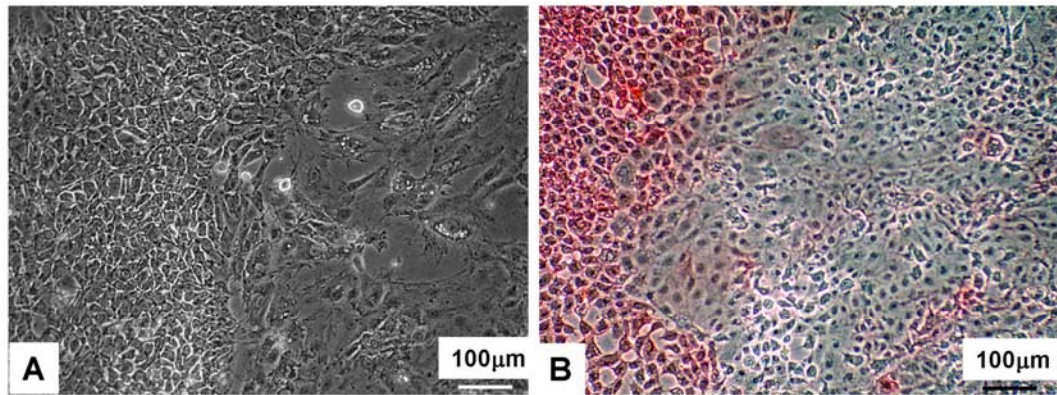


Figure 6:

Differentiation seen in hPSC maintained on Matrigel: WA09 hESCs maintained on MatrigelTM in growth medium without additional supplementation produce (A) heterogeneous undifferentiated and differentiated cells within the colonies (A) and stain positive/negative for alkaline phosphatase (B). Scale bar = 100 μ m.

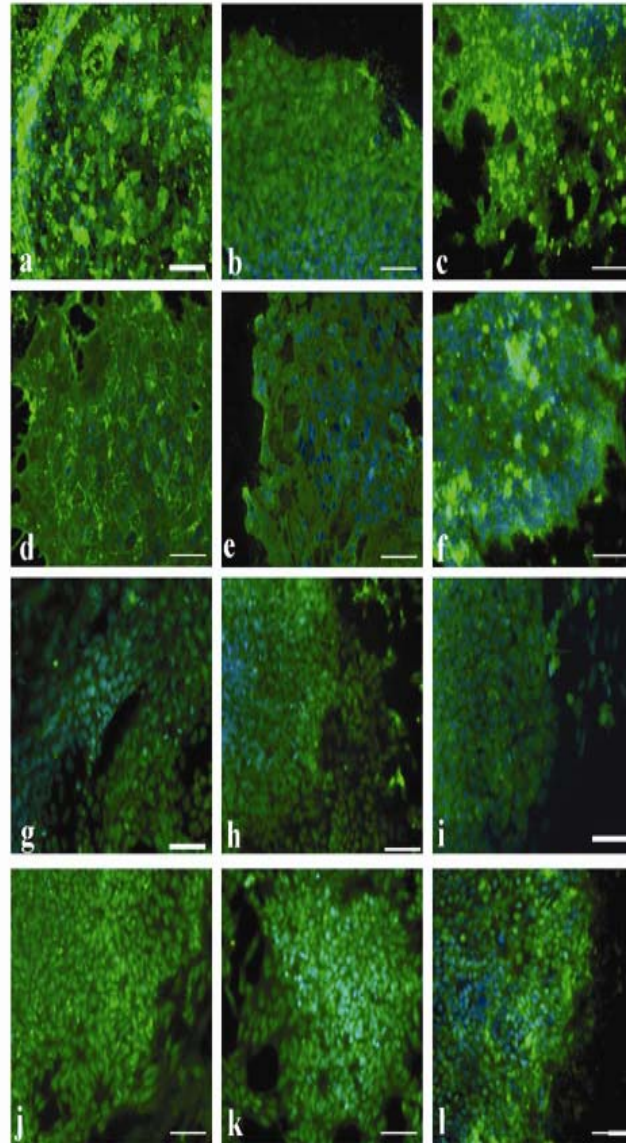


Figure 7:

Pluripotent markers expressed in hPSCs maintained on acellular substrates: Positive expression of stage specific embryonic antigen (SSEA4) (a-f) in WA09 (a, b, c) and hiPSC (d, e, f) propagated for 15 passages on MEF (a, d), aHFF (b, e) and aHDF (c, f). Expression of OCT4 (g-l) in WA09 (g, h, i) and hiPSC (j, k, l) propagated for 15 passages on MEF (g,j), aHFF (h,k) and aHDF (i,l) was observed. All slides were stained with DAPI (blue) to identify cell nuclei. Scale bar = 50 μ m.

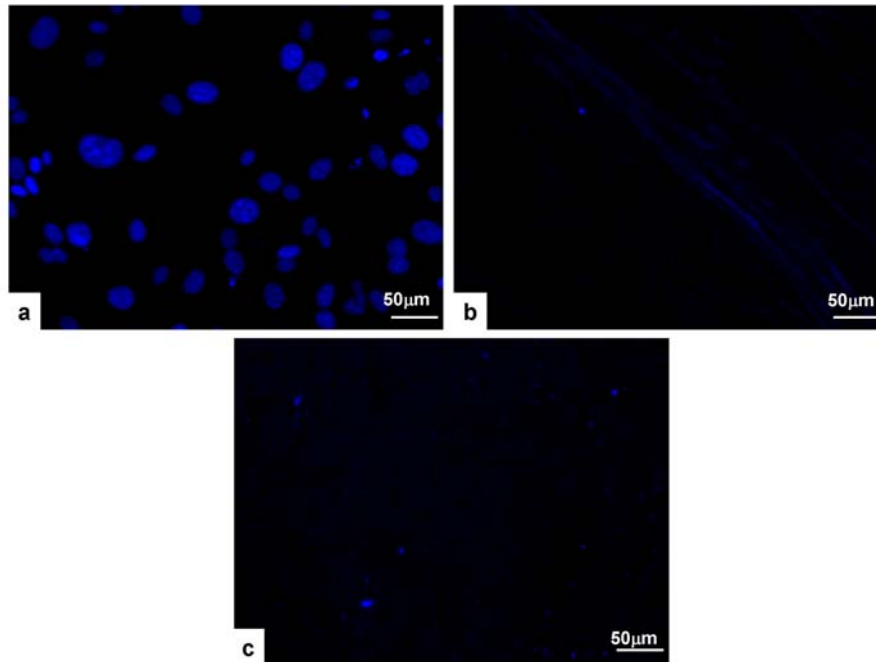


Figure 8:
Decellularization causes loss of nuclear material. (A) Fibroblasts stain positive for DAPI indicating intact nuclei. (B) Acellular fibroblasts and (C) MatrigelTM exhibit minimal staining for DAPI, indicating absence of nuclear material. Scale bar = 50 μm.

Gene expression analysis validates acellular substrates for stable undifferentiated hPSC propagation

Differential expression of pluripotency markers (POU5F1, NANOG and SOX2) was expressed as CT values normalized against the 18S rRNA housekeeping gene for each sample. For the purposes of the comparisons across the different experimental conditions, the Δ CT values of each marker within each experimental sample are presented against that of MEFs, as this eliminates the requirement for normalization with the calibrator.

Comparable Δ CT values of all the pluripotent genes across different culture conditions and cell lines are indicative of the maintenance of undifferentiated state of hPSCs on acellular substrates (Figure 9). Statistical analyses indicated no significant difference ($p > 0.05$) in the 12 different comparisons for the pluripotency markers tested between hPSCs propagated on the acellular substrates and those propagated on MEFs. However, a significant difference ($p < 0.05$) was observed for only one comparison in the case of POU5F1 expression within hiPSCs grown on aHFFs. In this particular case, there was a three-fold decrease in POU5F1 expression; however the expression of NANOG and SOX2 within this experimental condition was comparable to that of those on MEFs.

Acellular substrates maintains in vitro differentiation potential

Functional pluripotency of the hPSCs was assessed by *in vitro* differentiation (ectoderm, endoderm and mesoderm) via formation of embryoid bodies. Differential expression of germ layer specific markers Neurogenic differentiation 1 (NEUROD1), Insulin-like Growth Factor 2 (IGF2) and α -Fetoprotein (AFP) were expressed as CT values normalized against the 18S rRNA housekeeping gene for each sample.

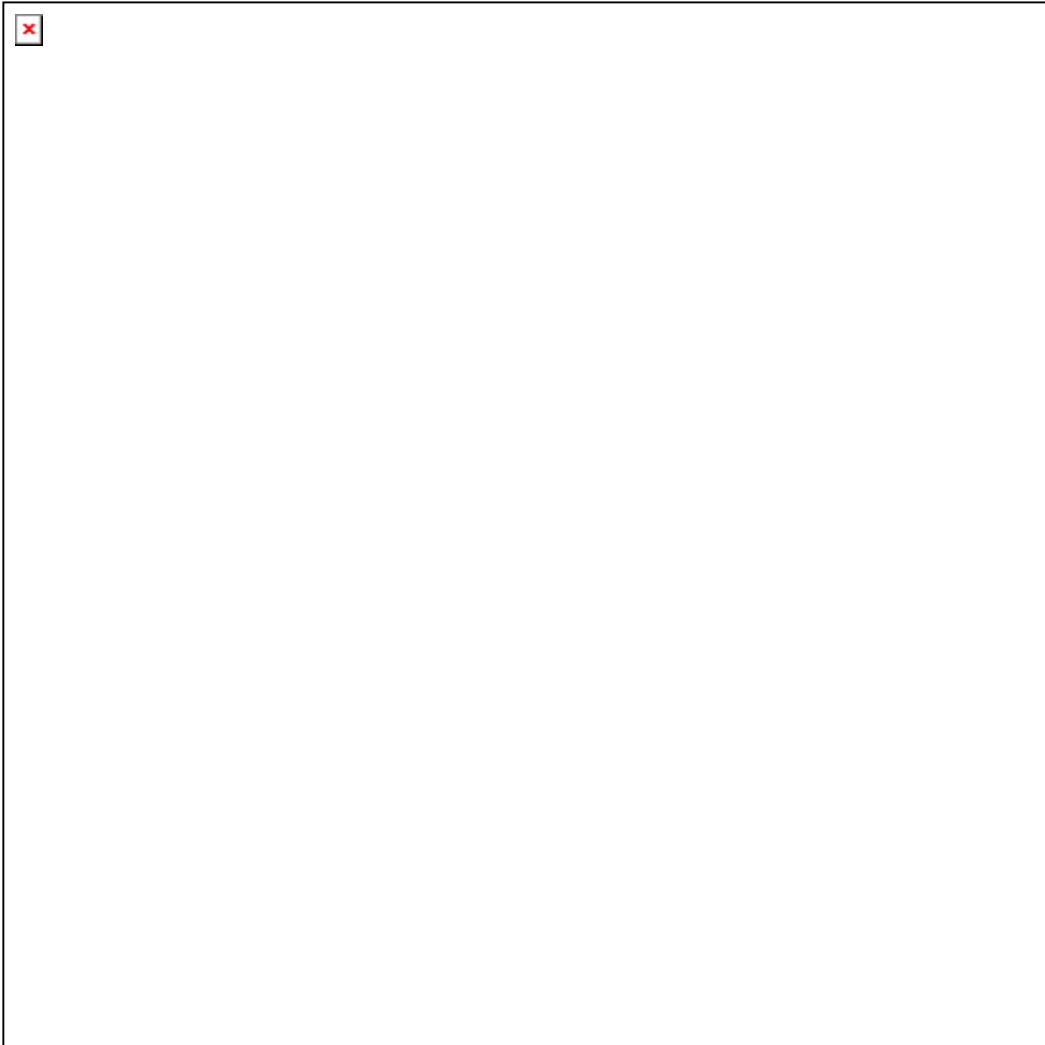


Figure 9:
Normalized gene expression of *undifferentiated markers* in WA09 (a) on MEFs (A); WA09 on acellular HFF (B) and WA09 on acellular HDFs (C). Normalized gene expression of *undifferentiated markers* in hiPSCs (b) on MEFs (A'); hiPSCs on acellular HFF (B') and hiPSCs (b) on acellular HDFs (C'). Significant difference ($p < 0.05$) between the group is indicated by the asterisk.

Statistical analyses indicated that the EBs generated from the WA09 and hiPSC on the different acellular substrates demonstrated significantly greater expression ($p < 0.01$) of all three germ layer specific markers analyzed (Figure 10 a, b) compared to their undifferentiated cells cultured in the same experimental conditions. Here, it is important to note that Δ CT values (normalized against 18S) should be interpreted counter-intuitively; where a lower value indicated higher expression. Comparative gene expression analysis based on fold change calculations also demonstrate increased expression of germ-layer specific markers in EBs generated from the WA09 and hiPSC on the different acellular substrates (Table 4). Further, the differentiation state of the hPSCs was quantified using the ‘expression index’ as a metric to compare the undifferentiated hPSCs against the EBs generated from the hPSCs grown under the same condition. For the two cell lines (WA09 and hiPSC) analyzed, the expression index of the undifferentiated sample (15 passages) was 251 and 612 on aHFFs (Figure 11 a, b) and 180 and 50 on aHDFs (Figure 11c, d), while the expression index of the 15-day old EBs was found to be 1.5 and 2 on aHFFs (Figure 11a, b) and 1.1 and 2.3 on aHDFs (Figure 11c, d).

In addition to the gene expression of markers indicative of germ layer formation in EBs, histological studies were performed to assess the morphology of the differentiated tissue. As shown in Figure 12 (a-r), histologic evidence of tri-lineage maturation was present in the EB-sections from hPSCs propagated on acellular substrates and on MEFs. Specifically, neuroepithelial differentiation was observed as mature-type neuroepithelial rosettes (Figure 12, a, d, g, j, m and p). Mesodermal differentiation was evident as fibrous

connective tissue (Figure 12 b, e, h, k, n and q), while endodermal differentiation was evident as secretory intestinal-type epithelia (Figure 12 c, f, i, l, o and r).

Cytogenetic analysis confirms feasibility of acellular substrates for stable hPSC undifferentiated.

In order to determine the stability of hPSCs propagated continuously on the acellular substrates, cytogenetic analysis was performed on twenty G-banded metaphase spreads from WA09 and hiPSC cells after 15 passages on acellular substrates. Nineteen cells from the WA09 sample demonstrated a normal female karyotype of 46,XX (Figure 13a), while one cell demonstrated a non-clonal chromosome aberration; 46,X,t(X;19)(q22, q13.3), which is most likely a technical artifact. In the case of hiPSCs, all twenty cells demonstrated a normal male karyotype of 46,XY (Figure 13b). None of the samples exhibited trisomies for chromosome 12 and/or 17, which are considered to be the common abnormalities observed in hPSC cultures [190].

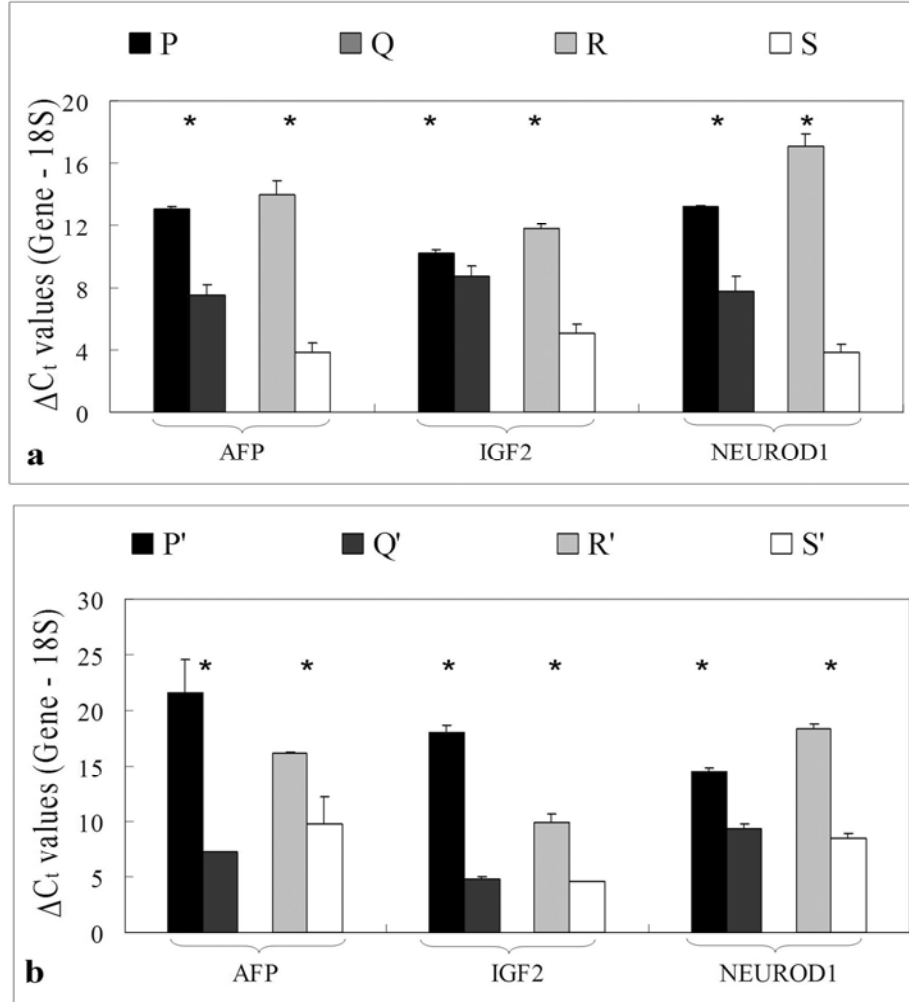


Figure 10:

Normalized gene expression of *germ layer specific markers* in (a) WA09 on acellular HFFs (P); EBs generated from WA09 on acellular HFFs (Q); hiPSC on acellular HFFs (R); and EBs generated from hiPSC on acellular HFFs (S). Normalized gene expression of *germ layer specific markers* in (b) WA09 on acellular HDFs (P'); EBs generated from WA09 on acellular HDFs (Q'); hiPSC on acellular HDFs (R'); and EBs generated from hiPSC on acellular HDFs (S'). Significant differential gene expression ($p < 0.01$) in all three lineage specific markers was observed.

Table 4:

Increase in gene expression of germ layer specific markers in embryoid bodies compared to their undifferentiated counterparts on different substrates is represented as fold change values. FC = Fold change, SD = Standard deviation

Fold change values of germ layer specific genes in embryoid bodies compared to their undifferentiated counterparts.

Substrates/Cell Line	FC \pm SD
<i>α-Fetoprotein -- Endodermal marker</i>	
aHFF – WA09	34.61 \pm 3.47
aHDF – WA09	523.9 \pm 204.2
aHFF – hiPS	87.67 \pm 2.51
aHDF - hiPS	9.26 \pm 0.72
<i>Insulin like growth factor 2 -- Mesodermal marker</i>	
aHFF – WA09	1.58 \pm 0.28
aHDF – WA09	25.9 \pm 8.7
aHFF – hiPS	240 \pm 33.9
aHDF - hiPS	5.9 \pm 0.04
<i>Neurogenic Differentiation marker 1-- Ectodermal marker</i>	
aHFF – WA09	30.9 \pm 1.7
aHDF – WA09	18866.4 \pm 7266.3
aHFF – hiPS	1.5 \pm 0.35
aHDF - hiPS	12.7 \pm 1.4



Figure 11:
QPCR analysis of undifferentiated hPSCs and differentiated EBs derived from hPSCs. Differential expression index of a) WA09 hPSC and WA09-derived EBs from acellular HFFs, b) WA09 hPSC and WA09-derived EBs from acellular HDFs, c) hiPSC and hiPSC-derived EBs from acellular HFFs and d) from acellular HDFs based on analysis of six genes (POU5F1, NANOG, SOX2, AFP, IGF2 and NEUROD1).

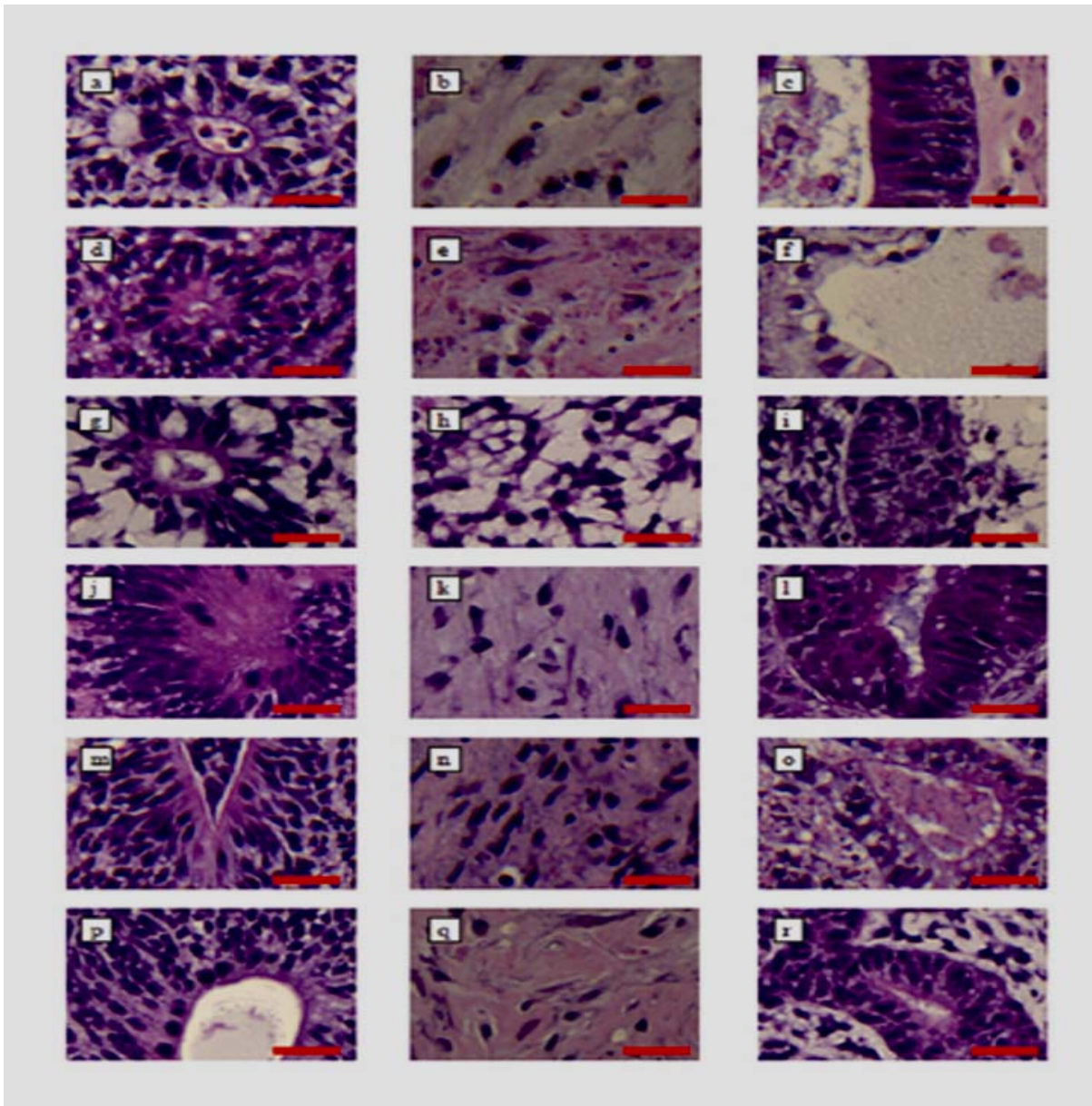


Figure 12:

Histologic evidence of tri-lineage differentiation in embryoid bodies generated from hPSCs. Shown are images of hematoxylin and eosin-stained histologic sections of EBs from WA09 propagated on MEFs as a positive control (top row, a-c); WA09 cells propagated on the acellular HFFs (second row, d-f) and acellular HDFs (third row, g-i) and hiPSC propagated on MEFs (fourth row, j-l) hiPSC propagated on acellular HFFs (fifth row m-o) and hiPSC propagated on acellular HDFs (bottom row p-r). Tri-lineage potential is demonstrated as ectodermal (neuroepithelial) differentiation (a, d, g, j, m and p); mesodermal (fibrous connective) differentiation (b, e, h, k, n and q) and endodermal (intestinal) differentiation (c, f, i, l, o and r). Magnification is 200x total (10x ocular, 20x objective). Each scale bar represents 50 μm in length.

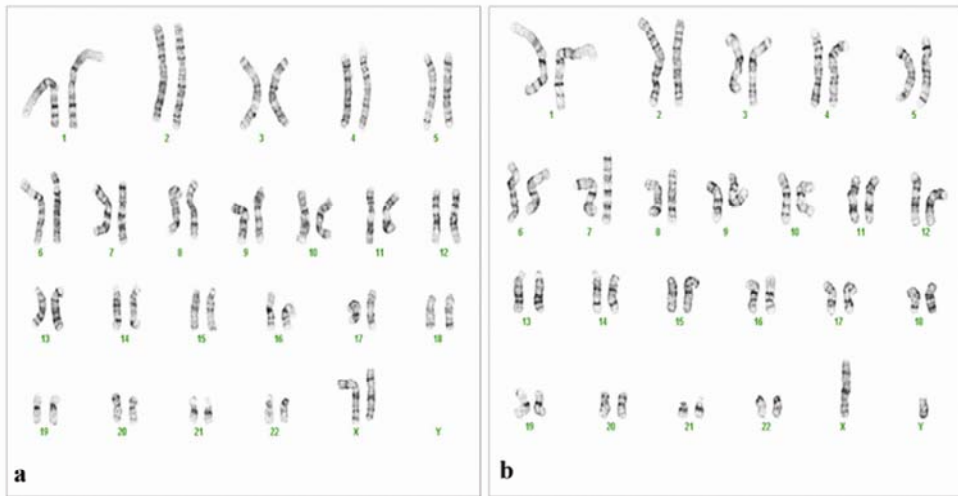


Figure 13:

Cytogenetic analysis on 20 metaphase spreads was performed on WA09 (a) and hiPSC (b) cultured on acellular HFFs. The G-banding karyotype of WA09 hESC after 15 passages on decellularized HFFs was 46,XX and that of hiPSCs was 46,XY.

Discussion

This study involves the development of a feeder-free system for stable undifferentiated hPSC propagation that demonstrates several significant steps towards the improvement of hPSC culture systems. The system developed was effective in its generation of a substrate of human origin and offered a viable alternative to traditional mouse feeder layer based systems. Further, other feeder-free systems have relied heavily on supplementation with excess basic fibroblast growth factor (bFGF) or MEF-CM for long term maintenance of hPSCs in their undifferentiated state. Given the cost ineffectiveness and the use of non-human derived components in those systems, our study has utilized growth medium without the need for conditioning prior to use on the acellular substrates. Furthermore, previous studies have reported the variability that exists between different hPSCs and the usefulness of comparing experimental outcomes across distinct hPSCs [202]. To demonstrate the efficacy of the acellular substrates, we used hPSCs from two embryonic (BG01v and WA09) in addition to an induced pluripotent stem cell from human fibroblasts in our studies. Positive expression of key pluripotent markers based on quantitative PCR and immunocytochemical analyses is a clear indicator of the sustained maintenance of self renewal of hPSCs on the acellular substrates. Quantitative PCR experimental outcomes validate the comparable expression of pluripotent genes, within the two hPSCs evaluated on the two different acellular substrates. Gene expression values of germ-layer specific markers analyzed within undifferentiated populations of cells related to high CT values are indicative of low differentiation within the hPSC colonies. Furthermore, the values based

on the EI demonstrate high values for undifferentiated hPSCs compared to differentiated samples (EBs) obtained from the hPSCs on the different substrates. A collective expression index based on up and down-regulated genes at any stage of hPSC culture is an attempt to quantify the level of differentiation in cells grown in different culture conditions. In this study, six markers; three pluripotency and three germ layer makers were used, with the robustness of such a metric increasing with the inclusion of more reporter genes. This method of PCR data representation is not susceptible to small changes in CT values and delivers a quality control indicator for the optimization of novel substrates in stable undifferentiated hPSC propagation. The expression indexes of hPSCs maintained on feeder-free substrates is comparatively lower than that of hPSCs propagated on MEFs (data not shown), as observed in this study and elsewhere [200]. The reason for this discrepancy is unknown; however the hPSCs maintained on acellular substrates display all characteristics of self-renewal and pluripotency that include tri-lineage differentiation potential as shown by histological analysis and are indistinguishable from each other in that regard.

In this study, we have used MEF-based feeder systems as a control for evaluating the usefulness of the human acellular substrates developed. Two immortalized human fibroblasts (foreskin and dermal) and decellularized substrates derived from the human fibroblasts were extensively characterized for stable hPSC propagation. Since MEFs have been used for the isolation, derivation and expansion of many of the existing hPSCs, we speculate that most of the hPSCs have developed a dependency on MEFs and MEF secreted components. The observed temporary transition effect related to some detectable

background differentiation during the early passages on the acellular substrates could have been a direct result of the period required for acclimatization of the hPSCs to the acellular substrates. However these transition effects subside for all hPSCs after the third passage on all the acellular substrates evaluated. In our culture system, the hPSCs were propagated in standard medium supplemented with 4ng/ml of bFGF, as opposed to 50-100 ng/ml bFGF in other reported feeder-free systems that have used MEF-CM or more defined medium [20, 192, 204]. The minimal requirement of supplementation demonstrates the efficacy of the acellular substrates in maintaining the undifferentiated state of the hPSCs without the need for conditioning of the medium or addition of higher bFGF concentrations. However, future efforts with regard to optimization of medium formulations might improve the propagation of stable hPSCs on the acellular substrates.

Previous studies have demonstrated the relevance of culture and passaging conditions on the genomic stability of hPSCs. Aneuploid cells have been observed in long-term culture of hESCs under feeder-free conditions, with trisomy 20 as the most frequent mutation [202], and trisomy 12 and 17 under feeder-based conditions [190]. In our studies, cytogenetic analyses conducted on hPSCs propagated on the acellular substrates demonstrate the absence of gross chromosomal abnormalities.

In conclusion, we have demonstrated the development and characterization of a human acellular substrate based feeder-free system as providing unique and functional benefits for stable undifferentiated hPSC propagation, as opposed to the common murine-based MatrigelTM substrate, that include reduced contamination potential due to extensive culture manipulations of parallel stem and feeder cultures, the potential for xeno-free scale-

up based on a thorough characterization of the substrate components and the reduced need for factor additives or medium conditioning. Further, the acellular substrate based system is devoid of non-human derived products and actively promotes long term propagation of hPSCs while maintaining self-renewal, and pluripotent characteristics and most importantly the genomic stability. It is possible that the matrix proteins might bind and sequester essential growth factors from the culture medium or might contain factors from fibroblasts which aid in the maintenance of self-renewal. Though this study does not eliminate the need for an additional cell line to be maintained in parallel, we are in the process of characterizing the core components of the ECM that will permit us to create defined matrices leading to elimination of maintenance of dual cultures. Alternately, lyophilization of the extracted substrates permit long-term storage for incorporation in hPSC culture as and when desired (Appendix D). Further understanding of the mechanism of action, modifications and optimization of the system will rely on a detailed characterization of the components of the extracellular matrix of the substrates and will contribute to a better understanding of the key physical cues required for hPSC self-renewal and for routine adaptation of the substrates for stable hPSC propagation.

CHAPTER 3: Characterization and application of human fibroblast-derived extracellular matrix for human pluripotent stem cell propagation

Abstract

Recent studies from our laboratory have shown that acellular substrates generated from human fibroblasts successfully maintained human pluripotent stem cells (hPSCs) in their undifferentiated state for extended periods. Towards better characterization of the core components in the substrates, we conducted proteomic analyses to identify the extracellular matrix (ECM) proteins in mouse embryonic and two human fibroblasts. Our studies identified heparan sulfate proteoglycan (HSPG) along with other major ECM proteins as core components of the substrates derived from mouse and human fibroblasts, these results were validated immunocytochemically. In our attempt to synthesize substrates that mimic the biological activity of fibroblast-deposited ECM, combinations of HSPG and other core ECM proteins were formulated and assessed for hPSC self-renewal. WA09 and BG01v hPSCs maintained on these substrates exhibit multiple characteristics of pluripotency that include (a) tight colony formation with typical stem cell morphology (b) positive expression of alkaline phosphatase (c) positive expression of SSEA3, SSEA4 and OCT4 based on immunocytochemical analyses (d) POU5F1, NANOG and SOX2 mRNA expression and (e) in-vitro differentiation and expression of germ-layer specific markers.

Our studies also reveal that although HSPG by itself does not support hPSC self-renewal, a substrate that combines HSPG and fibronectin is sufficient for undifferentiated propagation of hPSCs. These studies form the basis for identification and development of appropriate ECM components in a substrate that synergistically promotes activation of adhesion and signaling pathways responsible for hPSC self-renewal.

Introduction

Human pluripotent stem cells (hPSCs) that include human embryonic stem cells (hESCs) and human induced pluripotent stem cells (hiPSCs) have the capacity to self-renew indefinitely or differentiate into the three primary germ layers and subsequently form specialized cell types [1, 2, 4, 5]. These unique characteristics of hPSCs make them suitable for use in regenerative biomedical therapies, drug testing platforms and as *in vitro* models for developmental biology studies. However, one of the major hurdles facing stem cell researchers is the ability to efficiently produce stable hPSCs prior to their use in different applications. Current methodologies provide limited opportunities for generating stable hPSC populations due to the lack of a thorough understanding of biochemical and biophysical cues required for unlimited self-renewal. Identification and characterization of key signaling factors, molecular pathways and extracellular matrix components responsible for self-renewal thus provide opportunities for the development of bioprocessing strategies for hPSC propagation systems [195].

Traditional methods for the derivation and subsequent propagation of hPSCs have involved the use of mouse embryonic fibroblasts (MEFs) as feeder layers, supplemented

with culture medium containing non-human derived serum [2, 189] . The risk of contamination with xenogenic pathogens under these culture conditions have led to the incorporation of growth factors such as basic fibroblast growth factor (bFGF) and serum replacers in hPSC propagation systems. Culture systems that use human feeders have also been identified to minimize association of hPSCs with nonhuman factors so as to develop propagation systems suitable for therapeutic applications [20]. Within an hPSC culture system, signaling molecules like basic fibroblast growth factor (FGF2) [34], Activin A [205], and noggin [206] have been shown to repress spontaneous differentiation rather than maintain self-renewal. Given that Activin A has also been shown to induce hPSC differentiation to the mesodermal lineage [106], there is a definite need for a better understanding of the mechanisms employed by the hPSCs to self-renew and/or differentiate.

Successful use of culture medium conditioned by mouse or human feeder cells in the maintenance of hPSCs demonstrates that the trophic factors secreted in the growth medium or the matrix deposited by the feeder layers [48], [207] play an important role in hPSC self-renewal. Proteomic analysis of mouse and human fibroblast conditioned medium have provided some preliminary insights into the feeder-derived factors that contribute to hPSC self-renewal[208, 209]. In these studies, a number of proteins of extracellular and intracellular origin of known biological functions have been detected, with the overall goal of identification of biological pathways responsible for hPSC self-renewal. However, given the consensus in the stem cell community of the absence of a

defined system for hPSC maintenance, it is believed that a number of unidentified factors may be required to maintain hPSC self-renewal [210].

Our current study utilized proteomic approaches to isolate and identify the proteins within the extracellular matrix in three well characterized feeder layers, human foreskin fibroblasts (HFF), human dermal fibroblasts (HDF) and mouse embryonic fibroblasts (MEF). Peptide identification involved two step liquid chromatography (LC) separation utilizing strong cation exchange (SCX) and reverse-phase sequential step elution followed by peptide sequence analysis using tandem mass spectrometry. Immunocytochemical analysis was used to validate the presence of key extracellular matrix proteins in the different feeder layers. To assess the efficacy of the ECMs identified, commercially available proteins were used to formulate ECM-protein based substrates (EPBS) and their ability to maintain undifferentiated hPSCs based on multiple evaluation criteria for pluripotency was studied. Our studies identified heparan sulfate proteoglycan (HSPG) as a core component of the EPBS developed for hPSC self-renewal with additional studies indicating that a combination of HSPG and fibronectin as being sufficient for hPSC self-renewal. Our results suggest that ECM components that contribute to adhesion and activation of pluripotency-related signaling pathways will play a critical role in the development of substrates for long-term stable hPSC propagation.

Materials and Methods

2.1 Preparation of acellular substrates from mouse and human feeders

Mouse embryonic fibroblasts (MEFs) were isolated from embryos derived from 13.5d CF1 pregnant mice, and maintained in Dulbecco's modified Eagle's medium with 4.5 g/L

glucose, 2mM L-Glutamine, 1% Penicillin/Streptomycin and 10% fetal bovine serum.

Human foreskin fibroblasts (HFFs) were maintained in Dulbecco's modified Eagle's medium with 4.5 g/L glucose, 2mM L-Glutamine, 1% Penicillin/Streptomycin and 10% cosmic calf serum and 2% Medium 199 (10x) to create a blend of basal medium

comprising of M199 and DMEM. Human dermal fibroblasts (HDFs) were maintained in Minimum Essential medium supplemented with 2mM L-Glutamine, 1%

Penicillin/Streptomycin, 15% fetal bovine serum, non-essential and essential amino acids, sodium pyruvate and vitamins.

Acellular substrates were generated by allowing the cultures (HFFs and HDFs) to proliferate 6 to 8 days past 100% confluency. In the case of MEFs, inactivated 6-8-day old MEFs seeded at a density of 300,000/ 35mm dish was used to generate acellular substrates. The plates were washed with sterile distilled water to remove traces of growth medium followed by a short exposure to 20mM NH₃ solution to lyse the fibroblasts leaving behind the deposited ECM. The substrates were thoroughly washed with phosphate buffered saline (PBS) to avoid the deleterious effects of the alkaline ammonia solution.

2.2 Preparation of samples derived from acellular substrates for proteomic analysis

Post acellularization as described above, the exposed extracellular protein matrix was scrapped off the tissue culture plate for processing. Given that different methodologies developed for protein processing and analysis can lead to different results, we decided to employ two independent methodologies as part of our proteomic analysis on the ECM substrates and pool together the data obtained. However, for the purposes of our studies, we only focused on ECM-proteins that were common in all three substrates that were

analyzed. The first method involved processing of the protein pellets and analysis based on previously published protocols [211, 212]. Proteins were denatured with 8M urea, reduced with DTT, alkylated with iodoacetamide and then digested overnight with trypsin in ammonium bicarbonate buffer. Resulting tryptic peptides were desalted on C8 cartridges (Michrom BioResources) and subjected to 2D Nano LC/MS/MS analyses on a Dionex nano LC system. For the first dimension separation we used 300 μm ID SCX column (PolyLC Polysulfoethyl A 150X.3mm, 5 μm , 200 A) using a 15 ammonium formate (in-house made, 0.8M solution) step gradient (0-100%, pH3.6-6.5) at flow rate 5 $\mu\text{l}/\text{min}$. Peptides eluted from SCX column are trapped on C4 precolumn (Dionex PepMap300, 5 μm , 300A, 300 μm ID X 5 mm), desalted (0.1% formic acid, 2% ACN) and then separated on 75 μm ID C18 column (Dionex NAN75-15-03-C18 PepMap100 stationary phase, 3 μm) using acetonitrile gradient at flow rate 200 nl/min and electrosprayed to LCQDeca XP Plus ion trap mass spectrometer. The mass spectrometer was operated in data-dependent mode. Survey full scan MS spectra were acquired from m/z 350 to 2000 and the four most abundant ions in were selected and fragmented to produce tandem mass spectra. The target ions already selected twice for MS/MS were dynamically excluded for 3 min. A normalized collision energy of 35% was used for peptide dissociation. The MS/MS spectra were recorded in the profile mode. The MS/MS data were analyzed using the SEQUEST search algorithm (Bioworks 3.2, Thermo) program against NCBI human and mouse protein database and its reversed complements, with a 1% false-positive rate used to obtain the peptide IDs. Spectra were searched allowing maximum mass deviation of 3 amu and 2 missed cleavage sites and only peptides showing fully tryptic termini were considered.

As part of the second independent method employed for proteomic analyses, the protein pellets were dissolved using 8M Urea in 10mM Tris Buffer at pH 8.0 followed by separation in 10% SDS-PAGE gel to filter out cellular debris. The gel section with the separated proteins was then divided into four pieces, for a crude reduction of sample complexity for use in mass spectrometric analysis. The gel pieces were transferred to a siliconized tube, washed and destained in 200 μ L 50% methanol overnight. The pieces were subsequently dehydrated in acetonitrile, rehydrated in 30 μ L of 10 mM dithiolthreitol (DTT) in 0.1 M ammonium bicarbonate and reduced at room temperature for 0.5 h. After removal of the DTT solution, samples were alkylated in 30 μ L 50 mM iodoacetamide in 0.1 M ammonium bicarbonate at room temperature for 30 min. This was followed by dehydration of the gel pieces in 100 μ L acetonitrile, and rehydration in 100 μ L 0.1 M ammonium bicarbonate, followed by complete drying by vacuum centrifugation. Further rehydration in 50 mM ammonium bicarbonate (20 ng/ μ L trypsin) on ice for 10 min was followed by removal of excess trypsin solution and addition of 20 μ L 50 mM ammonium bicarbonate solution. The sample was digested overnight at 37 °C and the peptides formed extracted from the polyacrylamide in two 30 μ L aliquots of 50% acetonitrile/5% formic acid. These extracts were combined and evaporated to 15 μ L for MS analysis.

2.3 Proteomic analysis

The Liquid Chromatography-Mass spectrometry (LC-MS) system consisted of a Thermo Electron Deca XP Plus mass spectrometer system with a nanospray ion source interfaced to a self-packed 8 cm x 75 μ m ID Phenomenex Jupiter (Torrance, CA) 10 μ m C18 reversed-phase capillary column. 5 μ L of the extract was injected onto the column using

pressure and the peptides eluted from the column by an acetonitrile/0.1 M acetic acid gradient at a flow rate of 0.4 μ L/min over 80 minutes. The nanospray ion source was operated at 2.8 kV. The digest was analyzed using the double play capability of the instrument acquiring full scan mass spectra to determine peptide molecular weights and product ion spectra to determine amino acid sequence in sequential scans. The data were analyzed by database searching using the Sequest search algorithm (Bioworks 3.2, Thermo) against IPI human and IPI mouse database (European Bioinformatics Institute).

2.4 Immunocytochemical validation of extracellular matrix proteins

Fibroblasts and acellular substrates derived from the fibroblasts were fixed using 4% paraformaldehyde in PBS. Fixed cells and substrates were incubated with primary antibodies: collagen I, collagen III, fibronectin and heparan sulfate proteoglycan (Abcam, Cambridge, MA). Goat anti-mouse IgG conjugated to Alexa 488 (Molecular Probes, Eugene, OR) was used as the secondary antibody for the collagens and fibronectin. Goat anti rat IgG conjugated to Alexa 594 (Molecular Probes, Eugene, OR) was used for HSPG. Fluorescent images were acquired using CoolSnap EZ camera (Photometrics, Tucson, AZ) mounted on a Nikon Eclipse TE 2000-S inverted microscope (Nikon, Melville, NY) with attached image analysis software. All image settings were controlled for uniform acquisition between samples. Specifically, uniform exposure time was maintained for images acquired from experimental samples as well as negative controls for background subtraction. All primary antibodies were obtained from Santa Cruz (Santa Cruz, CA), unless otherwise stated.

2.5 Formulation of different ECM-protein based substrates for hPSC propagation.

Commercially available proteins corresponding to basement membrane of Engelbreth-Holm-Swarm mouse sarcoma derived heparan sulfate proteoglycan (HSPG) and laminin at concentrations of $10\text{ng}/\text{cm}^2$ and $1\text{mg}/\text{cm}^2$ respectively; human plasma derived Fibronectin (Fn) (Millipore, Billerica, MA) and Vitronectin (Vn) at concentrations of $3\mu\text{g}/\text{cm}^2$ and $10\text{ng}/\text{cm}^2$ respectively were used to formulate the combinatorial ECM protein based substrates (EPBS) for evaluation in hPSC propagation. Different concentrations of the ECM proteins were initially tested to determine the appropriate combinations for use in the testing for hPSC maintenance. Tissue culture plates were treated with the different formulations and allowed to incubate for one hour at room temperature prior to seeding with hPSCs. The different combinations of the four ECM proteins tested were HSPG-Fn (HF), HSPG-Ln (HL), HSPG-Vn (HV), HSPG-Fn-Ln (HFL), HSPG-Fn-Vn (HFV), HSPG-Ln-Vn (HLV) and HSPG-Fn-Ln-Vn (HFLV). The purpose of this combinatorial study was to examine the specific effects of HSPG in promoting adhesion and maintenance of pluripotent capabilities of two different hPSCs. All proteins were acquired from Sigma unless otherwise specified.

2.6 Evaluation of pluripotent capabilities of hPSCs on ECM-based substrates

Human pluripotent stem cells (karyotypically normal WA09s and karyotypically abnormal BG01v) were routinely maintained in direct co-culture with MEFs in DMEM/F12 supplemented with 20% knockout serum replacement, 0.1mM β -mercaptoethanol, 1% non-essential amino acids, $100\text{U}/\text{ml}$ penicillin, $100\text{mg}/\text{ml}$ streptomycin and $4\text{ ng}/\text{ml}$ basic fibroblast growth factor. For the purposes of testing, WA09 and BG01v hPSCs were transferred from MEFs onto 35mm dishes coated with different EPBS in growth medium

supplemented with 100ng/ml of bFGF, and subcultured by treatment with collagenase for upto 5 passages.

Routine staining for alkaline phosphatase was performed as per manufacturer instructions (Vector Labs) and as published previously [213]. Immunostaining of hPSCs on the EPBS and in suspension for cytopsin applications was also based on previously published protocols [214]. Fixed cells were incubated with primary antibodies: OCT4 (Santacruz Biotechnology, Santa cruz, CA), SSEA3 and SSEA-4 (Millipore, Temecula, CA). Goat anti-mouse IgG conjugated to Alexa 488 for OCT4 and SSEA4 and goat anti-mouse IgM conjugated to Alexa flour 594 for SSEA3 (Molecular Probes, Eugene, OR) were used as secondary antibodies. Fluorescent images were acquired using a Nikon Eclipse TE 2000-S inverted microscope (Nikon) with attached image analysis software. All image settings were controlled for uniform acquisition between samples. Specifically, uniform exposure time was maintained for images acquired from experimental samples as well as negative controls for background subtraction.

The cytopsin apparatus was assembled and used based on previously published protocols [215]. A plastic slide, in this case the plastic base of a 4 well Permanox® chamber slide was used, holes were punched to facilitate the formation of a monolayer of cells onto a cleaned glass slide. 3MM filter paper (Whatman Int. Ltd., Maidstone, England) with holes corresponding to those on the plastic slide with 0.1-10 µl micropipette cut in half was wedged between the slides. A second uncut micropipette tip is inserted into the first and a small volume of the cell suspension was deposited into the apparatus followed by centrifugation at 1000rpm for the generation of the monolayer. Fluorescent images were

acquired using a Nikon Eclipse TE 2000-S inverted microscope (Nikon) with attached image analysis software. All image settings were controlled for uniform acquisition between samples as described earlier. For a quantitative analysis of SSEA3/SSEA4 expression on two different EPBS, the number of positively stained cells within three independent regions of interest was counted and the mean values reported. (Appendix D)

In vitro differentiation potential of hPSCs propagated on EPBS was assessed by the generation of embryoid bodies (EBs). To generate embryoid bodies (EBs), hPSC colonies were divided into clumps of about 100-300 cells and resuspended in ultra-low attachment conditions, in growth medium devoid of bFGF, with media changes every 3-4 days for 15 days.

mRNA for gene expression analyses was isolated from hPSCs propagated under different conditions and from EBs after 15 days in suspension using Trizol (Invitrogen, Carlsbad, CA) and quantified using BioMate3 UV-VIS Spectrophotometer (Thermo Scientific, Waltham, MA). cDNA was synthesized from 1 μ g of RNA using cDNA reverse transcription kit (Applied Biosystems, Foster City, CA). Expression of pluripotent genes Octamer Binding Transcription Factor-4 (POU5F1), SRY (Sex Determining Region-Y) Box-2 (SOX2), NANOG, and germ layer specific genes, Neurogenic differentiation 1 (NEUROD1), Insulin-like Growth Factor 2 (IGF2) and α -Fetoprotein (AFP) (Table 3) was analyzed using quantitative real time RT-PCR. (qPCR). qPCR was performed in an ABI HT7900 system and the data was acquired using Sequence Detection System software (SDS v2.2.1, Applied Biosystems). Gene expression data (three replicates) were acquired and SDS software was used to estimate relative fold change values using Δ CT quantitation

methods. Endogenous 18S ribosomal RNA was used for normalization in all the samples.

Relative gene expression for hPSCs propagated on EPBS was assessed against hPSCs propagated on MEFs. Relative gene expression of differentiated EBs obtained from different conditions was assessed against undifferentiated hPSCs propagated under the original condition. Expression Index (EI) was used to determine the relative differentiation state of cells, and was based on the average CT values from triplicate measurements. Expression Index (EI) was used to determine the relative differentiation state of cells [200, 201] and was based on the average CT values from triplicate measurements. An expression ratio of two or more genes was determined using a mathematical model based on the geometric average of assessed genes, previously described in detail,[201] given by the following equation:

$$EI = K_{RS} \frac{\sqrt[m]{(1 + E_{gene1m})^{Ct_{gene1m}} \cdot (1 + E_{gene2m})^{Ct_{gene2m}} \dots (1 + E_{genem})^{Ct_{genem}}}}{\sqrt[n]{(1 + E_{gene1n})^{Ct_{gene1n}} \cdot (1 + E_{gene2n})^{Ct_{gene2n}} \dots (1 + E_{genen})^{Ct_{genen}}}}$$

E is the PCR efficiency calculated from dilution series of purified PCR products, CT is the threshold cycle, and m and n are the numbers of genes that are up and down regulated upon differentiation respectively. K_{RS} is the relative sensitivity constant and was not determined as it does not affect relative comparisons between samples.

Results

Proteomic analysis of acellular substrates.

Proteomic analysis of acellular MEFs, HFFs and HDFs were conducted given the ability of these acellular substrates to maintain multiple hPSCs in their undifferentiated state [207]. In our previous study, hPSCs propagated on acellular substrates were indistinguishable by multiple criteria, including colony morphology, expression of pluripotency protein markers, tri-lineage in-vitro differentiation potential and gene expression patterns, from hPSCs cultured directly on a fibroblast feeder layer. It was thus postulated that proteomic analyses of ECM components of the feeders would provide insights into proteins involved in adhesion and activation of key signaling pathways. ECM proteins were acquired by decellularizing post-confluent feeder cells, followed by digestion with urea, and analysis using LC – MS/MS.

A total of 519, 426 and 514 proteins were identified in acellular MEF, HFFs and HDFs respectively, with only peptides identified as possessing fully tryptic termini with cross-correlation scores greater than 1.8 for singly charged peptides, 2.25 for doubly charged peptides, 3.0 for triply charged peptides and 3.75 for quadruple charged and higher used for peptide identification. The proteins were GO annotated into broad classifications of cellular compartment (CC), biological function (BP) and molecular function (MF) using PIPE (Protein Information and Property Explorer at <http://pipe.systemsbio.net> [216]) Further annotation of the identified proteins to increasing levels of specificity was performed using PIPE (Figure 14).

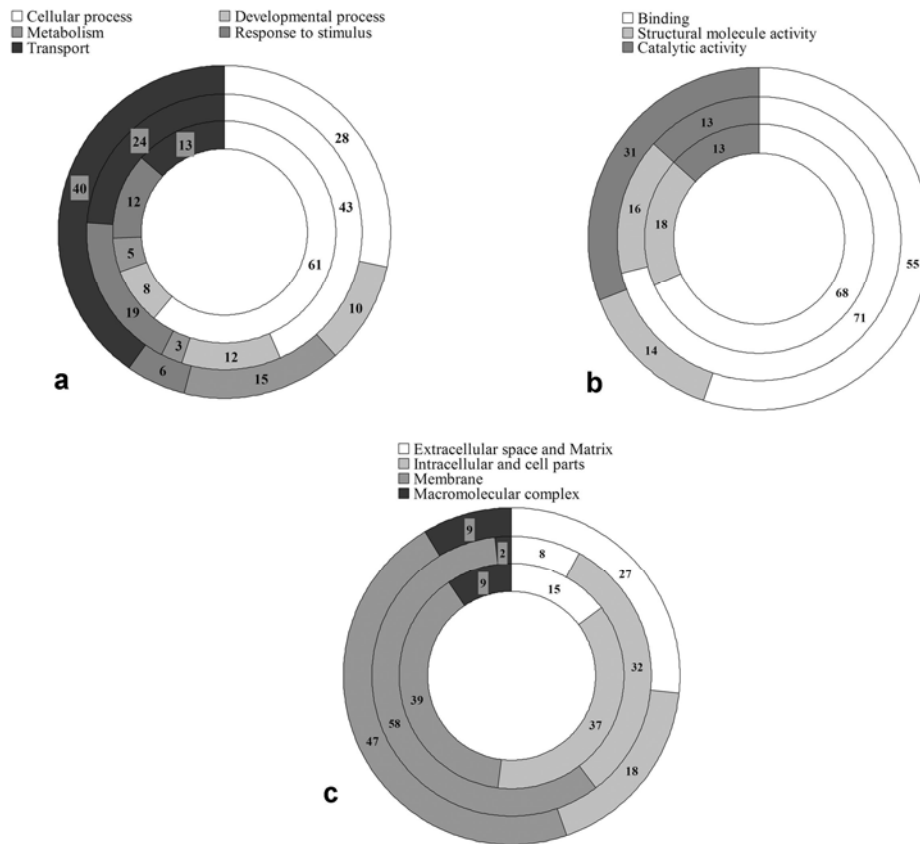


Figure 14:
 Functional biological and cellular profiles of the proteins identified in the three acellular substrates of MEF, HFFs and HDFs. The circles in the figure depict the molecular function (a), biological function (b) and cellular compartment (c) in acellular HDF (inner circle), acellular HFF (middle circle) and acellular MEFs (outer circle).

Our analysis primarily focused on membrane and extracellular matrix proteins in order to identify key proteins and signaling pathways involved in the maintenance of hPSC self-renewal. We observed that 75, 16 and 25 of the cellular compartment annotated proteins originated from the extracellular matrix, while 132, 114, 66 proteins were annotated as membrane proteins in MEFs, HFFs and HDFs respectively. The remaining proteins identified and annotated were non-membranous, originating from intracellular organelles. In each substrate analyzed, there were approximately 100 proteins that did not correspond to a GO annotation and it is expected that in-depth annotation will reveal their biological relevance within the cell.

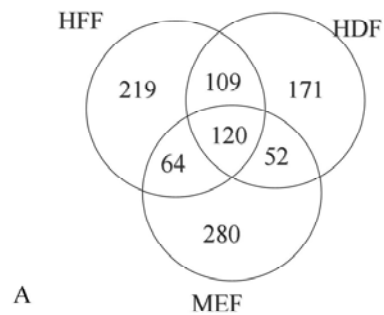
In total, acellular MEFs, HFFs and HDFs had 112 proteins in common, among which 20, 8 and 8 were extracellular matrix proteins and 30, 24 and 24 were membrane proteins respectively. Our analysis seems to indicate that the mouse substrate is richer in extracellular and membranous proteins than the human substrates analyzed. Proteins common to all three substrates constituted 11.8%, those that were common to two substrates ranged between 5.1 to 10.7%, where proteins common between HDF-HFF constituted 5.1%, between HDF-MEF 6.3% and between HFF-MEF 10.7% of the total proteins identified Figure 15 .

The three broad categories were further classified into a) cellular processes, developmental processes, metabolism, stimulus response and transport in BP; b) binding, structural molecular activity and catalytic activity in MF; and c) extracellular space and matrix, intracellular and cell parts, membrane and macromolecular complex in CC. Comparisons within each functional group clearly indicate the similarities between the

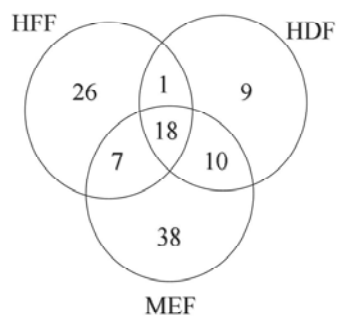
human substrates (Figure 14, inner circles). This study was primarily conducted to identify extracellular matrix proteins involved in self-renewal and maintenance of pluripotency within both mouse and human substrates. Table 5 lists several proteins that constituted the extracellular matrix and plasma membrane of the feeder layers. Based on the comprehensive list of proteins, a summary of the ECM proteins as well as growth/differentiation factors that might actively contribute to long term pluripotentiality of hPSCs was also generated (Table 6).

Immunocytochemical validation of ECM components

Since mass spectrometry is at best a semi-quantitative analytical method, we have attempted to corroborate the results obtained using immunostaining for some of the major ECM proteins identified. Antibodies were used against major ECM proteins identified in all three substrates; Collagen I, Collagen III, Fibronectin and HSPG. Results confirmed the presence of these proteins using immunofluorescence within the ECM of the human fibroblast feeders and their acellular substrates (Figure 16 i,ii). Our results also indicate that minimal residual nuclear material was observed based on the absence of 4',6-diamidino-2-phenylindole (DAPI) stain within the acellular substrates (Figure 16 iii,iv). Similar results were observed in MEF and MEF derived acellular substrates (Figure 17).



A



B

Figure 15:

Distribution of 1015 proteins identified in the three acellular substrates, acellular HDFs, acellular HFFs and acellular MEFs. (A). Distribution of 109 *extracellular matrix* proteins found in the acellular substrates of HDFs, HFFs, MEFs. (B).

Table 5:

List of proteins in the three acellular substrates pertaining to cellular compartment identified using LC-MS/MS

Protein identified and biological classification (In all three substrates)			
Extracellular matrix, space and plasma membrane	Collagen, type I, alpha 1 Collagen, type I, alpha 2 Collagen, VI, alpha 3 Collagen, XII, alpha 1 Fibronectin 1 Gelsolin Integrin beta 1 (fibronectin receptor beta) Keratin 1 Keratin 2 Keratin 8 Keratin 10 Lectin, galactose binding, soluble 3 Thrombospondin 1 Heparan sulfate proteoglycan/Perlacan Serpine peptidase inhibitor Scavenger receptor class B, member 2	Intracellular and cytoplasm	Actin, alpha 2, Actin, beta, Actin, gamma 1 Annexin A1 Annexin A2 Annexin A5 Annexin A6 Calreticulin Calumenin Calnexin Caveolin 1 Cofilin 1 Filamin A Filamin C Glyceraldehyde-3-phosphate dehydrogenase Lamin A/C Septin 2 Plectin 1 Transgelin Vimentin Elastin microfibril interfacier 1
Heat Shock proteins	Heat shock 70kDa protein 1-like Heat shock 70kDa protein 2 Heat shock 70kDa protein 5 Heat shock 70kDa protein 8 Heat shock protein 90kDa alpha Heat shock 60kDa protein 1 Heat shock protein 90, beta		
Protein identified and biological classification (In aHFF and aHDF)			
Extracellular matrix, space and plasma membrane	Activated leukocyte cell adhesion molecule CD 44 molecule CD59 molecule CD99 molecule CD26 Tenascin C (hexabrachion)	Intracellular and cytoplasm	Actin, gamma 2 Actinin, alpha 1 Actinin, alpha 4 Eukaryotic translation elongation factor 1 gamma Filamin B, beta Lactate dehydrogenase A Protein kinase C substrate Keratin 9
Heat Shock proteins	Heat shock 70kDa protein 7 Heat shock 70kDa protein 9 Heat shock 27kDa protein 1		

Table 6:

Proteins of interest that might contribute to the maintenance of self renewal in hPSCs

Collagens	Required for the structural integrity of the matrix. Previously used in ES cultures both as an additive to the growth medium and a substrate. Found in secreted medium as well as the deposited ECM layer	[208-210, 217]
TGFb family	Related signaling proteins latent TGFb binding protein (LTBP) 2 and 3 were found to be present in the substrates and have been implicated in the critical role of controlling and targeting TGFb to sites of storage or activation. The TGFb superfamily include: Bone morphogenetic proteins (BMPs), Growth and differentiation factors (GDFs), Anti-müllerian hormone (AMH), Activin, Nodal and TGFβ's, with several of these implicated in the maintenance of hPSC self-renewal	[194, 205, 206, 218-221]
Thrombospondin	Thrombospondin 1 is an adhesive glycoprotein, mediates cell-cell and cell-matrix interactions. Multiple domains bind to a number of ECM proteins including fibronectin and collagens. Associated with various biological functions such as cell attachment, cell aggregation and angiogenesis and involved in the activation of TGFβ. Increased expression of thrombospondin1 has been observed in response to platelet derived growth factor, FGF2 and TGFβ	[208, 222, 223]
Biglycan	Biglycan and decorin are small proteoglycans known to interact with collagens and growth factors as TGFβ. Interactions of these proteoglycans with growth factors are known to modulate the function of growth factors.	[224-228]
Periostin	Osteoblast specific factor was found in proteomic analyses of both feeder layer conditioned medium and deposited ECM. Periostin is known to bind to heparin and induces cell attachment and spreading	[208, 209, 229, 230]
Follistatin	Follistatin is known to bind and regulate the activity of TGFb family members	[231, 232]

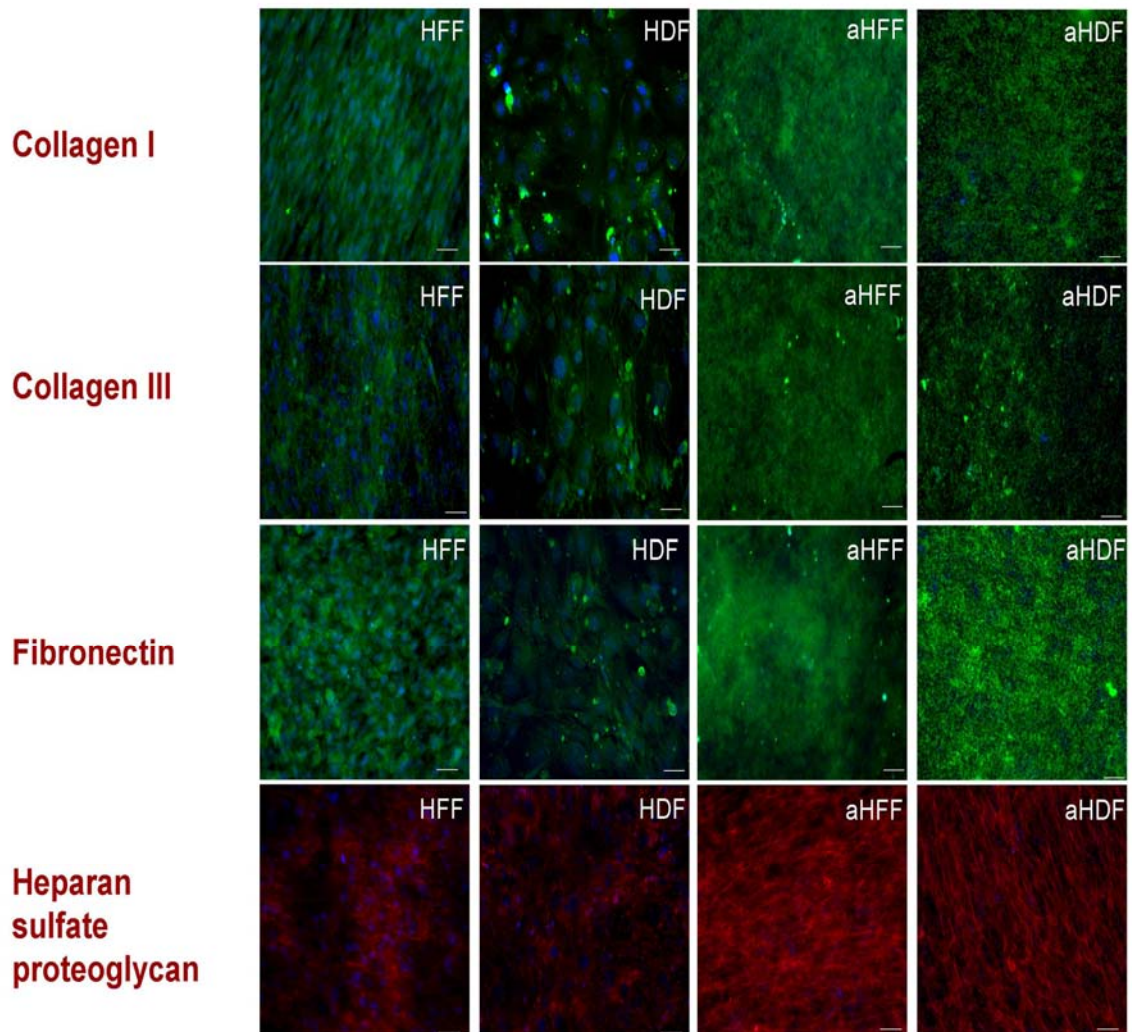


Figure 16:
 Immunocytochemical validation of the presence of major constituents of the extracellular matrix; Collagen I (A), Collagen III (B), Fibronectin (C), and heparan sulfate proteoglycan (D) on HFFs (i), acellular HFFs (ii), HDFs (iii) and acellular HDFs (iv).

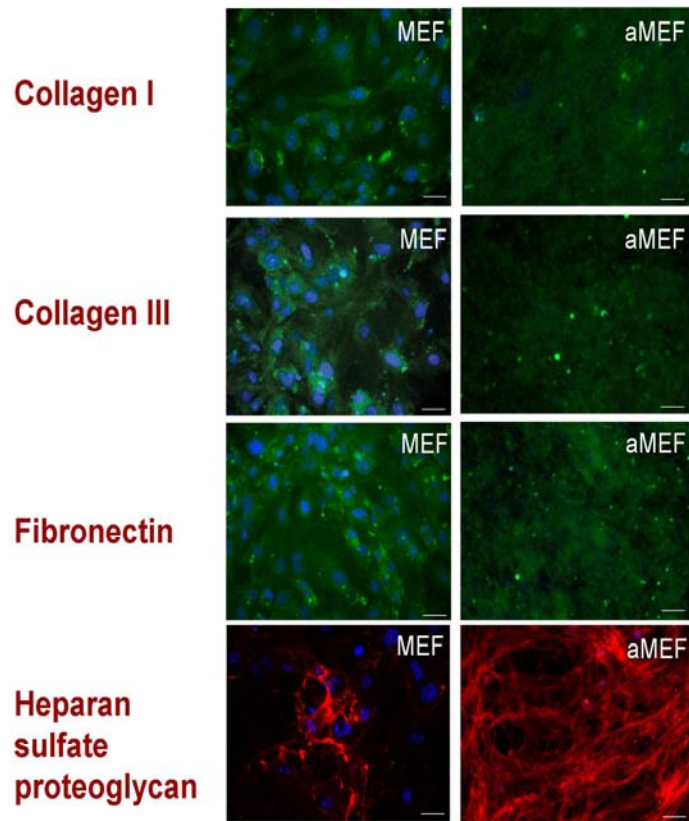


Figure 17:
Immunocytochemical validation of the presence of major constituents of the extracellular matrix; Collagen I (A), Collagen IV (B), Fibronectin (C), and heparan sulfate proteoglycan (D), on MEFs (i), acellular MEFs (ii).

3.3. hPSC adhesion and propagation on ECM-protein based substrates.

Furthermore, we attempted to generate a combinatorial EBPS of commercially available proteins that mimic naturally deposited ECM, and test their ability to maintain pluripotency in hPSCs for extended periods. In our study, given that HSPG and Fn was identified in all three substrates, we used these proteins in combination with other previously tested ECM proteins; Ln [233] and Vn[234]. Different combinations of HSPG, Fn, Ln and Vn was investigated with the primary focus on HSPG. Karyotypically normal WA09 and aneuploid BG01v hPSCs were cultured on MEFs prior to transfer onto the EPBS substrates. The hPSCs propagated on specific EPBS maintained a high nuclear to cytoplasmic ratio, representative of actively dividing cells (Figure 18). Positive expression of alkaline phosphatase (AP) at each passage is indicative of the ability of the EPBS to maintain hPSCs for extended periods (Figure 18). Of all the different combinations tested, HF showed the maximum colony attachment and proliferation based on quantitative analysis of AP expression (Figure 19). In the combinations that did not include Fn, (HL, HV, HLV), cell attachment progressively decreased over passaging time. Our results suggest that the addition of Ln and Vn to the HF mixture (i.e. HFL, HFV and HFLV) presented suitable substrates for propagation however did not contribute to the enhancement of the attachment and proliferative properties of the HF mixture. The number of AP positive colonies in the HFLV substrate was similar to that on HF, hence we can conclude that the use of HF is sufficient for a suitable and a cost-effective ECM substrate for hPSC propagation. Individual testing of HSPG and Fn for their attachment and proliferation capabilities demonstrated that HSPG alone did not support attachment

whereas although Fn permitted hPSC adhesion, in the absence of any other ECM protein greater differentiation was observed within the colonies (Figure 20). Our preliminary studies involving hPSC propagation on EPBS was conducted in growth medium containing 4ng/ml of bFGF. However, the hPSC colonies did not express the standard pluripotent characteristic of in vitro differentiation potential. In order to ensure the maintenance of pluripotent characteristics, higher concentrations of bFGF were used in our studies.

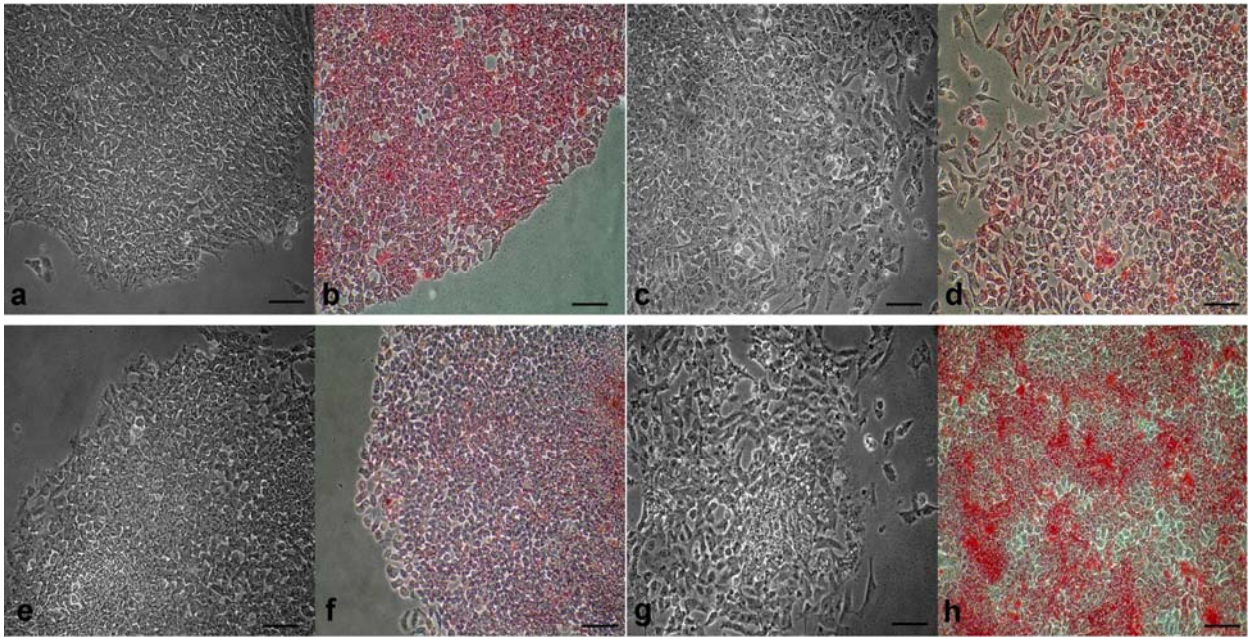


Figure 18:

Phase contrast images of human pluripotent stem cells, WA09 (a,e) and BG01v (c,g) and positive expression of alkaline phosphatase in WA09 (b,f) and BG01v (d,h) grown on ECM-based protein substrates Heparan sulfate proteoglycan – Fibronectin (HF) (a-d) and Heparan sulfate proteoglycan-Fibronectin-Laminin-Vitronectin, (HFLV) (e-h).

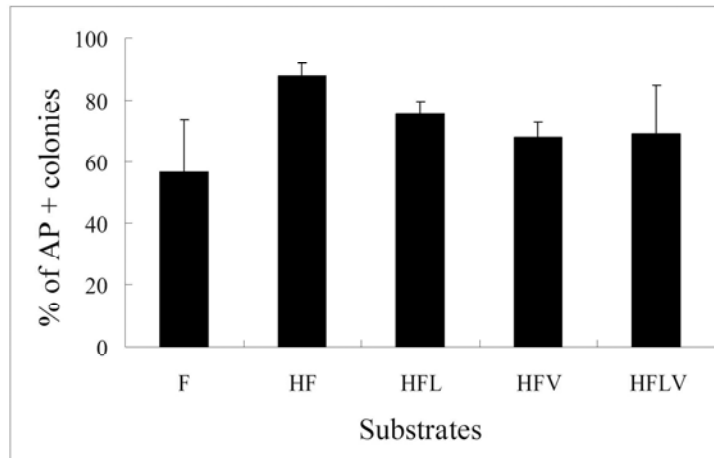


Figure 19:
Percentage of Alkaline Phosphatase positive colonies within different combinatorial-ECM-protein based substrates namely Heparan sulfate proteoglycan-Fibronectin (HF), Heparan sulfate proteoglycan-Fibronectin-Laminin (HFL), Heparan sulfate proteoglycan-Fibronectin-Vitronectin (HFV) and Heparan sulfate proteoglycan-Fibronectin-Laminin – Vitronectin (HFLV)

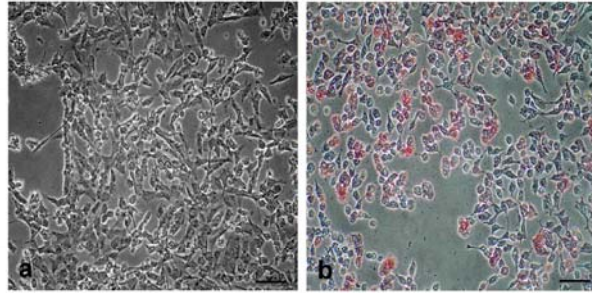


Figure 20:

Progressive differentiation of hPSCs propagated on fibronectin substrates. The absence of alkaline phosphatase staining in sections of the colony is indicative of loss of stemness.

Characterization of hPSCs on ECM-protein based substrates.

Further characterization of the hPSCs cultured on the different EPBS was based on immunocytochemical analysis for detection of pluripotent markers SSEA4 and OCT4. Results demonstrate that WA09 cells maintained tight colony boundaries while BG01v cells were observed to have taken a more fibroblastic spindle shape (Figure 21 a,c,e,g). Though BG01v cells do not appear morphologically similar to normal hPSCs, characterization using immunocytochemistry and gene expression using qPCR indicate no loss of stemness. Using the cytopsin apparatus, we also quantified the percentage of hPSCs that were positive for cell surface markers SSEA3 and SSEA4 expression. Results showed comparable expression of these markers in hPSCs grown on both HF and HFLV substrates. WA09 cells cultured on HF showed that 91% and 89.7% of the cell population stained for SSEA3 and SSEA4, whereas 81.4% and 80.4% were positively stained on HFLV substrates (Figure 22 a). Similarly, in BG01v hPSCs, 98.2 and 93% were positive for SSEA3 and SSEA4 on HF substrates and 94.9 and 89.6% for SSEA3 and SSEA4 on HFLV substrates (Figure 22 b).

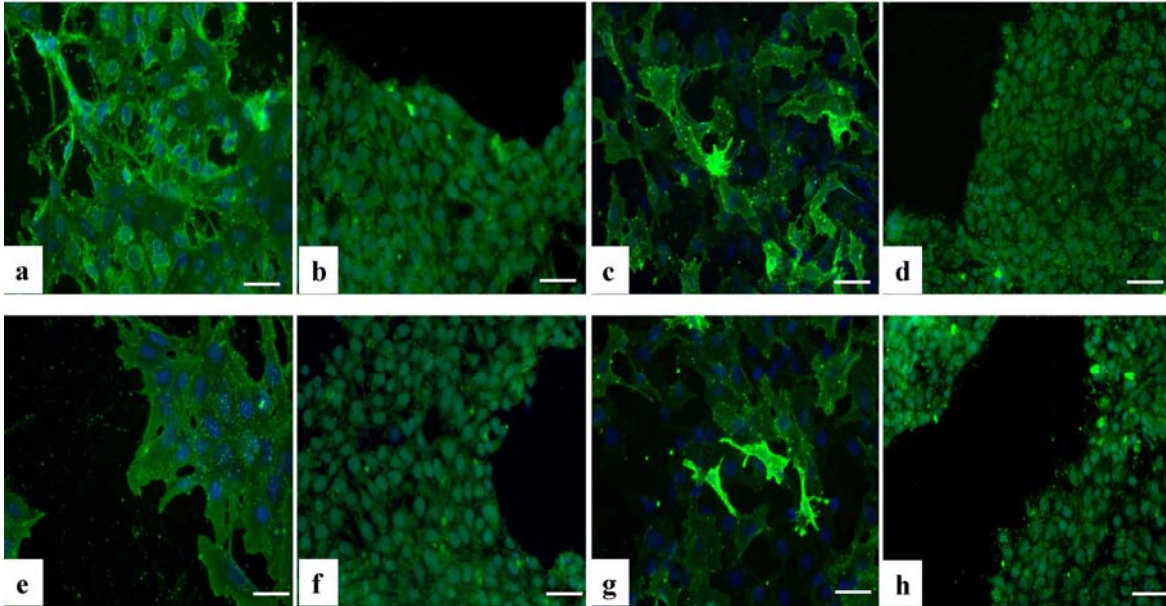


Figure 21:

Immunofluorescence staining of hPSCs for pluripotency markers stage specific embryonic antigen 4 (SSEA4) in WA09 (a,e) and BG01v (c,g) and transcription factor OCT4 WA09 (b,f) and BG01v (d,h) grown on ECM-protein based substrates Heparan sulfate proteoglycan-Fibronectin (HF) (a-d) and Heparan sulfate proteoglycan-Fibronectin-Laminin –Vitronectin (HFLV) (e-h). Scale bar = 50 μ m.

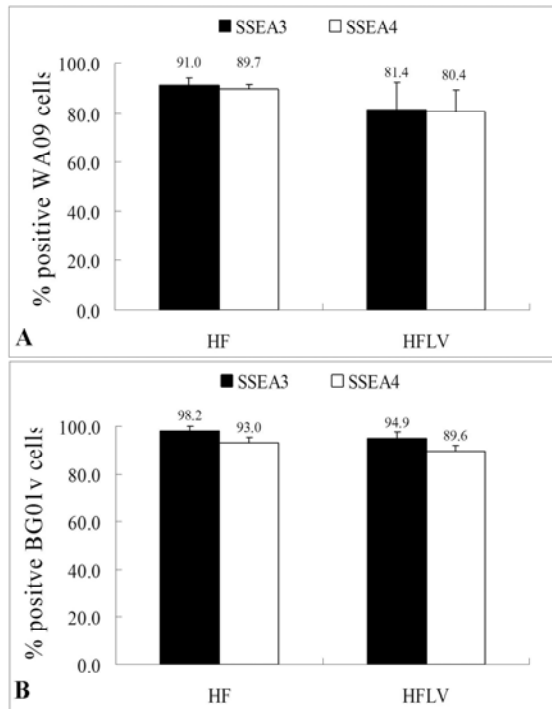


Figure 22:
Quantitative expression of pluripotency markers SSEA3 and SSEA4 on ECM-protein based substrates Heparan sulfate proteoglycan-Fibronectin (HF) and Heparan sulfate proteoglycan-Fibronectin-Laminin-Vitronectin (HFLV) in WA09 (A) and BG01v (B) hPSCs.

Differential expression of pluripotency markers (POU5F1, NANOG and SOX2) was presented as CT values normalized against the 18S rRNA housekeeping gene for each experimental condition. For the purposes of the comparisons, the Δ CT values of each marker within the different experimental sample are presented against that of MEFs. This eliminates the requirement for normalization with the calibrator. Comparable Δ CT values of OCT4 and SOX2 genes were seen across different culture conditions and are indicative of the maintenance of the undifferentiated state of hPSCs on protein substrates; HF and HFLV (Figure 23 a). Statistical analyses using Student's t-test indicated no significant difference ($p > 0.05$) in the different comparisons for the pluripotency markers tested between hPSCs propagated on the EPBS and those propagated on MEFs. However in the case of NANOG, there was reduced expression on both the HF and HFLV substrates when compared to those propagated on MEFs (Figure 23 a). Functional pluripotency of the hPSCs via the formation of embryoid bodies was assessed by *in vitro* differentiation (ectoderm, endoderm and mesoderm). Differential expression of germ layer specific markers NEUROD1 (ectoderm), IGF2 (mesoderm) and AFP (endoderm) were presented as CT values normalized against the 18S rRNA housekeeping gene for each sample and further compared to undifferentiated cells cultured in the same experimental conditions. Statistical analyses indicated that the EBs generated from the WA09 on the different ECM protein substrates demonstrated significantly greater expression ($p < 0.01$) of all three germ layer specific markers analyzed (Figure 23 b) compared to the undifferentiated cells. Here, it is important to note that Δ CT values (normalized against 18S) should be interpreted counter-intuitively; where a lower value indicated higher expression and vice versa.

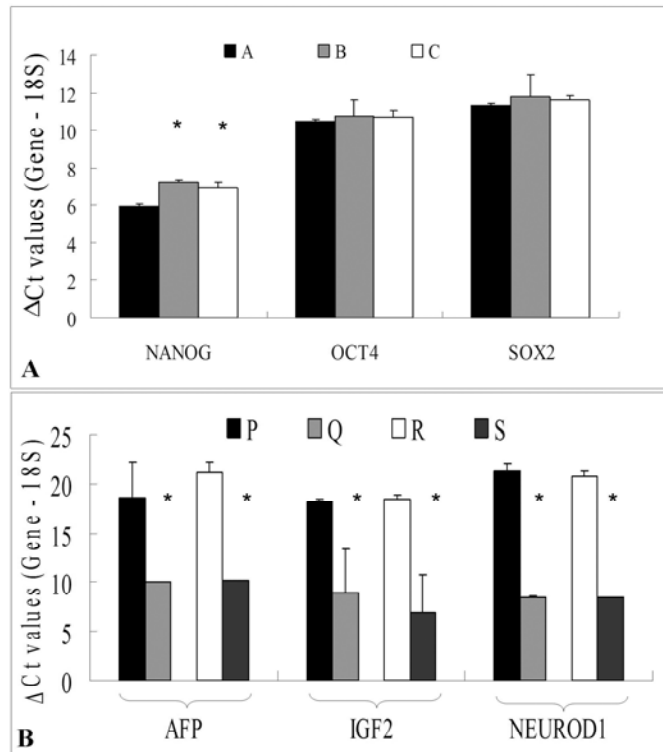


Figure 23:

Normalized gene expression of *undifferentiated markers* in WA09 on MEFS (A) WA09 on Heparan sulfate proteoglycan-Fibronectin (HF) (B) and WA09 on Heparan sulfate proteoglycan-Fibronectin-Laminin –Vitronectin (HFLV) (C). Significant difference ($p < 0.05$) between the group is shown by (*). (b) Normalized gene expression of *germ layer specific markers* in WA09 on Heparan sulfate proteoglycan-Fibronectin (P), EB generated from WA09 on Heparan sulfate proteoglycan-Fibronectin (Q), WA09 on Heparan sulfate proteoglycan-Fibronectin-Laminin –Vitronectin and EB generated from WA09 on Heparan sulfate proteoglycan-Fibronectin-Laminin –Vitronectin. Significant differential gene expression ($p < 0.01$) in all three lineage specific markers was observed

Further, the differentiation state of the hPSCs was quantified using the ‘expression index’ as a metric to compare the undifferentiated hPSCs against the EBs generated from the hPSCs grown under the same condition as well as across different culture conditions. For the karyotypically normal WA09 hPSC, the expression index of the undifferentiated sample was 2859 on HF and 3411 on HFLV while the expression index of the 15-day old EBs derived from WA09 was found to be 0.03 and 0.02 on HF and HFLV respectively (Figure 24). Although the EI values for hPSCs on HFLV were higher when compared to those grown on HF substrates, there is no difference in the potential of HF substrates for hPSC maintenance compared to HFLV substrates, based on all other characterization studies. A summary of the different protein combinations tested and the response of hPSCs to the substrates is tabulated in Table 7

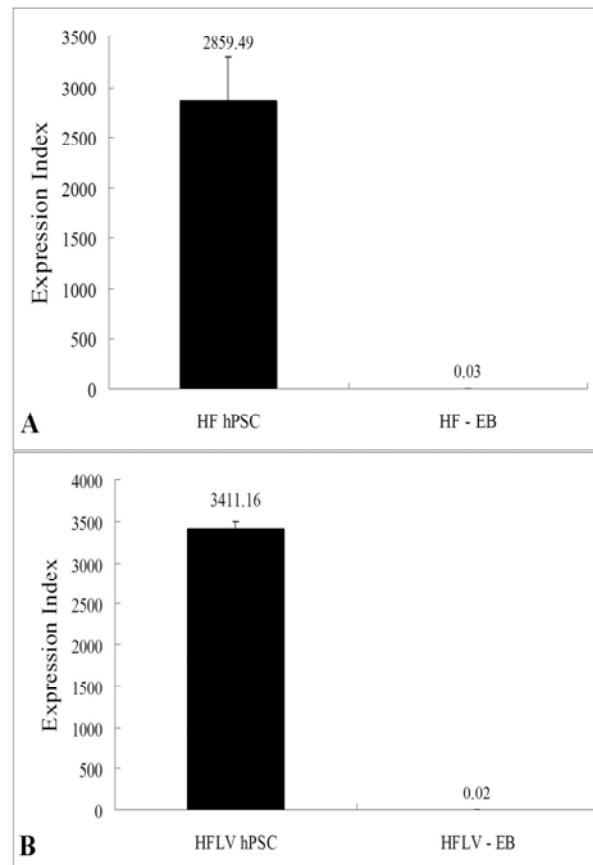


Figure 24: Differential expression index of a) WA09 hPSC and WA09 EBs derived from Heparan sulfate proteoglycan-Fibronectin (HF) substrates and b) WA09 hPSC and WA09 derived EBs from Heparan sulfate proteoglycan-Fibronectin-Laminin –Vitronectin (HFLV) based on analysis of six genes (POU5F1, NANOG, SOX2, AFP, IGF2 and NEUROD1).

Table 7:

A tabulated summary of the different ECM combination tested and hPSC response to these substrate with respect to adhesion, differentiation and pluripotency markers

Properties Substrates		Adhesion	Differentiation (AP expression)		Pluripotency marker expression			
					SSEA4	Oct4		
	WA09							
	BG01v							
H		-	-	N/A	N/A	N/A	N/A	N/A
F		+	+	+/-	+/-	+/-	+/-	+/-
HF		++	++	-	+	+	+	+
HFL		+	+	-	+	+	+	+
HFV		+	+	-	+	+	+	+
HLV		+/-	+/-	+/-	+/-	+/-	+/-	+/-
HFLV		++	++	-	+	+	+	+

Key: +/- decreased expression of the property over time; ++ increased expression

Discussion

Till date, there have been few reports that have focused on the identification and characterization of secreted factors from MEFs, HFFs, HDFs [208, 209] that contribute to hPSC self-renewal. Our study is the first to employ a proteomics approach to identify components of the ECM that maintain hPSC self-renewal. The substrates revealed a complex network of extracellular and intracellular proteins of varying biological functions. The presence of cytosolic and nuclear proteins in our results is indicative of the difficulties in isolating a pure ECM sample. In conditioned medium proteomic studies, the highest percentage of proteins identified comprised of ECM components [208, 209]. Of the proteins identified in the conditioned medium, heparan sulfate proteoglycan (HSPG), Biglycan, Periostin, Fibronectin and Collagens were concurrently found within the acellular substrates (Table 5). Since both acellular substrates and conditioned media can support hPSC self-renewal independently of each other and has the aforementioned proteins in common, we can speculate that core ECM proteins in the human fibroblasts are sufficient in promoting hPSC self-renewal. In our studies, HSPG was found to be present in all three substrates and a critical component of the ECM substrate that promoted hPSC self-renewal. HSPGs are present in the extracellular matrix and cell membranes ubiquitously and covalently attach to several core proteins[235]. Several growth factors, cytokines and physiological relevant molecules have been shown to bind to the sulfated regions of HS chains[236]. HS chains have also been shown to regulate various biological signaling pathways such as fibroblast growth factors (FGFs), Wnt and hedgehog (Hh) and

BMP[237], pathways that have been implicated in maintenance of hPSC self-renewal. FGF2 has been previously shown to be extremely important in maintaining pluripotency in hPSCs[192]. HS increases the affinity of FGF2 to its receptor [238-240] and allows for stabilization of FGF2 within the growth medium, which is subsequently responsible for maintenance of hPSC self-renewal [241]. Additionally, HSPG regulates the extrinsic signaling pathways of the β catenin/Wnt pathway required for the expression of NANOG, which is essential for the maintenance of pluripotency in mESCs[242], and a core component of the pluripotency transcription network in hESCs [243].

In our studies, fibronectin was found to be present in all three substrates and a critical component of the ECM substrate that promoted hPSC self-renewal. Fibronectin is a high molecular weight glycoprotein secreted and organised by fibroblast cells into an insoluble component of the extracellular matrix[244]. The ability of fibronectin to maintain undifferentiated hPSCs has been previously reported with supplementation using conditioned medium or high FGF2 concentrations in growth medium [20, 245]. The interaction between fibronectin and hPSC has been demonstrated to be through integrin α 5 β 1, a major receptor for fibronectin [246]. Several integrins subunits (α 5, α 6, α v, β 1 and β 2) were shown to be highly expressed in hPSCs indicating the active role of several ECM proteins in the cell-extracellular matrix interaction for attachment and propagation [20, 48, 234, 247, 248].

Other important adhesive proteins and signaling molecules were identified in our analysis are listed in Table 6 [194, 217-232]. In our studies, immunocytochemical analyses validated the presence of multiple ECM proteins in both the cellular as well as acellular

substrates and allows us to qualitatively conclude that the decellularization process causes minimal loss of ECM (Fn, Collagens and HSPG). From all the different EPBS combinations tested, our results suggest that the combinatorial use of HSPG and Fn is sufficient for the maintenance of hPSC self-renewal. Although previous studies have shown that Ln and Vn individually [233, 234], as well as in combination with HSPG and Fn in our studies have been shown to support self renewal, the use of HSPG-Fn as a substrate provides a cost-effective and sufficient alternative to the use of feeder layer or feeder conditioned medium. The property of Fn to elicit an adhesion response from most fibroblasts is attributed to integrin binding domains, however heparan binding domains on Fn is known to contribute to the adhesion of normal fibroblasts, in melanoma and neuroblastoma cells[249-251]. Integrins such as $\alpha 5\beta 1$ are the key mediators of integrin-ligand interaction in Fn through primary receptors as the RGD motif of repeat III₁₀[252]. Signaling through proteoglycans such as syndecan-4 in addition to integrin signaling is required for rearrangement of the actin cytoskeleton into bundled stress fibers and focal adhesion formation[253, 254]. Focal adhesions are signaling complexes that result in stable cell-matrix interactions and contributes not only to cell adhesion but to dynamic changes in gene expression, apoptosis regulation, and control of the cell cycle[255]. In addition to HSPG as a co-factor in FGF signaling, recent studies have shown that the addition of HS increases the binding affinity of FGF to its receptors by several fold [238, 241]. Several modeling studies describe the interaction as a dimer of FGF ligands bound to a dimer of FGF receptors stabilized by a cell surface-anchored HSPG[256, 257]. Thus, the presence of HSPG in the EPBS as well as endogenous cell surface HSPG that contribute to FGF2

sequestration and cell-matrix focal adhesion formations might be an important component of the substrate involved in hPSC self-renewal (Figure 25).

Conclusions

This study provides the first detailed characterization of acellular substrates that have demonstrated the propensity to maintain hPSC self-renewal for extended periods, followed by generation of EPBS based on the data obtained from proteomic analyses. In an attempt to design a substrate that mimics naturally occurring biological substrates, we have observed that HSPG plays an important role in the maintenance of hPSC self-renewal. In conjunction with Fn, HSPG yields a substrate that can maintain hPSCs in their undifferentiated state over multiple passages. Our results also showed that the presence of other ECM proteins in the EPBS did not contribute to any additional benefit to the HSPG-Fn combination. However any EBPS combination lacking Fn did not support hPSC adhesion and propagation without any supplementation of the growth medium. Our understanding is that the combinatorial effects of the interactions of HSPG with Fn to create a matrix on the tissue culture polystyrene (TCPS) surface, cell membrane bound HSPG with Fn that allow for focal adhesion contacts on the matrix as well as the ability of HSPG sequester growth factors such as FGF2 and TGF β which in turn activate various downstream self-renewal activators play a critical role in the ability of HSPG-Fn substrate to maintain undifferentiated hPSCs (Figure 25). Growth factors and other cytokines that are present in small quantities are not detected either due to the stringent search parameters or due to the MS instrument selecting only the most abundant ions for sequencing. It is

known that hPSC pluripotency relies heavily on exogenous supplementation of the culture medium with growth factors. Thus the identification of growth factors present in the acellular substrates and sequestered within the matrix is vital. Further analysis of the substrates that maintain hPSC pluripotency using techniques involving the quantification of proteins such as isotope-coded affinity tags (ICAT) or isobaric tag for relative and absolute quantitation (iTRAQ) would allow for better understanding of the dose dependent effects of proteins and growth factors. Furthermore, information on the relative abundance of proteins and their inhibitors would be of great significance in the development of substrates that synergistically promotes activation of adhesion and signaling pathways responsible for hPSC self-renewal.

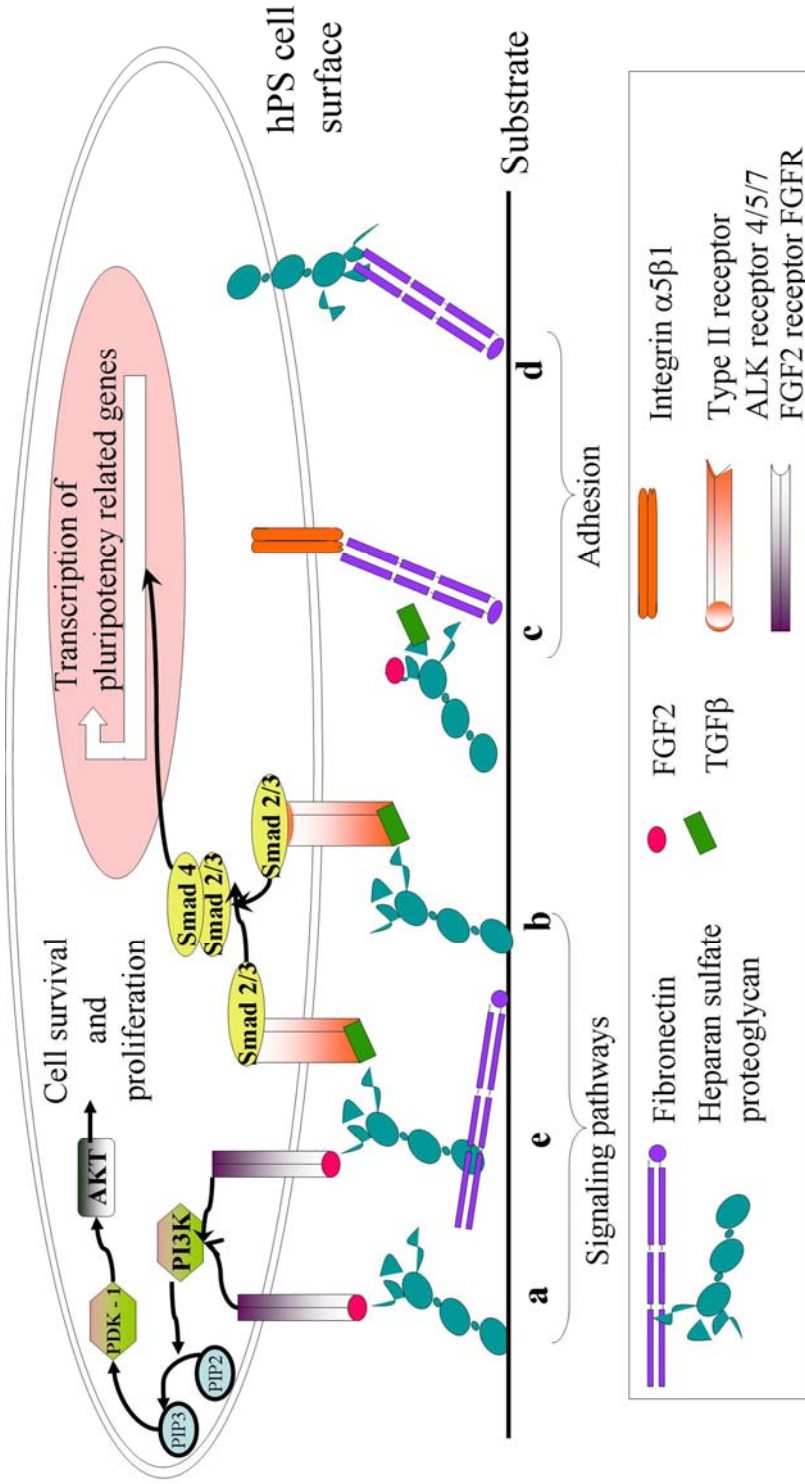


Figure 25: Schematic of the potential synergistic adhesion and signaling pathway interactions that occurs between the hPSC cell surface and the substrate that contributes to hPSC self-renewal. Signaling factors that are associated with self renewal depicted are A) Association of Fn with HSPG and further HSPG sequestered bFGF binding to cell membrane bound FGF receptor FGFR triggers the intracellular signaling cascades; such as PI3K cascade that activates pluripotency-associated transcription factors in the nucleus. B) HSPG sequestered TGFβ signaling via Activin Receptor-Like Kinase (ALK) 4,5 and 7 triggers the activation of Smad 2/3 signaling pathway that activates pluripotency-associated transcription factors in the nucleus. Adhesion based strategies C) Fn-Integrin associated adhesion of hPSCs to substrate D) Heparan based adhesion (focal contacts) of hPSCs to substrate and E) HSPG bound to Fn (via heparan binding sites) with sequestered TGFβ and bFGF and activation of the respective signaling cascades

CHAPTER 4: Propagation of human embryonic and induced pluripotent stem cells in an indirect co-culture system

Abstract

We have developed and validated a microporous poly(ethylene terephthalate) membrane-based indirect co-culture system for human pluripotent stem cell (hPSC) propagation, which allows real-time conditioning of the culture medium with human fibroblasts while maintaining the complete separation of the two cell types. The propagation and pluripotent characteristics of the hESC human embryonic stem cell (hESC) line and a human induced pluripotent stem cell (hiPSC) line were studied in prolonged culture in this system. We report that hPSCs cultured on membranes by indirect co-culture with fibroblasts were indistinguishable by multiple criteria from hPSCs cultured directly on a fibroblast feeder layer. Thus this co-culture system is a significant advance in hPSC culture methods, providing a facile stem cell expansion system with continuous medium conditioning while preventing mixing of hPSCs and feeder cells. This membrane culture method will enable testing of novel feeder cells and differentiation studies using co-culture with other cell types, and will simplify stepwise changes in culture conditions for staged differentiation protocols

Introduction

Human pluripotent stem cells (hPSCs) that include human embryonic stem cells (hESCs) and human induced pluripotent stem cells (hiPSCs) are capable of self-renewal and differentiation into multiple cell types [1, 2, 4, 5]. Traditional culturing of hPSCs involves direct contact with a supporting feeder cell layer, such as mouse embryonic fibroblasts (MEFs), to support their undifferentiated growth [258]. These feeder cells not only secrete extracellular matrix (ECM) components crucial for attachment of hPSCs, but also contribute yet unidentified essential nutrients and growth factors to help maintain hPSCs in a pluripotent state. Because of their potential in tissue engineering and clinical applications, there is a great deal of interest in improving methods for the scalable expansion and differentiation of hPSCs. Feeder cell layers provide an excellent growth substrate for the proper attachment of hPSCs that generally do not adhere to tissue culture treated plastic. One issue of hESC and hiPSC lines propagation in direct contact with a feeder layer however, is that it allows for the intermixing of cell types [17]. Recent culture improvements include using human rather than mouse fibroblasts as feeder layers [20, 22, 23, 259] to eliminate potential cross-species pathogen contamination, however separation of the feeder from the stem cells for passage or other manipulations still remains a technical challenge. On this front, progress in the development of feeder-free methods has been made using purified substrates such as Matrigel, fibronectin or laminin to allow for attachment [48]. In these feeder-free culture systems, hPSCs are propagated in growth medium previously pre-conditioned separately by fibroblast feeder cells then transferred to the hPSC culture. Commercially available culture media have recently been offered as

alternatives to conditioned medium[204]. However, these media are expensive and use exceedingly high levels of synthetic growth factors (e.g., as much as 100 ng/mL bFGF, IGF, BMPs, etc) to achieve maintenance of undifferentiated hPSC cultures limiting their cost effectiveness for scale-up. In addition to cost concerns of these additives, there remains concern that prolonged continuous culture in completely feeder-free culture may lead to undesirable changes in hPSC karyotype or phenotype [260].

In an effort to simplify hPSC culture without compromising the quality of the cells, we have evaluated a microporous membrane-based indirect co-culture (MBIC) system that physically separates hPSCs from the feeder layer, while allowing for continuous conditioning of the medium by the feeder cells. It was recently reported that undifferentiated hESCs could be successfully cultured on microporous membranes separated from a MEF feeder layer attached directly to the opposite side of the membranes [261]. In their study, the investigators concluded that direct contact was still necessary where a membrane pore size of 3.0 μm was required that allowed direct contact between the feeders and the hESCs through cellular extensions across the pores.

In this study, we report the first use of an MBIC method for maintaining undifferentiated hPSCs, in which cell type mixing between the stem cells and the feeder cells is eliminated due to the absence of physical contact between the two. We show that hPSCs cultured across a membrane from human feeder cells are indistinguishable from those cultured in contact with the feeders, based on colony morphology, expression of pluripotency protein markers, in-vitro differentiation into the three different germ layers and global gene expression profiles. Use of a MBIC system for the expansion of human

hPSCs, where the stem cells and the feeder cells are separated by a microporous membrane partition, allows for an economical alternative to synthetic media-based feeder free system that is amenable to scale up. In addition, the complete separation of the feeders simplifies the testing of multiple culture conditions for optimal hPSC growth, by enabling rapid changes in conditions, such as testing differentiation factors and/or other types of co-cultured cells, without having to dissociate and replat the cells

Materials and methods

Generation of inactivated human feeder layers and acellular substrates from human feeders. Human foreskin fibroblasts (HFFs) were maintained in Dulbecco's modified Eagle's medium with 4.5 g/L glucose, 2mM L-Glutamine, 1% Penicillin/Streptomycin and 10% cosmic calf serum (HyClone, Logan, UT) and 2% Medium 199 (10x) (Gibco, Gaithersburg, MD) to create a basal media blend of DMEM and M199. Inactivation of the feeders was achieved by incubation in 10 μ g/ml of Mitomycin C (MMc), a mitotic inhibitor for 2 hours. Post-incubation, the cells were thoroughly washed with PBS 6 times, followed by trypsinization and additional 3 washes in media. The cells were then plated at a density of 300,000 cells/35mm dish.

Acellular substrates were generated by allowing the HFF cultures to proliferate 6-8 days past 100% confluency within the 6-well tissue culture dishes (Sigma-Aldrich) of a Millicell[®] 1.0 μ m polyethylene terephthalate (PET) inserts with hanging geometry (Millipore, Billerica, MA). The inserts were washed with sterile distilled water to remove traces of growth medium followed by a short exposure to 20mM NH₃ solution to expose the deposited ECM. The substrates were thoroughly washed with phosphate buffered

saline (PBS) to avoid the deleterious effects of the alkaline ammonia solution. A schematic depicting the microporous membrane culture system within a 6-well dish is shown in Figure 26.

Propagation of hPSCs and hPSC-derived cells. Karyotypically normal diploid stem cell lines WA09 and hiPSC (WiCell Research Institute, Madison, WI) were transferred from mouse feeder layers onto the acellular matrices within the inserts. Parallel studies were also carried out using fibronectin coating supporting BG01v cells (Bresagen, Athens, GA), a rapidly dividing, karyotypically aneuploid cell line [198, 199, 213], within the inserts. For fibronectin coating, the inserts were incubated for 24 hours at 37°C with 30 µg/mL human fibronectin (Millipore) diluted in 0.2% porcine gelatin (Sigma-Aldrich). The hPSCs were maintained in DMEM/F12 supplemented with 20% knockout serum replacement, 0.1mM β-mercaptoethanol, 1% non-essential amino acids, 100U/ml penicillin, 100mg/ml streptomycin and 4ng/ml basic fibroblast growth factor, bFGF (Gibco, Gaithersburg, MD). Cells were subcultured by either mechanical dissociation or by gentle trituration; the colonies were split into clumps of 100-200 cells and transferred to a fresh substrate coated insert.

WA09-derived extraembryonic endoderm-like (XE) cells utilized for global gene expression comparisons were generated using the method described [262]. XE cells are polygonal, flat cells that grow in monolayer and resemble fibroblasts in morphology. XE cells were grown in DMEM+10% FBS at 37°C/5% CO₂. XE cells were fed on alternate days and passaged weekly with 0.05% trypsin (Gibco).

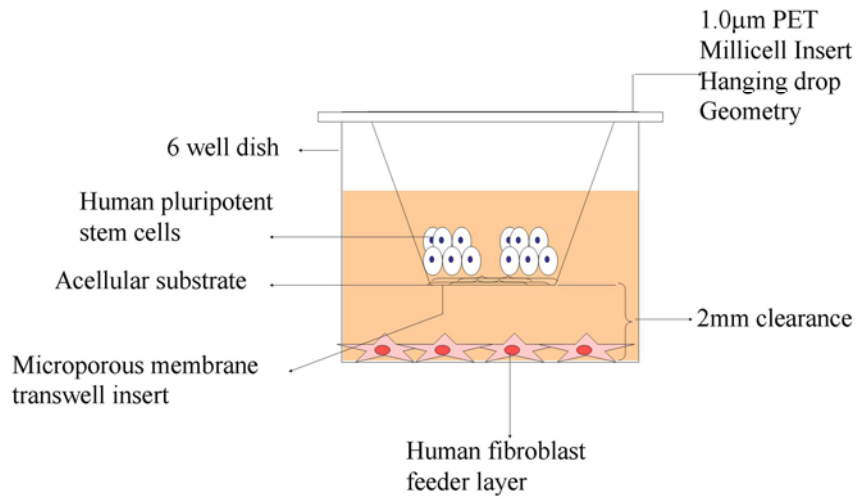


Figure 26:
Schematic of a Microporous Membrane-based indirect co-culture system. HPSCs attach to extracellular matrix (ECM) coated microporous membranes of transwell inserts, which hang inside a 6-well tissue culture dish by plastic projections. HFF- Human foreskin fibroblast.

Alkaline Phosphatase assay. Staining for alkaline phosphatase was performed as per manufacturer instructions (Vector Labs). Briefly, the cells were washed with deionized water to remove traces of media. The final solution was prepared by the addition of the three constituents provided in 0.2M Tris HCl buffer, pH 8.0. The hPSCs were incubated in the final mixture for 40 minutes in the dark and images acquired using a Nikon TS100 Microscope.

Antibodies and Immunocytochemical analysis. hPSCs cultured on the acellular substrates were transferred onto 4 chambered glass slides. 4% paraformaldehyde in PBS was used for fixation, permeabilization for intracellular markers was achieved with 0.2% Triton X-100 in PBS and blocked with normal goat serum. Fixed cells were incubated with primary antibodies: OCT4 (SantaCruz Biotechnology) and SSEA-4 (Chemicon, Temecula, CA). Goat anti-mouse IgG conjugated to Alexa 488 (Molecular Probes, Eugene, OR) was used as secondary antibody. Fluorescent images were acquired using a CoolSnap EZ camera (Photometrics, Tucson, AZ) mounted on a Nikon Eclipse TE 2000-S inverted microscope (Nikon, Melville, NY) with attached image analysis software. All image settings were controlled for uniform acquisition between samples. Specifically, uniform exposure time was maintained for images acquired from experimental samples as well as negative controls for background subtraction.

In vitro differentiation of hPSCs and histology of hPSC-derived embryoid bodies. To generate embryoid bodies (EBs), hPSCs were dissociated using collagenase and resuspended in growth medium devoid of bFGF. EB formation was facilitated using suspension culture, where cells at a density of 25,000 cells/ml were suspended from a

petri-dish lid in 20 μ l droplets. After 5 days, the EBs were transferred to agarose plates to facilitate further differentiation with media changes every 3-4 days for a total differentiation duration of 15 days. EBs were prepared for morphological analysis by fixation in 3.7% paraformaldehyde (PFA) in 1.5ml microfuge tubes at approximately 15-25 EBs per tube. Once fixed overnight, EBS were rinsed with PBS to remove PFA, resuspended in 200 μ l melted 4% low melting point agarose (Sigma Aldrich) at 42°C and incubated for 2 hours to allow settling. Final pelleting and agarose solidification was performed with brief room temperature centrifugation at 500g. Agarose embedded samples were removed as single plugs and processed by dehydration with increasing ethanol concentration to 100% followed by xylene and paraffination in a Leica TP1020 tissue processor. Hematoxylin and Eosin (H&E) staining was performed on microscope slide mounted 5 μ m sections in a Leica Autostainer XL workstation. Images were acquired using an Olympus BX51 microscope using the default imaging parameters.

RNA isolation and real time reverse transcription polymerase chain reaction. RNA was isolated from hPSCs and propagated for 15 passages under different conditions and from EBs after 15 days in suspension using Trizol (Invitrogen, Carlsbad, CA) and quantified using BioMate3 UV-VIS Spectrophotometer (Thermo Scientific, Waltham, MA). cDNA was synthesized from 1 μ g of RNA using cDNA reverse transcription kit (Applied Biosystems, Foster City, CA). Expression of pluripotent genes and differentiation markers (Table 3) within undifferentiated and differentiated samples was analyzed using quantitative real time RT-PCR. PCR was performed in an ABI HT7900 system and the

data was acquired using Sequence Detection System software (SDS v2.2.1, Applied Biosystems).

Gene expression data (three replicates) were acquired and SDS software was used to estimate relative fold change values using Δ CT quantitation methods. Endogeneous 18S ribosomal RNA was used for normalization. Relative gene expression for hPSCs propagated in the MBIC system was assessed against hPSCs propagated on acellular HFFs. However, relative gene expression of differentiated EBs obtained from different conditions was assessed against hPSCs propagated under the original condition. Expression Index (EI) was used to determine the relative differentiation state of cells [200]. EI was based on the average CT values from triplicate measurements. An expression ratio of two or more genes was determined using a mathematical model based on the geometric average of assessed genes, previously described in detail [201], given by the following equation:

$$EI = K_{RS} \frac{\sqrt[m]{(1 + E_{gene1m})^{Ct_{gene1m}} \cdot (1 + E_{gene2m})^{Ct_{gene2m}} \dots (1 + E_{genem})^{Ct_{genem}}}}{\sqrt[n]{(1 + E_{gene1n})^{Ct_{gene1n}} \cdot (1 + E_{gene2n})^{Ct_{gene2n}} \dots (1 + E_{genen})^{Ct_{genen}}}}$$

E is the PCR efficiency calculated from dilution series of purified PCR products, Ct is the threshold cycle, and m and n are the numbers of genes that are up and down regulated upon differentiation respectively. K_{RS} is the relative sensitivity constant and was not determined as it does not affect relative comparisons between samples.

Scanning Electron Microscopy (SEM) analysis of membranes and hPSC colonies. To verify that matrix coating did not clog the pores of the MBIC system, transwell insert samples were prepared for SEM analysis. Briefly, PET insert membrane samples were washed twice with PBS to remove any excess ECM, culture medium, or cell debris.

Samples were then fixed in 2% glutaraldehyde in 0.1 M sodium cacodylate buffer and subsequently dehydrated in increasing concentrations of ethanol. Following dehydration, samples were dried, mounted on an aluminum stub, sputter coated with platinum, and examined with a Zeiss EVO 50 XVP Scanning Electron Microscope (Zeiss, Thornwood, NJ). SEM analysis of hPSC colonies was performed by fixation in 4% glutaraldehyde followed by three washes in 0.1M Cacodylate Buffer pH 7.2 with 0.1M Sucrose. Cells were treated with 1% Osmium Tetroxide in 0.1M Cacodylate Buffer pH 7.2 followed by a 0.1M Cacodylate Buffer pH 7.2 rinse. Samples were dried by incubation in increasing percentage of ethanol (25 to 100%). SEM images were acquired by coating with ~ 150Å gold for contrast enhancement and electrical continuity. Membranes were removed from inserts with a scalpel before microscopy. Representative images were collected in the FEI Quanta FEG ESEM 200 under high vacuum at 15 keV.

Gene expression profiling, data collection and analysis. Whole-genome gene expression data was obtained in duplicate from karyotypically normal WA09 hESCs maintained for 10 passages in (a) direct co-culture with HFF, (b) microporous membrane-based indirect co-culture with hFFs, and (c) feeder-free in HFF-conditioned medium. In addition, we profiled three replicates of WA09-derived differentiated XE cells, and two replicates of hFFs. Total RNA was extracted using the Mirvana Total RNA extraction kit (Ambion). mRNA labeling and amplification was performed using the Totalprep kit. Whole-genome gene expression profiling was then performed using Illumina human WGA-6 version 2 gene expression arrays according to the manufacturer's protocol. Data processing and

normalization was performed in BeadStudio (Illumina). Clustering and statistical analyses were performed using MATISSE, based on previously developed methods [263].

Results

In-direct co-culture allows expansion of hPSCs without feeder-cell contact

Our initial experiments focused on developing appropriate culture conditions in which the hPSCs would successfully attach to the membranes, prior to use in MBIC studies. Our studies showed that hPSC lines did not attach to tissue culture-treated 1.0 μm PET inserts without prior treatment, whereas coating the inserts with 30 $\mu\text{g}/\text{mL}$ fibronectin diluted in 0.2% porcine gelatin for 24 hours or generation of human acellular substrates within the inserts allowed for hPSC attachment.

To test the feasibility of MBIC to support undifferentiated growth of WA09 hESC and iPS lines using standard growth medium, we first demonstrated that both hPSC lines could be successfully cultured for over 10 generations on 1.0 μm PET inserts in co-culture with MEFs and subsequently with HFFs as shown in the SEM micrographs (Figure 27). In all of our studies, the feeder cells were attached to the bottom of the well, rather than the bottom of the microporous membrane. hPSCs cultured in the MBIC system retained cell and colony morphology characteristics of undifferentiated cultures.

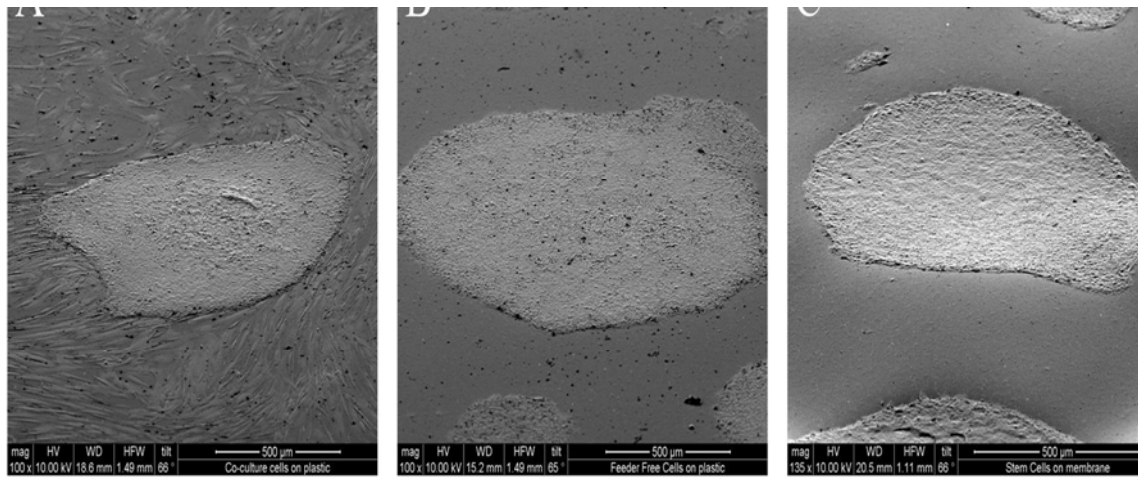


Figure 27:

Scanning electron micrograph of WA09 hESCs co-cultured and passaged five times with human foreskin fibroblasts on plastic (A), feeder free on plastic with conditioned media (B) or by indirect co-culture on 1mm PET membrane (C).

Specifically, these cells maintained a high nuclear to cytoplasmic ratio representative of rapidly dividing undifferentiated hPSCs, and have distinct colony boundaries. Positive expression of alkaline phosphatase, a reliable marker of pluripotency [264], is indicative of sustained stemness in the hPSCs maintained on the inserts (Figure 28 a,b).

In-direct co-culture maintains undifferentiated state of three different hPSCs

Attachment and long term undifferentiated propagation of hPSCs on acellular substrates within the MBIC system was validated by the expression of transcription factor OCT4 and cell surface marker SSEA4 immunocytochemically and mRNA expression. At intermittent passages as well as on passage 10, karyotypically normal hPSCs within the MBIC system expressed all pluripotency markers (Figure 28 c, d e and f). To evaluate the relative gene expression of pluripotency as well as germ layer specific genes, RNA from hPSCs maintained within the MBIC system for 15 passages was isolated and analyzed by quantitative RT-PCR. Samples were obtained in triplicates from hPSCs within the MBIC system and directly compared to hPSCs propagated on acellular substrates on tissue culture polystyrene (TCPS). Expression of pluripotency markers (OCT4, SOX2, NANOG) was presented as CT values normalized against the 18S housekeeping gene for each sample. As shown in Figure 29 c, comparable Δ CT values across different culture conditions and cell lines is indicative of maintenance of the undifferentiated state in the MBIC system. Statistical analyses indicated no significant difference ($p > 0.05$) between hPSCs propagated in the MBIC system and those propagated on acellular substrates on TCPS. Further, the differentiation state of the hPSCs was quantified using the ‘expression index’ as a metric to compare the undifferentiated hPSCs against EBs obtained in the MBIC system. Using the

CT values and corresponding PCR efficiency for the transcript of interest, a ratio of the geometric averages of the up-regulated and the down-regulated genes in the appropriate undifferentiated/differentiated sample was obtained. For the two cell lines (WA09 and hiPSC) analyzed, the expression index of the undifferentiated sample (15 passages) was 90 and 137, while the expression index of the 15-day old EBs was found to be 0.4 and 0.55 (Figure 29 a & b).

In-direct co-culture maintains in vitro differentiation potential

Functional pluripotency of the hPSCs cultured on acellular substrates was tested by in vitro differentiation by embryoid body formation and germ layer identification (ectoderm, endoderm and mesoderm). hPSC colonies were manually cut into clumps of about 100-300 cells and resuspended in ultra-low attachment conditions, an agarose coated Petri dish.

Within 5-6 days, cystic EBs were formed with high efficiency. After 15 days, total RNA was isolated from the EBs and analyzed by real time PCR. Statistical analyses indicated that the EBs generated under the MBIC system demonstrated significantly high expression ($p < 0.01$) of all germ layer specific markers analyzed (Figure 29d). In addition to the expression of markers indicative of germ layer formation in the EBs, histological studies were performed to assess the morphology of the differentiated tissue. Detailed examination of the EB-sections from hPSCs propagated under direct co-culture and in the MBIC system demonstrates the formation of complex structures such as neuroepithelial tubes, fibrous connective tissue and intestinal gut (Figure 30).

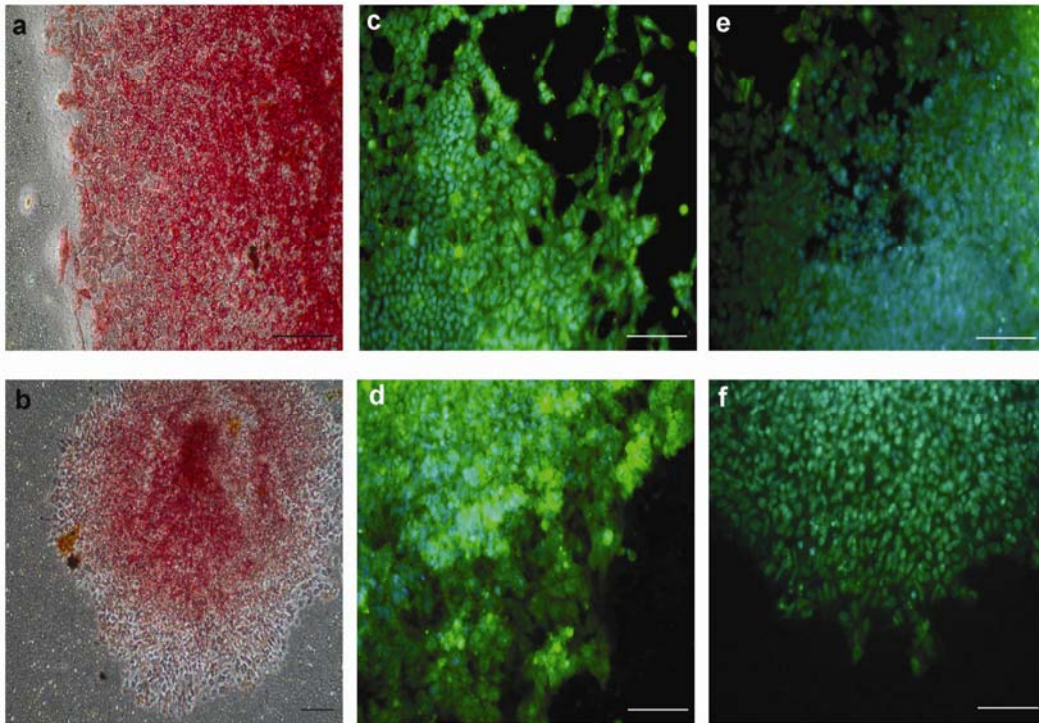


Figure 28:

Morphology and pluripotency markers on hPSCs grown within the millicell culture system: WA09 hESCs and hiPSCs maintain alkaline phosphatase, Stage specific embryonic antigen (SSEA4) and POU5F1 expression after 10 passages in membrane-based culture. WA09 (a,c,e) and hiPSC (b,d,f) grown in direct co-culture with HFFs are positive for alkaline phosphates (a,b), SSEA4 (c,d) and POU5F1 (e,f). Scale bar = 100 μ m.

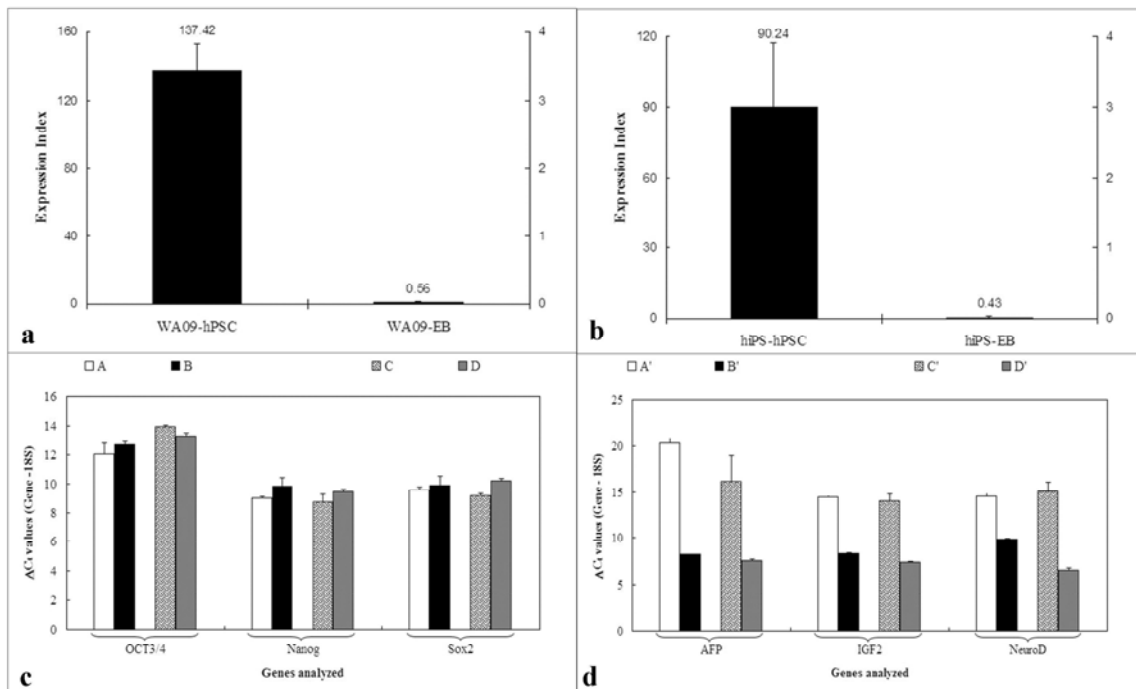


Figure 29:

Quantitative real time polymerase chain reaction (QPCR) analysis of undifferentiated hPSCs and differentiated EBs derived from hPSCs. Differential expression index of a) WA09 hPSC and WA09-derived EBs and b) hiPSC and hiPSC-derived EBs, based on analysis of six genes (OCT4, NANOG, SOX2, AFP, IGF2 and NEUROD1). (c) Normalized gene expression of undifferentiated markers in WA09 on acellular HFF (A); WA09 in MBIC system (B); hiPSC on acellular HFF (C) and hiPSC in MBIC system (D). There is no significant difference ($p > 0.01$) between the groups ($n=3$) indicating comparable pluripotent gene expression. (d) Normalized gene expression of differentiated markers in WA09 in MBIC system (A'); EBs generated from WA09 in MBIC system (B'); hiPSC in MBIC system (C'); and EBs generated from hiPSC in MBIC system (D'). Significant differential gene expression ($p < 0.01$) in all three lineage specific markers was observed.

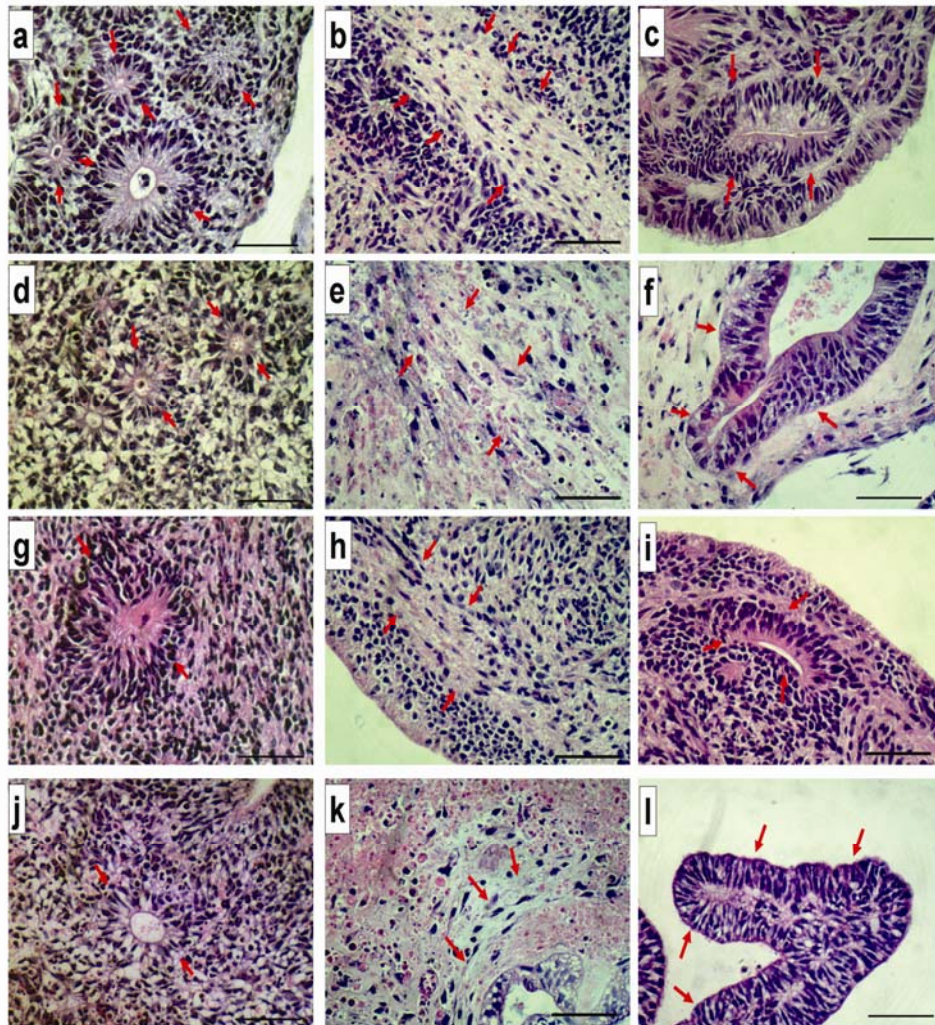


Figure 30:
 Histologic Evidence of Tri-Lineage Differentiation in embryoid bodies generated from hPSCs. Shown are images of hematoxylin and eosin-stained histologic sections of EBs from WA09 propagated on MEFs as a positive control (top row, a-c); WA09 cells propagated on the MBIC system (middle row, d-f) and hiPSC propagated in the MBIC system (bottom row, g-i). Tri-lineage potential is demonstrated as ectodermal (neuroepithelial) differentiation (a, d, and f); mesodermal (fibrous connective) differentiation (b, e, and g) and endodermal (intestinal) differentiation (c, f, and i). Magnification is 200x total (10x ocular, 20x objective). Each scale bar represents 50 μm in length.

Global gene expression analysis validates indirect co-culture for hPSC propagation.

Genome-wide gene expression profiles of undifferentiated karyotypically normal WA09 hESCs in direct co-culture with HFF feeder cells (standard), in indirect co-culture (MBIC), and feeder-free in HFF-conditioned media (feeder-free) were very similar (Figure 31). The correlation coefficients among the three culture conditions were very high (Table 8), with a limited number of genes showing differential expression among them (Figure 32, top diagram). The XE cells are fibroblast-like cells differentiated from the WA09 hESC line. The numbers of differentially expressed genes (Figure 31) and the correlation coefficients among the three cell types (Table 8) support the notion that the XE cells have a phenotype between that of undifferentiated hESCs and HFFs, but more closely related to the HFF phenotype. The large majority of the genes differentially expressed between undifferentiated hESCs and XE cells are also differentially expressed between hESCs and HFFs (2741 out of 3057, or 91%, Figure 32.). Similar results are found when the comparisons are performed against hESCs grown under the three culture conditions (Figure 32). The expression profiles for the hESCs grown under the MBIC and feeder-free conditions were more closely related to each other than those grown under standard conditions (Figure 31). This result is not entirely unexpected, as the hESCs in the feeder-free and MBIC conditions are exposed to HFF-generated soluble factors without direct contact with HFFs, while the hESCs in the standard condition have both access to soluble factors and direct contact with HFFs. Differentially expressed genes were examined for enrichment in GO categories and targets of ESC-related transcriptional regulators (14 transcriptional regulators examined, listed with references in Table 9).

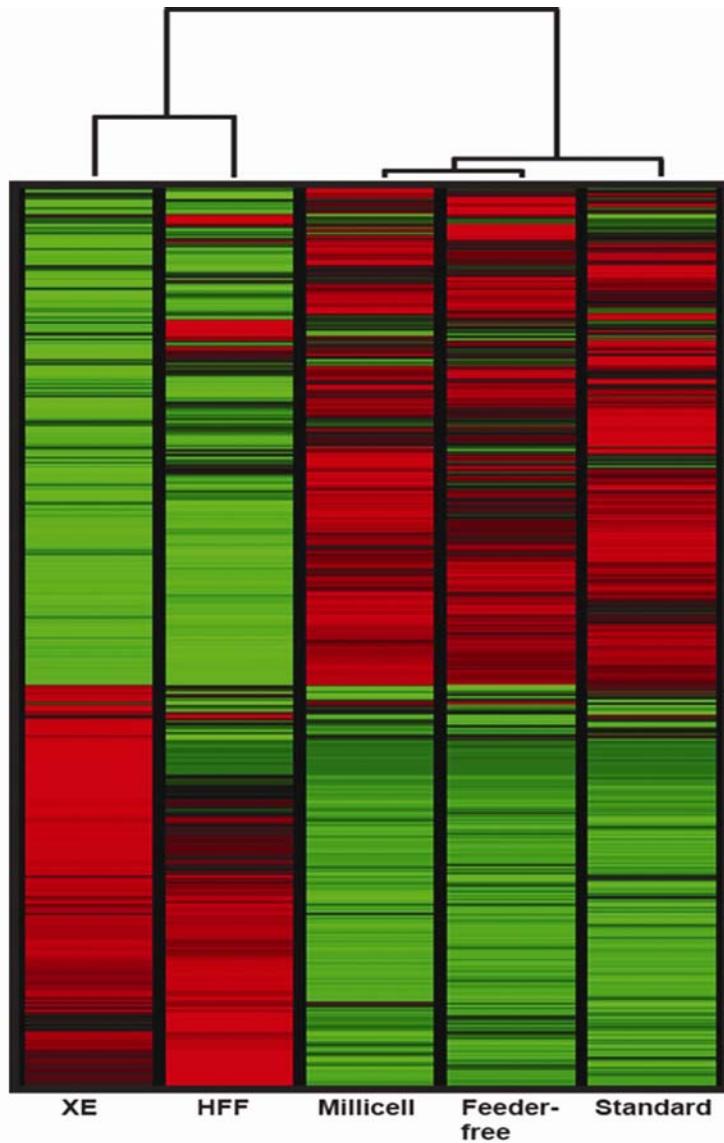



Figure 31:


Agglomerative hierarchical clustering by average distance, using the Pearson correlation coefficient as the distance measure. The lengths of the branches on the dendrogram are proportional to the average distance in global expression between sample types, and the heatmap showing expression displays row-normalized intensity values for the 7,373 genes significantly differentially expressed between at least two sample types. XE: WA09-derived extraembryonic endoderm-like cells. HFF: human foreskin fibroblasts. Undifferentiated WA09 hESCs were maintained with HFFs in indirect coculture (Millicell), on Matrigel with HFF-conditioned media (Feeder-Free), and on an HFF feeder layer (Standard).

Table 8:

R^2 correlation coefficients between expression profiles of different culture conditions (in pink boxes) and numbers of significantly differentially expressed genes (FDR < 0.05, minimum fold-change of 1.3) between pairs of culture conditions (in violet boxes).

	Standard	Feeder-free	Millicell	XE	HFF
Standard	---	0.9796	0.9795	0.8087	0.7718
Feeder-free	160	---	0.9865	0.8279	0.7917
Millicell	260	14	---	0.8112	0.7750
XE	2984	2763	3269	---	0.9347
HFF	5870	5709	5934	626	---

 = r^2 correlation coefficient

 = #differentially expressed genes, FDR < 0.05

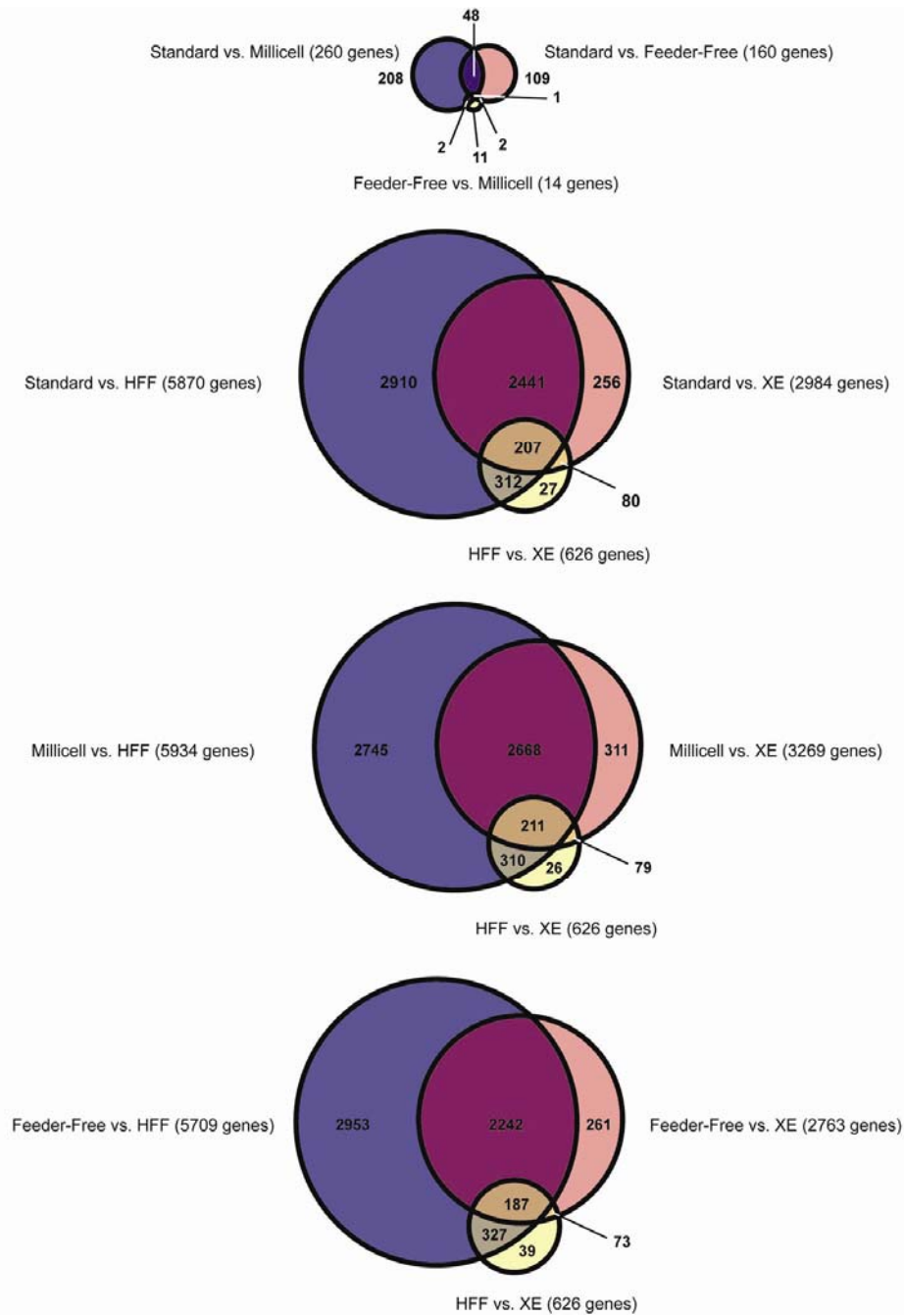


Figure 32:

Venn diagrams indicating the overlap between the sets of genes significantly differentially expressed (FDR < 0.05) between pairs of samples. The top diagram shows results for the hESCs cultured in the three different conditions. The lower three diagrams show results among hESCs, HFFs and XE cells, with the data for each hESC culture conditions shown in a separate diagram. The sizes of the circles are proportional to the number of genes represented

Table 9:

14 transcriptional regulators examined in the enrichment analysis in Figure 6. Lists of target genes were extracted from the referenced papers, which identified targets of transcriptional regulators from ChIP-Chip data

Comparison	Number of genes	GO biological process	p-value	# targets	Transcription Factor Targets	p-value	# targets
Standard > FF	36		NS				
Standard < FF	176	development	0.019	35	NANOG	2.37E-05	33
					Dax1 mouse	3.00E-03	29
					TCF3	6.45E-07	40
					POU5F1	0.000825	32
Standard > MILLICELL	83	cell communication	0.045	32	PcG mouse	0.025	6
Standard < MILLICELL	174		NS		Dax1 mouse	5.58E-05	33
FF > MILLICELL	21		NS				
FF < MILLICELL	1		NS				

Two significantly enriched GO categories (Development and Cell communication) were found (Table 10). Moreover, there was significant enrichment for targets of the pluripotency-associated transcription factors OCT4/POU5F1, NANOG, DAX1, and TCF3 in the set of genes expressed at significantly higher levels in cells cultured under Feeder-Free or MBIC conditions compared to the Standard condition. OCT4/POU5F1 and NANOG are of course two of the transcription factors most closely associated with pluripotency. In mouse ES cells, DAX1 has been shown to physically interact with SOX2 and NANOG [243, 265], as well as to have predicted promoter binding sites for the core pluripotency-associated transcription factors [266]. OCT4/POU5F1, NANOG, SOX2, and TCF3 co-occupy the promoter regions of a large number of pluripotency-associated and lineage-specific genes, and it has recently been suggested that TCF3 be added to the short list of core transcription factors thought to be critical to the maintenance of the pluripotent state [265, 267]. Although the number of differentially expressed genes between the hESCs grown in standard vs. MBIC and Standard vs. feeder-free conditions were small, the enrichment of targets of these transcription factors in the set of genes more highly expressed in the MBIC and feeder-Free conditions suggests that, if anything, they are more conducive to the maintenance of pluripotency than the standard condition involving direct co-culture with feeders.

Table 10:

TF-targets and GO categories enriched in sets of genes differentially expressed among the three hESC culture conditions. The numbers of genes in each category are listed in the second column (e.g. there are 36 genes expressed at significantly lower levels in the Standard culture condition compared to the Feeder-Free condition). Enrichments for genes in particular Gene Ontology (GO) categories are listed in column 3 (with the associated p-values in column 4), and enrichments for targets of transcription factors are indicated in the fifth column (with the associate p-values in column 6). p-values are Bonferroni corrected for multiple testing. NS = not significant.

Annotation	# of genes	Organism	Reference
E2F4 targets	1479	Human	[268]
NANOG targets	1427	Human	
OCT4/POU5F1 targets	1614	Human	
SOX2 targets	1356	Human	
TCF3 targets	1677	Human	[269]
Methylated promoters	624	Mouse	[270]
Unmethylated promoters	3486	Mouse	
Polycomb bound promoters	284	Mouse	
Dax1 targets	1493	Mouse	[243]
Klf4 targets	1510	Mouse	
Myc targets	3018	Mouse	
Nacl targets	670	Mouse	
Rex1 targets	1282	Mouse	
Zfp281 targets	519	Mouse	

Discussion

This study demonstrates several important steps towards hPSC culture improvement. First, the MBIC system was effective in segregating hPSCs from feeder layers. Alkaline phosphatase analysis of feeder layers below showed negative AP staining, thus indicating that hPSCs did not traverse the microporous membranes (data not shown). In addition to successful physical separation of cell types, we have demonstrated MEFs can be replaced with HFFs, which eliminates any potential exposure to xenotropic pathogens. Previous studies have reported the variability that exists between different pluripotent stem cells and the need to compare experimental results between two distinct cell lines [271]. To demonstrate the ubiquity of the MBIC methods, we used hPSCs from multiple embryonic as well as an induced stem cell from human fibroblasts in our studies.

Furthermore, in contrast to conventional conditioned medium protocols, where feeder-secreted nutrients and growth factors in the conditioned medium have a limited storage capability once removed from the feeder cells resulting in the requirement to be produced in parallel to the hPSCs culture in which they will be used, the MBIC system achieves a dynamic and sustained conditioning of the medium – similar to that achieved by direct contact cultures – while simultaneously achieving clean and thorough cell segregation.

While many of the essential nutritive factors secreted by feeder layers have not been identified, this system demonstrates that hPSCs attached to a substrate only need access to the nutrients in the medium, and do not require direct interaction with feeder cells. Another important component of hPSC culture is the passaging technique used for expansion.

Traditional methods have involved labor-intensive mechanical passaging or use of bulk dissociation agents like collagenase, trypsin or EDTA-based reagents. There is published data to demonstrate that bulk passaging methods, although easy to adopt for hPSC culture has a tendency to result in chromosomal abnormalities in long-term culture. It is useful to note that the passaging methodology developed in the MBIC system involves a simple step of gently washing and triturating the hPSCs with medium and transfer onto fresh inserts. This passaging methodology within the MBIC system has potential for the reduction of chromosomal abnormalities on hPSCs in long-term culture and propagation. The bench scale demonstration of feasibility of the MBIC culture system presented here has scope for refinement and scale up that could facilitate the design of culture systems for both self-renewal and differentiation of hPSCs.

Our findings are in contradiction to those presented in an earlier study, where results suggested that a porous membrane based system only functions in the propagation of hESCs plated to the apical (top) face of the membrane if the feeder cells are grown directly on the basolateral (bottom) face of the insert[261]. Though the two studies are somewhat similar, the previous study used different feeder layers (STO strain MEFs[261] vs. CF-1 strain MEFs derived in-house, used in our study), which could potentially contribute to the differences observed between our two studies. The results from the previous MBIC based study suggests that there exists intrinsic sensitivity to a variety of parameters such as cell types, cell seeding densities, media change schedule, etc. that would require optimization. However, the study presented here clearly demonstrates, based on multiple measured experimental outcomes that the MBIC system can propagate hPSCs in long term culture

without the feeder layer attached to the opposing membrane side as well as without any physical contact.

Global gene expression profiling of our samples using whole-genome gene expression microarrays revealed that hESCs cultured under Standard, Feeder-Free, and MBIC conditions were very similar. However, a small but significant set of genes demonstrated differences in gene expression among undifferentiated hESCs grown in the three different conditions, particularly between cells cultured in the Standard vs. MBIC and Standard vs. Feeder-Free conditions. Our results also suggest that the XE cell phenotype lies between that of undifferentiated hESCs and HFFs, but is much closer to the HFF phenotype.

We envision cells as occupying discrete phenotypic states, stabilized by networks of interacting regulatory molecules, such as transcription factors, epigenetic marks, and miRNAs. If the cells are perturbed sufficiently (e.g. if undifferentiated cells are exposed to chemicals such as retinoic acid or TPA), they can be induced to change phenotypic states. However, small perturbations can be compensated for by subtle changes in the regulatory network. We believe that we may be seeing evidence for these mechanisms at work in the hPSCs cultured under different conditions, with the differences in culture conditions causing small changes in gene expression of pluripotency-associated genes, but no change in the overall pluripotent phenotype. The relative phenotypes of the cell types studied can be illustrated in the model (Figure 33), where the hPSCs cultured under the Feeder-Free and MBIC conditions lie at slightly different positions in the same general phenotypic state as hPSC cultured under standard conditions, the HFFs occupy a markedly different phenotypic state, and the XEs are located between the hPSCs and HFFs, but closer to the

HFFs. Our findings also support the notion that global gene expression may be a more sensitive method for detecting subtle but potentially biologically important differences between cell populations than standard phenotypic assays [272]. There are several ways to improve this new MBIC system, particularly in the area of cell attachment. In this study, we used a mixture of fibronectin and gelatin for promoting cell attachment in our initial assessment of the system. A traditional substrate used for hPSC involves use of Matrigel, which includes laminin and peptidoglycans in addition to the collagen found in porcine gelatin. [204]. Our study has demonstrated use of acellular substrates derived from human fibroblasts that provide the relevant physical cues for attachment within the MBIC system. We believe that the acellular substrates present the hPSCs with an environment that is molecularly similar to what is used in direct co-culture systems. Furthermore, use of the same fibroblast line as a feeder to provide the chemical cues for real time conditioning of the media renders the MBIC system an economically feasible alternate to use of other purified ECMs like fibronectin or laminin. It is important to note that during the transition stages from direct co-culture to the MBIC system, a certain level of spontaneous differentiation is observed, hPSCs formed both undifferentiated colonies with tight boundaries as well as heterogeneous colonies containing a population of differentiated cells at the colony boundaries and between colonies as seen in earlier studies [20, 48]. However, the hPSCs recovered quickly to maintain their undifferentiated state over many passages in the MBIC system.

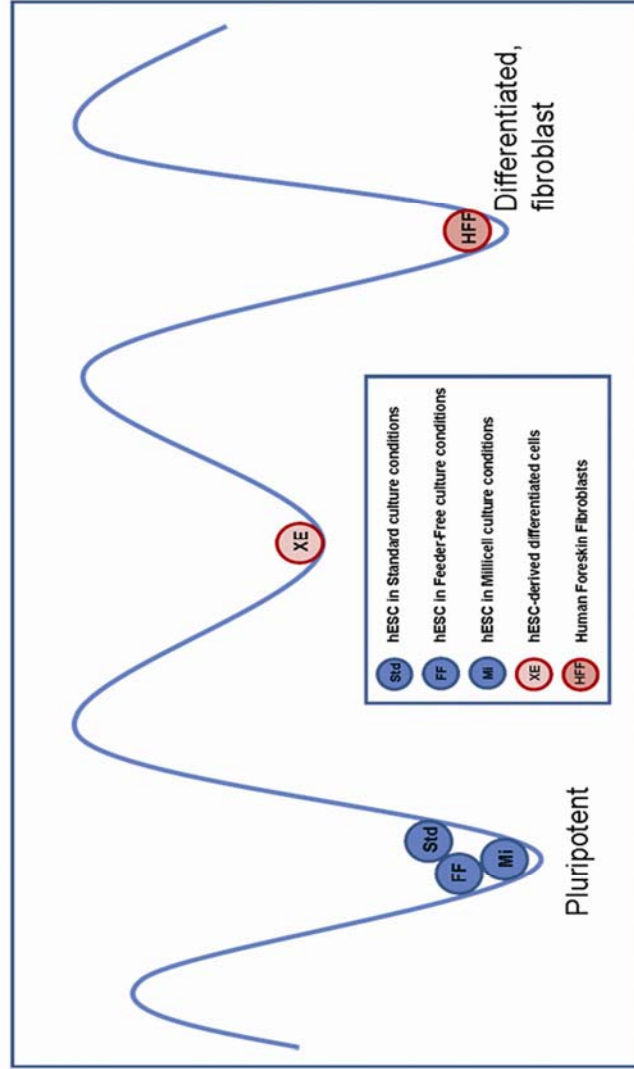


Figure 33: Relationships between the five cell types analyzed in the global gene expression studies. The cells can occupy discrete phenotypic states, stabilized by networks of interacting regulatory molecules, such as transcription factors, epigenetic factors, and miRNAs. Stable cellular phenotypes are shown as “energy wells,” while transitions between stable phenotypes are shown as “energy barriers.” Cell types are shown as colored circles, and occupy stable phenotypic states.

Development and characterization of defined substrates for hPSC propagation should greatly enhance the ability of hPSCs to attach to the insert surface [195].

Two considerations for improvement in the MBIC system are the polymer type that constitutes the insert, and pore size. For this study, we used a PET membrane, but other commercially available polymers deserve further analysis. As shown by the previous study, [261], pore size clearly can have an effect on the diffusion of nutrients across the membrane, in addition to having an effect on the topography of the insert. The membrane surface in the MBIC system is fundamentally different than the surface of TCPS dishes that are widely used in tissue culture, and different polymer variations need to be explored to develop an economically feasible system for hPSC propagation.

Importantly, the potential uses of the MBIC system extend beyond expansion of undifferentiated hPSCs. It is expected that this system will find applications in expansion of any pluripotent cell type as we have shown with hiPSC that are propagated under similar culture conditions used for hESCs [4, 5]. In addition to the pluripotent expansion of hPSCs, the applicability of the MBIC system is amenable to the directed differentiation to adult stem cells into specific, mature cell types [273]. Similar methodologies could be developed for controlling the differentiation of hPSCs, as well as gaining an increased understanding of the nuances of the differentiation process such as defining cues that require direct contact and/or soluble factors. For example, the use of OP9 mouse stromal cell co-culture has been demonstrated for obtaining enriched populations of hESC-derived, CD34+ hematopoietic progenitors [274]. The ability to utilize the MBIC system to induce differentiation of hPSCs by co-culture with inducing cell types would eliminate the

inevitable mixing of cells, resulting in a more purified cell population. Furthermore, if a human stromal cell type or other inducing cell types could substitute the widely used animal stromal lines for differentiation pathways, the MBIC system would assist with cell segregation to a degree where the resulting hPSC derivatives might be clinically useful.

Conclusions

In conclusion, we have demonstrated the characterization of the MBIC system as providing functional and unique benefits over prior innovations in the undifferentiated propagation of hPSCs including reducing the burden of expensive purified factor additives, contamination potential due to extensive culture manipulations of parallel stem and feeder cultures, and the amenability to scale-up to larger culture systems composed of separated hPSC expansion and media conditioning compartments separated by a porous membrane partition. Thus, the MBIC system presented provides a versatile and cost-effective solution for eliminating cell mixing in hPSC co-cultures while retaining the benefits of the presence of feeder cells in their conditioning of the media and providing essential factors to promote pluripotency. Further modifications and optimization of this system and a detailed characterization of hPSCs in long-term cultures should allow for routine adaptation of the MBIC system in hPSC propagation and directed differentiation.

CHAPTER 5: Conclusions and Future Directions

Conclusions

The impetus for this study was the identification and development of substrates that were devoid of non-human components for long term undifferentiated propagation of human pluripotent stem cells (hPSCs). To achieve this, the ECM deposited by mouse and human feeder layers were analyzed and characterized for cellular compatibility. Further characterization based on mass spectrometry revealed proteins involved in maintenance of self-renewal. The information was in turn used to generate defined substrates from commercially available proteins, and evaluated for maintenance of hPSC self-renewal. The study was conducted in three parts.

First, the capability of the acellular substrates to maintain long term undifferentiated propagation of two embryonic and one induced pluripotent stem cell lines was investigated (Chapter 2 and Appendix A). Characterization studies were based on morphological, immunocytochemical expression of pluripotent markers, gene expression of pluripotent and germ layer specific markers and in vitro differentiation. Results from these experiments supported the following conclusions:

- Human fibroblast derived ECM based substrate can maintain undifferentiated propagation of stable hPSCs.

- Absence of additional supplementation of the growth medium such as increased concentration of growth factors or the use of conditioned medium suggests that human acellular substrates are sufficient for maintenance of hPSC self-renewal in the long-term.

Second, to elucidate the composition of the substrates and identify key proteins or growth factors involved in hPSC self-renewal, proteomic analysis was performed on the substrates derived from human fibroblasts. The results obtained from proteomic analysis and further characterization of the ECM components supported the following conclusions:

- Heparan sulfate proteoglycan and fibronectin are core components of the ECM in all fibroblasts analyzed (MEFs, HFFs and HDFs).
- The use of commercially available HSPG and Fn to synthesize ECM-based substrates have demonstrated the potential to develop defined substrates that exhibit equivalent capabilities to maintain hPSC self-renewal as that exhibited by the acellular substrates.
- The combination of HSPG and Fn contribute to the synergistic activation of adhesion and signaling pathways that are necessary for hPSC self-renewal.

Third, the acellular substrates within microporous membrane-based inserts were evaluated in the development of indirect co-culture systems and controlled microenvironments for hPSC self-renewal. Results from these experiments supported the following conclusions:

- The application of acellular substrate coated microporous membranes provides a microenvironment that contributes to the synergistic action of biophysical and

biochemical cues (from the ECM coated membrane and real-time conditioning of the growth medium) for hPSC self-renewal.

- This system provides a versatile and cost-effective solution that prevents cell mixing in hPSC co-cultures for pluripotency and differentiation studies without feeder cell contamination.

Future directions

The studies conducted in this research have opened avenues for further investigation in the following areas a) characterization of signaling molecules and ECM proteins that contribute to hPSC self-renewal, b) design, synthesis and incorporation of peptides that represent biologically active sites in key proteins within the culture system and c) design of microenvironment that will contribute to efficient sub-culturing methodologies for hPSC propagation. These studies could be accomplished through the following specific aims:

Specific Aim 1: Analyze the acellular substrates using methodologies capable of measuring concentrations of relevant proteins across substrates.

The purpose of this aim will be to improve upon the results acquired from the proteomic analyses presented in this dissertation. Concentration dependence of growth factors such as bFGF on hPSC self-renewal is indicative of the need to detect concentration of proteins and the growth factors in substrates. Results from quantification techniques such as isotope-coded affinity tags (ICAT) or isobaric tag for relative and

absolute quantitation (iTRAQ) might be useful in determining the abundance of proteins and subsequent translation of that information to the synthesis of ECM substrates using commercially available proteins[209].

Specific Aim 2: Design and generate peptide based substrates that support adhesion and undifferentiated propagation of hPSCs

Based on results obtained from ECM-based substrates for hPSC attachment and propagation, synthetic peptides can be designed that can recapitulate the different combinations of protein required for hPSC self-renewal. A library of peptides based on the active sites of core ECM proteins such as fibronectin, heparan sulfate proteoglycan, vitronectin, laminin and collagens could be probed to arrive at the best combination that engage the appropriate integrins and allow for hPSC adhesion. Engaging syndecan on hPSC cell membranes have been shown to allow cell attachment onto peptide treated surfaces and support undifferentiated hPSC propagation[275]. Results obtained from the proposed experiments have the potential to provide further evidence in support of the results presented in this dissertation (Chapter 3).

Specific Aim 3: Design controlled microenvironments for propagation and maintenance of hPSCs within a 3D microwell based culture system.

Microwell slides that house 600 microwells of 100 x 100 μm lateral dimensions coated with non-human Matrigel^(TM) have been shown to be capable of supporting long term undifferentiated cultures of hPSCs [72]. Preliminary studies using microwell slides

coated with murine fibroblast derived acellular substrates have demonstrated the potential to sustain hPSCs for a period of 60 days (Appendix D). It is expected that use of human fibroblast-derived acellular substrates or the appropriate combination of proteins/peptides will elicit similar results and lead to the generation of a humanized system. Such a system will also lead to the development of a viable alternative to current labor-intensive and inefficient subculturing techniques used.

Literature Cited

Literature Cited

1. Reubinoff, B.E., Pera, M.F., Fong, C.Y., *et al.*, *Embryonic stem cell lines from human blastocysts: somatic differentiation in vitro*. Nat Biotechnol, 2000. **18**(4): p. 399-404.
2. Thomson, J.A., Itskovitz-Eldor, J., Shapiro, S.S., *et al.*, *Embryonic stem cell lines derived from human blastocysts*. Science, 1998. **282**(5391): p. 1145-7.
3. Nakagawa, M., Koyanagi, M., Tanabe, K., *et al.*, *Generation of induced pluripotent stem cells without Myc from mouse and human fibroblasts*. Nat Biotechnol, 2008. **26**(1): p. 101-6.
4. Takahashi, K., Tanabe, K., Ohnuki, M., *et al.*, *Induction of pluripotent stem cells from adult human fibroblasts by defined factors*. Cell, 2007. **131**(5): p. 861-72.
5. Yu, J., Vodyanik, M.A., Smuga-Otto, K., *et al.*, *Induced pluripotent stem cell lines derived from human somatic cells*. Science, 2007. **318**(5858): p. 1917-20.
6. Evans, M.J. and Kaufman, M.H., *Establishment in culture of pluripotential cells from mouse embryos*. Nature, 1981. **292**(5819): p. 154-6.
7. Thomson, J.A., Kalishman, J., Golos, T.G., *et al.*, *Isolation of a primate embryonic stem cell line*. Proc Natl Acad Sci U S A, 1995. **92**(17): p. 7844-8.

8. Donahue, R.E., Kessler, S.W., Bodine, D., *et al.*, *Helper virus induced T cell lymphoma in nonhuman primates after retroviral mediated gene transfer*. J Exp Med, 1992. **176**(4): p. 1125-35.
9. Frondoza, C.G., Tanner, K.T., Jones, L.C., *et al.*, *Polymethylmethacrylate particles enhance DNA and protein synthesis of human fibroblasts in vitro*. J Biomed Mater Res, 1993. **27**(5): p. 611-7.
10. Newman, K.D. and McBurney, M.W., *Poly(D,L lactic-co-glycolic acid) microspheres as biodegradable microcarriers for pluripotent stem cells*. Biomaterials, 2004. **25**(26): p. 5763-71.
11. Iannaccone, P.M., Taborn, G.U., Garton, R.L., *et al.*, *Pluripotent embryonic stem cells from the rat are capable of producing chimeras*. Dev Biol, 1994. **163**(1): p. 288-92.
12. Sukoyan, M.A., Golubitsa, A.N., Zhelezova, A.I., *et al.*, *Isolation and cultivation of blastocyst-derived stem cell lines from American mink (Mustela vison)*. Mol Reprod Dev, 1992. **33**(4): p. 418-31.
13. Doetschman, T., Williams, P., and Maeda, N., *Establishment of hamster blastocyst-derived embryonic stem (ES) cells*. Dev Biol, 1988. **127**(1): p. 224-7.

14. Graves, K.H. and Moreadith, R.W., *Derivation and characterization of putative pluripotential embryonic stem cells from preimplantation rabbit embryos*. Mol Reprod Dev, 1993. **36**(4): p. 424-33.
15. Notarianni, E., Galli, C., Laurie, S., *et al.*, *Derivation of pluripotent, embryonic cell lines from the pig and sheep*. J Reprod Fertil Suppl, 1991. **43**: p. 255-60.
16. Thomson, J.A., Kalishman, J., Golos, T.G., *et al.*, *Pluripotent cell lines derived from common marmoset (Callithrix jacchus) blastocysts*. Biol Reprod, 1996. **55**(2): p. 254-9.
17. Martin, M.J., Muotri, A., Gage, F., *et al.*, *Human embryonic stem cells express an immunogenic nonhuman sialic acid*. Nat Med, 2005. **11**(2): p. 228-32.
18. Price PJ , Goldsborough MD, and Tilkins, M., *Embryonic stem cell serum replacement*, Invitrogen., Editor. 1998.
19. Amit, M., Carpenter, M.K., Inokuma, M.S., *et al.*, *Clonally derived human embryonic stem cell lines maintain pluripotency and proliferative potential for prolonged periods of culture*. Dev Biol, 2000. **227**(2): p. 271-8.
20. Amit, M., Shariki, C., Margulets, V., *et al.*, *Feeder layer- and serum-free culture of human embryonic stem cells*. Biol Reprod, 2004. **70**(3): p. 837-45.

21. Inzunza, J., Gertow, K., Stromberg, M.A., *et al.*, *Derivation of human embryonic stem cell lines in serum replacement medium using postnatal human fibroblasts as feeder cells*. *Stem Cells*, 2005. **23**(4): p. 544-9.
22. Amit, M., Margulets, V., Segev, H., *et al.*, *Human feeder layers for human embryonic stem cells*. *Biol Reprod*, 2003. **68**(6): p. 2150-6.
23. Choo, A.B., Padmanabhan, J., Chin, A.C., *et al.*, *Expansion of pluripotent human embryonic stem cells on human feeders*. *Biotechnol Bioeng*, 2004. **88**(3): p. 321-31.
24. Hovatta, O., Mikkola, M., Gertow, K., *et al.*, *A culture system using human foreskin fibroblasts as feeder cells allows production of human embryonic stem cells*. *Hum Reprod*, 2003. **18**(7): p. 1404-9.
25. Richards, M., Fong, C.Y., Chan, W.K., *et al.*, *Human feeders support prolonged undifferentiated growth of human inner cell masses and embryonic stem cells*. *Nat Biotechnol*, 2002. **20**(9): p. 933-6.
26. Richards, M., Tan, S., Fong, C.Y., *et al.*, *Comparative evaluation of various human feeders for prolonged undifferentiated growth of human embryonic stem cells*. *Stem Cells*, 2003. **21**(5): p. 546-56.
27. Cheng, L., Hammond, H., Ye, Z., *et al.*, *Human adult marrow cells support prolonged expansion of human embryonic stem cells in culture*. *Stem Cells*, 2003. **21**(2): p. 131-42.

28. Lee, J.B., Song, J.M., Lee, J.E., *et al.*, *Available human feeder cells for the maintenance of human embryonic stem cells*. *Reproduction*, 2004. **128**(6): p. 727-35.
29. Genbacev, O., Krtolica, A., Zdravkovic, T., *et al.*, *Serum-free derivation of human embryonic stem cell lines on human placental fibroblast feeders*. *Fertil Steril*, 2005. **83**(5): p. 1517-29.
30. Kim, S.J., Song, C.H., Sung, H.J., *et al.*, *Human placenta-derived feeders support prolonged undifferentiated propagation of a human embryonic stem cell line, SNUhES3: comparison with human bone marrow-derived feeders*. *Stem Cells Dev*, 2007. **16**(3): p. 421-8.
31. Stojkovic, P., Lako, M., Stewart, R., *et al.*, *An autogeneic feeder cell system that efficiently supports growth of undifferentiated human embryonic stem cells*. *Stem Cells*, 2005. **23**(3): p. 306-14.
32. Miyamoto, K., Hayashi, K., Suzuki, T., *et al.*, *Human placenta feeder layers support undifferentiated growth of primate embryonic stem cells*. *Stem Cells*, 2004. **22**(4): p. 433-40.
33. Kristensen, D.M., Kalisz, M., and Nielsen, J.H., *Cytokine signalling in embryonic stem cells*. *Apmis*, 2005. **113**(11-12): p. 756-72.

34. Xu, C., Rosler, E., Jiang, J., *et al.*, *Basic fibroblast growth factor supports undifferentiated human embryonic stem cell growth without conditioned medium.* Stem Cells, 2005. **23**(3): p. 315-23.
35. Ernst, M., Oates, A., and Dunn, A.R., *Gp130-mediated signal transduction in embryonic stem cells involves activation of Jak and Ras/mitogen-activated protein kinase pathways.* J Biol Chem, 1996. **271**(47): p. 30136-43.
36. Guo, D., Jia, Q., Song, H.Y., *et al.*, *Vascular endothelial cell growth factor promotes tyrosine phosphorylation of mediators of signal transduction that contain SH2 domains. Association with endothelial cell proliferation.* J Biol Chem, 1995. **270**(12): p. 6729-33.
37. Zimrin, A.B., Pepper, M.S., McMahon, G.A., *et al.*, *An antisense oligonucleotide to the notch ligand jagged enhances fibroblast growth factor-induced angiogenesis in vitro.* J Biol Chem, 1996. **271**(51): p. 32499-502.
38. Nichols, J., Evans, E.P., and Smith, A.G., *Establishment of germ-line-competent embryonic stem (ES) cells using differentiation inhibiting activity.* Development, 1990. **110**(4): p. 1341-8.
39. Smith, A.G., Heath, J.K., Donaldson, D.D., *et al.*, *Inhibition of pluripotential embryonic stem cell differentiation by purified polypeptides.* Nature, 1988. **336**(6200): p. 688-90.

40. Williams, R.L., Hilton, D.J., Pease, S., *et al.*, *Myeloid leukaemia inhibitory factor maintains the developmental potential of embryonic stem cells*. *Nature*, 1988. **336**(6200): p. 684-7.
41. Niwa, H., Burdon, T., Chambers, I., *et al.*, *Self-renewal of pluripotent embryonic stem cells is mediated via activation of STAT3*. *Genes Dev*, 1998. **12**(13): p. 2048-60.
42. Makino, H., Hasuda, H., and Ito, Y., *Immobilization of leukemia inhibitory factor (LIF) to culture murine embryonic stem cells*. *J Biosci Bioeng*, 2004. **98**(5): p. 374-9.
43. Nur, E.K.A., Ahmed, I., Kamal, J., *et al.*, *Three-dimensional nanofibrillar surfaces promote self-renewal in mouse embryonic stem cells*. *Stem Cells*, 2006. **24**(2): p. 426-33.
44. Paling, N.R., Wheadon, H., Bone, H.K., *et al.*, *Regulation of embryonic stem cell self-renewal by phosphoinositide 3-kinase-dependent signaling*. *J Biol Chem*, 2004. **279**(46): p. 48063-70.
45. Kleinman, H.K., McGarvey, M.L., Hassell, J.R., *et al.*, *Basement membrane complexes with biological activity*. *Biochemistry*, 1986. **25**(2): p. 312-8.

46. Kleinman, H.K., McGarvey, M.L., Liotta, L.A., *et al.*, *Isolation and characterization of type IV procollagen, laminin, and heparan sulfate proteoglycan from the EHS sarcoma*. *Biochemistry*, 1982. **21**(24): p. 6188-93.
47. Vukicevic, S., Kleinman, H.K., Luyten, F.P., *et al.*, *Identification of multiple active growth factors in basement membrane Matrigel suggests caution in interpretation of cellular activity related to extracellular matrix components*. *Exp Cell Res*, 1992. **202**(1): p. 1-8.
48. Xu, C., Inokuma, M.S., Denham, J., *et al.*, *Feeder-free growth of undifferentiated human embryonic stem cells*. *Nat Biotechnol*, 2001. **19**(10): p. 971-4.
49. Takashima, A. and Grinnell, F., *Human keratinocyte adhesion and phagocytosis promoted by fibronectin*. *J Invest Dermatol*, 1984. **83**(5): p. 352-8.
50. Yoshida, K., Chambers, I., Nichols, J., *et al.*, *Maintenance of the pluripotential phenotype of embryonic stem cells through direct activation of gp130 signalling pathways*. *Mech Dev*, 1994. **45**(2): p. 163-71.
51. Humphrey, R.K., Beattie, G.M., Lopez, A.D., *et al.*, *Maintenance of pluripotency in human embryonic stem cells is STAT3 independent*. *Stem Cells*, 2004. **22**(4): p. 522-30.

52. Stojkovic, P., Lako, M., Przyborski, S., *et al.*, *Human-Serum Matrix Supports Undifferentiated Growth of Human Embryonic Stem Cells*. *Stem Cells*, 2005. **23**(7): p. 895-902.
53. Gerecht, S., Burdick, J.A., Ferreira, L.S., *et al.*, *Hyaluronic acid hydrogel for controlled self-renewal and differentiation of human embryonic stem cells*. *Proc Natl Acad Sci U S A*, 2007. **104**(27): p. 11298-303.
54. Toole, B.P., *Hyaluronan in morphogenesis*. *J Intern Med*, 1997. **242**(1): p. 35-40.
55. Jen, A.C., Wake, M.C., and Mikos, A.G., *Review: Hydrogels for cell immobilization*. *Biotechnol Bioeng*, 1996. **50**(4): p. 357-64.
56. Putnam, A.J. and Mooney, D.J., *Tissue engineering using synthetic extracellular matrices*. *Nat Med*, 1996. **2**(7): p. 824-6.
57. Shoichet, M.S., Li, R.H., White, M.L., *et al.*, *Stability of hydrogels used in cell encapsulation: An in vitro comparison of alginate and agarose*. *Biotechnol Bioeng*, 1996. **50**(4): p. 374-81.
58. Cukierman, E., Pankov, R., Stevens, D.R., *et al.*, *Taking cell-matrix adhesions to the third dimension*. *Science*, 2001. **294**(5547): p. 1708-12.
59. Cukierman, E., Pankov, R., and Yamada, K.M., *Cell interactions with three-dimensional matrices*. *Curr Opin Cell Biol*, 2002. **14**(5): p. 633-9.

60. Harrison, J., Pattanawong, S., Forsythe, J.S., *et al.*, *Colonization and maintenance of murine embryonic stem cells on poly(alpha-hydroxy esters)*. *Biomaterials*, 2004. **25**(20): p. 4963-70.
61. Harrison, J., Melville, A.J., Forsythe, J.S., *et al.*, *Sintered hydroxyfluorapatites--IV: The effect of fluoride substitutions upon colonisation of hydroxyapatites by mouse embryonic stem cells*. *Biomaterials*, 2004. **25**(20): p. 4977-86.
62. Horak, D., Kroupova, J., Slouf, M., *et al.*, *Poly(2-hydroxyethyl methacrylate)-based slabs as a mouse embryonic stem cell support*. *Biomaterials*, 2004. **25**(22): p. 5249-60.
63. Kroupova, J., Horak, D., Pachernik, J., *et al.*, *Functional polymer hydrogels for embryonic stem cell support*. *J Biomed Mater Res B Appl Biomater*, 2006. **76**(2): p. 315-25.
64. Cetinkaya, G., Turkoglu, H., Arat, S., *et al.*, *LIF-immobilized nonwoven polyester fabrics for cultivation of murine embryonic stem cells*. *J Biomed Mater Res A*, 2007. **81**(4): p. 911-9.
65. Ouyang, A., Ng, R., and Yang, S.T., *Long-term culturing of undifferentiated embryonic stem cells in conditioned media and three-dimensional fibrous matrices without extracellular matrix coating*. *Stem Cells*, 2007. **25**(2): p. 447-54.

66. Massia, S.P. and Hubbell, J.A., *An RGD spacing of 440 nm is sufficient for integrin alpha V beta 3-mediated fibroblast spreading and 140 nm for focal contact and stress fiber formation.* J Cell Biol, 1991. **114**(5): p. 1089-100.
67. Palecek, S.P., Loftus, J.C., Ginsberg, M.H., *et al.*, *Integrin-ligand binding properties govern cell migration speed through cell-substratum adhesiveness.* Nature, 1997. **385**(6616): p. 537-40.
68. Khademhosseini, A., Suh, K.Y., Yang, J.M., *et al.*, *Layer-by-layer deposition of hyaluronic acid and poly-L-lysine for patterned cell co-cultures.* Biomaterials, 2004. **25**(17): p. 3583-92.
69. Gerecht, S., Townsend, S.A., Pressler, H., *et al.*, *A porous photocurable elastomer for cell encapsulation and culture.* Biomaterials, 2007. **28**(32): p. 4826-35.
70. Wang, Y., Ameer, G.A., Sheppard, B.J., *et al.*, *A tough biodegradable elastomer.* Nat Biotechnol, 2002. **20**(6): p. 602-6.
71. Wang, Y., Kim, Y.M., and Langer, R., *In vivo degradation characteristics of poly(glycerol sebacate).* J Biomed Mater Res A, 2003. **66**(1): p. 192-7.
72. Mohr, J.C., de Pablo, J.J., and Palecek, S.P., *3-D microwell culture of human embryonic stem cells.* Biomaterials, 2006. **27**(36): p. 6032-42.

73. Li, Y.J., Chung, E.H., Rodriguez, R.T., *et al.*, *Hydrogels as artificial matrices for human embryonic stem cell self-renewal*. J Biomed Mater Res A, 2006. **79**(1): p. 1-5.
74. Nie, Y., Bergendahl, V., Hei, D.J., *et al.*, *Scalable culture and cryopreservation of human embryonic stem cells on microcarriers*. Biotechnol Prog, 2009. **25**(1): p. 20-31.
75. Phillips, B.W., Horne, R., Lay, T.S., *et al.*, *Attachment and growth of human embryonic stem cells on microcarriers*. J Biotechnol, 2008. **138**(1-2): p. 24-32.
76. Anderson, D.G., Levenberg, S., and Langer, R., *Nanoliter-scale synthesis of arrayed biomaterials and application to human embryonic stem cells*. Nat Biotechnol, 2004. **22**(7): p. 863-6.
77. Derda, R., Li, L., Orner, B.P., *et al.*, *Defined substrates for human embryonic stem cell growth identified from surface arrays*. ACS Chem Biol, 2007. **2**(5): p. 347-55.
78. Green, J.J., Zhou, B.Y., Mitalipova, M.M., *et al.*, *Nanoparticles for gene transfer to human embryonic stem cell colonies*. Nano Lett, 2008. **8**(10): p. 3126-30.
79. Yang, F., Green, J.J., Dinio, T., *et al.*, *Gene delivery to human adult and embryonic cell-derived stem cells using biodegradable nanoparticulate polymeric vectors*. Gene Ther, 2009. **16**(4): p. 533-46.

80. Amit, M., Margulets, V., Segev, H., *et al.*, *Human Feeder Layers for Human Embryonic Stem Cells*. Biol Reprod, 2003. **68**(6): p. 2150-2156.
81. Hovatta, O., Mikkola, M., Gertow, K., *et al.*, *A culture system using human foreskin fibroblasts as feeder cells allows production of human embryonic stem cells*. Hum. Reprod., 2003. **18**(7): p. 1404-1409.
82. Richards, M., Fong, C.-Y., Chan, W.-K., *et al.*, *Human feeders support prolonged undifferentiated growth of human inner cell masses and embryonic stem cells*. Nat Biotech, 2002. **20**(9): p. 933-936.
83. Richards, M., Tan, S., Fong, C.-Y., *et al.*, *Comparative Evaluation of Various Human Feeders for Prolonged Undifferentiated Growth of Human Embryonic Stem Cells*. Stem Cells, 2003. **21**(5): p. 546-556.
84. Cheng, L., Hammond, H., Ye, Z., *et al.*, *Human Adult Marrow Cells Support Prolonged Expansion of Human Embryonic Stem Cells in Culture*. Stem Cells, 2003. **21**(2): p. 131-142.
85. Lee, J.B., Song, J.M., Lee, J.E., *et al.*, *Available human feeder cells for the maintenance of human embryonic stem cells*. Reproduction, 2004. **128**(6): p. 727-735.

86. Genbacev, O., Krtolica, A., Zdravkovic, T., *et al.*, *Serum-free derivation of human embryonic stem cell lines on human placental fibroblast feeders*. *Fertility and Sterility*, 2005. **83**(5): p. 1517-1529.
87. Kim, S.J., Song, C.H., Sung, H.J., *et al.*, *Human Placenta-Derived Feeders Support Prolonged Undifferentiated Propagation of a Human Embryonic Stem Cell Line, SNUhES3: Comparison with Human Bone Marrow-Derived Feeders*. *Stem Cells and Development*, 2007. **16**(3): p. 421-428.
88. Stojkovic, P., Lako, M., Stewart, R., *et al.*, *An Autogeneic Feeder Cell System That Efficiently Supports Growth of Undifferentiated Human Embryonic Stem Cells*. *Stem Cells*, 2005. **23**(3): p. 306-314.
89. Wang, Q., Fang, Z.F., Jin, F., *et al.*, *Derivation and Growing Human Embryonic Stem Cells on Feeders Derived from Themselves*. *Stem Cells*, 2005. **23**(9): p. 1221-1227.
90. Makino, H., Hasuda, H., and Ito, Y., *Immobilization of leukemia inhibitory factor (LIF) to culture murine embryonic stem cells*. *Journal of Bioscience and Bioengineering*, 2004. **98**(5): p. 374-379.
91. Xu, C., Inokuma, M.S., Denham, J., *et al.*, *Feeder-free growth of undifferentiated human embryonic stem cells*. *Nat Biotech*, 2001. **19**(10): p. 971-974.

92. Klimanskaya, I., Chung, Y., Meisner, L., *et al.*, *Human embryonic stem cells derived without feeder cells*. *The Lancet*, 2005. **365**(9471): p. 1636-1641.
93. Gerecht, S., Burdick, J.A., Ferreira, L.S., *et al.*, *Hyaluronic acid hydrogel for controlled self-renewal and differentiation of human embryonic stem cells*. *Proceedings of the National Academy of Sciences*, 2007. **104**(27): p. 11298-11303.
94. Harrison, J., Pattanawong, S., Forsythe, J.S., *et al.*, *Colonization and maintenance of murine embryonic stem cells on poly([alpha]-hydroxy esters)*. *Biomaterials*, 2004. **25**(20): p. 4963-4970.
95. Harrison, J., Melville, A.J., Forsythe, J.S., *et al.*, *Sintered hydroxyfluorapatites--IV: the effect of fluoride substitutions upon colonisation of hydroxyapatites by mouse embryonic stem cells*. *Biomaterials*, 2004. **25**(20): p. 4977-4986.
96. Ouyang, A., Ng, R., and Yang, S.-T., *Long-Term Culturing of Undifferentiated Embryonic Stem Cells in Conditioned Media and Three-Dimensional Fibrous Matrices Without Extracellular Matrix Coating*. *Stem Cells*, 2007. **25**(2): p. 447-454.
97. Gerecht, S., Townsend, S.A., Pressler, H., *et al.*, *A porous photocurable elastomer for cell encapsulation and culture*. *Biomaterials*, 2007. **28**(32): p. 4826-4835.
98. Mohr, J.C., de Pablo, J.J., and Palecek, S.P., *3-D microwell culture of human embryonic stem cells*. *Biomaterials*, 2006. **27**(36): p. 6032-6042.

99. Martin, G.R. and Evans, M.J., *Differentiation of clonal lines of teratocarcinoma cells: formation of embryoid bodies in vitro*. Proc Natl Acad Sci U S A, 1975. **72**(4): p. 1441-5.
100. Bain, G., Kitchens, D., Yao, M., *et al.*, *Embryonic stem cells express neuronal properties in vitro*. Dev Biol, 1995. **168**(2): p. 342-57.
101. Buttery, L.D., Bourne, S., Xynos, J.D., *et al.*, *Differentiation of osteoblasts and in vitro bone formation from murine embryonic stem cells*. Tissue Eng, 2001. **7**(1): p. 89-99.
102. Dani, C., Smith, A.G., Dessolin, S., *et al.*, *Differentiation of embryonic stem cells into adipocytes in vitro*. J Cell Sci, 1997. **110** (**Pt 11**): p. 1279-85.
103. Doetschman, T.C., Eistetter, H., Katz, M., *et al.*, *The in vitro development of blastocyst-derived embryonic stem cell lines: formation of visceral yolk sac, blood islands and myocardium*. J Embryol Exp Morphol, 1985. **87**: p. 27-45.
104. Fraichard, A., Chassande, O., Bilbaut, G., *et al.*, *In vitro differentiation of embryonic stem cells into glial cells and functional neurons*. J Cell Sci, 1995. **108** (**Pt 10**): p. 3181-8.
105. Kramer, J., Hegert, C., Guan, K., *et al.*, *Embryonic stem cell-derived chondrogenic differentiation in vitro: activation by BMP-2 and BMP-4*. Mech Dev, 2000. **92**(2): p. 193-205.

106. Schuldiner, M., Yanuka, O., Itskovitz-Eldor, J., *et al.*, *Effects of eight growth factors on the differentiation of cells derived from human embryonic stem cells.* Proc Natl Acad Sci U S A, 2000. **97**(21): p. 11307-12.
107. Smith, A.G., *Embryo-derived stem cells: of mice and men.* Annu Rev Cell Dev Biol, 2001. **17**: p. 435-62.
108. Jiang, J., Au, M., Lu, K., *et al.*, *Generation of insulin-producing islet-like clusters from human embryonic stem cells.* Stem Cells, 2007. **25**(8): p. 1940-53.
109. Schroeder, I.S., Rolletschek, A., Blyszczuk, P., *et al.*, *Differentiation of mouse embryonic stem cells to insulin-producing cells.* Nat Protoc, 2006. **1**(2): p. 495-507.
110. Moore, R.N., Dasgupta, A., Rajaei, N., *et al.*, *Enhanced differentiation of embryonic stem cells using co-cultivation with hepatocytes.* Biotechnol Bioeng, 2008. **101**(6): p. 1332-43.
111. Teratani, T., Yamamoto, H., Aoyagi, K., *et al.*, *Direct hepatic fate specification from mouse embryonic stem cells.* Hepatology, 2005. **41**(4): p. 836-46.
112. Atala, A., Kim, W., Paige, K.T., *et al.*, *Endoscopic treatment of vesicoureteral reflux with a chondrocyte-alginate suspension.* J Urol, 1994. **152**(2 Pt 2): p. 641-3; discussion 644.
113. Rowley, J.A., Madlambayan, G., and Mooney, D.J., *Alginate hydrogels as synthetic extracellular matrix materials.* Biomaterials, 1999. **20**(1): p. 45-53.

114. Fang, S., Qiu, Y.D., Mao, L., *et al.*, *Differentiation of embryoid-body cells derived from embryonic stem cells into hepatocytes in alginate microbeads in vitro*. *Acta Pharmacol Sin*, 2007. **28**(12): p. 1924-30.
115. Yamashita, Y., Shimada, M., Tsujita, E., *et al.*, *Polyurethane foam/spheroid culture system using human hepatoblastoma cell line (Hep G2) as a possible new hybrid artificial liver*. *Cell Transplant*, 2001. **10**(8): p. 717-22.
116. Matsumoto, K., Mizumoto, H., Nakazawa, K., *et al.*, *Hepatic differentiation of mouse embryonic stem cells in a three-dimensional culture system using polyurethane foam*. *J Biosci Bioeng*, 2008. **105**(4): p. 350-4.
117. Matsumoto, K., Mizumoto, H., Nakazawa, K., *et al.*, *Hepatic differentiation of mouse embryonic stem cells in a bioreactor using polyurethane/spheroid culture*. *Transplant Proc*, 2008. **40**(2): p. 614-6.
118. Mizumoto, H., Aoki, K., Nakazawa, K., *et al.*, *Hepatic differentiation of embryonic stem cells in HF/organoid culture*. *Transplant Proc*, 2008. **40**(2): p. 611-3.
119. Lavon, N., Yanuka, O., and Benvenisty, N., *Differentiation and isolation of hepatic-like cells from human embryonic stem cells*. *Differentiation*, 2004. **72**(5): p. 230-8.
120. Rambhatla, L., Chiu, C.P., Kundu, P., *et al.*, *Generation of hepatocyte-like cells from human embryonic stem cells*. *Cell Transplant*, 2003. **12**(1): p. 1-11.

121. Shirahashi, H., Wu, J., Yamamoto, N., *et al.*, *Differentiation of human and mouse embryonic stem cells along a hepatocyte lineage*. *Cell Transplant*, 2004. **13**(3): p. 197-211.
122. Baharvand, H., Hashemi, S.M., Kazemi Ashtiani, S., *et al.*, *Differentiation of human embryonic stem cells into hepatocytes in 2D and 3D culture systems in vitro*. *Int J Dev Biol*, 2006. **50**(7): p. 645-52.
123. Chadwick, K., Wang, L., Li, L., *et al.*, *Cytokines and BMP-4 promote hematopoietic differentiation of human embryonic stem cells*. *Blood*, 2003. **102**(3): p. 906-15.
124. Hubner, K., Fuhrmann, G., Christenson, L.K., *et al.*, *Derivation of oocytes from mouse embryonic stem cells*. *Science*, 2003. **300**(5623): p. 1251-6.
125. Kehat, I., Kenyagin-Karsenti, D., Snir, M., *et al.*, *Human embryonic stem cells can differentiate into myocytes with structural and functional properties of cardiomyocytes*. *J Clin Invest*, 2001. **108**(3): p. 407-14.
126. Levenberg, S., Golub, J.S., Amit, M., *et al.*, *Endothelial cells derived from human embryonic stem cells*. *Proc Natl Acad Sci U S A*, 2002. **99**(7): p. 4391-6.
127. Toyooka, Y., Tsunekawa, N., Akasu, R., *et al.*, *Embryonic stem cells can form germ cells in vitro*. *Proc Natl Acad Sci U S A*, 2003. **100**(20): p. 11457-62.

128. Xu, C., Police, S., Rao, N., *et al.*, *Characterization and enrichment of cardiomyocytes derived from human embryonic stem cells*. *Circ Res*, 2002. **91**(6): p. 501-8.
129. Zhan, X., Dravid, G., Ye, Z., *et al.*, *Functional antigen-presenting leucocytes derived from human embryonic stem cells in vitro*. *Lancet*, 2004. **364**(9429): p. 163-71.
130. Nakano, T., Kodama, H., and Honjo, T., *Generation of lymphohematopoietic cells from embryonic stem cells in culture*. *Science*, 1994. **265**(5175): p. 1098-101.
131. Palacios, R., Golunski, E., and Samaridis, J., *In vitro generation of hematopoietic stem cells from an embryonic stem cell line*. *Proc Natl Acad Sci U S A*, 1995. **92**(16): p. 7530-4.
132. Hirashima, M., Kataoka, H., Nishikawa, S., *et al.*, *Maturation of embryonic stem cells into endothelial cells in an in vitro model of vasculogenesis*. *Blood*, 1999. **93**(4): p. 1253-63.
133. Nishikawa, S.I., Nishikawa, S., Hirashima, M., *et al.*, *Progressive lineage analysis by cell sorting and culture identifies FLK1+VE-cadherin+ cells at a diverging point of endothelial and hemopoietic lineages*. *Development*, 1998. **125**(9): p. 1747-57.

134. McCloskey, K.E., Stice, S.L., and Nerem, R.M., *In vitro derivation and expansion of endothelial cells from embryonic stem cells*. *Methods Mol Biol*, 2006. **330**: p. 287-301.
135. Nishikawa, S.I., Hirashima, M., Nishikawa, S., *et al.*, *Cell biology of vascular endothelial cells*. *Ann N Y Acad Sci*, 2001. **947**: p. 35-40; discussion 41.
136. Chen, S.S., Fitzgerald, W., Zimmerberg, J., *et al.*, *Cell-cell and cell-extracellular matrix interactions regulate embryonic stem cell differentiation*. *Stem Cells*, 2007. **25**(3): p. 553-61.
137. Liu, H., Collins, S.F., and Suggs, L.J., *Three-dimensional culture for expansion and differentiation of mouse embryonic stem cells*. *Biomaterials*, 2006. **27**(36): p. 6004-14.
138. Mosesson, M.W. and Amrani, D.L., *The structure and biologic activities of plasma fibronectin*. *Blood*, 1980. **56**(2): p. 145-58.
139. Francis, S.E., Goh, K.L., Hodivala-Dilke, K., *et al.*, *Central roles of alpha5beta1 integrin and fibronectin in vascular development in mouse embryos and embryoid bodies*. *Arterioscler Thromb Vasc Biol*, 2002. **22**(6): p. 927-33.
140. Ferreira, L.S., Gerecht, S., Fuller, J., *et al.*, *Bioactive hydrogel scaffolds for controllable vascular differentiation of human embryonic stem cells*. *Biomaterials*, 2007. **28**(17): p. 2706-17.

141. Battista, S., Guarnieri, D., Borselli, C., *et al.*, *The effect of matrix composition of 3D constructs on embryonic stem cell differentiation*. *Biomaterials*, 2005. **26**(31): p. 6194-207.
142. Liu, H. and Roy, K., *Biomimetic three-dimensional cultures significantly increase hematopoietic differentiation efficacy of embryonic stem cells*. *Tissue Eng*, 2005. **11**(1-2): p. 319-30.
143. Kaufman, D.S., Hanson, E.T., Lewis, R.L., *et al.*, *Hematopoietic colony-forming cells derived from human embryonic stem cells*. *Proc Natl Acad Sci U S A*, 2001. **98**(19): p. 10716-21.
144. Gerecht-Nir, S., Cohen, S., Ziskind, A., *et al.*, *Three-dimensional porous alginate scaffolds provide a conducive environment for generation of well-vascularized embryoid bodies from human embryonic stem cells*. *Biotechnol Bioeng*, 2004. **88**(3): p. 313-20.
145. Inanc, B., Elcin, A.E., and Elcin, Y.M., *Effect of osteogenic induction on the in vitro differentiation of human embryonic stem cells cocultured with periodontal ligament fibroblasts*. *Artif Organs*, 2007. **31**(11): p. 792-800.
146. Hauselmann, H.J., Fernandes, R.J., Mok, S.S., *et al.*, *Phenotypic stability of bovine articular chondrocytes after long-term culture in alginate beads*. *J Cell Sci*, 1994. **107 (Pt 1)**: p. 17-27.

147. Petit, B., Masuda, K., D'Souza, A.L., *et al.*, *Characterization of crosslinked collagens synthesized by mature articular chondrocytes cultured in alginate beads: comparison of two distinct matrix compartments*. *Exp Cell Res*, 1996. **225**(1): p. 151-61.
148. Tanaka, H., Murphy, C.L., Murphy, C., *et al.*, *Chondrogenic differentiation of murine embryonic stem cells: effects of culture conditions and dexamethasone*. *J Cell Biochem*, 2004. **93**(3): p. 454-62.
149. Garreta, E., Genove, E., Borros, S., *et al.*, *Osteogenic differentiation of mouse embryonic stem cells and mouse embryonic fibroblasts in a three-dimensional self-assembling peptide scaffold*. *Tissue Eng*, 2006. **12**(8): p. 2215-27.
150. Randle, W.L., Cha, J.M., Hwang, Y.S., *et al.*, *Integrated 3-dimensional expansion and osteogenic differentiation of murine embryonic stem cells*. *Tissue Eng*, 2007. **13**(12): p. 2957-70.
151. Hwang, N.S., Kim, M.S., Sampattavanich, S., *et al.*, *Effects of three-dimensional culture and growth factors on the chondrogenic differentiation of murine embryonic stem cells*. *Stem Cells*, 2006. **24**(2): p. 284-91.
152. Hwang, N.S., Varghese, S., Theprungsirikul, P., *et al.*, *Enhanced chondrogenic differentiation of murine embryonic stem cells in hydrogels with glucosamine*. *Biomaterials*, 2006. **27**(36): p. 6015-23.

153. Homicz, M.R., Schumacher, B.L., Sah, R.L., *et al.*, *Effects of serial expansion of septal chondrocytes on tissue-engineered neocartilage composition*. *Otolaryngol Head Neck Surg*, 2002. **127**(5): p. 398-408.
154. Bielby, R.C., Christodoulou, I.S., Pryce, R.S., *et al.*, *Time- and concentration-dependent effects of dissolution products of 58S sol-gel bioactive glass on proliferation and differentiation of murine and human osteoblasts*. *Tissue Eng*, 2004. **10**(7-8): p. 1018-26.
155. Bielby, R.C., Pryce, R.S., Hench, L.L., *et al.*, *Enhanced derivation of osteogenic cells from murine embryonic stem cells after treatment with ionic dissolution products of 58S bioactive sol-gel glass*. *Tissue Eng*, 2005. **11**(3-4): p. 479-88.
156. Bielby, R.C., Boccaccini, A.R., Polak, J.M., *et al.*, *In vitro differentiation and in vivo mineralization of osteogenic cells derived from human embryonic stem cells*. *Tissue Eng*, 2004. **10**(9-10): p. 1518-25.
157. Kang, X., Xie, Y., Powell, H.M., *et al.*, *Adipogenesis of murine embryonic stem cells in a three-dimensional culture system using electrospun polymer scaffolds*. *Biomaterials*, 2007. **28**(3): p. 450-8.
158. Flaim, C.J., Chien, S., and Bhatia, S.N., *An extracellular matrix microarray for probing cellular differentiation*. *Nat Methods*, 2005. **2**(2): p. 119-25.

159. Flaim, C.J., Teng, D., Chien, S., *et al.*, *Combinatorial signaling microenvironments for studying stem cell fate*. *Stem Cells Dev*, 2008. **17**(1): p. 29-39.
160. Reubinoff, B.E., Itsykson, P., Turetsky, T., *et al.*, *Neural progenitors from human embryonic stem cells*. *Nat Biotechnol*, 2001. **19**(12): p. 1134-40.
161. Nistor, G.I., Totoiu, M.O., Haque, N., *et al.*, *Human embryonic stem cells differentiate into oligodendrocytes in high purity and myelinate after spinal cord transplantation*. *Glia*, 2005. **49**(3): p. 385-96.
162. Park, S., Lee, K.S., Lee, Y.J., *et al.*, *Generation of dopaminergic neurons in vitro from human embryonic stem cells treated with neurotrophic factors*. *Neurosci Lett*, 2004. **359**(1-2): p. 99-103.
163. Perrier, A.L., Tabar, V., Barberi, T., *et al.*, *Derivation of midbrain dopamine neurons from human embryonic stem cells*. *Proc Natl Acad Sci U S A*, 2004. **101**(34): p. 12543-8.
164. Wiles, M.V. and Johansson, B.M., *Embryonic stem cell development in a chemically defined medium*. *Exp Cell Res*, 1999. **247**(1): p. 241-8.
165. Kawasaki, H., Mizuseki, K., Nishikawa, S., *et al.*, *Induction of midbrain dopaminergic neurons from ES cells by stromal cell-derived inducing activity*. *Neuron*, 2000. **28**(1): p. 31-40.

166. Kawasaki, H., Suemori, H., Mizuseki, K., *et al.*, *Generation of dopaminergic neurons and pigmented epithelia from primate ES cells by stromal cell-derived inducing activity*. Proc Natl Acad Sci U S A, 2002. **99**(3): p. 1580-5.
167. Willerth, S.M., Arendas, K.J., Gottlieb, D.I., *et al.*, *Optimization of fibrin scaffolds for differentiation of murine embryonic stem cells into neural lineage cells*. Biomaterials, 2006. **27**(36): p. 5990-6003.
168. Yamazoe, H. and Iwata, H., *Efficient generation of dopaminergic neurons from mouse embryonic stem cells enclosed in hollow fibers*. Biomaterials, 2006. **27**(28): p. 4871-80.
169. Levenberg, S., Huang, N.F., Lavik, E., *et al.*, *Differentiation of human embryonic stem cells on three-dimensional polymer scaffolds*. Proc Natl Acad Sci U S A, 2003. **100**(22): p. 12741-6.
170. Levenberg, S., Burdick, J.A., Kraehenbuehl, T., *et al.*, *Neurotrophin-induced differentiation of human embryonic stem cells on three-dimensional polymeric scaffolds*. Tissue Eng, 2005. **11**(3-4): p. 506-12.
171. Cao, Y., Croll, T.I., Cooper-White, J.J., *et al.*, *Production and surface modification of polylactide-based polymeric scaffolds for soft-tissue engineering*. Methods Mol Biol, 2004. **238**: p. 87-112.

172. Lees, J.G., Lim, S.A., Croll, T., *et al.*, *Transplantation of 3D scaffolds seeded with human embryonic stem cells: biological features of surrogate tissue and teratoma-forming potential*. *Regen Med*, 2007. **2**(3): p. 289-300.
173. Moore, R.N., Dasgupta, A., Rajaei, N., *et al.*, *Enhanced differentiation of embryonic stem cells using co-cultivation with hepatocytes*. *Biotechnol Bioeng*, 2008.
174. Buttery, L.D.K., Bourne, S., Xynos, J.D., *et al.*, *Differentiation of Osteoblasts and in Vitro Bone Formation from Murine Embryonic Stem Cells*. *Tissue Engineering*, 2001. **7**(1): p. 89-99.
175. Kawasaki, H., Mizuseki, K., Nishikawa, S., *et al.*, *Induction of Midbrain Dopaminergic Neurons from ES Cells by Stromal Cell-Derived Inducing Activity*. *Neuron*, 2000. **28**(1): p. 31-40.
176. Nishikawa, S.I., Nishikawa, S., Hirashima, M., *et al.*, *Progressive lineage analysis by cell sorting and culture identifies FLK1+VE-cadherin+ cells at a diverging point of endothelial and hemopoietic lineages*. *Development*, 1998. **125**(9): p. 1747-1757.
177. Liu, H., Collins, S.F., and Suggs, L.J., *Three-dimensional culture for expansion and differentiation of mouse embryonic stem cells*. *Biomaterials*, 2006. **27**(36): p. 6004-6014.

178. Ferreira, L.S., Gerecht, S., Fuller, J., *et al.*, *Bioactive hydrogel scaffolds for controllable vascular differentiation of human embryonic stem cells*. *Biomaterials*, 2007. **28**(17): p. 2706-2717.
179. Battista, S., Guarnieri, D., Borselli, C., *et al.*, *The effect of matrix composition of 3D constructs on embryonic stem cell differentiation*. *Biomaterials*, 2005. **26**(31): p. 6194-6207.
180. Randle, W.L., Cha, J.M., Hwang, Y.-S., *et al.*, *Integrated 3-Dimensional Expansion and Osteogenic Differentiation of Murine Embryonic Stem Cells*. *Tissue Engineering*, 2007. **13**(12): p. 2957-2970.
181. Garreta, E., Genove, E., Borros, S., *et al.*, *Osteogenic Differentiation of Mouse Embryonic Stem Cells and Mouse Embryonic Fibroblasts in a Three-Dimensional Self-Assembling Peptide Scaffold*. *Tissue Engineering*, 2006. **12**(8): p. 2215-2227.
182. Liu, H. and Roy, K., *Biomimetic Three-Dimensional Cultures Significantly Increase Hematopoietic Differentiation Efficacy of Embryonic Stem Cells*. *Tissue Engineering*, 2005. **11**(1-2): p. 319-330.
183. Hwang, N.S., Kim, M.S., Sampattavanich, S., *et al.*, *Effects of Three-Dimensional Culture and Growth Factors on the Chondrogenic Differentiation of Murine Embryonic Stem Cells*. *Stem Cells*, 2006. **24**(2): p. 284-291.

184. Hwang, N.S., Varghese, S., Theprungsirikul, P., *et al.*, *Enhanced chondrogenic differentiation of murine embryonic stem cells in hydrogels with glucosamine*. *Biomaterials*, 2006. **27**(36): p. 6015-6023.
185. Kang, X., Xie, Y., Powell, H.M., *et al.*, *Adipogenesis of murine embryonic stem cells in a three-dimensional culture system using electrospun polymer scaffolds*. *Biomaterials*, 2007. **28**(3): p. 450-458.
186. Yamazoe, H. and Iwata, H., *Efficient generation of dopaminergic neurons from mouse embryonic stem cells enclosed in hollow fibers*. *Biomaterials*, 2006. **27**(28): p. 4871-4880.
187. Bielby, R.C., Boccaccini, A.R., Polak, J.M., *et al.*, *In Vitro Differentiation and In Vivo Mineralization of Osteogenic Cells Derived from Human Embryonic Stem Cells*. *Tissue Engineering*, 2004. **10**(9-10): p. 1518-1525.
188. Levenberg, S., Huang, N.F., Lavik, E., *et al.*, *Differentiation of human embryonic stem cells on three-dimensional polymer scaffolds*. *Proceedings of the National Academy of Sciences of the United States of America*, 2003. **100**(22): p. 12741-12746.
189. Shambloott, M.J., Axelman, J., Wang, S., *et al.*, *Derivation of pluripotent stem cells from cultured human primordial germ cells*. *Proc Natl Acad Sci U S A*, 1998. **95**(23): p. 13726-31.

190. Mitalipova, M.M., Rao, R.R., Hoyer, D.M., *et al.*, *Preserving the genetic integrity of human embryonic stem cells*. *Nat Biotechnol*, 2005. **23**(1): p. 19-20.
191. Heng, B.C., Liu, H., and Cao, T., *Feeder cell density--a key parameter in human embryonic stem cell culture*. *In Vitro Cell Dev Biol Anim*, 2004. **40**(8-9): p. 255-7.
192. Levenstein, M.E., Ludwig, T.E., Xu, R.H., *et al.*, *Basic fibroblast growth factor support of human embryonic stem cell self-renewal*. *Stem Cells*, 2006. **24**(3): p. 568-74.
193. Sato, N., Meijer, L., Skaltsounis, L., *et al.*, *Maintenance of pluripotency in human and mouse embryonic stem cells through activation of Wnt signaling by a pharmacological GSK-3-specific inhibitor*. *Nat Med*, 2004. **10**(1): p. 55-63.
194. Vallier, L., Alexander, M., and Pedersen, R.A., *Activin/Nodal and FGF pathways cooperate to maintain pluripotency of human embryonic stem cells*. *J Cell Sci*, 2005. **118**(Pt 19): p. 4495-509.
195. Abraham, S., Eroshenko, N., and Rao, R.R., *Role of bioinspired polymers in determination of pluripotent stem cell fate*. *Regen Med*, 2009. **4**(4): p. 561-78.
196. Stojkovic, M., Lako, M., Stojkovic, P., *et al.*, *Derivation of human embryonic stem cells from day-8 blastocysts recovered after three-step in vitro culture*. *Stem Cells*, 2004. **22**(5): p. 790-7.

197. Gospodarowicz, D., Delgado, D., and Vlodavsky, I., *Permissive effect of the extracellular matrix on cell proliferation in vitro*. Proc Natl Acad Sci U S A, 1980. **77**(7): p. 4094-8.
198. Plaia, T.W., Josephson, R., Liu, Y., *et al.*, *Characterization of a new NIH-registered variant human embryonic stem cell line, BG01V: a tool for human embryonic stem cell research*. Stem Cells, 2006. **24**(3): p. 531-46.
199. Zeng, X., Chen, J., Liu, Y., *et al.*, *BG01V: a variant human embryonic stem cell line which exhibits rapid growth after passaging and reliable dopaminergic differentiation*. Restor Neurol Neurosci, 2004. **22**(6): p. 421-8.
200. Noaksson, K., Zoric, N., Zeng, X., *et al.*, *Monitoring differentiation of human embryonic stem cells using real-time PCR*. Stem Cells, 2005. **23**(10): p. 1460-7.
201. Stahlberg, A., Aman, P., Ridell, B., *et al.*, *Quantitative real-time PCR method for detection of B-lymphocyte monoclonality by comparison of kappa and lambda immunoglobulin light chain expression*. Clin Chem, 2003. **49**(1): p. 51-9.
202. Carpenter, M.K., Rosler, E.S., Fisk, G.J., *et al.*, *Properties of four human embryonic stem cell lines maintained in a feeder-free culture system*. Dev Dyn, 2004. **229**(2): p. 243-58.

203. O'Connor, M.D., Kardel, M.D., Iosfina, I., *et al.*, *Alkaline phosphatase-positive colony formation is a sensitive, specific, and quantitative indicator of undifferentiated human embryonic stem cells*. *Stem Cells*, 2008. **26**(5): p. 1109-16.
204. Ludwig, T.E., Bergendahl, V., Levenstein, M.E., *et al.*, *Feeder-independent culture of human embryonic stem cells*. *Nat Methods*, 2006. **3**(8): p. 637-46.
205. Beattie, G.M., Lopez, A.D., Bucay, N., *et al.*, *Activin A maintains pluripotency of human embryonic stem cells in the absence of feeder layers*. *Stem Cells*, 2005. **23**(4): p. 489-95.
206. Wang, G., Zhang, H., Zhao, Y., *et al.*, *Noggin and bFGF cooperate to maintain the pluripotency of human embryonic stem cells in the absence of feeder layers*. *Biochem Biophys Res Commun*, 2005. **330**(3): p. 934-42.
207. Abraham, S., Sheridan, D.S., Miller, B., *et al.*, *Stable propagation of human embryonic and induced pluripotent stem cells on decellularized human substrates*. 2010, Virginia Commonwealth University.
208. Prowse, A.B., McQuade, L.R., Bryant, K.J., *et al.*, *A proteome analysis of conditioned media from human neonatal fibroblasts used in the maintenance of human embryonic stem cells*. *Proteomics*, 2005. **5**(4): p. 978-89.
209. Prowse, A.B., McQuade, L.R., Bryant, K.J., *et al.*, *Identification of potential pluripotency determinants for human embryonic stem cells following proteomic*

- analysis of human and mouse fibroblast conditioned media*. J Proteome Res, 2007. **6**(9): p. 3796-807.
210. Ludwig, T.E., Levenstein, M.E., Jones, J.M., *et al.*, *Derivation of human embryonic stem cells in defined conditions*. Nat Biotechnol, 2006. **24**(2): p. 185-7.
211. Roberts, S.B., Robichaux, J.L., Chavali, A.K., *et al.*, *Proteomic and network analysis characterize stage-specific metabolism in Trypanosoma cruzi*. BMC Syst Biol, 2009. **3**: p. 52.
212. Xu, P., Alves, J.M., Kitten, T., *et al.*, *Genome of the opportunistic pathogen Streptococcus sanguinis*. J Bacteriol, 2007. **189**(8): p. 3166-75.
213. Mitalipova, M., Calhoun, J., Shin, S., *et al.*, *Human embryonic stem cell lines derived from discarded embryos*. Stem Cells, 2003. **21**(5): p. 521-6.
214. Calhoun, J.D., Rao, R.R., Warrenfeltz, S., *et al.*, *Transcriptional profiling of initial differentiation events in human embryonic stem cells*. Biochem Biophys Res Commun, 2004. **323**(2): p. 453-64.
215. Sisino, G., Bellavia, D., Corallo, M., *et al.*, *A homemade cytospin apparatus*. Anal Biochem, 2006. **359**(2): p. 283-4.
216. Ramos, H., Shannon, P., and Aebersold, R., *The protein information and property explorer: an easy-to-use, rich-client web application for the management and functional analysis of proteomic data*. Bioinformatics, 2008. **24**(18): p. 2110-1.

217. Yao, S., Chen, S., Clark, J., *et al.*, *Long-term self-renewal and directed differentiation of human embryonic stem cells in chemically defined conditions.* Proc Natl Acad Sci U S A, 2006. **103**(18): p. 6907-12.
218. James, D., Levine, A.J., Besser, D., *et al.*, *TGFbeta/activin/nodal signaling is necessary for the maintenance of pluripotency in human embryonic stem cells.* Development, 2005. **132**(6): p. 1273-82.
219. Oklu, R. and Hesketh, R., *The latent transforming growth factor beta binding protein (LTBP) family.* Biochem J, 2000. **352 Pt 3**: p. 601-10.
220. Qi, X., Li, T.G., Hao, J., *et al.*, *BMP4 supports self-renewal of embryonic stem cells by inhibiting mitogen-activated protein kinase pathways.* Proc Natl Acad Sci U S A, 2004. **101**(16): p. 6027-32.
221. Watabe, T. and Miyazono, K., *Roles of TGF-beta family signaling in stem cell renewal and differentiation.* Cell Res, 2009. **19**(1): p. 103-15.
222. Adams, J.C., *Thrombospondin-1.* Int J Biochem Cell Biol, 1997. **29**(6): p. 861-5.
223. Crawford, S.E., Stellmach, V., Murphy-Ullrich, J.E., *et al.*, *Thrombospondin-1 is a major activator of TGF-beta1 in vivo.* Cell, 1998. **93**(7): p. 1159-70.
224. Iozzo, R.V., *The biology of the small leucine-rich proteoglycans. Functional network of interactive proteins.* J Biol Chem, 1999. **274**(27): p. 18843-6.

225. Ruoslahti, E. and Yamaguchi, Y., *Proteoglycans as modulators of growth factor activities*. Cell, 1991. **64**(5): p. 867-9.
226. Schonherr, E., Hausser, H., Beavan, L., *et al.*, *Decorin-type I collagen interaction. Presence of separate core protein-binding domains*. J Biol Chem, 1995. **270**(15): p. 8877-83.
227. Schonherr, E., Witsch-Prehm, P., Harrach, B., *et al.*, *Interaction of biglycan with type I collagen*. J Biol Chem, 1995. **270**(6): p. 2776-83.
228. Yamaguchi, Y., Mann, D.M., and Ruoslahti, E., *Negative regulation of transforming growth factor-beta by the proteoglycan decorin*. Nature, 1990. **346**(6281): p. 281-4.
229. Bao, S., Ouyang, G., Bai, X., *et al.*, *Periostin potently promotes metastatic growth of colon cancer by augmenting cell survival via the Akt/PKB pathway*. Cancer Cell, 2004. **5**(4): p. 329-39.
230. Sugiura, T., Takamatsu, H., Kudo, A., *et al.*, *Expression and characterization of murine osteoblast-specific factor 2 (OSF-2) in a baculovirus expression system*. Protein Expr Purif, 1995. **6**(3): p. 305-11.
231. Iemura, S., Yamamoto, T.S., Takagi, C., *et al.*, *Direct binding of follistatin to a complex of bone-morphogenetic protein and its receptor inhibits ventral and*

- epidermal cell fates in early Xenopus embryo*. Proc Natl Acad Sci U S A, 1998. **95**(16): p. 9337-42.
232. Sidis, Y., Tortoriello, D.V., Holmes, W.E., *et al.*, *Follistatin-related protein and follistatin differentially neutralize endogenous vs. exogenous activin*. Endocrinology, 2002. **143**(5): p. 1613-24.
233. Li, Y., Powell, S., Brunette, E., *et al.*, *Expansion of human embryonic stem cells in defined serum-free medium devoid of animal-derived products*. Biotechnol Bioeng, 2005. **91**(6): p. 688-98.
234. Braam, S.R., Zeinstra, L., Litjens, S., *et al.*, *Recombinant vitronectin is a functionally defined substrate that supports human embryonic stem cell self-renewal via alphavbeta5 integrin*. Stem Cells, 2008. **26**(9): p. 2257-65.
235. Esko, J.D. and Selleck, S.B., *Order out of chaos: assembly of ligand binding sites in heparan sulfate*. Annu Rev Biochem, 2002. **71**: p. 435-71.
236. Bernfield, M., Gotte, M., Park, P.W., *et al.*, *Functions of cell surface heparan sulfate proteoglycans*. Annu Rev Biochem, 1999. **68**: p. 729-77.
237. Lin, X., *Functions of heparan sulfate proteoglycans in cell signaling during development*. Development, 2004. **131**(24): p. 6009-21.
238. Harmer, N.J., *Insights into the role of heparan sulphate in fibroblast growth factor signalling*. Biochem Soc Trans, 2006. **34**(Pt 3): p. 442-5.

239. Nugent, M.A. and Edelman, E.R., *Kinetics of basic fibroblast growth factor binding to its receptor and heparan sulfate proteoglycan: a mechanism for cooperativity*. *Biochemistry*, 1992. **31**(37): p. 8876-83.
240. Roghani, M., Mansukhani, A., Dell'Era, P., *et al.*, *Heparin increases the affinity of basic fibroblast growth factor for its receptor but is not required for binding*. *J Biol Chem*, 1994. **269**(6): p. 3976-84.
241. Levenstein, M.E., Berggren, W.T., Lee, J.E., *et al.*, *Secreted proteoglycans directly mediate human embryonic stem cell-basic fibroblast growth factor 2 interactions critical for proliferation*. *Stem Cells*, 2008. **26**(12): p. 3099-107.
242. Sasaki, N., Okishio, K., Ui-Tei, K., *et al.*, *Heparan sulfate regulates self-renewal and pluripotency of embryonic stem cells*. *J Biol Chem*, 2008. **283**(6): p. 3594-606.
243. Kim, J., Chu, J., Shen, X., *et al.*, *An extended transcriptional network for pluripotency of embryonic stem cells*. *Cell*, 2008. **132**(6): p. 1049-61.
244. Wierzbicka-Patynowski, I. and Schwarzbauer, J.E., *The ins and outs of fibronectin matrix assembly*. *J Cell Sci*, 2003. **116**(Pt 16): p. 3269-76.
245. Baxter, M.A., Camarasa, M.V., Bates, N., *et al.*, *Analysis of the distinct functions of growth factors and tissue culture substrates necessary for the long-term self-renewal of human embryonic stem cell lines*. *Stem Cell Res*, 2009.

246. Hayashi, Y., Furue, M.K., Okamoto, T., *et al.*, *Integrins regulate mouse embryonic stem cell self-renewal*. *Stem Cells*, 2007. **25**(12): p. 3005-15.
247. Hoffman, L.M. and Carpenter, M.K., *Human embryonic stem cell stability*. *Stem Cell Rev*, 2005. **1**(2): p. 139-44.
248. Rowland, T.J., Miller, L.M., Blaschke, A.J., *et al.*, *Roles of Integrins in Human Induced Pluripotent Stem Cell Growth on Matrigel and Vitronectin*. *Stem Cells Dev*, 2009.
249. Haugen, P.K., Letourneau, P.C., Drake, S.L., *et al.*, *A cell-surface heparan sulfate proteoglycan mediates neural cell adhesion and spreading on a defined sequence from the C-terminal cell and heparin binding domain of fibronectin, FN-C/H II*. *J Neurosci*, 1992. **12**(7): p. 2597-608.
250. McCarthy, J.B., Hagen, S.T., and Furcht, L.T., *Human fibronectin contains distinct adhesion- and motility-promoting domains for metastatic melanoma cells*. *J Cell Biol*, 1986. **102**(1): p. 179-88.
251. Woods, A., Longley, R.L., Tumova, S., *et al.*, *Syndecan-4 binding to the high affinity heparin-binding domain of fibronectin drives focal adhesion formation in fibroblasts*. *Arch Biochem Biophys*, 2000. **374**(1): p. 66-72.

252. Pytela, R., Pierschbacher, M.D., and Ruoslahti, E., *Identification and isolation of a 140 kd cell surface glycoprotein with properties expected of a fibronectin receptor*. Cell, 1985. **40**(1): p. 191-8.
253. Bloom, L., Ingham, K.C., and Hynes, R.O., *Fibronectin regulates assembly of actin filaments and focal contacts in cultured cells via the heparin-binding site in repeat III13*. Mol Biol Cell, 1999. **10**(5): p. 1521-36.
254. Woods, A., Couchman, J.R., Johansson, S., *et al.*, *Adhesion and cytoskeletal organisation of fibroblasts in response to fibronectin fragments*. Embo J, 1986. **5**(4): p. 665-70.
255. Woods, A. and Couchman, J.R., *Syndecan-4 and focal adhesion function*. Curr Opin Cell Biol, 2001. **13**(5): p. 578-83.
256. Pellegrini, L., Burke, D.F., von Delft, F., *et al.*, *Crystal structure of fibroblast growth factor receptor ectodomain bound to ligand and heparin*. Nature, 2000. **407**(6807): p. 1029-34.
257. Walker, A., Turnbull, J.E., and Gallagher, J.T., *Specific heparan sulfate saccharides mediate the activity of basic fibroblast growth factor*. J Biol Chem, 1994. **269**(2): p. 931-5.
258. Dravid, G., Hammond, H., and Cheng, L., *Culture of human embryonic stem cells on human and mouse feeder cells*. Methods Mol Biol, 2006. **331**: p. 91-104.

259. Hovatta, O. and Skottman, H., *Feeder-free derivation of human embryonic stem-cell lines*. Lancet, 2005. **365**(9471): p. 1601-3.
260. Mannello, F. and Tonti, G.A., *Concise review: no breakthroughs for human mesenchymal and embryonic stem cell culture: conditioned medium, feeder layer, or feeder-free; medium with fetal calf serum, human serum, or enriched plasma; serum-free, serum replacement nonconditioned medium, or ad hoc formula? All that glitters is not gold!* Stem Cells, 2007. **25**(7): p. 1603-9.
261. Kim, S., Ahn, S.E., Lee, J.H., *et al.*, *A novel culture technique for human embryonic stem cells using porous membranes*. Stem Cells, 2007. **25**(10): p. 2601-9.
262. Gonzalez, R., Loring, J.F., and Snyder, E.Y., *Preparation of autogenic human feeder cells for growth of human embryonic stem cells*. Curr Protoc Stem Cell Biol, 2008. **Chapter 1**: p. Unit 1C 5 1-1C 5 15.
263. Ulitsky, I. and Shamir, R., *Identification of functional modules using network topology and high-throughput data*. BMC Syst Biol, 2007. **1**: p. 8.
264. Sheridan, S.D., Gil, S., Wilgo, M., *et al.*, *Microporous membrane growth substrates for embryonic stem cell culture and differentiation*. Methods Cell Biol, 2008. **86**: p. 29-57.

265. Wang, J., Rao, S., Chu, J., *et al.*, *A protein interaction network for pluripotency of embryonic stem cells*. *Nature*, 2006. **444**(7117): p. 364-8.
266. Zhou, Q., Chipperfield, H., Melton, D.A., *et al.*, *A gene regulatory network in mouse embryonic stem cells*. *Proc Natl Acad Sci U S A*, 2007. **104**(42): p. 16438-43.
267. Marson, A., Levine, S.S., Cole, M.F., *et al.*, *Connecting microRNA genes to the core transcriptional regulatory circuitry of embryonic stem cells*. *Cell*, 2008. **134**(3): p. 521-33.
268. Boyer, L.A., Lee, T.I., Cole, M.F., *et al.*, *Core transcriptional regulatory circuitry in human embryonic stem cells*. *Cell*, 2005. **122**(6): p. 947-56.
269. Cole, M.F., Johnstone, S.E., Newman, J.J., *et al.*, *Tcf3 is an integral component of the core regulatory circuitry of embryonic stem cells*. *Genes Dev*, 2008. **22**(6): p. 746-55.
270. Fouse, S.D., Shen, Y., Pellegrini, M., *et al.*, *Promoter CpG methylation contributes to ES cell gene regulation in parallel with Oct4/Nanog, PcG complex, and histone H3 K4/K27 trimethylation*. *Cell Stem Cell*, 2008. **2**(2): p. 160-9.
271. Rao, R.R., Calhoun, J.D., Qin, X., *et al.*, *Comparative transcriptional profiling of two human embryonic stem cell lines*. *Biotechnol Bioeng*, 2004. **88**(3): p. 273-86.

272. Muller, F.J., Laurent, L.C., Kostka, D., *et al.*, *Regulatory networks define phenotypic classes of human stem cell lines*. *Nature*, 2008. **455**(7211): p. 401-5.
273. Breems, D.A., Blokland, E.A., Siebel, K.E., *et al.*, *Stroma-contact prevents loss of hematopoietic stem cell quality during ex vivo expansion of CD34+ mobilized peripheral blood stem cells*. *Blood*, 1998. **91**(1): p. 111-7.
274. Vodyanik, M.A., Bork, J.A., Thomson, J.A., *et al.*, *Human embryonic stem cell-derived CD34+ cells: efficient production in the coculture with OP9 stromal cells and analysis of lymphohematopoietic potential*. *Blood*, 2005. **105**(2): p. 617-26.
275. Meng, Y., Eshghi, S., Li, Y.J., *et al.*, *Characterization of integrin engagement during defined human embryonic stem cell culture*. *Faseb J*, 2009.

Appendix A

Additional Figures for Chapter 2

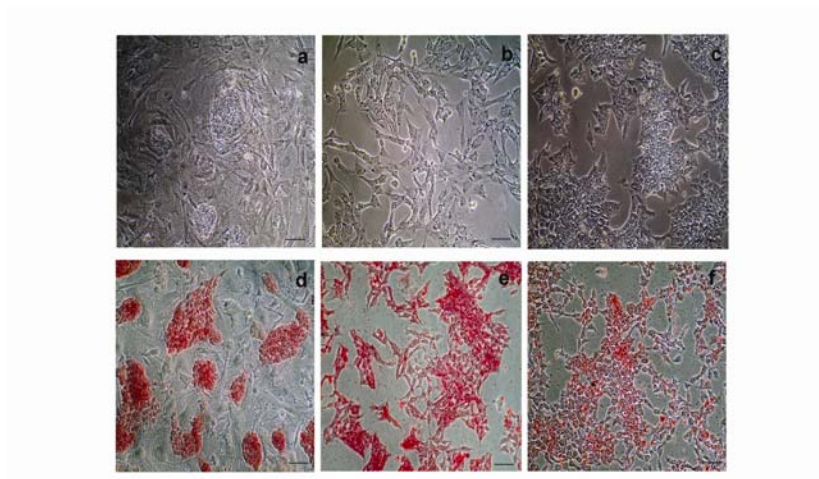


Figure 1: Karyotypically abnormal BG01v hESCs maintain high nuclear to cytoplasmic ratio and tight boundaries on control, MEFs (a) and spread out to form a continuous layer on acellular HFF (b) and HDF substrates (c). Positive expression of alkaline phosphatase in BG01v ES cells propagated for 15 passages on MEF (d), aHFF (e) and aHDF (f) was observed, Scale bar = 100 μ m.

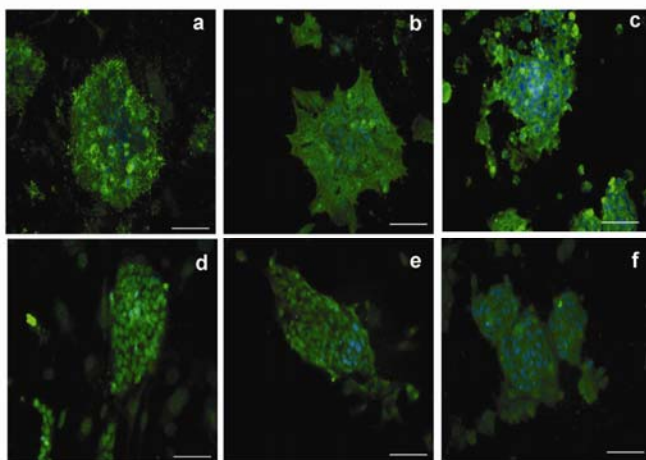


Figure 2: Positive expression of stage specific embryonic antigen (SSEA4) (a-c) in BG01v ES cells propagated for 15 passages on MEF (a), aHFF (b) and aHDF (c). Expression of OCT4 (d-f) in BG01v cells propagated for 15 passages on MEF (d), aHFF (e) and aHDF (f) was observed, Scale bar = 100 μ m.

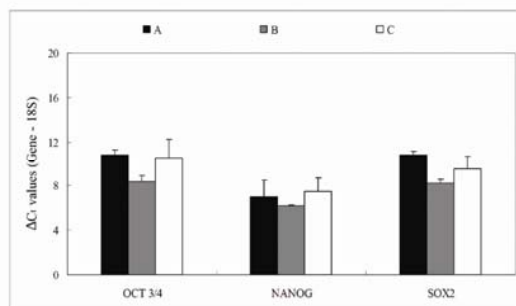


Figure 3: Normalized gene expression of *undifferentiated markers* in BG01v on MEFs (A); BG01v on acellular HFF (B) and WA09 on acellular HDFs (C). There is no significant difference ($p > 0.01$) between the groups ($n=3$) indicating comparable pluripotent gene expression.

Appendix B

Tables of proteins identified in proteomic analysis in all three substrates acellular MEFs, acellular HFFs and acellular HDFs.

Results acquired from proteomic analysis of acellular MEFs

Proteins	Gene Symbol	Description	Biological Process_max	Molecular Function_max	Cellular Component_max
11459	Acta1	actin, alpha 1, skeletal muscle	muscle contraction (GO:0006936)	ATP binding (GO:0005524)	actin cytoskeleton (GO:0015629)
11461	Actb	actin, beta, cytoplasmic		ATP binding (GO:0005524)	cytosol (GO:0005829)
11657	Alb	albumin	transport (GO:0006810)	copper ion binding (GO:0005507)	cytoplasm (GO:0005737)
11749	Anxa6	annexin A6	calcium ion transport (GO:0006816)	calcium ion binding (GO:0005509)	perinuclear region of cytoplasm (GO:0048471)
11946	Atp5a1	ATP synthase, H+ transporting, mitochondrial F1 complex, alpha subunit, isoform 1	ATP synthesis coupled proton transport (GO:0015986)	hydrogen ion transporting ATP synthase activity, rotational mechanism (GO:0046933)	mitochondrial inner membrane (GO:0005743)
12306	Anxa2	annexin A2	fibrinolysis (GO:0042730)	phospholipase inhibitor activity (GO:0004859)	stress fiber (GO:0001725)
12406	Serpinh1	serine (or cysteine) peptidase inhibitor, clade H, member 1	response to stress (GO:0006950)	serine-type endopeptidase inhibitor activity (GO:0004867)	endoplasmic reticulum (GO:0005783)
12842	Col1a1	collagen, type I, alpha 1	phosphate transport (GO:0006817)	extracellular matrix structural constituent (GO:0005201)	cytoplasm (GO:0005737)
12843	Col1a2	collagen, type I, alpha 2	phosphate transport (GO:0006817)	extracellular matrix structural constituent (GO:0005201)	cytoplasm (GO:0005737)
13346	Des	desmin	muscle development (GO:0007517)	structural constituent of cytoskeleton (GO:0005200)	Z disc (GO:0030018)
13628	Eef1a2	eukaryotic translation elongation factor 1 alpha 2	anti-apoptosis (GO:0006916)	GTPase activity (GO:0003924)	nucleus (GO:0005634)
14115	Fbln2	fibulin 2		calcium ion binding (GO:0005509)	proteinaceous extracellular matrix (GO:0005578)
14118	Fbn1	fibrillin 1		calcium ion binding (GO:0005509)	microfibril (GO:0001527)
14268	Fn1	fibronectin 1	transmembrane receptor protein tyrosine kinase signaling pathway (GO:0007169)	heparin binding (GO:0008201)	apical plasma membrane (GO:0016324)
14735	Gpc4	glypican 4			anchored to membrane (GO:0031225)
14827	Pdia3	protein disulfide isomerase associated 3	positive regulation of apoptosis (GO:0043065)	protein disulfide isomerase activity (GO:0003756)	endoplasmic reticulum (GO:0005783)
15482	Hspa1l	heat shock protein 1-like	spermatogenesis (GO:0007283)	ATP binding (GO:0005524)	
15530	Hspg2	perlecan (heparan sulfate proteoglycan 2)	protein localization (GO:0008104)	protein binding (GO:0005515)	proteinaceous extracellular matrix (GO:0005578)
16412	Itgb1	integrin beta 1 (fibronectin receptor beta)	sarcomere organization (GO:0045214)	integrin binding (GO:0005178)	integrin complex (GO:0008305)
16661	Krt10	keratin 10		protein binding (GO:0005515)	keratin filament (GO:0045095)
16691	Krt8	keratin 8	tumor necrosis factor-mediated signaling pathway (GO:0033209)	protein binding (GO:0005515)	Z disc (GO:0030018)
16905	Lmna	lamin A	nuclear membrane organization and biogenesis (GO:0006998)	protein binding (GO:0005515)	lamin filament (GO:0005638)
16952	Anxa1	annexin A1	regulation of cell proliferation (GO:0042127)	phospholipase A2 inhibitor activity (GO:0019834)	nucleus (GO:0005634)
17254	Slc3a2	solute carrier family 3 (activators of dibasic and neutral amino acid transport), member 2	amino acid transport (GO:0006865)	cation binding (GO:0043169)	integral to membrane (GO:0016021)
17880	Myh11	myosin, heavy polypeptide 11, smooth muscle	smooth muscle contraction (GO:0006939)	ATP binding (GO:0005524)	striated muscle thick filament (GO:0005863)
17886	Myh9	myosin, heavy polypeptide 9, non-muscle	meiotic spindle organization and biogenesis (GO:0000212)	actin-dependent ATPase activity (GO:0030898)	cell-cell adherens junction (GO:0005913)
19132	Prph	peripherin	intermediate filament cytoskeleton organization and biogenesis (GO:0045104)	protein binding (GO:0005515)	neurofilament (GO:0005883)
21825	Thbs1	thrombospondin 1	negative regulation of angiogenesis (GO:0016525)	heparin binding (GO:0008201)	extracellular space (GO:0005615)

21838	Thy1	thymus cell antigen 1, theta	retinal cone cell development (GO:0046549)		anchored to external side of plasma membrane (GO:0031362)
22073	Prss3	protease, serine, 3		serine-type endopeptidase activity (GO:0004252)	cellular_component (GO:0005575)
22186	Uba52	ubiquitin A-52 residue ribosomal protein fusion product 1	protein modification process (GO:0006464)	structural constituent of ribosome (GO:0003735)	nucleus (GO:0005634)
22352	Vim	vimentin	intermediate filament-based process (GO:0045103)	protein binding (GO:0005515)	type III intermediate filament (GO:0045098)
54652	Cacna1f	calcium channel, voltage-dependent, alpha 1F subunit	cellular calcium ion homeostasis (GO:0006874)	voltage-gated calcium channel activity (GO:0005245)	integral to membrane of membrane fraction (GO:0000299)
66395	Ahnak	AHNAK nucleoprotein (desmoyokin)	intracellular signaling cascade (GO:0007242)		intercellular junction (GO:0005911)
71853	Pdia6	protein disulfide isomerase associated 6	cell redox homeostasis (GO:0045454)	protein disulfide isomerase activity (GO:0003756)	endoplasmic reticulum (GO:0005783)
77579	Myh10	myosin, heavy polypeptide 10, non-muscle	substrate-bound cell migration, cell extension (GO:0006930)	actin-dependent ATPase activity (GO:0030898)	stress fiber (GO:0001725)
81601	Htatip	HIV-1 tat interactive protein, homolog (human)	positive regulation of transcription from RNA polymerase II promoter (GO:0045944)	histone acetyltransferase activity (GO:0004402)	chromatin (GO:0000785)
101706	Numa1	nuclear mitotic apparatus protein 1		tubulin binding (GO:0015631)	nucleus (GO:0005634)
109624	Cald1	caldesmon 1	regulation of smooth muscle contraction (GO:0006940)	actin binding (GO:0003779)	actin cap (GO:0030478)
223915	Krt73	keratin 73		structural molecule activity (GO:0005198)	intermediate filament (GO:0005882)
223917	Krt79	keratin 79		structural molecule activity (GO:0005198)	intermediate filament (GO:0005882)
230594	Zcchc11	zinc finger, CCHC domain containing 11	negative regulation of NF-kappaB transcription factor activity (GO:0032088)	zinc ion binding (GO:0008270)	nucleus (GO:0005634)
236892	EG236892	predicted gene, EG236892			
238831	Ppwd1	peptidylprolyl isomerase domain and WD repeat containing 1	mRNA processing (GO:0006397)	peptidyl-prolyl cis-trans isomerase activity (GO:0003755)	spliceosome (GO:0005681)
11464	Actc1	actin, alpha, cardiac	muscle thin filament assembly (GO:0030240)	ATP binding (GO:0005524)	actin cytoskeleton (GO:0015629)
11632	Aip	aryl-hydrocarbon receptor-interacting protein	protein folding (GO:0006457)	transcription cofactor activity (GO:0003712)	membrane fraction (GO:0005624)
11750	Anxa7	annexin A7	cellular calcium ion homeostasis (GO:0006874)	calcium ion binding (GO:0005509)	nucleus (GO:0005634)
11757	Prdx3	peroxiredoxin 3	oxidation reduction (GO:0055114)	identical protein binding (GO:0042802)	mitochondrion (GO:0005739)
11853	Rhoc	ras homolog gene family, member C	small GTPase mediated signal transduction (GO:0007264)	GTP binding (GO:0005525)	nucleus (GO:0005634)
11947	Atp5b	ATP synthase, H+ transporting mitochondrial F1 complex, beta subunit	ATP synthesis coupled proton transport (GO:0015986)	hydrogen-exporting ATPase activity, phosphorylative mechanism (GO:0008553)	mitochondrial inner membrane (GO:0005743)
12317	Calr	calreticulin	cortical actin cytoskeleton organization and biogenesis (GO:0030866)	zinc ion binding (GO:0008270)	microsome (GO:0005792)
12330	Canx	calnexin	protein folding (GO:0006457)	calcium ion binding (GO:0005509)	endoplasmic reticulum (GO:0005783)
12331	Cap1	CAP, adenylate cyclase-associated protein 1 (yeast)	receptor-mediated endocytosis (GO:0006898)	actin binding (GO:0003779)	cortical actin cytoskeleton (GO:0030864)
12336	Capns1	calpain, small subunit 1		calcium-dependent cysteine-type endopeptidase activity (GO:0004198)	cytoplasm (GO:0005737)
12345	Capzb	capping protein (actin filament) muscle Z-line, beta	barbed-end actin filament capping (GO:0051016)	actin binding (GO:0003779)	intercalated disc (GO:0014704)
12417	Cbx3	chromobox homolog 3 (Drosophila HP1 gamma)	chromatin assembly or disassembly (GO:0006333)	chromatin binding (GO:0003682)	nuclear centromeric heterochromatin (GO:0031618)
12419	Cbx5	chromobox homolog 5 (Drosophila HP1a)	chromatin assembly or disassembly (GO:0006333)	chromatin binding (GO:0003682)	nuclear heterochromatin (GO:0005720)
12492	Scarb2	scavenger receptor class B, member 2	cell adhesion (GO:0007155)	receptor activity (GO:0004872)	lysosome (GO:0005764)
12540	Cdc42	cell division cycle 42 homolog (S. cerevisiae)	filopodium formation (GO:0046847)	GTPase activity (GO:0003924)	filopodium (GO:0030175)

12631	Cfl1	cofilin 1, non-muscle	actin filament organization (GO:0007015)	actin binding (GO:0003779)	cortical actin cytoskeleton (GO:0030864)
12751	Tpp1	tripeptidyl peptidase I	proteolysis (GO:0006508)	serine-type endopeptidase activity (GO:0004252)	lysosome (GO:0005764)
12814	Col11a1	collagen, type XI, alpha 1	phosphate transport (GO:0006817)	extracellular matrix structural constituent (GO:0005201)	cytoplasm (GO:0005737)
12825	Col3a1	collagen, type III, alpha 1	phosphate transport (GO:0006817)	extracellular matrix structural constituent (GO:0005201)	cytoplasm (GO:0005737)
12831	Col5a1	collagen, type V, alpha 1	phosphate transport (GO:0006817)	heparin binding (GO:0008201)	collagen type V (GO:0005588)
12866	Cox7a2	cytochrome c oxidase, subunit VIIa 2		cytochrome-c oxidase activity (GO:0004129)	mitochondrial inner membrane (GO:0005743)
12903	Crabp1	cellular retinoic acid binding protein I	transport (GO:0006810)	retinal binding (GO:0016918)	cytoplasm (GO:0005737)
12934	Dpysl2	dihydropyrimidinase-like 2	nervous system development (GO:0007399)	hydrolase activity (GO:0016787)	mitochondrion (GO:0005739)
13030	Ctsb	cathepsin B	proteolysis (GO:0006508)	cysteine-type endopeptidase activity (GO:0004197)	lysosome (GO:0005764)
13040	Ctss	cathepsin S	proteolysis (GO:0006508)	cysteine-type endopeptidase activity (GO:0004197)	lysosome (GO:0005764)
13205	Ddx3x	DEAD/H (Asp-Glu-Ala-Asp/His) box polypeptide 3, X-linked		ATP binding (GO:0005524)	nucleus (GO:0005634)
13207	Ddx5	DEAD (Asp-Glu-Ala-Asp) box polypeptide 5	mRNA processing (GO:0006397)	ATP binding (GO:0005524)	nucleus (GO:0005634)
13627	Eef1a1	eukaryotic translation elongation factor 1 alpha 1	translation (GO:0006412)	GTP binding (GO:0005525)	cytoplasm (GO:0005737)
13629	Eef2	eukaryotic translation elongation factor 2	translation (GO:0006412)	GTPase activity (GO:0003924)	cytoplasm (GO:0005737)
13885	Esd	esterase D/formylglutathione hydrolase		S-formylglutathione hydrolase activity (GO:0018738)	cytoplasmic membrane-bounded vesicle (GO:0016023)
14230	Fkbp10	FK506 binding protein 10	protein folding (GO:0006457)	peptidyl-prolyl cis-trans isomerase activity (GO:0003755)	endoplasmic reticulum (GO:0005783)
14314	Fstl1	folliculin-like 1		heparin binding (GO:0008201)	extracellular space (GO:0005615)
14319	Fth1	ferritin heavy chain 1	cellular iron ion homeostasis (GO:0006879)	ferric iron binding (GO:0008199)	
14376	Ganab	alpha glucosidase 2 alpha neutral subunit	N-glycan processing (GO:0006491)	glucosidase activity (GO:0015926)	endoplasmic reticulum (GO:0005783)
14678	Gnai2	guanine nucleotide binding protein (G protein), alpha inhibiting 2	G-protein signaling, adenylate cyclase inhibiting pathway (GO:0007193)	GTPase activity (GO:0003924)	
14679	Gnai3	guanine nucleotide binding protein (G protein), alpha inhibiting 3	G-protein coupled receptor protein signaling pathway (GO:0007186)	GTPase activity (GO:0003924)	heterotrimeric G-protein complex (GO:0005834)
14688	Gnb1	guanine nucleotide binding protein (G protein), beta 1	phototransduction, visible light (GO:0007603)	GTPase activity (GO:0003924)	heterotrimeric G-protein complex (GO:0005834)
14693	Gnb2	guanine nucleotide binding protein (G protein), beta 2	G-protein coupled receptor protein signaling pathway (GO:0007186)	GTPase activity (GO:0003924)	heterotrimeric G-protein complex (GO:0005834)
14696	Gnb4	guanine nucleotide binding protein (G protein), beta 4	G-protein coupled receptor protein signaling pathway (GO:0007186)	GTPase activity (GO:0003924)	heterotrimeric G-protein complex (GO:0005834)
14824	Gm	granulin	positive regulation of epithelial cell proliferation (GO:0050679)	phospholipase A2 activity (GO:0004623)	mitochondrion (GO:0005739)
14828	Hspa5	heat shock protein 5	ER overload response (GO:0006983)	ATP binding (GO:0005524)	endoplasmic reticulum (GO:0005783)
15382	Hnrnpa1	heterogeneous nuclear ribonucleoprotein A1	mRNA processing (GO:0006397)	RNA binding (GO:0003723)	nucleus (GO:0005634)
15387	Hnrmpk	heterogeneous nuclear ribonucleoprotein K	mRNA processing (GO:0006397)	DNA binding (GO:0003677)	nucleus (GO:0005634)
15388	Hnrnpl	heterogeneous nuclear ribonucleoprotein L	mRNA processing (GO:0006397)	RNA binding (GO:0003723)	pronucleus (GO:0045120)
15481	Hspa8	heat shock protein 8	chaperone cofactor-dependent protein folding (GO:0051085)	ATPase activity, coupled (GO:0042623)	cytoplasm (GO:0005737)
15510	Hspd1	heat shock protein 1 (chaperonin)	protein folding (GO:0006457)	ATP binding (GO:0005524)	mitochondrial inner membrane (GO:0005743)

15512	Hspa2	heat shock protein 2	response to stress (GO:0006950)	ATP binding (GO:0005524)	mitochondrion (GO:0005739)
15516	Hsp90ab1	heat shock protein 90kDa alpha (cytosolic), class B member 1	protein folding (GO:0006457)	ATP binding (GO:0005524)	mitochondrion (GO:0005739)
15519	Hsp90aa1	heat shock protein 90, alpha (cytosolic), class A member 1	positive regulation of cytotoxic T cell differentiation (GO:0045585)	ATP binding (GO:0005524)	cytosol (GO:0005829)
16211	Kpnb1	karyopherin (importin) beta 1	ribosomal protein import into nucleus (GO:0006610)	protein transporter activity (GO:0008565)	nucleus (GO:0005634)
16592	Fabp5	fatty acid binding protein 5, epidermal	phosphatidylcholine biosynthetic process (GO:0006656)	lipid binding (GO:0008289)	cytoplasm (GO:0005737)
16665	Krt15	keratin 15		structural molecule activity (GO:0005198)	intermediate filament (GO:0005882)
16678	Krt1	keratin 1		structural molecule activity (GO:0005198)	intermediate filament (GO:0005882)
16681	Krt2	keratin 2		structural molecule activity (GO:0005198)	intermediate filament (GO:0005882)
16687	Krt6a	keratin 6A	intermediate filament organization (GO:0045109)	structural molecule activity (GO:0005198)	intermediate filament (GO:0005882)
16777	Lamb1-1	laminin B1 subunit 1	cell adhesion (GO:0007155)	enzyme binding (GO:0019899)	laminin-10 complex (GO:0043259)
16852	Lgals1	lectin, galactose binding, soluble 1	myoblast differentiation (GO:0045445)	galactose binding (GO:0005534)	extracellular space (GO:0005615)
16854	Lgals3	lectin, galactose binding, soluble 3	skeletal development (GO:0001501)	IgE binding (GO:0019863)	nucleus (GO:0005634)
16976	Lrpap1	low density lipoprotein receptor-related protein associated protein 1		heparin binding (GO:0008201)	endoplasmic reticulum (GO:0005783)
17118	Marcks	myristoylated alanine rich protein kinase C substrate		actin binding (GO:0003779)	germinal vesicle (GO:0042585)
17534	Mrc2	mannose receptor, C type 2	endocytosis (GO:0006897)	calcium ion binding (GO:0005509)	integral to membrane (GO:0016021)
17931	Ppp1r12a	protein phosphatase 1, regulatory (inhibitor) subunit 12A		phosphoprotein phosphatase activity (GO:0004721)	cytoplasm (GO:0005737)
17975	Ncl	nucleolin		DNA binding (GO:0003677)	nucleus (GO:0005634)
18102	Nme1	non-metastatic cells 1, protein (NM23A) expressed in	GTP biosynthetic process (GO:0006183)	ATP binding (GO:0005524)	microsome (GO:0005792)
18103	Nme2	non-metastatic cells 2, protein (NM23B) expressed in	GTP biosynthetic process (GO:0006183)	ATP binding (GO:0005524)	mitochondrion (GO:0005739)
18148	Npm1	nucleophosmin 1	regulation of DNA damage response, signal transduction by p53 class mediator (GO:0043516)	rRNA binding (GO:0019843)	nucleus (GO:0005634)
18220	Nucb1	nucleobindin 1		calcium ion binding (GO:0005509)	Golgi apparatus (GO:0005794)
18451	P4ha1	procollagen-proline, 2-oxoglutarate 4-dioxygenase (proline 4-hydroxylase), alpha 1 polypeptide	peptidyl-proline hydroxylation to 4-hydroxy-L-proline (GO:0018401)	procollagen-proline 4-dioxygenase activity (GO:0004656)	endoplasmic reticulum (GO:0005783)
18452	P4ha2	procollagen-proline, 2-oxoglutarate 4-dioxygenase (proline 4-hydroxylase), alpha II polypeptide	peptidyl-proline hydroxylation to 4-hydroxy-L-proline (GO:0018401)	procollagen-proline 4-dioxygenase activity (GO:0004656)	endoplasmic reticulum (GO:0005783)
18453	P4hb	prolyl 4-hydroxylase, beta polypeptide	peptidyl-proline hydroxylation to 4-hydroxy-L-proline (GO:0018401)	procollagen-proline 4-dioxygenase activity (GO:0004656)	microsome (GO:0005792)
18477	Prdx1	peroxiredoxin 1	regulation of NF-kappaB import into nucleus (GO:0042345)	peroxiredoxin activity (GO:0051920)	nucleus (GO:0005634)
18483	Palm	paralemmin	negative regulation of cAMP biosynthetic process (GO:0030818)	D3 dopamine receptor binding (GO:0031750)	cytoplasm (GO:0005737)
18537	Pcmt1	protein-L-isoaspartate (D-aspartate) O-methyltransferase 1	protein amino acid methylation (GO:0006479)	protein-L-isoaspartate (D-aspartate) O-methyltransferase activity (GO:0004719)	cytoplasm (GO:0005737)
18746	Pkm2	pyruvate kinase, muscle	glycolysis (GO:0006096)	pyruvate kinase activity (GO:0004743)	mitochondrion (GO:0005739)
19025	Ctsa	cathepsin A	proteolysis (GO:0006508)	serine carboxypeptidase activity (GO:0004185)	lysosome (GO:0005764)
19156	Psap	prosaposin	sphingolipid metabolic process (GO:0006665)		lysosome (GO:0005764)
19170	Psmb1	proteasome (prosome, macropain) subunit, beta	ubiquitin-dependent protein catabolic process	threonine endopeptidase activity (GO:0004298)	nucleus (GO:0005634)

		type 1	(GO:0006511)		
19173	Psmb5	proteasome (prosome, macropain) subunit, beta type 5	proteasomal ubiquitin-dependent protein catabolic process (GO:0043161)	threonine endopeptidase activity (GO:0004298)	nucleus (GO:0005634)
19186	Psmc1	proteasome (prosome, macropain) 28 subunit, alpha	antigen processing and presentation of exogenous antigen (GO:0019884)	proteasome activator activity (GO:0008538)	cytosol (GO:0005829)
19205	Ptbp1	polypyrimidine tract binding protein 1	mRNA processing (GO:0006397)	RNA binding (GO:0003723)	nucleus (GO:0005634)
19326	Rab11b	RAB11B, member RAS oncogene family	small GTPase mediated signal transduction (GO:0007264)	GTP binding (GO:0005525)	cytoplasmic membrane-bounded vesicle (GO:0016023)
19656	Rbmxrt	RNA binding motif protein, X chromosome retrogene	mRNA processing (GO:0006397)	RNA binding (GO:0003723)	nucleus (GO:0005634)
19983	Rpl5	ribosomal protein L5	translation (GO:0006412)	5S rRNA binding (GO:0008097)	nucleus (GO:0005634)
20102	Rps4x	ribosomal protein S4, X-linked	translation (GO:0006412)	rRNA binding (GO:0019843)	cytosolic small ribosomal subunit (GO:0022627)
20194	S100a10	S100 calcium binding protein A10 (calpactin)		calcium ion binding (GO:0005509)	
20333	Sec22b	SEC22 vesicle trafficking protein homolog B (S. cerevisiae)	ER to Golgi vesicle-mediated transport (GO:0006888)		Golgi membrane (GO:0000139)
20334	Sec23a	SEC23A (S. cerevisiae)	ER to Golgi vesicle-mediated transport (GO:0006888)	zinc ion binding (GO:0008270)	COPII vesicle coat (GO:0030127)
20362	8-Sep	septin 8	cell cycle (GO:0007049)	GTP binding (GO:0005525)	septin complex (GO:0031105)
20740	Sdna2	spectrin alpha 2	barbed-end actin filament capping (GO:0051016)	actin binding (GO:0003779)	fascia adherens (GO:0005916)
20742	Sdna2	spectrin beta 2	barbed-end actin filament capping (GO:0051016)	actin binding (GO:0003779)	nucleus (GO:0005634)
20867	Stip1	stress-induced phosphoprotein 1	response to stress (GO:0006950)	binding (GO:0005488)	nucleus (GO:0005634)
20901	Strap	serine/threonine kinase receptor associated protein	negative regulation of transcription from RNA polymerase II promoter (GO:0000122)	receptor binding (GO:0005102)	nucleus (GO:0005634)
20911	Stxbp2	syntaxin binding protein 2	vesicle docking during exocytosis (GO:0006904)	syntaxin binding (GO:0019905)	
21881	Tkt	transketolase	regulation of growth (GO:0040008)	transketolase activity (GO:0004802)	
22027	Hsp90b1	heat shock protein 90, beta (Grp94), member 1	protein folding (GO:0006457)	ATP binding (GO:0005524)	endoplasmic reticulum (GO:0005783)
22074	Try4	trypsin 4		serine-type endopeptidase activity (GO:0004252)	cellular_component (GO:0005575)
22154	Tubb5	tubulin, beta 5	spindle assembly (GO:0051225)	GTPase activity (GO:0003924)	microtubule (GO:0005874)
22240	Dpysl3	dihydropyrimidinase-like 3	nervous system development (GO:0007399)	hydrolase activity (GO:0016787)	cytoplasm (GO:0005737)
22333	Vdac1	voltage-dependent anion channel 1	apoptosis (GO:0006915)	voltage-gated anion channel activity (GO:0008308)	mitochondrial outer membrane (GO:0005741)
22334	Vdac2	voltage-dependent anion channel 2	anion transport (GO:0006820)	voltage-gated anion channel activity (GO:0008308)	mitochondrial outer membrane (GO:0005741)
22627	Ywhae	tyrosine 3-monooxygenase/tryptophan 5-monooxygenase activation protein, epsilon polypeptide	negative regulation of protein amino acid dephosphorylation (GO:0035308)	monooxygenase activity (GO:0004497)	mitochondrion (GO:0005739)
26388	Ifi202b	interferon activated gene 202B			nucleus (GO:0005634)
26433	Plod3	procollagen-lysine, 2-oxoglutarate 5-dioxygenase 3	protein modification process (GO:0006464)	iron ion binding (GO:0005506)	endoplasmic reticulum (GO:0005783)
26442	Psmc5	proteasome (prosome, macropain) subunit, alpha type 5	ubiquitin-dependent protein catabolic process (GO:0006511)	threonine endopeptidase activity (GO:0004298)	nucleus (GO:0005634)
26949	Vat1	vesicle amine transport protein 1 homolog (T californica)	oxidation reduction (GO:0055114)	zinc ion binding (GO:0008270)	
27041	G3bp1	Ras-GTPase-activating protein SH3-domain binding protein 1	transport (GO:0006810)	ATP binding (GO:0005524)	nucleus (GO:0005634)
52398	SEPT11	septin 11	cell cycle (GO:0007049)	GTP binding (GO:0005525)	septin complex (GO:0031105)

53328	Pgrmc1	progesterone receptor membrane component 1		transition metal ion binding (GO:0046914)	microsome (GO:0005792)
53379	Hnrnpa2b1	heterogeneous nuclear ribonucleoprotein A2/B1	mRNA processing (GO:0006397)	RNA binding (GO:0003723)	nucleus (GO:0005634)
53857	Tuba8	tubulin, alpha 8	microtubule cytoskeleton organization and biogenesis (GO:0000226)	GTPase activity (GO:0003924)	microtubule (GO:0005874)
54401	Ywhab	tyrosine 3-monooxygenase/tryptophan 5-monooxygenase activation protein, beta polypeptide	protein targeting (GO:0006605)	monooxygenase activity (GO:0004497)	cytoplasm (GO:0005737)
54609	Ubqln2	ubiquilin 2	protein modification process (GO:0006464)		nucleus (GO:0005634)
55944	Eif3d	eukaryotic translation initiation factor 3, subunit D	translation (GO:0006412)	translation initiation factor activity (GO:0003743)	
56085	Ubqln1	ubiquilin 1	protein modification process (GO:0006464)	intermediate filament binding (GO:0019215)	nucleus (GO:0005634)
56491	Vapb	vesicle-associated membrane protein, associated protein B and C		structural molecule activity (GO:0005198)	integral to membrane (GO:0016021)
56692	Map2k1ip1	mitogen-activated protein kinase kinase 1 interacting protein 1	activation of MAPKK activity (GO:0000186)	kinase activity (GO:0016301)	late endosome (GO:0005770)
56735	Krt71	keratin 71	cytoskeleton organization and biogenesis (GO:0007010)	structural constituent of cytoskeleton (GO:0005200)	intermediate filament (GO:0005882)
66073	Txndc12	thioredoxin domain containing 12 (endoplasmic reticulum)	cell redox homeostasis (GO:0045454)	protein-disulfide reductase (glutathione) activity (GO:0019153)	endoplasmic reticulum (GO:0005783)
66427	Cyb5b	cytochrome b5 type B	transport (GO:0006810)	iron ion binding (GO:0005506)	mitochondrial inner membrane (GO:0005743)
66870	Serp1	Serpine1 mRNA binding protein 1		RNA binding (GO:0003723)	nucleus (GO:0005634)
67300	Cltc	clathrin, heavy polypeptide (Hc)	intracellular protein transport (GO:0006886)	protein binding (GO:0005515)	clathrin coat of trans-Golgi network vesicle (GO:0030130)
67454	1200009F10Rik	RIKEN cDNA 1200009F10 gene	induction of apoptosis (GO:0006917)	protein binding (GO:0005515)	endoplasmic reticulum (GO:0005783)
68585	Rtn4	reticulon 4	negative regulation of axon extension (GO:0030517)	protein binding (GO:0005515)	integral to endoplasmic reticulum membrane (GO:0030176)
68682	Slc44a2	solute carrier family 44, member 2	transport (GO:0006810)		integral to membrane (GO:0016021)
68794	Finc	filamin C, gamma (actin binding protein 280)	actin filament-based process (GO:0030029)	actin binding (GO:0003779)	actin cytoskeleton (GO:0015629)
69162	Sec31a	SEC31 homolog A (S. cerevisiae)	protein transport (GO:0015031)		endosome (GO:0005768)
69386	Hist1h4h	histone cluster 1, H4h	nucleosome assembly (GO:0006334)	DNA binding (GO:0003677)	nucleus (GO:0005634)
71679	Atp5h	ATP synthase, H+ transporting, mitochondrial F0 complex, subunit d	ATP synthesis coupled proton transport (GO:0015986)	hydrogen ion transporting ATP synthase activity, rotational mechanism (GO:0046933)	mitochondrial inner membrane (GO:0005743)
71770	Ap2b1	adaptor-related protein complex 2, beta 1 subunit	intracellular protein transport (GO:0006886)	clathrin binding (GO:0030276)	transport vesicle (GO:0030133)
72333	Pald	palladin, cytoskeletal associated protein		actin binding (GO:0003779)	nucleus (GO:0005634)
77055	Krt76	keratin 76			intermediate filament (GO:0005882)
80294	Pofut2	protein O-fucosyltransferase 2	fucose metabolic process (GO:0006004)	peptide-O-fucosyltransferase activity (GO:0046922)	endoplasmic reticulum (GO:0005783)
81910	Rrbp1	ribosome binding protein 1	intracellular protein transport across a membrane (GO:0065002)	receptor activity (GO:0004872)	integral to endoplasmic reticulum membrane (GO:0030176)
83397	Akap12	A kinase (PRKA) anchor protein (gravin) 12	protein targeting (GO:0006605)	receptor signaling complex scaffold activity (GO:0030159)	cytoskeleton (GO:0005856)
93695	Gpnmb	glycoprotein (transmembrane) nmb	cell adhesion (GO:0007155)	heparin binding (GO:0008201)	integral to plasma membrane (GO:0005887)
97122	Hist2h4	histone cluster 2, H4	nucleosome assembly (GO:0006334)	DNA binding (GO:0003677)	nucleus (GO:0005634)
97908	Hist1h3g	histone cluster 1, H3g	nucleosome assembly (GO:0006334)	DNA binding (GO:0003677)	nucleus (GO:0005634)
98238	Lrrc59	leucine rich repeat containing 59		protein binding (GO:0005515)	microsome (GO:0005792)

109168	5730596K20Rik	RIKEN cDNA 5730596K20 gene		GTPase activity (GO:0003924)	integral to membrane (GO:0016021)
109672	Cyb5	cytochrome b-5	fatty acid metabolic process (GO:0006631)	stearoyl-CoA 9-desaturase activity (GO:0004768)	microsome (GO:0005792)
109754	Cyb5r3	cytochrome b5 reductase 3	sterol biosynthetic process (GO:0016126)	cytochrome-b5 reductase activity (GO:0004128)	mitochondrial inner membrane (GO:0005743)
110611	Hdlbp	high density lipoprotein (HDL) binding protein	steroid metabolic process (GO:0008202)	RNA binding (GO:0003723)	nucleus (GO:0005634)
114228	Prss1	protease, serine, 1 (trypsin 1)			
192176	Flna	filamin, alpha	early endosome to late endosome transport (GO:0045022)	protein kinase C binding (GO:0005080)	trans-Golgi network (GO:0005802)
208263	Tor1aip1	torsin A interacting protein 1		lamin binding (GO:0005521)	nucleus (GO:0005634)
216197	Ckap4	cytoskeleton-associated protein 4		protein binding (GO:0005515)	endoplasmic reticulum (GO:0005783)
227613	Tubb2c	tubulin, beta 2c	microtubule-based movement (GO:0007018)	GTPase activity (GO:0003924)	microtubule (GO:0005874)
229279	Hnrnpa3	heterogeneous nuclear ribonucleoprotein A3	mRNA processing (GO:0006397)	RNA binding (GO:0003723)	nucleus (GO:0005634)
230257	Rod1	ROD1 regulator of differentiation 1 (S. pombe)	mRNA processing (GO:0006397)	RNA binding (GO:0003723)	nucleus (GO:0005634)
235072	SEPT7	septin 7	cell cycle (GO:0007049)	GTP binding (GO:0005525)	synaptosome (GO:0019717)
4232	MEST	mesoderm specific transcript homolog (mouse)	mesoderm development (GO:0007498)	protein binding (GO:0005515)	integral to membrane (GO:0016021)
11363	Acadl	acyl-Coenzyme A dehydrogenase, long-chain	fatty acid metabolic process (GO:0006631)	long-chain-acyl-CoA dehydrogenase activity (GO:0004466)	mitochondrion (GO:0005739)
11429	Aco2	aconitase 2, mitochondrial	tricarboxylic acid cycle (GO:0006099)	aconitate hydratase activity (GO:0003994)	mitochondrion (GO:0005739)
11465	Actg1	actin, gamma, cytoplasmic 1	sarcomere organization (GO:0045214)	ATP binding (GO:0005524)	actin cytoskeleton (GO:0015629)
11472	Actn2	actinin alpha 2	muscle contraction (GO:0006936)	thyroid hormone receptor coactivator activity (GO:0030375)	Z disc (GO:0030018)
11475	Acta2	actin, alpha 2, smooth muscle, aorta		ATP binding (GO:0005524)	cytoskeleton (GO:0005856)
11555	Adrb2	adrenergic receptor, beta 2	G-protein signaling, adenylate cyclase activating pathway (GO:0007189)	beta2-adrenergic receptor activity (GO:0004941)	nucleus (GO:0005634)
11669	Aldh2	aldehyde dehydrogenase 2, mitochondrial	oxidation reduction (GO:0055114)	aldehyde dehydrogenase (NAD) activity (GO:0004029)	mitochondrion (GO:0005739)
11740	Slc25a5	solute carrier family 25 (mitochondrial carrier, adenine nucleotide translocator), member 5	transport (GO:0006810)	transporter activity (GO:0005215)	mitochondrial inner membrane (GO:0005743)
11746	Anxa4	annexin A4	kidney development (GO:0001822)	calcium ion binding (GO:0005509)	apical plasma membrane (GO:0016324)
11747	Anxa5	annexin A5	negative regulation of coagulation (GO:0050819)	calcium ion binding (GO:0005509)	
11773	Ap2m1	adaptor protein complex AP-2, mu1	intracellular protein transport (GO:0006886)	protein binding (GO:0005515)	clathrin coat of coated pit (GO:0030132)
11820	App	amyloid beta (A4) precursor protein	smooth endoplasmic reticulum calcium ion homeostasis (GO:0051563)	serine-type endopeptidase inhibitor activity (GO:0004867)	Golgi apparatus (GO:0005794)
11886	Asah1	N-acylsphingosine amidohydrolase 1		ceramidase activity (GO:0017040)	lysosome (GO:0005764)
11928	Atp1a1	ATPase, Na+/K+ transporting, alpha 1 polypeptide	regulation of cellular pH (GO:0030641)	sodium:potassium-exchanging ATPase activity (GO:0005391)	microsome (GO:0005792)
11938	Atp2a2	ATPase, Ca++ transporting, cardiac muscle, slow twitch 2	cellular calcium ion homeostasis (GO:0006874)	calcium-transporting ATPase activity (GO:0005388)	microsome (GO:0005792)
11944	Atp4a	ATPase, H+/K+ exchanging, gastric, alpha polypeptide	potassium ion transport (GO:0006813)	hydrogen:potassium-exchanging ATPase activity (GO:0008900)	integral to membrane (GO:0016021)
11949	Atp5c1	ATP synthase, H+ transporting, mitochondrial F1 complex, gamma polypeptide 1	ATP synthesis coupled proton transport (GO:0015986)	hydrogen ion transporting ATP synthase activity, rotational mechanism (GO:0046933)	mitochondrial inner membrane (GO:0005743)
11950	Atp5f1	ATP synthase, H+ transporting, mitochondrial F0 complex, subunit b, isoform 1	ATP synthesis coupled proton transport (GO:0015986)	hydrogen ion transporting ATP synthase activity, rotational mechanism (GO:0046933)	mitochondrial inner membrane (GO:0005743)
12034	Phb2	prohibitin 2	regulation of transcription, DNA-dependent (GO:0006355)	receptor activity (GO:0004872)	mitochondrial inner membrane (GO:0005743)

12304	Pdia4	protein disulfide isomerase associated 4	cell redox homeostasis (GO:0045454)	protein disulfide isomerase activity (GO:0003756)	endoplasmic reticulum (GO:0005783)
12313	Calm1	calmodulin 1	positive regulation of DNA binding (GO:0043388)	calcium ion binding (GO:0005509)	
12314	Calm2	calmodulin 2	G-protein coupled receptor protein signaling pathway (GO:0007186)	calcium ion binding (GO:0005509)	cytoplasm (GO:0005737)
12315	Calm3	calmodulin 3	G-protein coupled receptor protein signaling pathway (GO:0007186)	calcium ion binding (GO:0005509)	cytoplasm (GO:0005737)
12321	Calu	calumenin		calcium ion binding (GO:0005509)	endoplasmic reticulum (GO:0005783)
12385	Ctnna1	catenin (cadherin associated protein), alpha 1	negative regulation of neuroblast proliferation (GO:0007406)	actin filament binding (GO:0051015)	zonula adherens (GO:0005915)
12387	Ctnnb1	catenin (cadherin associated protein), beta 1	negative regulation of osteoclast differentiation (GO:0045671)	double-stranded DNA binding (GO:0003690)	fascia adherens (GO:0005916)
12388	Ctnnd1	catenin (cadherin associated protein), delta 1	regulation of transcription, DNA-dependent (GO:0006355)	protein binding (GO:0005515)	nucleus (GO:0005634)
12389	Cav1	caveolin, caveolae protein 1	inactivation of MAPK activity (GO:0000188)	protease activator activity (GO:0016504)	integral to plasma membrane (GO:0005887)
12390	Cav2	caveolin 2	negative regulation of endothelial cell proliferation (GO:0001937)	protein homodimerization activity (GO:0042803)	integral to plasma membrane (GO:0005887)
12520	Cd81	CD 81 antigen	positive regulation of B cell proliferation (GO:0030890)		integral to membrane (GO:0016021)
12527	Cd9	CD9 antigen	fusion of sperm to egg plasma membrane (GO:0007342)	protein binding (GO:0005515)	integral to membrane (GO:0016021)
12797	Cnn1	calponin 1	actomyosin structure organization and biogenesis (GO:0031032)	actin binding (GO:0003779)	
12816	Col12a1	collagen, type XII, alpha 1	phosphate transport (GO:0006817)	protein binding (GO:0005515)	cytoplasm (GO:0005737)
12835	Col6a3	collagen, type VI, alpha 3		structural molecule activity (GO:0005198)	extracellular space (GO:0005615)
12837	Col8a1	collagen, type VIII, alpha 1	phosphate transport (GO:0006817)	protein binding (GO:0005515)	cytoplasm (GO:0005737)
12858	Cox5a	cytochrome c oxidase, subunit Va		iron ion binding (GO:0005506)	mitochondrial inner membrane (GO:0005743)
12861	Cox6a1	cytochrome c oxidase, subunit VI a, polypeptide 1		cytochrome-c oxidase activity (GO:0004129)	mitochondrion (GO:0005739)
12974	Cs	citrate synthase	tricarboxylic acid cycle (GO:0006099)	citrate (Si)-synthase activity (GO:0004108)	mitochondrion (GO:0005739)
13200	Ddost	dolichyl-di-phosphooligosaccharide-protein glycotransferase	protein amino acid N-linked glycosylation via asparagine (GO:0018279)	dolichyl-diphosphooligosaccharide-protein glycotransferase activity (GO:0004579)	endoplasmic reticulum (GO:0005783)
13382	Dld	dihydrolipoamide dehydrogenase	regulation of membrane potential (GO:0042391)	FAD binding (GO:0050660)	acrosomal matrix (GO:0043159)
13427	Dync1i2	dynein cytoplasmic 1 intermediate chain 2		motor activity (GO:0003774)	microtubule (GO:0005874)
13717	Eln	elastin	stress fiber formation (GO:0043149)	extracellular matrix structural constituent (GO:0005201)	proteinaceous extracellular matrix (GO:0005578)
13849	Ephx1	epoxide hydrolase 1, microsomal	aromatic compound catabolic process (GO:0019439)	epoxide hydrolase activity (GO:0004301)	microsome (GO:0005792)
14089	Fap	fibroblast activation protein	proteolysis (GO:0006508)	serine-type endopeptidase activity (GO:0004252)	integral to membrane (GO:0016021)
14113	Fbl	fibrillarin	rRNA processing (GO:0006364)	methyltransferase activity (GO:0008168)	Cajal body (GO:0015030)
14119	Fbn2	fibrillin 2	embryonic limb morphogenesis (GO:0030326)	calcium ion binding (GO:0005509)	microfibril (GO:0001527)
14251	Flot1	flotillin 1			integral to membrane (GO:0016021)
14433	Gapdh	glyceraldehyde-3-phosphate dehydrogenase	glycolysis (GO:0006096)	glyceraldehyde-3-phosphate dehydrogenase (phosphorylating) activity (GO:0004365)	mitochondrion (GO:0005739)
14660	Gls	glutaminase	glutamine catabolic process (GO:0006543)	glutaminase activity (GO:0004359)	
14661	Glud1	glutamate dehydrogenase 1	transmembrane receptor protein tyrosine kinase signaling pathway (GO:0007169)	ATP binding (GO:0005524)	mitochondrial inner membrane (GO:0005743)
14674	Gna13	guanine nucleotide binding protein, alpha 13	Rho protein signal transduction (GO:0007266)	GTPase activity (GO:0003924)	heterotrimeric G-protein complex

					(GO:0005834)
14694	Gnb21	guanine nucleotide binding protein (G protein), beta polypeptide 2 like 1	activation of protein kinase C activity (GO:0007205)	GTPase activity (GO:0003924)	heterotrimeric G-protein complex (GO:0005834)
14719	Got2	glutamate oxaloacetate transaminase 2, mitochondrial	aspartate biosynthetic process (GO:0006532)	aspartate transaminase activity (GO:0004069)	mitochondrial inner membrane (GO:0005743)
14886	Gtf2i	general transcription factor II I	regulation of transcription, DNA-dependent (GO:0006355)	DNA binding (GO:0003677)	nucleus (GO:0005634)
14919	Gucy2e	guanylate cyclase 2e	cGMP biosynthetic process (GO:0006182)	ATP binding (GO:0005524)	integral to membrane (GO:0016021)
14950	H13	histocompatibility 13		aspartic-type endopeptidase activity (GO:0004190)	endoplasmic reticulum (GO:0005783)
14957	Hist1h1d	histone cluster 1, H1d	nucleosome assembly (GO:0006334)	DNA binding (GO:0003677)	nucleus (GO:0005634)
14958	H1f0	H1 histone family, member 0	nucleosome assembly (GO:0006334)	DNA binding (GO:0003677)	nucleus (GO:0005634)
15211	Hexa	hexosaminidase A	ganglioside catabolic process (GO:0006689)	beta-N-acetylhexosaminidase activity (GO:0004563)	lysosome (GO:0005764)
15289	Hmgb1	high mobility group box 1	regulation of transcription, DNA-dependent (GO:0006355)	heparin binding (GO:0008201)	chromatin (GO:0000785)
15364	Hmga2	high mobility group AT-hook 2	regulation of transcription, DNA-dependent (GO:0006355)	DNA binding (GO:0003677)	nuclear chromosome (GO:0000228)
15369	Hmox2	heme oxygenase (decycling) 2	heme oxidation (GO:0006788)	iron ion binding (GO:0005506)	microsome (GO:0005792)
15441	Hp1bp3	heterochromatin protein 1, binding protein 3	nucleosome assembly (GO:0006334)	DNA binding (GO:0003677)	nucleus (GO:0005634)
15502	Dnaja1	DnaJ (Hsp40) homolog, subfamily A, member 1	androgen receptor signaling pathway (GO:0030521)	zinc ion binding (GO:0008270)	membrane (GO:0016020)
15951	Iff204	interferon activated gene 204	DNA damage response, signal transduction by p53 class mediator resulting in induction of apoptosis (GO:0042771)	transcription cofactor activity (GO:0003712)	nucleus (GO:0005634)
16906	Lmnb1	lamin B1		structural molecule activity (GO:0005198)	lamin filament (GO:0005638)
16971	Lrp1	low density lipoprotein receptor-related protein 1	apoptotic cell clearance (GO:0043277)	calcium ion binding (GO:0005509)	nucleus (GO:0005634)
16997	Ltbp2	latent transforming growth factor beta binding protein 2	metabolic process (GO:0008152)	calcium ion binding (GO:0005509)	extracellular region (GO:0005576)
16998	Ltbp3	latent transforming growth factor beta binding protein 3	transforming growth factor beta receptor signaling pathway (GO:0007179)	calcium ion binding (GO:0005509)	proteinaceous extracellular matrix (GO:0005578)
17150	Mfap2	microfibrillar-associated protein 2			microfibril (GO:0001527)
17257	Mecp2	methyl CpG binding protein 2	negative regulation of transcription, DNA-dependent (GO:0045892)	mRNA binding (GO:0003729)	heterochromatin (GO:0000792)
17276	Mela	melanoma antigen	transposition (GO:0032196)	RNA-directed DNA polymerase activity (GO:0003964)	integral to membrane (GO:0016021)
17448	Mdh2	malate dehydrogenase 2, NAD (mitochondrial)	glycolysis (GO:0006096)	L-malate dehydrogenase activity (GO:0030060)	mitochondrial inner membrane (GO:0005743)
17470	Cd200	Cd200 antigen		protein binding (GO:0005515)	integral to membrane (GO:0016021)
17709	COX2	cytochrome c oxidase subunit II	transport (GO:0006810)	copper ion binding (GO:0005507)	mitochondrion (GO:0005739)
17758	Mtap4	microtubule-associated protein 4	negative regulation of microtubule depolymerization (GO:0007026)		microtubule (GO:0005874)
17904	Myl6	myosin, light polypeptide 6, alkali, smooth muscle and non-muscle	muscle filament sliding (GO:0030049)	calcium ion binding (GO:0005509)	unconventional myosin complex (GO:0016461)
17995	Ndufv1	NADH dehydrogenase (ubiquinone) flavoprotein 1	mitochondrial electron transport, NADH to ubiquinone (GO:0006120)	NADH dehydrogenase (ubiquinone) activity (GO:0008137)	mitochondrial inner membrane (GO:0005743)
18000	SEPT2	septin 2	cytokinesis (GO:0000910)	GTPase activity (GO:0003924)	synaptosome (GO:0019717)
18186	Nrp1	neuropilin 1	negative regulation of axon extension (GO:0030517)	semaphorin receptor activity (GO:0017154)	integral to membrane (GO:0016021)
18194	Nsdhl	NAD(P) dependent steroid dehydrogenase-like	sterol biosynthetic process (GO:0016126)	3-beta-hydroxy-delta5-steroid dehydrogenase activity (GO:0003854)	integral to membrane (GO:0016021)

18242	Oat	ornithine aminotransferase		ornithine-oxo-acid transaminase activity (GO:0004587)	mitochondrion (GO:0005739)
18596	Pdgfrb	platelet derived growth factor receptor, beta polypeptide	regulation of peptidyl-tyrosine phosphorylation (GO:0050730)	vascular endothelial growth factor receptor activity (GO:0005021)	integral to membrane (GO:0016021)
18654	Pgf	placental growth factor	ureteric bud branching (GO:0001658)	growth factor activity (GO:0008083)	extracellular space (GO:0005615)
18673	Phb	prohibitin	DNA replication (GO:0006260)		mitochondrial inner membrane (GO:0005743)
18674	Slc25a3	solute carrier family 25 (mitochondrial carrier, phosphate carrier), member 3	transport (GO:0006810)	symporter activity (GO:0015293)	mitochondrial inner membrane (GO:0005743)
18810	Plec1	plectin 1		actin binding (GO:0003779)	cytoskeleton (GO:0005856)
18984	Por	P450 (cytochrome) oxidoreductase	oxidation reduction (GO:0055114)	iron ion binding (GO:0005506)	microsome (GO:0005792)
19012	Ppap2a	phosphatidic acid phosphatase 2a	diacylglycerol biosynthetic process (GO:0006651)	phosphatidate phosphatase activity (GO:0008195)	integral to plasma membrane (GO:0005887)
19035	Ppib	peptidylprolyl isomerase B	protein folding (GO:0006457)	peptidyl-prolyl cis-trans isomerase activity (GO:0003755)	endoplasmic reticulum (GO:0005783)
19223	Ptgis	prostaglandin I2 (prostacyclin) synthase	prostaglandin biosynthetic process (GO:0001516)	iron ion binding (GO:0005506)	endoplasmic reticulum (GO:0005783)
19353	Rac1	RAS-related C3 botulinum substrate 1	embryonic olfactory bulb interneuron precursor migration (GO:0021831)	GTPase activity (GO:0003924)	cytoplasmic membrane-bounded vesicle (GO:0016023)
19384	Ran	RAN, member RAS oncogene family	protein import into nucleus (GO:0006606)	GTPase activity (GO:0003924)	nucleus (GO:0005634)
19672	Rcn1	reticulocalbin 1		calcium ion binding (GO:0005509)	endoplasmic reticulum (GO:0005783)
19896	Rpl10a	ribosomal protein L10A	translation (GO:0006412)	structural constituent of ribosome (GO:0003735)	ribosome (GO:0005840)
19899	Rpl18	ribosomal protein L18	translation (GO:0006412)	structural constituent of ribosome (GO:0003735)	cytoplasm (GO:0005737)
19921	Rpl19	ribosomal protein L19	translation (GO:0006412)	RNA binding (GO:0003723)	cytosolic large ribosomal subunit (GO:0022625)
19944	Rpl29	ribosomal protein L29	translation (GO:0006412)	structural constituent of ribosome (GO:0003735)	ribosome (GO:0005840)
19951	Rpl32	ribosomal protein L32	translation (GO:0006412)	RNA binding (GO:0003723)	cytosolic large ribosomal subunit (GO:0022625)
19988	Rpl6	ribosomal protein L6	translation (GO:0006412)	structural constituent of ribosome (GO:0003735)	ribosome (GO:0005840)
19989	Rpl7	ribosomal protein L7	translation (GO:0006412)	RNA binding (GO:0003723)	large ribosomal subunit (GO:0015934)
20014	Rpn2	ribophorin II	protein amino acid N-linked glycosylation via asparagine (GO:0018279)	dolichyl-diphosphooligosaccharide-protein glycotransferase activity (GO:0004579)	endoplasmic reticulum (GO:0005783)
20044	Rps14	ribosomal protein S14	translation (GO:0006412)	RNA binding (GO:0003723)	cytosolic small ribosomal subunit (GO:0022627)
20068	Rps17	ribosomal protein S17	translation (GO:0006412)	structural constituent of ribosome (GO:0003735)	cytosolic small ribosomal subunit (GO:0022627)
20091	Rps3a	ribosomal protein S3a	translation (GO:0006412)	structural constituent of ribosome (GO:0003735)	nucleus (GO:0005634)
20116	Rps8	ribosomal protein S8			ribosome (GO:0005840)
20195	S100a11	S100 calcium binding protein A11 (calgizzarin)	spermatogenesis (GO:0007283)	cytokine activity (GO:0005125)	cytoplasm (GO:0005737)
20340	Glg1	golgi apparatus protein 1		fibroblast growth factor binding (GO:0017134)	Golgi apparatus (GO:0005794)
20501	Slc16a1	solute carrier family 16 (monocarboxylic acid transporters), member 1	organic anion transport (GO:0015711)	secondary active monocarboxylate transmembrane transporter activity (GO:0015355)	integral to membrane (GO:0016021)
20818	Srpb	signal recognition particle receptor, B subunit		GTP binding (GO:0005525)	endoplasmic reticulum (GO:0005783)
21345	Tagln	transgelin	cytoskeleton organization and biogenesis (GO:0007010)		cytoplasm (GO:0005737)
21402	Skp1a	S-phase kinase-associated protein 1A	ubiquitin-dependent protein catabolic process (GO:0006511)	kinase activity (GO:0016301)	SCF ubiquitin ligase complex (GO:0019005)
21762	Psm2	proteasome (prosome, macropain) 26S subunit, non-ATPase, 2			cytosol (GO:0005829)

21894	Tln1	talín 1	cortical actin cytoskeleton organization and biogenesis (GO:0030866)	actin binding (GO:0003779)	focal adhesion (GO:0005925)
21917	Tmpo	thymopoietin	regulation of transcription (GO:0045449)	hormone activity (GO:0005179)	chromatin (GO:0000785)
22004	Tpm2	tropomyosin 2, beta	muscle contraction (GO:0006936)	actin binding (GO:0003779)	cytoskeleton (GO:0005856)
22121	Rpl13a	ribosomal protein L13a	translation (GO:0006412)	structural constituent of ribosome (GO:0003735)	large ribosomal subunit (GO:0015934)
22143	Tuba1b	tubulin, alpha 1B	microtubule-based movement (GO:0007018)	GTPase activity (GO:0003924)	microtubule (GO:0005874)
22146	Tuba1c	tubulin, alpha 1C	microtubule-based movement (GO:0007018)	GTPase activity (GO:0003924)	microtubule (GO:0005874)
22187	Ubb	ubiquitin B	protein modification process (GO:0006464)	protein binding (GO:0005515)	nucleus (GO:0005634)
22335	Vdac3	voltage-dependent anion channel 3	nerve-nerve synaptic transmission (GO:0007270)	voltage-gated anion channel activity (GO:0008308)	mitochondrial outer membrane (GO:0005741)
22385	Baz1b	bromodomain adjacent to zinc finger domain, 1B	chromatin remodeling (GO:0006338)	zinc ion binding (GO:0008270)	centromeric heterochromatin (GO:0005721)
22608	Ybx1	Y box protein 1	mRNA processing (GO:0006397)	single-stranded DNA binding (GO:0003697)	nucleus (GO:0005634)
23825	Banf1	barrier to autointegration factor 1	provirus integration (GO:0019047)	DNA binding (GO:0003677)	nucleus (GO:0005634)
23876	Fbln5	fibulin 5	cell adhesion (GO:0007155)	calcium ion binding (GO:0005509)	extracellular space (GO:0005615)
23937	Mab21l2	mab-21-like 2 (C. elegans)	camera-type eye development (GO:0043010)		nucleus (GO:0005634)
23943	Mbc2	membrane bound C2 domain containing protein			integral to membrane (GO:0016021)
26914	H2afy	H2A histone family, member Y	nucleosome assembly (GO:0006334)	DNA binding (GO:0003677)	Barr body (GO:0001740)
26942	Spag1	sperm associated antigen 1	single fertilization (GO:0007338)	GTP binding (GO:0005525)	cytoplasm (GO:0005737)
26961	Rpl8	ribosomal protein L8	translation (GO:0006412)	rRNA binding (GO:0019843)	cytosolic large ribosomal subunit (GO:0022625)
27050	Rps3	ribosomal protein S3	translation (GO:0006412)	RNA binding (GO:0003723)	small ribosomal subunit (GO:0015935)
27061	Bcap31	B-cell receptor-associated protein 31	apoptosis (GO:0006915)	receptor activity (GO:0004872)	integral to plasma membrane (GO:0005887)
27176	Rpl7a	ribosomal protein L7a	translation (GO:0006412)	structural constituent of ribosome (GO:0003735)	polysomal ribosome (GO:0042788)
27367	Rpl3	ribosomal protein L3	translation (GO:0006412)	structural constituent of ribosome (GO:0003735)	cytoplasm (GO:0005737)
27425	Atp5l	ATP synthase, H+ transporting, mitochondrial F0 complex, subunit g	ATP synthesis coupled proton transport (GO:0015986)	hydrogen-exporting ATPase activity, phosphorylative mechanism (GO:0008553)	mitochondrial inner membrane (GO:0005743)
28080	Atp5o	ATP synthase, H+ transporting, mitochondrial F1 complex, O subunit	ATP synthesis coupled proton transport (GO:0015986)	hydrogen-exporting ATPase activity, phosphorylative mechanism (GO:0008553)	mitochondrion (GO:0005739)
28185	Tomm70a	translocase of outer mitochondrial membrane 70 homolog A (yeast)		receptor activity (GO:0004872)	mitochondrion (GO:0005739)
28295	D10Jhu81e	DNA segment, Chr 10, Johns Hopkins University 81 expressed			mitochondrion (GO:0005739)
30960	Vapa	vesicle-associated membrane protein, associated protein A		structural molecule activity (GO:0005198)	endoplasmic reticulum (GO:0005783)
50706	Postn	periostin, osteoblast specific factor	extracellular matrix organization and biogenesis (GO:0030198)	heparin binding (GO:0008201)	proteinaceous extracellular matrix (GO:0005578)
50790	Acs14	acyl-CoA synthetase long-chain family member 4	fatty acid metabolic process (GO:0006631)	long-chain-fatty-acid-CoA ligase activity (GO:0004467)	peroxisome (GO:0005777)
51788	H2afz	H2A histone family, member Z	nucleosome assembly (GO:0006334)	DNA binding (GO:0003677)	Barr body (GO:0001740)
52377	Rcn3	reticulocalbin 3, EF-hand calcium binding domain		calcium ion binding (GO:0005509)	endoplasmic reticulum (GO:0005783)
53322	Nucb2	nucleobindin 2	cellular calcium ion homeostasis (GO:0006874)	calcium ion binding (GO:0005509)	nuclear outer membrane (GO:0005640)
53421	Sec61a1	Sec61 alpha 1 subunit (S. cerevisiae)	intracellular protein transport across a membrane (GO:0065002)	P-P-bond-hydrolysis-driven protein transmembrane transporter activity (GO:0015450)	endoplasmic reticulum (GO:0005783)

54637	Praf2	PRA1 domain family 2	protein transport (GO:0015031)		integral to membrane (GO:0016021)
56334	Tmed2	transmembrane emp24 domain trafficking protein 2	protein transport (GO:0015031)	protein binding (GO:0005515)	Golgi apparatus (GO:0005794)
56401	Lepre1	leprecan 1	protein metabolic process (GO:0019538)	procollagen-proline 3-dioxygenase activity (GO:0019797)	nucleus (GO:0005634)
56428	Mtch2	mitochondrial carrier homolog 2 (C. elegans)	transport (GO:0006810)	binding (GO:0005488)	mitochondrial inner membrane (GO:0005743)
56451	Suclq1	succinate-CoA ligase, GDP-forming, alpha subunit	tricarboxylic acid cycle (GO:0006099)	succinate-CoA ligase (ADP-forming) activity (GO:0004775)	mitochondrial inner membrane (GO:0005743)
56454	Aldh18a1	aldehyde dehydrogenase 18 family, member A1	proline biosynthetic process (GO:0006561)	glutamate 5-kinase activity (GO:0004349)	mitochondrion (GO:0005739)
56457	Clptm1	cleft lip and palate associated transmembrane protein 1	regulation of T cell differentiation in the thymus (GO:0033081)		external side of plasma membrane (GO:0009897)
56463	Snd1	staphylococcal nuclease and tudor domain containing 1	RNA interference (GO:0016246)	nuclease activity (GO:0004518)	nucleus (GO:0005634)
56702	Hist1h1b	histone cluster 1, H1b	nucleosome assembly (GO:0006334)	DNA binding (GO:0003677)	nucleus (GO:0005634)
57170	Dolpp1	dolichyl pyrophosphate phosphatase 1	protein amino acid N-linked glycosylation (GO:0006487)	dolichyl/diphosphatase activity (GO:0047874)	integral to endoplasmic reticulum membrane (GO:0030176)
57377	Gcs1	glucosidase 1	oligosaccharide metabolic process (GO:0009311)	mannosyl-oligosaccharide glucosidase activity (GO:0004573)	endoplasmic reticulum (GO:0005783)
59021	Rab2a	RAB2A, member RAS oncogene family	small GTPase mediated signal transduction (GO:0007264)	GTP binding (GO:0005525)	endoplasmic reticulum (GO:0005783)
64660	Mrps24	mitochondrial ribosomal protein S24		structural constituent of ribosome (GO:0003735)	mitochondrial small ribosomal subunit (GO:0005763)
65019	Rpl23	ribosomal protein L23	ribosomal protein import into nucleus (GO:0006610)	structural constituent of ribosome (GO:0003735)	nucleolus (GO:0005730)
65106	Arf6ip5	ADP-ribosylation factor-like 6 interacting protein 5	L-glutamate transport (GO:0015813)	protein binding (GO:0005515)	endoplasmic reticulum (GO:0005783)
65970	Lima1	LIM domain and actin binding 1		zinc ion binding (GO:0008270)	actin cytoskeleton (GO:0015629)
65973	Asph	aspartate-beta-hydroxylase	peptidyl-amino acid modification (GO:0018193)	peptide-aspartate beta-dioxygenase activity (GO:0004597)	integral to endoplasmic reticulum membrane (GO:0030176)
66052	Sdhc	succinate dehydrogenase complex, subunit C, integral membrane protein	tricarboxylic acid cycle (GO:0006099)	iron ion binding (GO:0005506)	mitochondrion (GO:0005739)
66141	Ifitm3	interferon induced transmembrane protein 3	negative regulation of cell proliferation (GO:0008285)		integral to membrane (GO:0016021)
66241	Tmem9	transmembrane protein 9	transport (GO:0006810)		lysosome (GO:0005764)
66480	Rpl15	ribosomal protein L15	translation (GO:0006412)	structural constituent of ribosome (GO:0003735)	ribosome (GO:0005840)
66525	Timm50	translocase of inner mitochondrial membrane 50 homolog (yeast)	release of cytochrome c from mitochondria (GO:0001836)	phosphoprotein phosphatase activity (GO:0004721)	mitochondrion (GO:0005739)
66656	Eef1d	eukaryotic translation elongation factor 1 delta (guanine nucleotide exchange protein)	translational elongation (GO:0006414)	translation elongation factor activity (GO:0003746)	eukaryotic translation elongation factor 1 complex (GO:0005853)
66673	Sorcs3	sortilin-related VPS10 domain containing receptor 3			integral to membrane (GO:0016021)
66861	Dnajc10	DnaJ (Hsp40) homolog, subfamily C, member 10	protein folding (GO:0006457)	heat shock protein binding (GO:0031072)	endoplasmic reticulum (GO:0005783)
66881	Pcyox1	prenylcysteine oxidase 1	prenylcysteine catabolic process (GO:0030328)	prenylcysteine oxidase activity (GO:0001735)	lysosome (GO:0005764)
66890	Lman2	lectin, mannose-binding 2	protein transport (GO:0015031)	calcium ion binding (GO:0005509)	Golgi apparatus (GO:0005794)
66945	Sdha	succinate dehydrogenase complex, subunit A, flavoprotein (Fp)	tricarboxylic acid cycle (GO:0006099)	succinate dehydrogenase (ubiquinone) activity (GO:0008177)	mitochondrial inner membrane (GO:0005743)
67003	Uqcrc2	ubiquinol cytochrome c reductase core protein 2	proteolysis (GO:0006508)	metalloendopeptidase activity (GO:0004222)	mitochondrial inner membrane (GO:0005743)
67040	Ddx17	DEAD (Asp-Glu-Ala-Asp) box polypeptide 17		ATP binding (GO:0005524)	nucleus (GO:0005634)
67097	Rps10	ribosomal protein S10		structural constituent of ribosome (GO:0003735)	cytoplasm (GO:0005737)

67115	Rpl14	ribosomal protein L14	translation (GO:0006412)	structural constituent of ribosome (GO:0003735)	ribosome (GO:0005840)
67154	Mtdh	Metadherin	regulation of transcription, DNA-dependent (GO:0006355)	DNA binding (GO:0003677)	tight junction (GO:0005923)
67166	Arl8b	ADP-ribosylation factor-like 8B	small GTPase mediated signal transduction (GO:0007264)	GTP binding (GO:0005525)	lysosome (GO:0005764)
67186	Rplp2	ribosomal protein, large P2	translational elongation (GO:0006414)	structural constituent of ribosome (GO:0003735)	ribosome (GO:0005840)
67273	Ndufa10	NADH dehydrogenase (ubiquinone) 1 alpha subcomplex 10	nucleobase, nucleoside, nucleotide and nucleic acid metabolic process (GO:0006139)	ATP binding (GO:0005524)	mitochondrion (GO:0005739)
67458	Ergic1	endoplasmic reticulum-golgi intermediate compartment (ERGIC) 1	vesicle-mediated transport (GO:0016192)		endoplasmic reticulum (GO:0005783)
67460	Decr1	2,4-dienoyl CoA reductase 1, mitochondrial	oxidation reduction (GO:0055114)	2,4-dienoyl-CoA reductase (NADPH) activity (GO:0008670)	mitochondrion (GO:0005739)
67552	H2afy3	H2A histone family, member Y3		DNA binding (GO:0003677)	nucleus (GO:0005634)
67622	Mxra7	matrix-remodelling associated 7			integral to membrane (GO:0016021)
67671	Rpl38	ribosomal protein L38	translation (GO:0006412)	structural constituent of ribosome (GO:0003735)	ribosome (GO:0005840)
67834	Idh3a	isocitrate dehydrogenase 3 (NAD+) alpha	tricarboxylic acid cycle (GO:0006099)	isocitrate dehydrogenase (NAD+) activity (GO:0004449)	mitochondrion (GO:0005739)
67891	Rpl4	ribosomal protein L4	translation (GO:0006412)	structural constituent of ribosome (GO:0003735)	ribosome (GO:0005840)
67938	Mylc2b	myosin light chain, regulatory B		calcium ion binding (GO:0005509)	myosin complex (GO:0016459)
68028	Rpl22l1	ribosomal protein L22 like 1	translation (GO:0006412)	structural constituent of ribosome (GO:0003735)	ribosome (GO:0005840)
68045	2700060E02Rik	RIKEN cDNA 2700060E02 gene			nucleus (GO:0005634)
68117	Apol	apolipoprotein O-like			mitochondrial inner membrane (GO:0005743)
68194	Ndufb4	NADH dehydrogenase (ubiquinone) 1 beta subcomplex 4	transport (GO:0006810)	NADH dehydrogenase (ubiquinone) activity (GO:0008137)	mitochondrial inner membrane (GO:0005743)
68294	Mfsd10	major facilitator superfamily domain containing 10	apoptosis (GO:0006915)	transporter activity (GO:0005215)	integral to membrane (GO:0016021)
68428	Steap3	STEAP family member 3	iron ion transport (GO:0006826)	ferric-chelate reductase activity (GO:0000293)	multivesicular body (GO:0005771)
68564	Nufip2	nuclear fragile X mental retardation protein interacting protein 2			nucleus (GO:0005634)
68581	Tmed10	transmembrane emp24-like trafficking protein 10 (yeast)	vesicle targeting, to, from or within Golgi (GO:0048199)		zymogen granule membrane (GO:0042589)
68796	1110039B18Rik	RIKEN cDNA 1110039B18 gene		calcium ion binding (GO:0005509)	integral to membrane (GO:0016021)
69617	Pitrm1	pitrilysin metalloproteinase 1	proteolysis (GO:0006508)	metalloendopeptidase activity (GO:0004222)	mitochondrion (GO:0005739)
70152	Mettl7a1	methyltransferase like 7A1		methyltransferase activity (GO:0008168)	
70186	2310056P07Rik	RIKEN cDNA 2310056P07 gene			integral to membrane (GO:0016021)
70350	Basp1	brain abundant, membrane attached signal protein 1	regulation of transcription, DNA-dependent (GO:0006355)	DNA binding (GO:0003677)	nucleus (GO:0005634)
70361	Lman1	lectin, mannose-binding, 1	ER to Golgi vesicle-mediated transport (GO:0006888)	sugar binding (GO:0005529)	sarcomere (GO:0030017)
70456	Brp44	brain protein 44			mitochondrion (GO:0005739)
70508	Bbx	bobby sox homolog (Drosophila)	regulation of transcription, DNA-dependent (GO:0006355)	DNA binding (GO:0003677)	nucleus (GO:0005634)
70575	Gfod2	glucose-fructose oxidoreductase domain containing 2	oxidation reduction (GO:0055114)	electron carrier activity (GO:0009055)	extracellular region (GO:0005576)
70804	Pgrmc2	progesterone receptor membrane component 2		transition metal ion binding (GO:0046914)	integral to membrane (GO:0016021)
71514	Sfpq	splicing factor proline/glutamine rich (polypyrimidine tract binding protein associated)	mRNA processing (GO:0006397)	DNA binding (GO:0003677)	nucleus (GO:0005634)

71960	Myh14	myosin, heavy polypeptide 14	regulation of cell shape (GO:0008360)	actin-dependent ATPase activity (GO:0030898)	stress fiber (GO:0001725)
72960	Top1mt	DNA topoisomerase 1, mitochondrial	DNA unwinding during replication (GO:0006268)	DNA topoisomerase type I activity (GO:0003917)	
73124	Golim4	golgi integral membrane protein 4	transport (GO:0006810)		endosome (GO:0005768)
74122	Tmem43	transmembrane protein 43			integral to membrane (GO:0016021)
74205	Acsl3	acyl-CoA synthetase long-chain family member 3	fatty acid metabolic process (GO:0006631)	long-chain-fatty-acid-CoA ligase activity (GO:0004467)	peroxisome (GO:0005777)
74551	Pck2	phosphoenolpyruvate carboxykinase 2 (mitochondrial)	gluconeogenesis (GO:0006094)	phosphoenolpyruvate carboxykinase (GTP) activity (GO:0004613)	mitochondrion (GO:0005739)
74776	Ppa2	pyrophosphatase (inorganic) 2	phosphate metabolic process (GO:0006796)	inorganic diphosphatase activity (GO:0004427)	mitochondrion (GO:0005739)
74840	Armet	arginine-rich, mutated in early stage tumors		growth factor activity (GO:0008083)	extracellular space (GO:0005615)
75909	Tmem49	transmembrane protein 49			integral to membrane (GO:0016021)
76267	Fads1	fatty acid desaturase 1	unsaturated fatty acid biosynthetic process (GO:0006636)	iron ion binding (GO:0005506)	endoplasmic reticulum (GO:0005783)
76293	Mfap4	microfibrillar-associated protein 4	signal transduction (GO:0007165)	calcium ion binding (GO:0005509)	microfibril (GO:0001527)
76299	Txndc4	thioredoxin domain containing 4 (endoplasmic reticulum)	response to unfolded protein (GO:0006986)		endoplasmic reticulum (GO:0005783)
76453	Prss23	protease, serine, 23	proteolysis (GO:0006508)	serine-type endopeptidase activity (GO:0004252)	extracellular space (GO:0005615)
76577	Ubx8	UBX domain containing 8			cytoplasm (GO:0005737)
76808	Rpl18a	ribosomal protein L18A	translation (GO:0006412)	structural constituent of ribosome (GO:0003735)	ribosome (GO:0005840)
76936	Hnrmpm	heterogeneous nuclear ribonucleoprotein M	mRNA processing (GO:0006397)	transmembrane receptor activity (GO:0004888)	integral to plasma membrane (GO:0005887)
77053	Unc84a	unc-84 homolog A (C. elegans)	nuclear membrane organization and biogenesis (GO:0006998)	zinc ion binding (GO:0008270)	integral to nuclear inner membrane (GO:0005639)
77134	Hnrnpa0	heterogeneous nuclear ribonucleoprotein A0		nucleic acid binding (GO:0003676)	ribonucleoprotein complex (GO:0030529)
78920	Dlst	dihydropyrimidinase S-succinyltransferase (E2 component of 2-oxo-glutarate complex)	tricarboxylic acid cycle (GO:0006099)	dihydropyrimidinase-residue succinyltransferase activity (GO:0004149)	mitochondrion (GO:0005739)
80838	Hist1h1a	histone cluster 1, H1a	nucleosome assembly (GO:0006334)	DNA binding (GO:0003677)	nucleus (GO:0005634)
93736	Aff4	AF4/FMR2 family, member 4	regulation of transcription, DNA-dependent (GO:0006355)		nucleus (GO:0005634)
97212	Hadha	hydroxyacyl-Coenzyme A dehydrogenase/3-ketoacyl-Coenzyme A thiolase/enoyl-Coenzyme A hydratase (trifunctional protein), alpha subunit	fatty acid beta-oxidation (GO:0006635)	3-hydroxyacyl-CoA dehydrogenase activity (GO:0003857)	mitochondrial inner membrane (GO:0005743)
100494	Zfand2a	zinc finger, AN1-type domain 2A		zinc ion binding (GO:0008270)	nucleus (GO:0005634)
100952	Emilin1	elastin microfibril interfacier 1	phosphate transport (GO:0006817)	extracellular matrix constituent conferring elasticity (GO:0030023)	cytoplasm (GO:0005737)
101739	Psp1	PC4 and SFRS1 interacting protein 1	regulation of transcription, DNA-dependent (GO:0006355)	DNA binding (GO:0003677)	nucleus (GO:0005634)
103080	SEPT10	septin 10	regulation of transcription, DNA-dependent (GO:0006355)	GTP binding (GO:0005525)	nucleus (GO:0005634)
103963	Rpn1	ribophorin I	protein amino acid glycosylation (GO:0006486)	dolichyl-diphosphooligosaccharide-protein glycotransferase activity (GO:0004579)	endoplasmic reticulum (GO:0005783)
104721	Ddx1	DEAD (Asp-Glu-Ala-Asp) box polypeptide 1	spliceosome assembly (GO:0000245)	ATPase activity (GO:0016887)	
105245	Txndc5	thioredoxin domain containing 5	cell redox homeostasis (GO:0045454)	isomerase activity (GO:0016853)	endoplasmic reticulum (GO:0005783)
108037	Shmt2	serine hydroxymethyltransferase 2 (mitochondrial)	one-carbon compound metabolic process (GO:0006730)	glycine hydroxymethyltransferase activity (GO:0004372)	mitochondrial inner membrane (GO:0005743)
108075	Ltbp4	latent transforming growth factor beta binding protein 4	transforming growth factor beta receptor signaling pathway (GO:0007179)	calcium ion binding (GO:0005509)	proteinaceous extracellular matrix (GO:0005578)

108989	Tpr	translocated promoter region			nuclear envelope (GO:0005635)
109154	2410014A08Rik	RIKEN cDNA 2410014A08 gene	protein targeting (GO:0006605)		integral to membrane (GO:0016021)
109905	Rap1a	RAS-related protein-1a	small GTPase mediated signal transduction (GO:0007264)	GTPase activity (GO:0003924)	intracellular (GO:0005622)
110052	Dek	DEK oncogene (DNA binding)		DNA binding (GO:0003677)	nucleus (GO:0005634)
110253	Triobp	TRIO and F-actin binding protein			nucleus (GO:0005634)
110446	Acat1	acetyl-Coenzyme A acetyltransferase 1	metabolic process (GO:0008152)	acetyl-CoA C-acetyltransferase activity (GO:0003985)	mitochondrial inner membrane (GO:0005743)
110842	EtfA	electron transferring flavoprotein, alpha polypeptide	transport (GO:0006810)	FAD binding (GO:0050660)	mitochondrial electron transfer flavoprotein complex (GO:0017133)
110911	Cds2	CDP-diacylglycerol synthase (phosphatidate cytidyltransferase) 2	phospholipid biosynthetic process (GO:0008654)	phosphatidate cytidyltransferase activity (GO:0004605)	mitochondrion (GO:0005739)
110954	Rpl10	ribosomal protein 10	translation (GO:0006412)	structural constituent of ribosome (GO:0003735)	ribosome (GO:0005840)
140481	Man2a2	mannosidase 2, alpha 2			mannosidase activity (GO:0015923)
195434	Utp14b	UTP14, U3 small nucleolar ribonucleoprotein, homolog B (yeast)	rRNA processing (GO:0006364)		nucleus (GO:0005634)
216136	Ilvbl	ilvB (bacterial acetolactate synthase)-like			integral to membrane (GO:0016021)
223650	Eppk1	epiplakin 1			cytoskeleton (GO:0005856)
223697	Unc84b	unc-84 homolog B (C. elegans)	nuclear membrane organization and biogenesis (GO:0006998)	protein binding (GO:0005515)	condensed nuclear chromosome (GO:0000794)
226646	Ndufs2	NADH dehydrogenase (ubiquinone) Fe-S protein 2	transport (GO:0006810)	NADH dehydrogenase (ubiquinone) activity (GO:0008137)	mitochondrion (GO:0005739)
227197	Ndufs1	NADH dehydrogenase (ubiquinone) Fe-S protein 1	mitochondrial electron transport, NADH to ubiquinone (GO:0006120)	NADH dehydrogenase (ubiquinone) activity (GO:0008137)	mitochondrion (GO:0005739)
227753	Gsn	gelsolin	barbed-end actin filament capping (GO:0051016)	actin binding (GO:0003779)	actin cytoskeleton (GO:0015629)
230709	Zmpste24	zinc metalloproteinase, STE24 homolog (S. cerevisiae)	prenylated protein catabolic process (GO:0030327)	metalloendopeptidase activity (GO:0004222)	endoplasmic reticulum (GO:0005783)
230753	Thrap3	thyroid hormone receptor associated protein 3	positive regulation of transcription from RNA polymerase II promoter (GO:0045944)	ATP binding (GO:0005524)	nucleus (GO:0005634)
230866	C230096C10Rik	RIKEN cDNA C230096C10 gene			integral to membrane (GO:0016021)
231086	Hadhb	hydroxyacyl-Coenzyme A dehydrogenase/3-ketoacyl-Coenzyme A thiolase/enoyl-Coenzyme A hydratase (trifunctional protein), beta subunit	fatty acid beta-oxidation (GO:0006635)	acetyl-CoA C-acyltransferase activity (GO:0003988)	mitochondrial inner membrane (GO:0005743)
231633	Tmem119	transmembrane protein 119			integral to membrane (GO:0016021)
233870	Tufm	Tu translation elongation factor, mitochondrial	translational elongation (GO:0006414)	GTPase activity (GO:0003924)	mitochondrial inner membrane (GO:0005743)
233908	Fus	fusion, derived from t(12;16) malignant liposarcoma (human)	positive regulation of transcription from RNA polymerase II promoter (GO:0045944)	zinc ion binding (GO:0008270)	nucleus (GO:0005634)
235339	Dlat	dihydropyrimidine S-acetyltransferase (E2 component of pyruvate dehydrogenase complex)	glycolysis (GO:0006096)	dihydropyrimidine-residue acetyltransferase activity (GO:0004742)	mitochondrial pyruvate dehydrogenase complex (GO:0005967)
238880	Actb2	actin, beta-like 2			actin cytoskeleton (GO:0015629)
241226	Itga8	integrin alpha 8	positive regulation of transforming growth factor beta receptor signaling pathway (GO:0030511)	calcium ion binding (GO:0005509)	integrin complex (GO:0008305)
242050	Igsf10	immunoglobulin superfamily, member 10	protein amino acid phosphorylation (GO:0006468)	vascular endothelial growth factor receptor activity (GO:0005021)	extracellular region (GO:0005576)
268301	Ankrd57	ankyrin repeat domain 57			
268977	Ltbp1	latent transforming growth factor beta binding protein 1	transforming growth factor beta receptor signaling pathway (GO:0007179)	calcium ion binding (GO:0005509)	proteinaceous extracellular matrix (GO:0005578)
276770	Eif5a	eukaryotic translation initiation factor 5A	translational initiation (GO:0006413)	translation initiation factor activity (GO:0003743)	nucleus (GO:0005634)

319168	Hist1h2ah	histone cluster 1, H2ah	nucleosome assembly (GO:0006334)	DNA binding (GO:0003677)	nucleus (GO:0005634)
319178	Hist1h2bb	histone cluster 1, H2bb	nucleosome assembly (GO:0006334)	DNA binding (GO:0003677)	nucleus (GO:0005634)
319195	Rpl17	ribosomal protein L17	translation (GO:0006412)	structural constituent of ribosome (GO:0003735) hydrolase activity, acting on ester bonds (GO:0016788)	large ribosomal subunit (GO:0015934)
328092	6530401N04Rik	RIKEN cDNA 6530401N04 gene	D-amino acid catabolic process (GO:0019478)		cytoplasm (GO:0005737)
338350	9330129D05Rik	RIKEN cDNA 9330129D05 gene	oxidation reduction (GO:0055114)	acyl-CoA dehydrogenase activity (GO:0003995)	extracellular space (GO:0005615)
384009	Glpr2	GLI pathogenesis-related 2			Golgi apparatus (GO:0005794)
404634	H2afy2	H2A histone family, member Y2	nucleosome assembly (GO:0006334)	DNA binding (GO:0003677)	Barr body (GO:0001740)

Results acquired from proteomic analysis of acellular HFF

Proteins	Gene Symbol	Description	Biological Process_max	Molecular Function_max	Cellular Component_max
37	ACADVL	acyl-Coenzyme A dehydrogenase, very long chain	fatty acid beta-oxidation (GO:0006635)	long-chain-acyl-CoA dehydrogenase activity (GO:0004466)	mitochondrial inner membrane (GO:0005743)
59	ACTA2	actin, alpha 2, smooth muscle, aorta		ATP binding (GO:0005524)	cytoskeleton (GO:0005856)
60	ACTB	actin, beta	sensory perception of sound (GO:0007605)	ATP binding (GO:0005524)	NuA4 histone acetyltransferase complex (GO:0035267)
197	AHSG	alpha-2-HS-glycoprotein	negative regulation of bone mineralization (GO:0030502)	cysteine protease inhibitor activity (GO:0004869)	extracellular space (GO:0005615)
231	AKR1B1	aldo-keto reductase family 1, member B1 (aldose reductase)	carbohydrate metabolic process (GO:0005975)	aldehyde reductase activity (GO:0004032)	cytosol (GO:0005829)
290	ANPEP	alanyl (membrane) aminopeptidase (aminopeptidase N, aminopeptidase M, microsomal aminopeptidase, CD13, p150)	proteolysis (GO:0006508)	aminopeptidase activity (GO:0004177)	integral to plasma membrane (GO:0005887)
292	SLC25A5	solute carrier family 25 (mitochondrial carrier; adenine nucleotide translocator), member 5	transport (GO:0006810)	adenine transmembrane transporter activity (GO:0015207)	mitochondrial inner membrane (GO:0005743)
301	ANXA1	annexin A1	anti-apoptosis (GO:0006916)	phospholipase A2 inhibitor activity (GO:0019834)	cornified envelope (GO:0001533)
302	ANXA2	annexin A2	skeletal development (GO:0001501)	phospholipase inhibitor activity (GO:0004859)	melanosome (GO:0042470)
304	ANXA2P2	annexin A2 pseudogene 2			
307	ANXA4	annexin A4	anti-apoptosis (GO:0006916)	phospholipase inhibitor activity (GO:0004859)	cytoplasm (GO:0005737)
308	ANXA5	annexin A5	anti-apoptosis (GO:0006916)	phospholipase inhibitor activity (GO:0004859)	cytoplasm (GO:0005737)
309	ANXA6	annexin A6		calcium ion binding (GO:0005509)	melanosome (GO:0042470)
310	ANXA7	annexin A7		voltage-gated calcium channel activity (GO:0005245)	
311	ANXA11	annexin A11	immune response (GO:0006955)	calcium ion binding (GO:0005509)	melanosome (GO:0042470)
476	ATP1A1	ATPase, Na+/K+ transporting, alpha 1 polypeptide	regulation of cellular pH (GO:0030641)	sodium:potassium-exchanging ATPase activity (GO:0005391)	melanosome (GO:0042470)
477	ATP1A2	ATPase, Na+/K+ transporting, alpha 2 (+) polypeptide	regulation of cellular pH (GO:0030641)	sodium:potassium-exchanging ATPase activity (GO:0005391)	integral to membrane (GO:0016021)
483	ATP1B3	ATPase, Na+/K+ transporting, beta 3 polypeptide	potassium ion transport (GO:0006813)	sodium:potassium-exchanging ATPase activity (GO:0005391)	melanosome (GO:0042470)
487	ATP2A1	ATPase, Ca++ transporting, cardiac muscle, fast twitch 1	positive regulation of fast-twitch skeletal muscle fiber contraction (GO:0031448)	calcium-transporting ATPase activity (GO:0005388)	sarcoplasmic reticulum membrane (GO:0033017)
488	ATP2A2	ATPase, Ca++ transporting, cardiac muscle, slow twitch 2	calcium ion transport (GO:0006816)	calcium-transporting ATPase activity (GO:0005388)	microsome (GO:0005792)
493	ATP2B4	ATPase, Ca++ transporting, plasma membrane 4	calcium ion transport (GO:0006816)	calcium-transporting ATPase activity (GO:0005388)	integral to plasma membrane (GO:0005887)
498	ATP5A1	ATP synthase, H+ transporting, mitochondrial F1 complex, alpha subunit 1, cardiac muscle	ATP synthesis coupled proton transport (GO:0015986)	hydrogen ion transporting ATP synthase activity, rotational mechanism (GO:0046933)	mitochondrial matrix (GO:0005759)
506	ATP5B	ATP synthase, H+ transporting, mitochondrial F1 complex, beta polypeptide	ATP synthesis coupled proton transport (GO:0015986)	hydrogen-exporting ATPase activity, phosphorylative mechanism (GO:0008553)	mitochondrial matrix (GO:0005759)
509	ATP5C1	ATP synthase, H+ transporting, mitochondrial F1 complex, gamma polypeptide 1	ATP synthesis coupled proton transport (GO:0015986)	hydrogen ion transporting ATP synthase activity, rotational mechanism (GO:0046933)	mitochondrial matrix (GO:0005759)
513	ATP5D	ATP synthase, H+ transporting, mitochondrial F1 complex, delta subunit	mitochondrial ATP synthesis coupled proton transport (GO:0042776)	hydrogen ion transporting ATP synthase activity, rotational mechanism (GO:0046933)	mitochondrial matrix (GO:0005759)
521	ATP5I	ATP synthase, H+ transporting, mitochondrial F0 complex, subunit E	ATP synthesis coupled proton transport (GO:0015986)	hydrogen ion transporting ATP synthase activity, rotational mechanism (GO:0046933)	mitochondrion (GO:0005739)
522	ATP5J	ATP synthase, H+ transporting, mitochondrial F0 complex, subunit F6	ATP synthesis coupled proton transport (GO:0015986)	hydrogen ion transporting ATP synthase activity, rotational mechanism (GO:0046933)	mitochondrion (GO:0005739)
539	ATP5O	ATP synthase, H+ transporting, mitochondrial F1 complex, O subunit (oligomycin sensitivity conferring protein)	mitochondrial ATP synthesis coupled proton transport (GO:0042776)	hydrogen ion transporting ATP synthase activity, rotational mechanism (GO:0046933)	mitochondrial matrix (GO:0005759)

540	ATP7B	ATPase, Cu++ transporting, beta polypeptide	cellular copper ion homeostasis (GO:0006878)	copper-exporting ATPase activity (GO:0004008)	late endosome (GO:0005770)
567	B2M	beta-2-microglobulin	antigen processing and presentation of peptide antigen via MHC class I (GO:0002474)	protein binding (GO:0005515)	early endosome membrane (GO:0031901)
682	BSG	basigin (Ok blood group)	cell surface receptor linked signal transduction (GO:0007166)	mannose binding (GO:0005537)	melanosome (GO:0042470)
811	CALR	calreticulin	cellular calcium ion homeostasis (GO:0006874)	zinc ion binding (GO:0008270)	endoplasmic reticulum (GO:0005783)
813	CALU	calumenin		calcium ion binding (GO:0005509)	melanosome (GO:0042470)
821	CANX	calnexin	protein folding (GO:0006457)	calcium ion binding (GO:0005509)	melanosome (GO:0042470)
836	CASP3	caspase 3, apoptosis-related cysteine peptidase	induction of apoptosis (GO:0006917)	cysteine-type peptidase activity (GO:0008234)	nucleoplasm (GO:0005654)
857	CAV1	caveolin 1, caveolae protein, 22kDa	cholesterol homeostasis (GO:0042632)	cholesterol binding (GO:0015485)	integral to plasma membrane (GO:0005887)
871	SERPINH1	serpin peptidase inhibitor, clade H (heat shock protein 47), member 1, (collagen binding protein 1)	response to unfolded protein (GO:0006986)	serine-type endopeptidase inhibitor activity (GO:0004867)	endoplasmic reticulum (GO:0005783)
919	CD247	CD247 molecule	cell surface receptor linked signal transduction (GO:0007166)	transmembrane receptor activity (GO:0004888)	integral to membrane (GO:0016021)
960	CD44	CD44 molecule (Indian blood group)	cell-matrix adhesion (GO:0007160)	hyaluronic acid binding (GO:0005540)	integral to plasma membrane (GO:0005887)
966	CD59	CD59 molecule, complement regulatory protein	cell surface receptor linked signal transduction (GO:0007166)	protein binding (GO:0005515)	anchored to membrane (GO:0031225)
975	CD81	CD81 molecule	phosphatidylinositol biosynthetic process (GO:0006661)	protein binding (GO:0005515)	integral to plasma membrane (GO:0005887)
989	SEPT7	septin 7	protein heterooligomerization (GO:0051291)	GTP binding (GO:0005525)	stress fiber (GO:0001725)
1012	CDH13	cadherin 13, H-cadherin (heart)	positive regulation of survival gene product expression (GO:0045885)	calcium ion binding (GO:0005509)	caveola (GO:0005901)
1072	CFL1	cofilin 1 (non-muscle)	anti-apoptosis (GO:0006916)	actin binding (GO:0003779)	nucleus (GO:0005634)
1244	ABCC2	ATP-binding cassette, sub-family C (CFTR/MRP), member 2	transport (GO:0006810)	ATPase activity (GO:0016887)	integral to plasma membrane (GO:0005887)
1329	COX5B	cytochrome c oxidase subunit Vb	respiratory gaseous exchange (GO:0007585)	zinc ion binding (GO:0008270)	mitochondrial inner membrane (GO:0005743)
1340	COX6B1	cytochrome c oxidase subunit Vlb polypeptide 1 (ubiquitous)	oxidation reduction (GO:0055114)	cytochrome-c oxidase activity (GO:0004129)	mitochondrion (GO:0005739)
1345	COX6C	cytochrome c oxidase subunit Vlc	generation of precursor metabolites and energy (GO:0006091)	cytochrome-c oxidase activity (GO:0004129)	mitochondrial inner membrane (GO:0005743)
1603	DAD1	defender against cell death 1	protein amino acid N-linked glycosylation via asparagine (GO:0018279)	dolichyl-diphosphooligosaccharide-protein glycotransferase activity (GO:0004579)	integral to membrane (GO:0016021)
1727	CYB5R3	cytochrome b5 reductase 3	iron ion transport (GO:0006826)	cytochrome-b5 reductase activity (GO:0004128)	mitochondrial outer membrane (GO:0005741)
1738	DLD	dihydropyrimidine dehydrogenase	cell redox homeostasis (GO:0045454)	FAD binding (GO:0050660)	mitochondrial matrix (GO:0005759)
1743	DLST	dihydropyrimidine S-succinyltransferase (E2 component of 2-oxo-glutarate complex)	tricarboxylic acid cycle (GO:0006099)	dihydropyrimidine-residue succinyltransferase activity (GO:0004149)	mitochondrial matrix (GO:0005759)
1917	EEF1A2	eukaryotic translation elongation factor 1 alpha 2	translational elongation (GO:0006414)	GTPase activity (GO:0003924)	nucleus (GO:0005634)
2197	FAU	Finkel-Biskis-Reilly murine sarcoma virus (FBR-MuSV) ubiquitously expressed	translational elongation (GO:0006414)	RNA binding (GO:0003723)	cytosolic small ribosomal subunit (GO:0022627)
2335	FN1	fibronectin 1	transmembrane receptor protein tyrosine kinase signaling pathway (GO:0007169)	heparin binding (GO:0008201)	ER-Golgi intermediate compartment (GO:0005793)
2597	GAPDH	glyceraldehyde-3-phosphate dehydrogenase	glycolysis (GO:0006096)	glyceraldehyde-3-phosphate dehydrogenase (phosphorylating) activity (GO:0004365)	cytoplasm (GO:0005737)
2923	PDIA3	protein disulfide isomerase family A, member 3	protein import into nucleus (GO:0006606)	phospholipase C activity (GO:0004629)	melanosome (GO:0042470)
3005	H1F0	H1 histone family, member 0	nucleosome assembly (GO:0006334)	DNA binding (GO:0003677)	nucleus (GO:0005634)
3006	HIST1H1C	histone cluster 1, H1c	nucleosome assembly (GO:0006334)	DNA binding (GO:0003677)	nucleus (GO:0005634)

3009	HIST1H1B	histone cluster 1, H1b	nucleosome assembly (GO:0006334)	DNA binding (GO:0003677)	nucleus (GO:0005634)
3032	HADHB	hydroxyacyl-Coenzyme A dehydrogenase/3-ketoacyl-Coenzyme A thiolase/enoyl-Coenzyme A hydratase (trifunctional protein), beta subunit	fatty acid beta-oxidation (GO:0006635)	acetyl-CoA C-acyltransferase activity (GO:0003988)	mitochondrial matrix (GO:0005759)
3039	HBA1	hemoglobin, alpha 1	oxygen transport (GO:0015671)	iron ion binding (GO:0005506)	hemoglobin complex (GO:0005833)
3046	HBE1	hemoglobin, epsilon 1	oxygen transport (GO:0015671)	iron ion binding (GO:0005506)	hemoglobin complex (GO:0005833)
3105	HLA-A	major histocompatibility complex, class I, A	antigen processing and presentation of peptide antigen via MHC class I (GO:0002474)	MHC class I receptor activity (GO:0032393)	integral to plasma membrane (GO:0005887)
3119	HLA-DQB1	major histocompatibility complex, class II, DQ beta 1	antigen processing and presentation of peptide or polysaccharide antigen via MHC class II (GO:0002504)	GTP binding (GO:0005525)	integral to membrane (GO:0016021)
3136	HLA-H	major histocompatibility complex, class I, H (pseudogene)	antigen processing and presentation of peptide antigen via MHC class I (GO:0002474)	MHC class I receptor activity (GO:0032393)	integral to plasma membrane (GO:0005887)
3159	HMGA1	high mobility group AT-hook 1	nucleosome disassembly (GO:0006337)	ligand-dependent nuclear receptor transcription coactivator activity (GO:0030374)	chromatin (GO:0000785)
3309	HSPA5	heat shock 70kDa protein 5 (glucose-regulated protein, 78kDa)		ATP binding (GO:0005524)	endoplasmic reticulum (GO:0005783)
3329	HSPD1	heat shock 60kDa protein 1 (chaperonin)	protein import into mitochondrial matrix (GO:0030150)	ATP binding (GO:0005524)	mitochondrial matrix (GO:0005759)
3336	HSPE1	heat shock 10kDa protein 1 (chaperonin 10)	caspase activation (GO:0006919)	ATP binding (GO:0005524)	mitochondrial matrix (GO:0005759)
3673	ITGA2	integrin, alpha 2 (CD49B, alpha 2 subunit of VLA-2 receptor)	integrin-mediated signaling pathway (GO:0007229)	magnesium ion binding (GO:0000287)	integrin complex (GO:0008305)
3688	ITGB1	integrin, beta 1 (fibronectin receptor, beta polypeptide, antigen CD29 includes MDF2, MSK12)	integrin-mediated signaling pathway (GO:0007229)	protein heterodimerization activity (GO:0046982)	melanosome (GO:0042470)
3833	KIFC1	kinesin family member C1	microtubule-based movement (GO:0007018)	ATP binding (GO:0005524)	early endosome (GO:0005769)
3848	KRT1	keratin 1 (epidermolytic hyperkeratosis)	fibrinolysis (GO:0042730)	receptor activity (GO:0004872)	cytoskeleton (GO:0005856)
3849	KRT2	keratin 2 (epidermal ichthyosis bullosa of Siemens)	epidermis development (GO:0008544)	structural constituent of cytoskeleton (GO:0005200)	intermediate filament (GO:0005882)
3855	KRT7	keratin 7	DNA replication (GO:0006260)	protein binding (GO:0005515)	intermediate filament (GO:0005882)
3857	KRT9	keratin 9 (epidermolytic palmoplantar keratoderma)	intermediate filament organization (GO:0045109)	structural constituent of cytoskeleton (GO:0005200)	intermediate filament (GO:0005882)
3858	KRT10	keratin 10 (epidermolytic hyperkeratosis; keratosis palmaris et plantaris)	epidermis development (GO:0008544)	protein binding (GO:0005515)	intermediate filament (GO:0005882)
4000	LMNA	lamin A/C		protein binding (GO:0005515)	nucleus (GO:0005634)
4158	MC2R	melanocortin 2 receptor (adrenocorticotropin hormone)	G-protein signaling, coupled to cyclic nucleotide second messenger (GO:0007187)	adrenocorticotropin receptor activity (GO:0004978)	integral to plasma membrane (GO:0005887)
4191	MDH2	malate dehydrogenase 2, NAD (mitochondrial)	glycolysis (GO:0006096)	L-malate dehydrogenase activity (GO:0030060)	mitochondrial matrix (GO:0005759)
4256	MGP	matrix Gla protein	regulation of bone mineralization (GO:0030500)	calcium ion binding (GO:0005509)	proteinaceous extracellular matrix (GO:0005578)
4257	MGST1	microsomal glutathione S-transferase 1		glutathione transferase activity (GO:0004364)	mitochondrial outer membrane (GO:0005741)
4267	CD99	CD99 molecule	cell adhesion (GO:0007155)	protein binding (GO:0005515)	integral to plasma membrane (GO:0005887)
4513	COX2	cytochrome c oxidase II	mitochondrial electron transport, cytochrome c to oxygen (GO:0006123)	copper ion binding (GO:0005507)	mitochondrion (GO:0005739)
4637	MYL6	myosin, light chain 6, alkali, smooth muscle and non-muscle	muscle filament sliding (GO:0030049)	actin-dependent ATPase activity (GO:0030898)	unconventional myosin complex (GO:0016461)
4697	NDUFA4	NADH dehydrogenase (ubiquinone) 1 alpha subcomplex, 4, 9kDa	mitochondrial electron transport, NADH to ubiquinone (GO:0006120)	NADH dehydrogenase (ubiquinone) activity (GO:0008137)	mitochondrion (GO:0005739)
4710	NDUFB4	NADH dehydrogenase (ubiquinone) 1 beta subcomplex, 4, 15kDa	mitochondrial electron transport, NADH to ubiquinone (GO:0006120)	NADH dehydrogenase (ubiquinone) activity (GO:0008137)	mitochondrion (GO:0005739)
4722	NDUFS3	NADH dehydrogenase (ubiquinone) Fe-S protein 3, 30kDa (NADH-coenzyme Q reductase)	induction of apoptosis (GO:0006917)	NADH dehydrogenase (ubiquinone) activity (GO:0008137)	mitochondrion (GO:0005739)

4907	NT5E	5'-nucleotidase, ecto (CD73)	nucleotide catabolic process (GO:0009166)	5'-nucleotidase activity (GO:0008253)	anchored to membrane (GO:0031225)
5033	P4HA1	procollagen-proline, 2-oxoglutarate 4-dioxygenase (proline 4-hydroxylase), alpha polypeptide I	protein metabolic process (GO:0019538)	procollagen-proline 4-dioxygenase activity (GO:0004656)	endoplasmic reticulum (GO:0005783)
5034	P4HB	procollagen-proline, 2-oxoglutarate 4-dioxygenase (proline 4-hydroxylase), beta polypeptide	peptidyl-proline hydroxylation to 4-hydroxy-L-proline (GO:0018401)	procollagen-proline 4-dioxygenase activity (GO:0004656)	melanosome (GO:0042470)
5144	PDE4D	phosphodiesterase 4D, cAMP-specific (phosphodiesterase E3 dunce homolog, Drosophila)	signal transduction (GO:0007165)	3',5'-cyclic-AMP phosphodiesterase activity (GO:0004115)	centrosome (GO:0005813)
5245	PHB	prohibitin	histone deacetylation (GO:0016575)	protein binding (GO:0005515)	mitochondrial inner membrane (GO:0005743)
5250	SLC25A3	solute carrier family 25 (mitochondrial carrier; phosphate carrier), member 3	generation of precursor metabolites and energy (GO:0006091)	phosphate carrier activity (GO:0015320)	mitochondrial inner membrane (GO:0005743)
5355	PLP2	proteolipid protein 2 (colonic epithelium-enriched)	cytokine and chemokine mediated signaling pathway (GO:0019221)	ion transmembrane transporter activity (GO:0015075)	endoplasmic reticulum (GO:0005783)
5375	PMP2	peripheral myelin protein 2	transport (GO:0006810)	lipid binding (GO:0008289)	cytoplasm (GO:0005737)
5378	PMS1	PMS1 postmeiotic segregation increased 1 (S. cerevisiae)	mismatch repair (GO:0006298)	ATP binding (GO:0005524)	nucleus (GO:0005634)
5479	PPIB	peptidylprolyl isomerase B (cyclophilin B)	protein folding (GO:0006457)	peptidyl-prolyl cis-trans isomerase activity (GO:0003755)	melanosome (GO:0042470)
5630	PRPH	peripherin		structural molecule activity (GO:0005198)	intermediate filament (GO:0005882)
5742	PTGS1	prostaglandin-endoperoxide synthase 1 (prostaglandin G/H synthase and cyclooxygenase)	prostaglandin biosynthetic process (GO:0001516)	iron ion binding (GO:0005506)	microsome (GO:0005792)
5862	RAB2A	RAB2A, member RAS oncogene family	ER to Golgi vesicle-mediated transport (GO:0006888)	GTPase activity (GO:0003924)	melanosome (GO:0042470)
5879	RAC1	ras-related C3 botulinum toxin substrate 1 (rho family, small GTP binding protein Rac1)	actin filament polymerization (GO:0030041)	GTPase activity (GO:0003924)	melanosome (GO:0042470)
5908	RAP1B	RAP1B, member of RAS oncogene family	small GTPase mediated signal transduction (GO:0007264)	GTP binding (GO:0005525)	cytoplasm (GO:0005737)
5932	RBBP8	retinoblastoma binding protein 8	regulation of transcription from RNA polymerase II promoter (GO:0006357)	protein binding (GO:0005515)	nucleus (GO:0005634)
6129	RPL7	ribosomal protein L7	translational elongation (GO:0006414)	RNA binding (GO:0003723)	cytosolic large ribosomal subunit (GO:0022625)
6141	RPL18	ribosomal protein L18	translational elongation (GO:0006414)	RNA binding (GO:0003723)	cytosolic large ribosomal subunit (GO:0022625)
6175	RPLP0	ribosomal protein, large, P0	translational elongation (GO:0006414)	RNA binding (GO:0003723)	cytosolic large ribosomal subunit (GO:0022625)
6181	RPLP2	ribosomal protein, large, P2	translational elongation (GO:0006414)	RNA binding (GO:0003723)	cytosolic large ribosomal subunit (GO:0022625)
6182	MRPL12	mitochondrial ribosomal protein L12	transcription from mitochondrial promoter (GO:0006390)	RNA binding (GO:0003723)	mitochondrial large ribosomal subunit (GO:0005762)
6184	RPN1	ribophorin I	protein amino acid N-linked glycosylation via asparagine (GO:0018279)	dolichyl-diphosphooligosaccharide-protein glycotransferase activity (GO:0004579)	melanosome (GO:0042470)
6185	RPN2	ribophorin II	protein amino acid N-linked glycosylation via asparagine (GO:0018279)	dolichyl-diphosphooligosaccharide-protein glycotransferase activity (GO:0004579)	endoplasmic reticulum (GO:0005783)
6201	RPS7	ribosomal protein S7	translational elongation (GO:0006414)	RNA binding (GO:0003723)	cytosolic small ribosomal subunit (GO:0022627)
6227	RPS21	ribosomal protein S21	translational elongation (GO:0006414)	RNA binding (GO:0003723)	cytosolic small ribosomal subunit (GO:0022627)
6233	RPS27A	ribosomal protein S27a	protein modification process (GO:0006464)	zinc ion binding (GO:0008270)	ribosome (GO:0005840)
6263	RYR3	ryanodine receptor 3	cellular calcium ion homeostasis (GO:0006874)	ryanodine-sensitive calcium-release channel activity (GO:0005219)	integral to plasma membrane (GO:0005887)
6275	S100A4	S100 calcium binding protein A4	epithelial to mesenchymal transition (GO:0001837)	calcium ion binding (GO:0005509)	
6281	S100A10	S100 calcium binding protein A10	signal transduction (GO:0007165)	calcium ion binding (GO:0005509)	

6282	S100A11	S100 calcium binding protein A11	negative regulation of DNA replication (GO:0008156)	calcium ion binding (GO:0005509)	nucleus (GO:0005634)
6342	SCP2	sterol carrier protein 2	steroid biosynthetic process (GO:0006694)	propanoyl-CoA C-acyltransferase activity (GO:0033814)	peroxisome (GO:0005777)
6554	SLC10A1	solute carrier family 10 (sodium/bile acid cotransporter family), member 1	sodium ion transport (GO:0006814)	bile acid:sodium symporter activity (GO:0008508)	integral to plasma membrane (GO:0005887)
6648	SOD2	superoxide dismutase 2, mitochondrial	response to superoxide (GO:0000303)	manganese ion binding (GO:0030145)	mitochondrial matrix (GO:0005759)
6745	SSR1	signal sequence receptor, alpha (translocon-associated protein alpha)	cotranslational protein targeting to membrane (GO:0006613)	calcium ion binding (GO:0005509)	endoplasmic reticulum (GO:0005783)
6748	SSR4	signal sequence receptor, delta (translocon-associated protein delta)	intracellular protein transport (GO:0006886)	calcium ion binding (GO:0005509)	endoplasmic reticulum (GO:0005783)
7070	THY1	Thy-1 cell surface antigen	retinal cone cell development (GO:0046549)	Rho GTPase activator activity (GO:0005100)	integral to plasma membrane (GO:0005887)
7184	HSP90B1	heat shock protein 90kDa beta (Grp94), member 1	anti-apoptosis (GO:0006916)	ATP binding (GO:0005524)	melanosome (GO:0042470)
7385	UQCRC2	ubiquinol-cytochrome c reductase core protein II	proteolysis (GO:0006508)	metalloendopeptidase activity (GO:0004222)	mitochondrion (GO:0005739)
7416	VDAC1	voltage-dependent anion channel 1	apoptotic program (GO:0008632)	voltage-gated anion channel activity (GO:0008308)	mitochondrial outer membrane (GO:0005741)
7417	VDAC2	voltage-dependent anion channel 2	anion transport (GO:0006820)	voltage-gated anion channel activity (GO:0008308)	mitochondrial outer membrane (GO:0005741)
7431	VIM	vimentin	cell motility (GO:0006928)	structural constituent of cytoskeleton (GO:0005200)	cytoskeleton (GO:0005856)
7855	FZD5	frizzled homolog 5 (Drosophila)	G-protein coupled receptor protein signaling pathway (GO:0007186)	non-G-protein coupled 7TM receptor activity (GO:0004926)	integral to plasma membrane (GO:0005887)
7857	SCG2	secretogranin II (chromogranin C)	induction of positive chemotaxis (GO:0050930)	cytokine activity (GO:0005125)	extracellular space (GO:0005615)
7879	RAB7A	RAB7A, member RAS oncogene family	endocytosis (GO:0006897)	GTPase activity (GO:0003924)	lysosome (GO:0005764)
8340	HIST1H2BL	histone cluster 1, H2bl	nucleosome assembly (GO:0006334)	DNA binding (GO:0003677)	nucleus (GO:0005634)
8349	HIST2H2BE	histone cluster 2, H2be	nucleosome assembly (GO:0006334)	DNA binding (GO:0003677)	nucleus (GO:0005634)
8803	SUCLA2	succinate-CoA ligase, ADP-forming, beta subunit	tricarboxylic acid cycle (GO:0006099)	succinate-CoA ligase (ADP-forming) activity (GO:0004775)	mitochondrion (GO:0005739)
8904	CPNE1	copine I	lipid metabolic process (GO:0006629)	phosphatidylserine binding (GO:0001786)	
9113	LATS1	LATS, large tumor suppressor, homolog 1 (Drosophila)	negative regulation of cyclin-dependent protein kinase activity (GO:0045736)	protein serine/threonine kinase activity (GO:0004674)	centrosome (GO:0005813)
9119	KRT75	keratin 75		structural molecule activity (GO:0005198)	intermediate filament (GO:0005882)
9131	AIFM1	apoptosis-inducing factor, mitochondrion-associated, 1	DNA damage response, signal transduction resulting in induction of apoptosis (GO:0008630)	FAD binding (GO:0050660)	nucleus (GO:0005634)
9341	VAMP3	vesicle-associated membrane protein 3 (cellubrevin)	protein complex assembly (GO:0006461)		integral to membrane (GO:0016021)
9377	COX5A	cytochrome c oxidase subunit Va		iron ion binding (GO:0005506)	mitochondrial inner membrane (GO:0005743)
9554	SEC22B	SEC22 vesicle trafficking protein homolog B (S. cerevisiae)	ER to Golgi vesicle-mediated transport (GO:0006888)	protein binding (GO:0005515)	melanosome (GO:0042470)
9555	H2AFY	H2A histone family, member Y	nucleosome assembly (GO:0006334)	DNA binding (GO:0003677)	Barr body (GO:0001740)
9902	MRC2	mannose receptor, C type 2	endocytosis (GO:0006897)	calcium ion binding (GO:0005509)	integral to membrane (GO:0016021)
10130	PDIA6	protein disulfide isomerase family A, member 6	protein folding (GO:0006457)	protein disulfide isomerase activity (GO:0003756)	melanosome (GO:0042470)
10211	FLOT1	flotillin 1		protein binding (GO:0005515)	melanosome (GO:0042470)
10398	MYL9	myosin, light chain 9, regulatory	regulation of muscle contraction (GO:0006937)	calcium ion binding (GO:0005509)	muscle myosin complex (GO:0005859)
10409	BASP1	brain abundant, membrane attached signal protein 1			cytoskeleton (GO:0005856)

10632	ATP5L	ATP synthase, H ⁺ transporting, mitochondrial F0 complex, subunit G	ATP synthesis coupled proton transport (GO:0015986)	hydrogen ion transporting ATP synthase activity, rotational mechanism (GO:0046933)	mitochondrion (GO:0005739)
10791	VAMP5	vesicle-associated membrane protein 5 (myobrevin)	skeletal muscle development (GO:0007519)		Golgi apparatus (GO:0005794)
10857	PGRMC1	progesterone receptor membrane component 1	transition metal ion binding (GO:0046914)		microsome (GO:0005792)
10874	NMU	neuromedin U	neuropeptide signaling pathway (GO:0007218)	receptor binding (GO:0005102)	extracellular region (GO:0005576)
10960	LMAN2	lectin, mannose-binding 2	protein transport (GO:0015031)	calcium ion binding (GO:0005509)	endoplasmic reticulum (GO:0005783)
10970	CKAP4	cytoskeleton-associated protein 4			integral to membrane (GO:0016021)
11161	C14orf1	chromosome 14 open reading frame 1	sterol biosynthetic process (GO:0016126)		transport vesicle (GO:0030133)
11331	PHB2	prohibitin 2	regulation of transcription, DNA-dependent (GO:0006355)	estrogen receptor binding (GO:0030331)	mitochondrial inner membrane (GO:0005743)
23049	SMG1	PI-3-kinase-related kinase SMG-1	phosphoinositide phosphorylation (GO:0046854)	protein serine/threonine kinase activity (GO:0004674)	nucleus (GO:0005634)
26135	SERBP1	SERPINE1 mRNA binding protein 1	regulation of mRNA stability (GO:0043488)	mRNA 3'-UTR binding (GO:0003730)	nucleus (GO:0005634)
28958	CCDC56	coiled-coil domain containing 56			integral to membrane (GO:0016021)
29058	C20orf30	chromosome 20 open reading frame 30			integral to membrane (GO:0016021)
29123	ANKRD11	ankyrin repeat domain 11			nucleus (GO:0005634)
29964	PRICKLE4	prickle homolog 4 (Drosophila)		zinc ion binding (GO:0008270)	
51449	PCYOX1	prenylcysteine oxidase 1	prenylated protein catabolic process (GO:0030327)	prenylcysteine oxidase activity (GO:0001735)	lysosome (GO:0005764)
51603	KIAA0859	KIAA0859	metabolic process (GO:0008152)	methyltransferase activity (GO:0008168)	
54732	TMED9	transmembrane emp24 protein transport domain containing 9	transport (GO:0006810)		endoplasmic reticulum (GO:0005783)
55035	NOL8	nucleolar protein 8	DNA replication (GO:0006260)	RNA binding (GO:0003723)	nucleus (GO:0005634)
55379	LRRC59	leucine rich repeat containing 59		protein binding (GO:0005515)	microsome (GO:0005792)
55697	VAC14	Vac14 homolog (S. cerevisiae)	signal transduction (GO:0007165)	receptor activity (GO:0004872)	cellular_component (GO:0005575)
55780	C6orf70	chromosome 6 open reading frame 70			integral to membrane (GO:0016021)
55970	GNG12	guanine nucleotide binding protein (G protein), gamma 12	G-protein coupled receptor protein signaling pathway (GO:0007186)	signal transducer activity (GO:0004871)	heterotrimeric G-protein complex (GO:0005834)
56926	NCLN	nicalin homolog (zebrafish)	protein processing (GO:0016485)		endoplasmic reticulum (GO:0005783)
57142	RTN4	reticulon 4	negative regulation of axon extension (GO:0030517)	protein binding (GO:0005515)	integral to endoplasmic reticulum membrane (GO:0030176)
57486	NLN	neurolysin (metallopeptidase M3 family)	proteolysis (GO:0006508)	metalloendopeptidase activity (GO:0004222)	mitochondrion (GO:0005739)
57620	STIM2	stromal interaction molecule 2	negative regulation of calcium ion transport via store-operated calcium channel (GO:0032235)	calcium ion binding (GO:0005509)	integral to endoplasmic reticulum membrane (GO:0030176)
57653	KIAA1529	KIAA1529			integral to membrane (GO:0016021)
58472	SQRDL	sulfide quinone reductase-like (yeast)		oxidoreductase activity (GO:0016491)	mitochondrion (GO:0005739)
58505	DC2	DC2 protein			integral to membrane (GO:0016021)
58528	RRAGD	Ras-related GTP binding D		GTP binding (GO:0005525)	nucleus (GO:0005634)
59338	PLEKHA1	pleckstrin homology domain containing, family A (phosphoinositide binding specific) member 1		phospholipid binding (GO:0005543)	nucleus (GO:0005634)
60559	SPCS3	signal peptidase complex subunit 3 homolog (S. cerevisiae)	signal peptide processing (GO:0006465)		microsome (GO:0005792)

79026	AHNAK	AHNAK nucleoprotein	nervous system development (GO:0007399)	protein binding (GO:0005515)	nucleus (GO:0005634)
79759	ZNF668	zinc finger protein 668	regulation of transcription, DNA-dependent (GO:0006355)	zinc ion binding (GO:0008270)	nucleus (GO:0005634)
81855	SFXN3	sideroflexin 3	iron ion transport (GO:0006826)	iron ion binding (GO:0005506)	mitochondrion (GO:0005739)
84669	USP32	ubiquitin specific peptidase 32	ubiquitin-dependent protein catabolic process (GO:0006511)	ubiquitin thiolesterase activity (GO:0004221)	membrane (GO:0016020)
84709	OSAP	ovary-specific acidic protein			integral to membrane (GO:0016021)
85235	HIST1H2AH	histone cluster 1, H2ah	nucleosome assembly (GO:0006334)	DNA binding (GO:0003677)	nucleus (GO:0005634)
90990	KIFC2	kinesin family member C2	microtubule-based movement (GO:0007018)	ATP binding (GO:0005524)	microtubule (GO:0005874)
91368	CDKN2AIP NL	CDKN2A interacting protein N-terminal like			
91662	NLRP12	NLR family, pyrin domain containing 12	release of cytoplasmic sequestered NF-kappaB (GO:0008588)	ATP binding (GO:0005524)	cytoplasm (GO:0005737)
94081	SFXN1	sideroflexin 1	iron ion transport (GO:0006826)	iron ion binding (GO:0005506)	mitochondrion (GO:0005739)
94239	H2AFV	H2A histone family, member V	nucleosome assembly (GO:0006334)	DNA binding (GO:0003677)	nucleus (GO:0005634)
112752	C14orf179	chromosome 14 open reading frame 179			
112802	KRT71	keratin 71		structural molecule activity (GO:0005198)	intermediate filament (GO:0005882)
116496	FAM129A	family with sequence similarity 129, member A			cellular_component (GO:0005575)
121457	IKIP	IKK interacting protein	induction of apoptosis (GO:0006917)	protein binding (GO:0005515)	endoplasmic reticulum (GO:0005783)
126328	NDUFA11	NADH dehydrogenase (ubiquinone) 1 alpha subcomplex, 11, 14.7kDa	transport (GO:0006810)		mitochondrion (GO:0005739)
139322	APOOL	apolipoprotein O-like			extracellular region (GO:0005576)
140465	MYL6B	myosin, light chain 6B, alkali, smooth muscle and non-muscle	muscle filament sliding (GO:0030049)	calcium ion binding (GO:0005509)	muscle myosin complex (GO:0005859)
162962	ZNF836	zinc finger protein 836	regulation of transcription, DNA-dependent (GO:0006355)	zinc ion binding (GO:0008270)	nucleus (GO:0005634)
221613	HIST1H2AA	histone cluster 1, H2aa	nucleosome assembly (GO:0006334)	DNA binding (GO:0003677)	nucleus (GO:0005634)
254528	C16orf73	chromosome 16 open reading frame 73			
255626	HIST1H2BA	histone cluster 1, H2ba	nucleosome assembly (GO:0006334)	DNA binding (GO:0003677)	nucleus (GO:0005634)
284119	PTRF	polymerase I and transcript release factor	transcription initiation from RNA polymerase I promoter (GO:0006361)	rRNA primary transcript binding (GO:0042134)	microsome (GO:0005792)
345651	ACTBL2	actin, beta-like 2		ATP binding (GO:0005524)	cytoskeleton (GO:0005856)
376940	ZC3H6	zinc finger CCCH-type containing 6		zinc ion binding (GO:0008270)	
606495	LOC606495	hypothetical protein LOC606495		cytochrome-b5 reductase activity (GO:0004128)	
47	ACLY	ATP citrate lyase	ATP catabolic process (GO:0006200)	succinate-CoA ligase (ADP-forming) activity (GO:0004775)	cytosol (GO:0005829)
71	ACTG1	actin, gamma 1	sensory perception of sound (GO:0007605)	ATP binding (GO:0005524)	cytoskeleton (GO:0005856)
81	ACTN4	actinin, alpha 4	positive regulation of sodium:hydrogen antiporter activity (GO:0032417)	actin filament binding (GO:0051015)	nucleus (GO:0005634)
87	ACTN1	actinin, alpha 1	regulation of apoptosis (GO:0042981)	actin binding (GO:0003779)	focal adhesion (GO:0005925)
88	ACTN2	actinin, alpha 2	microspike biogenesis (GO:0030035)	FAT2 1 binding (GO:0051374)	focal adhesion (GO:0005925)
143	PARP4	poly (ADP-ribose) polymerase family, member 4	protein amino acid ADP-ribosylation (GO:0006471)	NAD+ ADP-ribosyltransferase activity (GO:0003950)	nucleus (GO:0005634)

214	ALCAM	activated leukocyte cell adhesion molecule	signal transduction (GO:0007165)	receptor binding (GO:0005102)	integral to plasma membrane (GO:0005887)
226	ALDOA	aldolase A, fructose-bisphosphate	glycolysis (GO:0006096)	fructose-bisphosphate aldolase activity (GO:0004332)	
396	ARHGDI2	Rho GDP dissociation inhibitor (GDI) alpha	anti-apoptosis (GO:0006916)	Rho GDP-dissociation inhibitor activity (GO:0005094)	cytoskeleton (GO:0005856)
515	ATP5F1	ATP synthase, H+ transporting, mitochondrial F0 complex, subunit B1	ATP synthesis coupled proton transport (GO:0015986)	hydrogen ion transporting ATP synthase activity, rotational mechanism (GO:0046933)	mitochondrial matrix (GO:0005759)
538	ATP7A	ATPase, Cu++ transporting, alpha polypeptide (Menkes syndrome)	T-helper cell differentiation (GO:0042093)	copper-exporting ATPase activity (GO:0004008)	trans-Golgi network transport vesicle (GO:0030140)
800	CALD1	caldesmon 1	muscle contraction (GO:0006936)	actin binding (GO:0003779)	cytoskeleton (GO:0005856)
832	CAPZB	capping protein (actin filament) muscle Z-line, beta	barbed-end actin filament capping (GO:0051016)	actin binding (GO:0003779)	cytoplasm (GO:0005737)
928	CD9	CD9 molecule	fusion of sperm to egg plasma membrane (GO:0007342)	protein binding (GO:0005515)	platelet alpha granule membrane (GO:0031092)
950	SCARB2	scavenger receptor class B, member 2	cell adhesion (GO:0007155)	receptor activity (GO:0004872)	lysosomal membrane (GO:0005765)
1147	CHUK	conserved helix-loop-helix ubiquitous kinase	I-kappaB phosphorylation (GO:0007252)	IkappaB kinase activity (GO:0008384)	nucleus (GO:0005634)
1173	AP2M1	adaptor-related protein complex 2, mu 1 subunit	regulation of defense response to virus by virus (GO:0050690)	protein binding (GO:0005515)	peroxisomal membrane (GO:0005778)
1212	CLTB	clathrin, light chain (Lcb)	intracellular protein transport (GO:0006886)	calcium ion binding (GO:0005509)	clathrin coat of trans-Golgi network vesicle (GO:0030130)
1213	CLTC	clathrin, heavy chain (Hc)	intracellular protein transport (GO:0006886)	protein binding (GO:0005515)	clathrin coat of trans-Golgi network vesicle (GO:0030130)
1265	CNN2	calponin 2	actomyosin structure organization and biogenesis (GO:0031032)	actin binding (GO:0003779)	intercellular junction (GO:0005911)
1277	COL1A1	collagen, type I, alpha 1	phosphate transport (GO:0006817)	extracellular matrix structural constituent (GO:0005201)	collagen type I (GO:0005584)
1278	COL1A2	collagen, type I, alpha 2	phosphate transport (GO:0006817)	extracellular matrix structural constituent (GO:0005201)	collagen type I (GO:0005584)
1293	COL6A3	collagen, type VI, alpha 3	phosphate transport (GO:0006817)	serine-type endopeptidase inhibitor activity (GO:0004867)	collagen type VI (GO:0005589)
1303	COL12A1	collagen, type XII, alpha 1	phosphate transport (GO:0006817)	extracellular matrix structural constituent conferring tensile strength (GO:0030020)	collagen type XII (GO:0005595)
1315	COPB1	coatamer protein complex, subunit beta 1	COPI coating of Golgi vesicle (GO:0048205)	protein binding (GO:0005515)	Golgi-associated vesicle (GO:0005798)
1429	CRYZ	crystallin, zeta (quinone reductase)	visual perception (GO:0007601)	NADPH:quinone reductase activity (GO:0003960)	cytoplasm (GO:0005737)
1465	CSRP1	cysteine and glycine-rich protein 1		zinc ion binding (GO:0008270)	nucleus (GO:0005634)
1495	CTNNA1	catenin (cadherin-associated protein), alpha 1, 102kDa	apical junction assembly (GO:0043297)	vinculin binding (GO:0017166)	actin cytoskeleton (GO:0015629)
1528	CYB5A	cytochrome b5 type A (microsomal)	generation of precursor metabolites and energy (GO:0006091)	aldo-keto reductase activity (GO:0004033)	mitochondrial outer membrane (GO:0005741)
1639	DCTN1	dynactin 1 (p150, glued homolog, Drosophila)	mitosis (GO:0007067)	protein binding (GO:0005515)	spindle pole (GO:0000922)
1650	DDOST	dolichyl-diphosphooligosaccharide-protein glycosyltransferase	protein amino acid terminal N-glycosylation (GO:0006496)	dolichyl-diphosphooligosaccharide-protein glycotransferase activity (GO:0004579)	microsome (GO:0005792)
1781	DYNC112	dynein, cytoplasmic 1, intermediate chain 2	microtubule-based movement (GO:0007018)	microtubule motor activity (GO:0003777)	microtubule (GO:0005874)
1803	DPP4	dipeptidyl-peptidase 4 (CD26, adenosine deaminase complexing protein 2)	regulation of cell-cell adhesion mediated by integrin (GO:0033632)	aminopeptidase activity (GO:0004177)	integral to membrane (GO:0016021)
1808	DPYSL2	dihydropyrimidinase-like 2	nervous system development (GO:0007399)	dihydropyrimidinase activity (GO:0004157)	cytoplasm (GO:0005737)
1915	EEF1A1	eukaryotic translation elongation factor 1 alpha 1	translational elongation (GO:0006414)	GTPase activity (GO:0003924)	cytosol (GO:0005829)
1933	EEF1B2	eukaryotic translation elongation factor 1 beta 2	translational elongation (GO:0006414)	translation elongation factor activity (GO:0003746)	cytosol (GO:0005829)
1936	EEF1D	eukaryotic translation elongation factor 1 delta (guanine nucleotide exchange protein)	positive regulation of I-kappaB kinase/NF-kappaB cascade (GO:0043123)	translation elongation factor activity (GO:0003746)	cytosol (GO:0005829)

1937	EEF1G	eukaryotic translation elongation factor 1 gamma	translational elongation (GO:0006414)	translation elongation factor activity (GO:0003746)	cytosol (GO:0005829)
1938	EEF2	eukaryotic translation elongation factor 2	translational elongation (GO:0006414)	GTPase activity (GO:0003924)	cytoplasm (GO:0005737)
2040	STOM	stomatin	protein homooligomerization (GO:0051260)	protein binding (GO:0005515)	melanosome (GO:0042470)
2271	FH	fumarate hydratase	tricarboxylic acid cycle (GO:0006099)	fumarate hydratase activity (GO:0004333)	mitochondrial matrix (GO:0005759)
2274	FHL2	four and a half LIM domains 2	androgen receptor signaling pathway (GO:0030521)	androgen receptor binding (GO:0050681)	nucleus (GO:0005634)
2314	FLII	flightless I homolog (Drosophila)	regulation of transcription, DNA-dependent (GO:0006355)	actin binding (GO:0003779)	centrosome (GO:0005813)
2316	FLNA	filamin A, alpha (actin binding protein 280)	positive regulation of transcription factor import into nucleus (GO:0042993)	actin filament binding (GO:0051015)	actin cytoskeleton (GO:0015629)
2317	FLNB	filamin B, beta (actin binding protein 278)	skeletal muscle development (GO:0007519)	actin binding (GO:0003779)	actin cytoskeleton (GO:0015629)
2318	FLNC	filamin C, gamma (actin binding protein 280)		actin binding (GO:0003779)	actin cytoskeleton (GO:0015629)
2495	FTH1	ferritin, heavy polypeptide 1	cellular iron ion homeostasis (GO:0006879)	ferric iron binding (GO:0008199)	plasma membrane (GO:0005886)
2547	XRCC6	X-ray repair complementing defective repair in Chinese hamster cells 6 (Ku autoantigen, 70kDa)	double-strand break repair via nonhomologous end joining (GO:0006303)	double-stranded DNA binding (GO:0003690)	nucleus (GO:0005634)
2697	GJA1	gap junction protein, alpha 1, 43kDa	sensory perception of sound (GO:0007605)	ion transmembrane transporter activity (GO:0015075)	integral to plasma membrane (GO:0005887)
2744	GLS	glutaminase	glutamine catabolic process (GO:0006543)	glutaminase activity (GO:0004359)	mitochondrial matrix (GO:0005759)
2746	GLUD1	glutamate dehydrogenase 1	glutamate catabolic process (GO:0006538)	ATP binding (GO:0005524)	mitochondrial matrix (GO:0005759)
2747	GLUD2	glutamate dehydrogenase 2	glutamate metabolic process (GO:0006536)	glutamate dehydrogenase activity (GO:0004352)	mitochondrial matrix (GO:0005759)
2782	GNB1	guanine nucleotide binding protein (G protein), beta polypeptide 1	acetylcholine receptor signaling, muscarinic pathway (GO:0007213)	GTPase activity (GO:0003924)	
2804	GOLGB1	golgin B1, golgi integral membrane protein	Golgi organization and biogenesis (GO:0007030)	protein binding (GO:0005515)	Golgi stack (GO:0005795)
2934	GSN	gelsolin (amyloidosis, Finnish type)	barbed-end actin filament capping (GO:0051016)	actin binding (GO:0003779)	actin cytoskeleton (GO:0015629)
2950	GSTP1	glutathione S-transferase pi	anti-apoptosis (GO:0006916)	glutathione transferase activity (GO:0004364)	cytoplasm (GO:0005737)
3007	HIST1H1D	histone cluster 1, H1d	nucleosome assembly (GO:0006334)	DNA binding (GO:0003677)	nucleus (GO:0005634)
3010	HIST1H1T	histone cluster 1, H1t	nucleosome assembly (GO:0006334)	DNA binding (GO:0003677)	nucleus (GO:0005634)
3017	HIST1H2BD	histone cluster 1, H2bd	nucleosome assembly (GO:0006334)	DNA binding (GO:0003677)	nucleus (GO:0005634)
3024	HIST1H1A	histone cluster 1, H1a	nucleosome assembly (GO:0006334)	DNA binding (GO:0003677)	nucleus (GO:0005634)
3094	HINT1	histidine triad nucleotide binding protein 1	signal transduction (GO:0007165)	protein kinase C binding (GO:0005080)	nucleus (GO:0005634)
3106	HLA-B	major histocompatibility complex, class I, B	antigen processing and presentation of peptide antigen via MHC class I (GO:0002474)	MHC class I receptor activity (GO:0032393)	integral to plasma membrane (GO:0005887)
3107	HLA-C	major histocompatibility complex, class I, C	antigen processing and presentation of peptide antigen via MHC class I (GO:0002474)	MHC class I receptor activity (GO:0032393)	axonemal dynein complex (GO:0005858)
3146	HMGB1	high-mobility group box 1	negative regulation of transcriptional preinitiation complex assembly (GO:0017055)	DNA bending activity (GO:0008301)	condensed chromosome (GO:0000793)
3181	HNRNPA2B1	heterogeneous nuclear ribonucleoprotein A2/B1	nuclear mRNA splicing, via spliceosome (GO:0000398)	single-stranded telomeric DNA binding (GO:0043047)	nucleus (GO:0005634)
3184	HNRNPD	heterogeneous nuclear ribonucleoprotein D (AU-rich element RNA binding protein 1, 37kDa)	nuclear mRNA splicing, via spliceosome (GO:0000398)	DNA binding (GO:0003677)	chromosome, telomeric region (GO:0000781)
3185	HNRNPF	heterogeneous nuclear ribonucleoprotein F	nuclear mRNA splicing, via spliceosome (GO:0000398)	RNA binding (GO:0003723)	nucleus (GO:0005634)
3295	HSD17B4	hydroxysteroid (17-beta) dehydrogenase 4	fatty acid metabolic process (GO:0006631)	3-hydroxyacyl-CoA dehydrogenase activity (GO:0003857)	peroxisomal matrix (GO:0005782)
3305	HSPA1L	heat shock 70kDa protein 1-like	response to unfolded protein (GO:0006986)	ATP binding (GO:0005524)	

3306	HSPA2	heat shock 70kDa protein 2	male meiosis (GO:0007140)	ATP binding (GO:0005524)	cell surface (GO:0009986)
3308	HSPA4	heat shock 70kDa protein 4	response to unfolded protein (GO:0006986)	ATP binding (GO:0005524)	cytoplasm (GO:0005737)
3311	HSPA7	heat shock 70kDa protein 7 (HSP70B)	response to unfolded protein (GO:0006986)	ATP binding (GO:0005524)	cellular_component (GO:0005575)
3312	HSPA8	heat shock 70kDa protein 8	protein folding (GO:0006457)	ATPase activity, coupled (GO:0042623)	melanosome (GO:0042470)
3313	HSPA9	heat shock 70kDa protein 9 (mortalin)	anti-apoptosis (GO:0006916)	ATP binding (GO:0005524)	mitochondrion (GO:0005739)
3315	HSPB1	heat shock 27kDa protein 1	anti-apoptosis (GO:0006916)	identical protein binding (GO:0042802)	nucleus (GO:0005634)
3320	HSP90AA1	heat shock protein 90kDa alpha (cytosolic), class A member 1	positive regulation of nitric oxide biosynthetic process (GO:0045429)	ATP binding (GO:0005524)	melanosome (GO:0042470)
3326	HSP90AB1	heat shock protein 90kDa alpha (cytosolic), class B member 1	positive regulation of nitric oxide biosynthetic process (GO:0045429)	ATP binding (GO:0005524)	melanosome (GO:0042470)
3382	ICA1	islet cell autoantigen 1, 69kDa	neurotransmitter transport (GO:0006836)	protein binding (GO:0005515)	secretory granule membrane (GO:0030667)
3417	IDH1	isocitrate dehydrogenase 1 (NADP+), soluble	tricarboxylic acid cycle (GO:0006099)	isocitrate dehydrogenase (NADP+) activity (GO:0004450)	peroxisome (GO:0005777)
3609	ILF3	interleukin enhancer binding factor 3, 90kDa	negative regulation of transcription, DNA-dependent (GO:0045892)	double-stranded RNA binding (GO:0003725)	nucleus (GO:0005634)
3611	ILK	integrin-linked kinase	protein amino acid phosphorylation (GO:0006468)	protein serine/threonine kinase activity (GO:0004674)	cell junction (GO:0030054)
3675	ITGA3	integrin, alpha 3 (antigen CD49C, alpha 3 subunit of VLA-3 receptor)	integrin-mediated signaling pathway (GO:0007229)	calcium ion binding (GO:0005509)	integrin complex (GO:0008305)
3685	ITGAV	integrin, alpha V (vitronectin receptor, alpha polypeptide, antigen CD51)	integrin-mediated signaling pathway (GO:0007229)	calcium ion binding (GO:0005509)	integrin complex (GO:0008305)
3704	ITPA	inosine triphosphatase (nucleoside triphosphate pyrophosphatase)	nucleotide metabolic process (GO:0009117)	nucleoside-triphosphate diphosphatase activity (GO:0047429)	cytoplasm (GO:0005737)
3799	KIF5B	kinesin family member 5B	vesicle transport along microtubule (GO:0047496)	ATP binding (GO:0005524)	kinesin complex (GO:0005871)
3843	IPO5	importin 5	NLS-bearing substrate import into nucleus (GO:0006607)	Ran GTPase binding (GO:0008536)	nucleus (GO:0005634)
3856	KRT8	keratin 8	cytoskeleton organization and biogenesis (GO:0007010)	protein binding (GO:0005515)	intermediate filament (GO:0005882)
3895	KTN1	kinectin 1 (kinesin receptor)	microtubule-based movement (GO:0007018)	receptor activity (GO:0004872)	integral to plasma membrane (GO:0005887)
3939	LDHA	lactate dehydrogenase A	anaerobic glycolysis (GO:0019642)	L-lactate dehydrogenase activity (GO:0004459)	cytosol (GO:0005829)
3958	LGALS3	lectin, galactoside-binding, soluble, 3		IgE binding (GO:0019863)	nucleus (GO:0005634)
3998	LMAN1	lectin, mannose-binding, 1	protein folding (GO:0006457)	mannose binding (GO:0005537)	Golgi membrane (GO:0000139)
4008	LMO7	LIM domain 7	protein ubiquitination (GO:0016567)	zinc ion binding (GO:0008270)	nucleus (GO:0005634)
4082	MARCKS	myristoylated alanine-rich protein kinase C substrate	cell motility (GO:0006928)	actin filament binding (GO:0051015)	actin cytoskeleton (GO:0015629)
4478	MSN	moesin	cell motility (GO:0006928)	receptor binding (GO:0005102)	cytoskeleton (GO:0005856)
4627	MYH9	myosin, heavy chain 9, non-muscle	membrane protein ectodomain proteolysis (GO:0006509)	actin-dependent ATPase activity (GO:0030898)	stress fiber (GO:0001725)
4629	MYH11	myosin, heavy chain 11, smooth muscle	muscle thick filament assembly (GO:0030241)	ATP binding (GO:0005524)	striated muscle thick filament (GO:0005863)
4638	MYLK	myosin light chain kinase	protein amino acid phosphorylation (GO:0006468)	myosin light chain kinase activity (GO:0004687)	
4691	NCL	nucleolin	angiogenesis (GO:0001525)	DNA binding (GO:0003677)	nucleus (GO:0005634)
4735	SEPT2	septin 2	cell cycle (GO:0007049)	GTP binding (GO:0005525)	nucleus (GO:0005634)
4736	RPL10A	ribosomal protein L10a	translational elongation (GO:0006414)	structural constituent of ribosome (GO:0003735)	cytosol (GO:0005829)
4841	NONO	non-POU domain containing, octamer-binding	mRNA processing (GO:0006397)	DNA binding (GO:0003677)	nucleus (GO:0005634)

4869	NPM1	nucleophosmin (nucleolar phosphoprotein B23, numatrin)	anti-apoptosis (GO:0006916)	transcription coactivator activity (GO:0003713)	centrosome (GO:0005813)
4914	NTRK1	neurotrophic tyrosine kinase, receptor, type 1	activation of adenylate cyclase activity (GO:0007190)	transmembrane receptor protein tyrosine kinase activity (GO:0004714)	integral to plasma membrane (GO:0005887)
5052	PRDX1	peroxiredoxin 1	skeletal development (GO:0001501)	peroxiredoxin activity (GO:0051920)	melanosome (GO:0042470)
5223	PGAM1	phosphoglycerate mutase 1 (brain)	glycolysis (GO:0006096)	bisphosphoglycerate 2-phosphatase activity (GO:0004083)	cytosol (GO:0005829)
5230	PGK1	phosphoglycerate kinase 1	glycolysis (GO:0006096)	ATP binding (GO:0005524)	cytoplasm (GO:0005737)
5339	PLEC1	plectin 1, intermediate filament binding protein 500kDa	cytoskeletal anchoring at plasma membrane (GO:0007016)	actin binding (GO:0003779)	cytoskeleton (GO:0005856)
5351	PLOD1	procollagen-lysine 1, 2-oxoglutarate 5-dioxygenase 1	hydroxylysine biosynthetic process (GO:0046947)	iron ion binding (GO:0005506)	rough endoplasmic reticulum membrane (GO:0030867)
5589	PRKCSH	protein kinase C substrate 80K-H	protein kinase cascade (GO:0007243)	calcium ion binding (GO:0005509)	endoplasmic reticulum (GO:0005783)
5682	PSMA1	proteasome (prosome, macropain) subunit, alpha type, 1	anaphase-promoting complex-dependent proteasomal ubiquitin-dependent protein catabolic process (GO:0031145)	threonine endopeptidase activity (GO:0004298)	nucleus (GO:0005634)
5686	PSMA5	proteasome (prosome, macropain) subunit, alpha type, 5	anaphase-promoting complex-dependent proteasomal ubiquitin-dependent protein catabolic process (GO:0031145)	threonine endopeptidase activity (GO:0004298)	nucleus (GO:0005634)
5689	PSMB1	proteasome (prosome, macropain) subunit, beta type, 1	anaphase-promoting complex-dependent proteasomal ubiquitin-dependent protein catabolic process (GO:0031145)	threonine endopeptidase activity (GO:0004298)	nucleus (GO:0005634)
5693	PSMB5	proteasome (prosome, macropain) subunit, beta type, 5	anaphase-promoting complex-dependent proteasomal ubiquitin-dependent protein catabolic process (GO:0031145)	threonine endopeptidase activity (GO:0004298)	nucleus (GO:0005634)
5705	PSMC5	proteasome (prosome, macropain) 26S subunit, ATPase, 5	anaphase-promoting complex-dependent proteasomal ubiquitin-dependent protein catabolic process (GO:0031145)	ATPase activity (GO:0016887)	nucleus (GO:0005634)
5708	PSMD2	proteasome (prosome, macropain) 26S subunit, non-ATPase, 2	anaphase-promoting complex-dependent proteasomal ubiquitin-dependent protein catabolic process (GO:0031145)	protein binding (GO:0005515)	cytosol (GO:0005829)
5713	PSMD7	proteasome (prosome, macropain) 26S subunit, non-ATPase, 7	anaphase-promoting complex-dependent proteasomal ubiquitin-dependent protein catabolic process (GO:0031145)	protein binding (GO:0005515)	cytosol (GO:0005829)
5813	PURA	purine-rich element binding protein A	DNA unwinding during replication (GO:0006268)	double-stranded telomeric DNA binding (GO:0003691)	nuclear chromosome, telomeric region (GO:0000784)
5814	PURB	purine-rich element binding protein B	regulation of transcription, DNA-dependent (GO:0006355)	single-stranded DNA binding (GO:0003697)	nucleus (GO:0005634)
5887	RAD23B	RAD23 homolog B (S. cerevisiae)	proteasomal ubiquitin-dependent protein catabolic process (GO:0043161)	single-stranded DNA binding (GO:0003697)	nucleus (GO:0005634)
6117	RPA1	replication protein A1, 70kDa	nucleotide-excision repair, DNA damage removal (GO:0000718)	single-stranded DNA binding (GO:0003697)	PML body (GO:0016605)
6119	RPA3	replication protein A3, 14kDa	nucleotide-excision repair, DNA damage removal (GO:0000718)	single-stranded DNA binding (GO:0003697)	nucleus (GO:0005634)
6122	RPL3	ribosomal protein L3	translational elongation (GO:0006414)	RNA binding (GO:0003723)	cytosolic large ribosomal subunit (GO:0022625)
6124	RPL4	ribosomal protein L4	translational elongation (GO:0006414)	RNA binding (GO:0003723)	cytosolic large ribosomal subunit (GO:0022625)
6125	RPL5	ribosomal protein L5	translational elongation (GO:0006414)	5S rRNA binding (GO:0008097)	cytosolic large ribosomal subunit (GO:0022625)
6128	RPL6	ribosomal protein L6	regulation of transcription, DNA-dependent (GO:0006355)	DNA binding (GO:0003677)	cytosolic large ribosomal subunit (GO:0022625)
6160	RPL31	ribosomal protein L31	translational elongation (GO:0006414)	RNA binding (GO:0003723)	cytosolic large ribosomal subunit (GO:0022625)
6165	RPL35A	ribosomal protein L35a	translational elongation (GO:0006414)	tRNA binding (GO:0000049)	cytosolic large ribosomal subunit (GO:0022625)
6176	RPLP1	ribosomal protein, large, P1	translational elongation (GO:0006414)	RNA binding (GO:0003723)	cytosolic large ribosomal subunit (GO:0022625)

6188	RPS3	ribosomal protein S3	translational elongation (GO:0006414)	RNA binding (GO:0003723)	cytosolic small ribosomal subunit (GO:0022627)
6189	RPS3A	ribosomal protein S3A	induction of apoptosis (GO:0006917)	RNA binding (GO:0003723)	cytosolic small ribosomal subunit (GO:0022627)
6206	RPS12	ribosomal protein S12	translational elongation (GO:0006414)	RNA binding (GO:0003723)	cytosolic small ribosomal subunit (GO:0022627)
6209	RPS15	ribosomal protein S15	translational elongation (GO:0006414)	structural constituent of ribosome (GO:0003735)	cytosolic small ribosomal subunit (GO:0022627)
6238	RRBP1	ribosome binding protein 1 homolog 180kDa (dog)	intracellular protein transport across a membrane (GO:0065002)	receptor activity (GO:0004872)	integral to endoplasmic reticulum membrane (GO:0030176)
6251	RSU1	Ras suppressor protein 1	signal transduction (GO:0007165)	protein binding (GO:0005515)	
6421	SFPQ	splicing factor proline/glutamine-rich (polypyrimidine tract binding protein associated)	mRNA processing (GO:0006397)	DNA binding (GO:0003677)	nucleus (GO:0005634)
6449	SGTA	small glutamine-rich tetratricopeptide repeat (TPR)-containing, alpha		protein binding (GO:0005515)	cytoplasm (GO:0005737)
6520	SLC3A2	solute carrier family 3 (activators of dibasic and neutral amino acid transport), member 2	calcium ion transport (GO:0006816)	calcium:sodium antiporter activity (GO:0005432)	melanosome (GO:0042470)
6708	SPTA1	spectrin, alpha, erythrocytic 1 (elliptocytosis 2)	barbed-end actin filament capping (GO:0051016)	actin filament binding (GO:0051015)	cytoskeleton (GO:0005856)
6709	SPTAN1	spectrin, alpha, non-erythrocytic 1 (alpha-fodrin)	barbed-end actin filament capping (GO:0051016)	actin binding (GO:0003779)	cytosol (GO:0005829)
6711	SPTBN1	spectrin, beta, non-erythrocytic 1	barbed-end actin filament capping (GO:0051016)	actin binding (GO:0003779)	nucleolus (GO:0005730)
6810	STX4	syntaxin 4	intracellular protein transport (GO:0006886)	SNAP receptor activity (GO:0005484)	vacuole (GO:0005773)
6876	TAGLN	transgelin	muscle development (GO:0007517)	actin binding (GO:0003779)	cytoplasm (GO:0005737)
7057	THBS1	thrombospondin 1	nervous system development (GO:0007399)	heparin binding (GO:0008201)	platelet alpha granule lumen (GO:0031093)
7086	TKT	transketolase (Wernicke-Korsakoff syndrome)	metabolic process (GO:0008152)	transketolase activity (GO:0004802)	cytosol (GO:0005829)
7158	TP53BP1	tumor protein p53 binding protein 1	positive regulation of transcription, DNA-dependent (GO:0045893)	DNA binding (GO:0003677)	nucleus (GO:0005634)
7162	TPBG	trophoblast glycoprotein	cell motility (GO:0006928)	protein binding (GO:0005515)	integral to plasma membrane (GO:0005887)
7169	TPM2	tropomyosin 2 (beta)	regulation of ATPase activity (GO:0043462)	actin binding (GO:0003779)	cytoskeleton (GO:0005856)
7171	TPM4	tropomyosin 4	cell motility (GO:0006928)	actin binding (GO:0003779)	cytoskeleton (GO:0005856)
7203	CCT3	chaperonin containing TCP1, subunit 3 (gamma)	protein folding (GO:0006457)	ATP binding (GO:0005524)	cytoskeleton (GO:0005856)
7295	TXN	thioredoxin	signal transduction (GO:0007165)	protein binding (GO:0005515)	cytosol (GO:0005829)
7296	TXNRD1	thioredoxin reductase 1	signal transduction (GO:0007165)	FAD binding (GO:0005660)	nucleus (GO:0005634)
7317	UBA1	ubiquitin-like modifier activating enzyme 1	DNA replication (GO:0006260)	ATP binding (GO:0005524)	
7345	UCHL1	ubiquitin carboxyl-terminal esterase L1 (ubiquitin thiolesterase)	protein deubiquitination (GO:0016579)	ubiquitin thiolesterase activity (GO:0004221)	cytoplasm (GO:0005737)
7407	VARS	valyl-tRNA synthetase	valyl-tRNA aminoacylation (GO:0006438)	valine-tRNA ligase activity (GO:0004832)	cytoplasm (GO:0005737)
7408	VASP	vasodilator-stimulated phosphoprotein	cell motility (GO:0006928)	actin binding (GO:0003779)	actin cytoskeleton (GO:0015629)
7414	VCL	vinculin	lamellipodium biogenesis (GO:0030032)	actin binding (GO:0003779)	focal adhesion (GO:0005925)
7415	VCP	valosin-containing protein	caspase activation (GO:0006919)	ATPase activity (GO:0016887)	microsome (GO:0005792)
7424	VEGFC	vascular endothelial growth factor C	positive regulation of cell proliferation (GO:0008284)	growth factor activity (GO:0008083)	platelet alpha granule lumen (GO:0031093)
7430	EZR	ezrin	actin filament bundle formation (GO:0051017)	actin filament binding (GO:0051015)	cortical cytoskeleton (GO:0030863)
7520	XRCC5	X-ray repair complementing defective repair in Chinese hamster cells 5 (double-strand-break	double-strand break repair via nonhomologous end joining (GO:0006303)	ATP binding (GO:0005524)	nucleus (GO:0005634)

		rejoining; Ku autoantigen, 80kDa)			
7529	YWHAB	tyrosine 3-monooxygenase/tryptophan 5-monooxygenase activation protein, beta polypeptide	activation of pro-apoptotic gene products (GO:0008633)	monooxygenase activity (GO:0004497)	melanosome (GO:0042470)
7532	YWHAG	tyrosine 3-monooxygenase/tryptophan 5-monooxygenase activation protein, gamma polypeptide	negative regulation of protein kinase activity (GO:0006469)	protein kinase C binding (GO:0005080)	cytoplasm (GO:0005737)
7534	YWHAZ	tyrosine 3-monooxygenase/tryptophan 5-monooxygenase activation protein, zeta polypeptide	anti-apoptosis (GO:0006916)	transcription factor binding (GO:0008134)	melanosome (GO:0042470)
8087	FXR1	fragile X mental retardation, autosomal homolog 1	skeletal muscle development (GO:0007519)	RNA binding (GO:0003723)	nucleolus (GO:0005730)
8218	CLTCL1	clathrin, heavy chain-like 1	receptor-mediated endocytosis (GO:0006898)	signal transducer activity (GO:0004871)	clathrin coat of trans-Golgi network vesicle (GO:0030130)
8290	HIST3H3	histone cluster 3, H3	nucleosome assembly (GO:0006334)	DNA binding (GO:0003677)	nucleus (GO:0005634)
8335	HIST1H2AB	histone cluster 1, H2ab	nucleosome assembly (GO:0006334)	DNA binding (GO:0003677)	nucleus (GO:0005634)
8411	EEA1	early endosome antigen 1	vesicle fusion (GO:0006906)	phosphatidylinositol binding (GO:0005545)	early endosome membrane (GO:0031901)
8531	CSDA	cold shock domain protein A	negative regulation of transcription from RNA polymerase II promoter (GO:0000122)	double-stranded DNA binding (GO:0003690)	nucleus (GO:0005634)
8615	USO1	USO1 homolog, vesicle docking protein (yeast)	vesicle fusion with Golgi apparatus (GO:0048280)	protein transporter activity (GO:0008565)	Golgi membrane (GO:0000139)
8661	EIF3A	eukaryotic translation initiation factor 3, subunit A	regulation of translational initiation (GO:0006446)	translation initiation factor activity (GO:0003743)	cytosol (GO:0005829)
8662	EIF3B	eukaryotic translation initiation factor 3, subunit B	translational initiation (GO:0006413)	translation initiation factor activity (GO:0003743)	cytosol (GO:0005829)
8666	EIF3G	eukaryotic translation initiation factor 3, subunit G	regulation of translational initiation (GO:0006446)	translation initiation factor activity (GO:0003743)	cytosol (GO:0005829)
8668	EIF3I	eukaryotic translation initiation factor 3, subunit I	regulation of translational initiation (GO:0006446)	translation initiation factor activity (GO:0003743)	cytosol (GO:0005829)
8971	H1FX	H1 histone family, member X	nucleosome assembly (GO:0006334)	DNA binding (GO:0003677)	nucleus (GO:0005634)
9093	DNAJA3	DnaJ (Hsp40) homolog, subfamily A, member 3	protein folding (GO:0006457)	zinc ion binding (GO:0008270)	mitochondrial matrix (GO:0005759)
9218	VAPA	VAMP (vesicle-associated membrane protein)-associated protein A, 33kDa	positive regulation of I-kappaB kinase/NF-kappaB cascade (GO:0043123)	protein heterodimerization activity (GO:0046982)	tight junction (GO:0005923)
9219	MTA2	metastasis associated 1 family, member 2	chromatin assembly or disassembly (GO:0006333)	zinc ion binding (GO:0008270)	histone deacetylase complex (GO:0000118)
9230	RAB11B	RAB11B, member RAS oncogene family	small GTPase mediated signal transduction (GO:0007264)	GTPase activity (GO:0003924)	plasma membrane (GO:0005886)
9276	COPB2	coatamer protein complex, subunit beta 2 (beta prime)	COPI coating of Golgi vesicle (GO:0048205)	protein binding (GO:0005515)	COPI vesicle coat (GO:0030126)
9590	AKAP12	A kinase (PRKA) anchor protein (gravin) 12	protein targeting (GO:0006605)	protein kinase A binding (GO:0051018)	cytoskeleton (GO:0005856)
9601	PDIA4	protein disulfide isomerase family A, member 4	protein secretion (GO:0009306)	protein disulfide isomerase activity (GO:0003756)	melanosome (GO:0042470)
9706	ULK2	unc-51-like kinase 2 (C. elegans)	axonogenesis (GO:0007409)	protein serine/threonine kinase activity (GO:0004674)	
9761	KIAA0152	KIAA0152			integral to membrane (GO:0016021)
9782	MATR3	matrin 3		zinc ion binding (GO:0008270)	nuclear inner membrane (GO:0005637)
9871	SEC24D	SEC24 related gene family, member D (S. cerevisiae)	ER to Golgi vesicle-mediated transport (GO:0006888)	zinc ion binding (GO:0008270)	COPII vesicle coat (GO:0030127)
9943	OXS1	oxidative-stress responsive 1	protein amino acid phosphorylation (GO:0006468)	protein serine/threonine kinase activity (GO:0004674)	
9961	MVP	major vault protein	mRNA transport (GO:0051028)		nucleus (GO:0005634)
10095	ARPC1B	actin related protein 2/3 complex, subunit 1B, 41kDa	cell motility (GO:0006928)	actin binding (GO:0003779)	cytoplasm (GO:0005737)

10109	ARPC2	actin related protein 2/3 complex, subunit 2, 34kDa	regulation of actin filament polymerization (GO:0030833)	actin binding (GO:0003779)	cytoskeleton (GO:0005856)
10483	SEC23B	Sec23 homolog B (<i>S. cerevisiae</i>)	ER to Golgi vesicle-mediated transport (GO:0006888)	zinc ion binding (GO:0008270)	COPII vesicle coat (GO:0030127)
10487	CAP1	CAP, adenylate cyclase-associated protein 1 (yeast)	activation of adenylate cyclase activity (GO:0007190)	actin binding (GO:0003779)	plasma membrane (GO:0005886)
10528	NOL5A	nucleolar protein 5A (56kDa with KKE/D repeat)	rRNA processing (GO:0006364)	RNA binding (GO:0003723)	nucleus (GO:0005634)
10540	DCTN2	dynactin 2 (p50)	microtubule-based process (GO:0007017)	protein binding (GO:0005515)	centrosome (GO:0005813)
10574	CCT7	chaperonin containing TCP1, subunit 7 (eta)	protein folding (GO:0006457)	ATP binding (GO:0005524)	cytoplasm (GO:0005737)
10575	CCT4	chaperonin containing TCP1, subunit 4 (delta)	protein folding (GO:0006457)	ATP binding (GO:0005524)	melanosome (GO:0042470)
10576	CCT2	chaperonin containing TCP1, subunit 2 (beta)	protein folding (GO:0006457)	ATP binding (GO:0005524)	cytosol (GO:0005829)
10606	PAICS	phosphoribosylaminoimidazole carboxylase, phosphoribosylaminoimidazole succinocarboxamide synthetase	'de novo' IMP biosynthetic process (GO:0006189)	ATP binding (GO:0005524)	phosphoribosylaminoimidazole carboxylase complex (GO:0009320)
10611	PDLIM5	PDZ and LIM domain 5		protein kinase C binding (GO:0005080)	actin cytoskeleton (GO:0015629)
10801	9-Sep	septin 9	protein heterooligomerization (GO:0051291)	GTPase activity (GO:0003924)	stress fiber (GO:0001725)
10935	PRDX3	peroxiredoxin 3	positive regulation of NF-kappaB transcription factor activity (GO:0051092)	alkyl hydroperoxide reductase activity (GO:0008785)	mitochondrion (GO:0005739)
10938	EHD1	EH-domain containing 1		GTPase activity (GO:0003924)	early endosome membrane (GO:0031901)
10963	STIP1	stress-induced-phosphoprotein 1 (Hsp70/Hsp90-organizing protein)	response to stress (GO:0006950)	binding (GO:0005488)	nucleus (GO:0005634)
10992	SF3B2	splicing factor 3b, subunit 2, 145kDa	nuclear mRNA splicing, via spliceosome (GO:0000398)	nucleic acid binding (GO:0003676)	nucleus (GO:0005634)
11034	DSTN	destrin (actin depolymerizing factor)	actin polymerization and/or depolymerization (GO:0008154)	actin binding (GO:0003779)	actin cytoskeleton (GO:0015629)
11316	COPE	coatamer protein complex, subunit epsilon	COPI coating of Golgi vesicle (GO:0048205)	protein binding (GO:0005515)	COPI vesicle coat (GO:0030126)
11328	FKBP9	FK506 binding protein 9, 63 kDa	protein folding (GO:0006457)	peptidyl-prolyl cis-trans isomerase activity (GO:0003755)	endoplasmic reticulum (GO:0005783)
11335	CBX3	chromobox homolog 3 (HP1 gamma homolog, <i>Drosophila</i>)	chromatin remodeling (GO:0006338)	protein domain specific binding (GO:0019904)	nuclear centromeric heterochromatin (GO:0031618)
22872	SEC31A	SEC31 homolog A (<i>S. cerevisiae</i>)	ER to Golgi vesicle-mediated transport (GO:0006888)	protein binding (GO:0005515)	COPII vesicle coat (GO:0030127)
22995	CEP152	centrosomal protein 152kDa			centrosome (GO:0005813)
23022	PALLD	palladin, cytoskeletal associated protein	cytoskeleton organization and biogenesis (GO:0007010)	muscle alpha-actinin binding (GO:0051371)	nucleus (GO:0005634)
23193	GANAB	glucosidase, alpha; neutral AB	carbohydrate metabolic process (GO:0005975)	glucan 1,3-alpha-glucosidase activity (GO:0033919)	melanosome (GO:0042470)
23307	FKBP15	FK506 binding protein 15, 133kDa	protein folding (GO:0006457)		cytoplasm (GO:0005737)
23345	SYNE1	spectrin repeat containing, nuclear envelope 1	nuclear organization and biogenesis (GO:0006997)	actin binding (GO:0003779)	nucleus (GO:0005634)
23446	SLC44A1	solute carrier family 44, member 1	choline transport (GO:0015871)	choline transmembrane transporter activity (GO:0015220)	integral to membrane (GO:0016021)
23461	ABCA5	ATP-binding cassette, sub-family A (ABC1), member 5	transport (GO:0006810)	ATPase activity (GO:0016887)	lysosomal membrane (GO:0005765)
23499	MACF1	microtubule-actin crosslinking factor 1	cell cycle arrest (GO:0007050)	microtubule binding (GO:0008017)	cytoskeleton (GO:0005856)
23603	CORO1C	coronin, actin binding protein, 1C	phagocytosis (GO:0006909)	actin binding (GO:0003779)	actin cytoskeleton (GO:0015629)
26509	FER1L3	fer-1-like 3, myoferlin (<i>C. elegans</i>)	muscle contraction (GO:0006936)		nucleus (GO:0005634)
26986	PABPC1	poly(A) binding protein, cytoplasmic 1	mRNA polyadenylation (GO:0006378)	poly(A) binding (GO:0008143)	nucleus (GO:0005634)

27020	NPTN	neuroplastin	positive regulation of long-term neuronal synaptic plasticity (GO:0048170)	cell adhesion molecule binding (GO:0050839)	integral to membrane (GO:0016021)
29766	TMOD3	tropomodulin 3 (ubiquitous)		actin binding (GO:0003779)	cytoskeleton (GO:0005856)
30846	EHD2	EH-domain containing 2		GTPase activity (GO:0003924)	nucleus (GO:0005634)
51087	YBX2	Y box binding protein 2	transcription from RNA polymerase II promoter (GO:0006366)	DNA binding (GO:0003677)	nucleus (GO:0005634)
51350	KRT76	keratin 76	cytoskeleton organization and biogenesis (GO:0007010)	structural molecule activity (GO:0005198)	intermediate filament (GO:0005882)
51742	ARID4B	AT rich interactive domain 4B (RBP1-like)	chromatin assembly or disassembly (GO:0006333)	DNA binding (GO:0003677)	chromatin (GO:0000785)
54997	TESC	tescalcin		magnesium ion binding (GO:0000287)	nucleus (GO:0005634)
55075	UACA	uveal autoantigen with coiled-coil domains and ankyrin repeats	viral reproduction (GO:0016032)		nucleus (GO:0005634)
55299	BXDC2	brix domain containing 2	ribosome biogenesis and assembly (GO:0042254)	protein binding (GO:0005515)	nucleus (GO:0005634)
55752	SEPT11	septin 11	protein heterooligomerization (GO:0051291)	GTP binding (GO:0005525)	stress fiber (GO:0001725)
55917	CTTNBP2NL	CTTNBP2 N-terminal like			actin cytoskeleton (GO:0015629)
56005	C19orf10	chromosome 19 open reading frame 10			extracellular region (GO:0005576)
56911	C21orf7	chromosome 21 open reading frame 7		protein binding (GO:0005515)	nucleus (GO:0005634)
56969	RPL23AP13	ribosomal protein L23a pseudogene 13		nucleotide binding (GO:0000166)	ribosome (GO:0005840)
57222	ERGIC1	endoplasmic reticulum-golgi intermediate compartment (ERGIC) 1	ER to Golgi vesicle-mediated transport (GO:0006888)	protein binding (GO:0005515)	Golgi membrane (GO:0000139)
60681	FKBP10	FK506 binding protein 10, 65 kDa	protein folding (GO:0006457)	peptidyl-prolyl cis-trans isomerase activity (GO:0003755)	endoplasmic reticulum (GO:0005783)
63971	KIF13A	kinesin family member 13A	microtubule-based movement (GO:0007018)	ATP binding (GO:0005524)	microtubule (GO:0005874)
64098	PARVG	parvin, gamma	cell-matrix adhesion (GO:0007160)	actin binding (GO:0003779)	cytoskeleton (GO:0005856)
65992	C20orf116	chromosome 20 open reading frame 116		protein binding (GO:0005515)	extracellular region (GO:0005576)
66005	CHID1	chitinase domain containing 1	chitin catabolic process (GO:0006032)	chitinase activity (GO:0004568)	lysosome (GO:0005764)
81035	COLEC12	collectin sub-family member 12	phosphate transport (GO:0006817)	scavenger receptor activity (GO:0005044)	integral to membrane (GO:0016021)
81567	TXNDC5	thioredoxin domain containing 5	anti-apoptosis (GO:0006916)	isomerase activity (GO:0016853)	endoplasmic reticulum (GO:0005783)
84936	ZFYVE19	zinc finger, FYVE domain containing 19		zinc ion binding (GO:0008270)	
113026	PLCD3	phospholipase C, delta 3	intracellular signaling cascade (GO:0007242)	phosphoinositide phospholipase C activity (GO:0004435)	cytoplasm (GO:0005737)
127829	ARL8A	ADP-ribosylation factor-like 8A	small GTPase mediated signal transduction (GO:0007264)	GTPase activity (GO:0003924)	lysosome (GO:0005764)
140597	TCEAL2	transcription elongation factor A (SII)-like 2	regulation of transcription, DNA-dependent (GO:0006355)		nucleus (GO:0005634)
145165	FAM10A4	family with sequence similarity 10, member A4 pseudogene		binding (GO:0005488)	cytoplasm (GO:0005737)
153562	MARVELD2	MARVEL domain containing 2	sensory perception of sound (GO:0007605)		tight junction (GO:0005923)
158358	KIAA2026	KIAA2026			
255101	CCDC108	coiled-coil domain containing 108		structural molecule activity (GO:0005198)	integral to membrane (GO:0016021)
255738	PCSK9	proprotein convertase subtilisin/kexin type 9	protein autoprocessing (GO:0016540)	calcium ion binding (GO:0005509)	extracellular space (GO:0005615)
283149	BCL9L	B-cell CLL/lymphoma 9-like	regulation of transcription, DNA-dependent (GO:0006355)		nucleus (GO:0005634)

338773	TMEM119	transmembrane protein 119			integral to membrane (GO:0016021)
348654	GEN1	Gen homolog 1, endonuclease (Drosophila)	DNA repair (GO:0006281)	endonuclease activity (GO:0004519)	nucleus (GO:0005634)
360132	FKBP9L	FK506 binding protein 9-like	protein folding (GO:0006457)	calcium ion binding (GO:0005509)	endoplasmic reticulum (GO:0005783)
388474	LOC388474	similar to ribosomal protein L7a	translation (GO:0006412)	structural constituent of ribosome (GO:0003735)	ribosome (GO:0005840)
388697	HRNR	hornerin	multicellular organismal development (GO:0007275)	calcium ion binding (GO:0005509)	
440686	HIST2H3PS2	histone cluster 2, H3, pseudogene 2	nucleosome assembly (GO:0006334)	DNA binding (GO:0003677)	nucleus (GO:0005634)
440733	LOC440733	similar to insulinoma protein (rig)	translation (GO:0006412)	structural constituent of ribosome (GO:0003735)	small ribosomal subunit (GO:0015935)
440915	FKSG30	kappa-actin		ATP binding (GO:0005524)	cytoskeleton (GO:0005856)
441531	PGAM4	phosphoglycerate mutase family member 4	glycolysis (GO:0006096)	bisphosphoglycerate 2-phosphatase activity (GO:0004083)	
554313	HIST2H4B	histone cluster 2, H4b	nucleosome assembly (GO:0006334)	DNA binding (GO:0003677)	nucleus (GO:0005634)
641455	P704P	prostate-specific P704P		protein binding (GO:0005515)	
646821	LOC646821	similar to beta-actin		protein binding (GO:0005515)	
653852	LOC653852	similar to Filamin-C (Gamma-filamin) (Filamin-2) (Protein FLNc) (Actin-binding-like protein) (ABP-L) (ABP-280-like protein)			
72	ACTG2	actin, gamma 2, smooth muscle, enteric		ATP binding (GO:0005524)	cytoskeleton (GO:0005856)
213	ALB	albumin	hemolysis by symbiont of host red blood cells (GO:0019836)	copper ion binding (GO:0005507)	platelet alpha granule lumen (GO:0031093)
3371	TNC	tenascin C (hexabrachion)	signal transduction (GO:0007165)	receptor binding (GO:0005102)	proteinaceous extracellular matrix (GO:0005578)
11117	EMILIN1	elastin microfibril interfacier 1	phosphate transport (GO:0006817)	extracellular matrix structural constituent (GO:0005201)	cytoplasm (GO:0005737)
26154	ABCA12	ATP-binding cassette, sub-family A (ABC1), member 12	lipid transport (GO:0006869)	ATPase activity (GO:0016887)	integral to membrane (GO:0016021)
55239	OGFOD1	2-oxoglutarate and iron-dependent oxygenase domain containing 1	protein metabolic process (GO:0019538)	iron ion binding (GO:0005506)	
374454	KRT77	keratin 77		structural molecule activity (GO:0005198)	intermediate filament (GO:0005882)

Results acquired from proteomic analysis of acellular HDF

Proteins	Gene Symbol	Description	Biological Process_max	Molecular Function_max	Cellular Component_max
290	ANPEP	alanyl (membrane) aminopeptidase (aminopeptidase N, aminopeptidase M, microsomal aminopeptidase, CD13, p150)	proteolysis (GO:0006508)	aminopeptidase activity (GO:0004177)	integral to plasma membrane (GO:0005887)
309	ANXA6	annexin A6		calcium ion binding (GO:0005509)	melanosome (GO:0042470)
483	ATP1B3	ATPase, Na ⁺ /K ⁺ transporting, beta 3 polypeptide	potassium ion transport (GO:0006813)	sodium:potassium-exchanging ATPase activity (GO:0005391)	melanosome (GO:0042470)
493	ATP2B4	ATPase, Ca ⁺⁺ transporting, plasma membrane 4	calcium ion transport (GO:0006816)	calcium-transporting ATPase activity (GO:0005388)	integral to plasma membrane (GO:0005887)
857	CAV1	caveolin 1, caveolae protein, 22kDa	cholesterol homeostasis (GO:0042632)	cholesterol binding (GO:0015485)	integral to plasma membrane (GO:0005887)
960	CD44	CD44 molecule (Indian blood group)	cell-matrix adhesion (GO:0007160)	hyaluronic acid binding (GO:0005540)	integral to plasma membrane (GO:0005887)
1072	CFL1	cofilin 1 (non-muscle)	anti-apoptosis (GO:0006916)	actin binding (GO:0003779)	nucleus (GO:0005634)
1277	COL1A1	collagen, type I, alpha 1	phosphate transport (GO:0006817)	extracellular matrix structural constituent (GO:0005201)	collagen type I (GO:0005584)
1291	COL6A1	collagen, type VI, alpha 1	phosphate transport (GO:0006817)	protein binding (GO:0005515)	collagen type VI (GO:0005589)
1292	COL6A2	collagen, type VI, alpha 2	phosphate transport (GO:0006817)	protein binding, bridging (GO:0030674)	cytoplasm (GO:0005737)
1293	COL6A3	collagen, type VI, alpha 3	phosphate transport (GO:0006817)	serine-type endopeptidase inhibitor activity (GO:0004867)	collagen type VI (GO:0005589)
1915	EEF1A1	eukaryotic translation elongation factor 1 alpha 1	translational elongation (GO:0006414)	GTPase activity (GO:0003924)	cytosol (GO:0005829)
1917	EEF1A2	eukaryotic translation elongation factor 1 alpha 2	translational elongation (GO:0006414)	GTPase activity (GO:0003924)	nucleus (GO:0005634)
2200	FBN1	fibrillin 1	skeletal development (GO:0011501)	transmembrane receptor activity (GO:0004888)	microfibril (GO:0001527)
2316	FLNA	filamin A, alpha (actin binding protein 280)	positive regulation of transcription factor import into nucleus (GO:0042993)	actin filament binding (GO:0051015)	actin cytoskeleton (GO:0015629)
2335	FN1	fibronectin 1	transmembrane receptor protein tyrosine kinase signaling pathway (GO:0007169)	heparin binding (GO:0008201)	ER-Golgi intermediate compartment (GO:0005793)
2597	GAPDH	glyceraldehyde-3-phosphate dehydrogenase	glycolysis (GO:0006096)	glyceraldehyde-3-phosphate dehydrogenase (phosphorylating) activity (GO:0004365)	cytoplasm (GO:0005737)
2778	GNAS	GNAS complex locus	G-protein signaling, adenylate cyclase activating pathway (GO:0007189)	GTPase activity (GO:0003924)	heterotrimeric G-protein complex (GO:0005834)
3105	HLA-A	major histocompatibility complex, class I, A	antigen processing and presentation of peptide antigen via MHC class I (GO:0002474)	MHC class I receptor activity (GO:0032393)	integral to plasma membrane (GO:0005887)
3136	HLA-H	major histocompatibility complex, class I, H (pseudogene)	antigen processing and presentation of peptide antigen via MHC class I (GO:0002474)	MHC class I receptor activity (GO:0032393)	integral to plasma membrane (GO:0005887)
3309	HSPA5	heat shock 70kDa protein 5 (glucose-regulated protein, 78kDa)		ATP binding (GO:0005524)	endoplasmic reticulum (GO:0005783)
3339	HSPG2	heparan sulfate proteoglycan 2	cell adhesion (GO:0007155)	protein binding (GO:0005515)	basement membrane (GO:0005604)
3688	ITGB1	integrin, beta 1 (fibronectin receptor, beta polypeptide, antigen CD29 includes MDF2, MSK12)	integrin-mediated signaling pathway (GO:0007229)	protein heterodimerization activity (GO:0046982)	melanosome (GO:0042470)
3849	KRT2	keratin 2 (epidermal ichthyosis bullosa of Siemens)	epidermis development (GO:0008544)	structural constituent of cytoskeleton (GO:0005200)	intermediate filament (GO:0005882)
3857	KRT9	keratin 9 (epidermolytic palmoplantar keratoderma)	intermediate filament organization (GO:0045109)	structural constituent of cytoskeleton (GO:0005200)	intermediate filament (GO:0005882)
3858	KRT10	keratin 10 (epidermolytic hyperkeratosis; keratosis palmaris et plantaris)	epidermis development (GO:0008544)	protein binding (GO:0005515)	intermediate filament (GO:0005882)

3888	KRT82	keratin 82		protein binding (GO:0005515)	intermediate filament (GO:0005882)
4000	LMNA	lamin A/C		protein binding (GO:0005515)	nucleus (GO:0005634)
4627	MYH9	myosin, heavy chain 9, non-muscle	membrane protein ectodomain proteolysis (GO:0006509)	actin-dependent ATPase activity (GO:0030898)	stress fiber (GO:0001725)
5315	PKM2	pyruvate kinase, muscle	glycolysis (GO:0006096)	pyruvate kinase activity (GO:0004743)	cytosol (GO:0005829)
5630	PRPH	peripherin		structural molecule activity (GO:0005198)	intermediate filament (GO:0005882)
6184	RPN1	ribophorin I	protein amino acid N-linked glycosylation via asparagine (GO:0018279)	dolichyl-diphosphooligosaccharide-protein glycotransferase activity (GO:0004579)	melanosome (GO:0042470)
6513	SLC2A1	solute carrier family 2 (facilitated glucose transporter), member 1	glucose transport (GO:0015758)	sugar:hydrogen symporter activity (GO:0005351)	melanosome (GO:0042470)
7011	TEP1	telomerase-associated protein 1	telomere maintenance via recombination (GO:0000722)	telomerase activity (GO:0003720)	chromosome, telomeric region (GO:0000781)
7057	THBS1	thrombospondin 1	nervous system development (GO:0007399)	heparin binding (GO:0008201)	platelet alpha granule lumen (GO:0031093)
7070	THY1	Thy-1 cell surface antigen	retinal cone cell development (GO:0046549)	Rho GTPase activator activity (GO:0005100)	integral to plasma membrane (GO:0005887)
7277	TUBA4A	tubulin, alpha 4a	microtubule-based movement (GO:0007018)	GTPase activity (GO:0003924)	microtubule (GO:0005874)
7431	VIM	vimentin	cell motility (GO:0006928)	structural constituent of cytoskeleton (GO:0005200)	cytoskeleton (GO:0005856)
8295	TRRAP	transformation/transcription domain-associated protein	histone acetylation (GO:0016573)	transcription cofactor activity (GO:0003712)	NuA4 histone acetyltransferase complex (GO:0035267)
23332	CLASP1	cytoplasmic linker associated protein 1	negative regulation of microtubule depolymerization (GO:0007026)	microtubule plus-end binding (GO:0051010)	kinetochore microtubule (GO:0005828)
25923	ATL3	atlastin 3		GTPase activity (GO:0003924)	integral to membrane (GO:0016021)
27127	SMC1B	structural maintenance of chromosomes 1B	meiosis (GO:0007126)	ATPase activity (GO:0016887)	nucleus (GO:0005634)
27253	PCDH17	protocadherin 17	homophilic cell adhesion (GO:0007156)	calcium ion binding (GO:0005509)	integral to membrane (GO:0016021)
54734	RAB39	RAB39, member RAS oncogene family	small GTPase mediated signal transduction (GO:0007264)	GTP binding (GO:0005525)	plasma membrane (GO:0005886)
57653	KIAA1529	KIAA1529			integral to membrane (GO:0016021)
79026	AHNAK	AHNAK nucleoprotein	nervous system development (GO:0007399)	protein binding (GO:0005515)	nucleus (GO:0005634)
219770	GJD4	gap junction protein, delta 4, 40.1kDa	cell communication (GO:0007154)		integral to membrane (GO:0016021)
284119	PTRF	polymerase I and transcript release factor	transcription initiation from RNA polymerase I promoter (GO:0006361)	rRNA primary transcript binding (GO:0042134)	microsome (GO:0005792)
81	ACTN4	actinin, alpha 4	positive regulation of sodium:hydrogen antiporter activity (GO:0032417)	actin filament binding (GO:0051015)	nucleus (GO:0005634)
87	ACTN1	actinin, alpha 1	regulation of apoptosis (GO:0042981)	actin binding (GO:0003779)	focal adhesion (GO:0005925)
214	ALCAM	activated leukocyte cell adhesion molecule	signal transduction (GO:0007165)	receptor binding (GO:0005102)	integral to plasma membrane (GO:0005887)
226	ALDOA	aldolase A, fructose-bisphosphate	glycolysis (GO:0006096)	fructose-bisphosphate aldolase activity (GO:0004332)	
274	BIN1	bridging integrator 1	regulation of endocytosis (GO:0030100)	protein binding (GO:0005515)	actin cytoskeleton (GO:0015629)
301	ANXA1	annexin A1	anti-apoptosis (GO:0006916)	phospholipase A2 inhibitor activity (GO:0019834)	cornified envelope (GO:0001533)
302	ANXA2	annexin A2	skeletal development (GO:0001501)	phospholipase inhibitor activity (GO:0004859)	melanosome (GO:0042470)
311	ANXA11	annexin A11	immune response (GO:0006955)	calcium ion binding (GO:0005509)	melanosome (GO:0042470)
522	ATP5J	ATP synthase, H+ transporting, mitochondrial F0 complex, subunit F6	ATP synthesis coupled proton transport (GO:0015986)	hydrogen ion transporting ATP synthase activity, rotational mechanism (GO:0046933)	mitochondrion (GO:0005739)

538	ATP7A	ATPase, Cu ⁺⁺ transporting, alpha polypeptide (Menkes syndrome)	T-helper cell differentiation (GO:0042093)	copper-exporting ATPase activity (GO:0004008)	trans-Golgi network transport vesicle (GO:0030140)
682	BSG	basigin (Ok blood group)	cell surface receptor linked signal transduction (GO:0007166)	mannose binding (GO:0005537)	melanosome (GO:0042470)
811	CALR	calreticulin	cellular calcium ion homeostasis (GO:0006874)	zinc ion binding (GO:0008270)	endoplasmic reticulum (GO:0005783)
813	CALU	calumenin		calcium ion binding (GO:0005509)	melanosome (GO:0042470)
821	CANX	calnexin	protein folding (GO:0006457)	calcium ion binding (GO:0005509)	melanosome (GO:0042470)
829	CAPZA1	capping protein (actin filament) muscle Z-line, alpha 1	barbed-end actin filament capping (GO:0051016)	actin binding (GO:0003779)	F-actin capping protein complex (GO:0008290)
832	CAPZB	capping protein (actin filament) muscle Z-line, beta	barbed-end actin filament capping (GO:0051016)	actin binding (GO:0003779)	cytoplasm (GO:0005737)
871	SERPINH1	serpin peptidase inhibitor, clade H (heat shock protein 47), member 1, (collagen binding protein 1)	response to unfolded protein (GO:0006986)	serine-type endopeptidase inhibitor activity (GO:0004867)	endoplasmic reticulum (GO:0005783)
950	SCARB2	scavenger receptor class B, member 2	cell adhesion (GO:0007155)	receptor activity (GO:0004872)	lysosomal membrane (GO:0005765)
966	CD59	CD59 molecule, complement regulatory protein	cell surface receptor linked signal transduction (GO:0007166)	protein binding (GO:0005515)	anchored to membrane (GO:0031225)
1192	CLIC1	chloride intracellular channel 1	chloride transport (GO:0006821)	voltage-gated chloride channel activity (GO:0005247)	nucleus (GO:0005634)
1212	CLTB	clathrin, light chain (Lcb)	intracellular protein transport (GO:0006886)	calcium ion binding (GO:0005509)	clathrin coat of trans-Golgi network vesicle (GO:0030130)
1278	COL1A2	collagen, type I, alpha 2	phosphate transport (GO:0006817)	extracellular matrix structural constituent (GO:0005201)	collagen type I (GO:0005584)
1465	CSRP1	cysteine and glycine-rich protein 1		zinc ion binding (GO:0008270)	nucleus (GO:0005634)
1528	CYB5A	cytochrome b5 type A (microsomal)	generation of precursor metabolites and energy (GO:0006091)	aldo-keto reductase activity (GO:0004033)	mitochondrial outer membrane (GO:0005741)
1727	CYB5R3	cytochrome b5 reductase 3	iron ion transport (GO:0006826)	cytochrome-b5 reductase activity (GO:0004128)	mitochondrial outer membrane (GO:0005741)
1803	DPP4	dipeptidyl-peptidase 4 (CD26, adenosine deaminase complexing protein 2)	regulation of cell-cell adhesion mediated by integrin (GO:0033632)	aminopeptidase activity (GO:0004177)	integral to membrane (GO:0016021)
1808	DPYSL2	dihydropyrimidinase-like 2	nervous system development (GO:0007399)	dihydropyrimidinase activity (GO:0004157)	cytoplasm (GO:0005737)
1809	DPYSL3	dihydropyrimidinase-like 3	nervous system development (GO:0007399)	dihydropyrimidinase activity (GO:0004157)	cytoplasm (GO:0005737)
1936	EEF1D	eukaryotic translation elongation factor 1 delta (guanine nucleotide exchange protein)	positive regulation of I-kappaB kinase/NF-kappaB cascade (GO:0043123)	translation elongation factor activity (GO:0003746)	cytosol (GO:0005829)
2023	ENO1	enolase 1, (alpha)	glycolysis (GO:0006096)	transcription corepressor activity (GO:0003714)	nucleus (GO:0005634)
2027	ENO3	enolase 3 (beta, muscle)	glycolysis (GO:0006096)	phosphopyruvate hydratase activity (GO:0004634)	phosphopyruvate hydratase complex (GO:0000015)
2271	FH	fumarate hydratase	tricarboxylic acid cycle (GO:0006099)	fumarate hydratase activity (GO:0004333)	mitochondrial matrix (GO:0005759)
2274	FHL2	four and a half LIM domains 2	androgen receptor signaling pathway (GO:0030521)	androgen receptor binding (GO:0050681)	nucleus (GO:0005634)
2317	FLNB	filamin B, beta (actin binding protein 278)	skeletal muscle development (GO:0007519)	actin binding (GO:0003779)	actin cytoskeleton (GO:0015629)
2318	FLNC	filamin C, gamma (actin binding protein 280)		actin binding (GO:0003779)	actin cytoskeleton (GO:0015629)
2734	GLG1	golgi apparatus protein 1		fibroblast growth factor binding (GO:0017134)	Golgi membrane (GO:0000139)
2923	PDIA3	protein disulfide isomerase family A, member 3	protein import into nucleus (GO:0006606)	phospholipase C activity (GO:0004629)	melanosome (GO:0042470)
2934	GSN	gelsolin (amyloidosis, Finnish type)	barbed-end actin filament capping (GO:0051016)	actin binding (GO:0003779)	actin cytoskeleton (GO:0015629)
2950	GSTP1	glutathione S-transferase pi	anti-apoptosis (GO:0006916)	glutathione transferase activity (GO:0004364)	cytoplasm (GO:0005737)
3012	HIST1H2AE	histone cluster 1, H2ae			

3017	HIST1H2BD	histone cluster 1, H2bd	nucleosome assembly (GO:0006334)	DNA binding (GO:0003677)	nucleus (GO:0005634)
3106	HLA-B	major histocompatibility complex, class I, B	antigen processing and presentation of peptide antigen via MHC class I (GO:0002474)	MHC class I receptor activity (GO:0032393)	integral to plasma membrane (GO:0005887)
3107	HLA-C	major histocompatibility complex, class I, C	antigen processing and presentation of peptide antigen via MHC class I (GO:0002474)	MHC class I receptor activity (GO:0032393)	axonemal dynein complex (GO:0005858)
3181	HNRNPA2B1	heterogeneous nuclear ribonucleoprotein A2/B1	nuclear mRNA splicing, via spliceosome (GO:0000398)	single-stranded telomeric DNA binding (GO:0043047)	nucleus (GO:0005634)
3184	HNRNPD	heterogeneous nuclear ribonucleoprotein D (AU-rich element RNA binding protein 1, 37kDa)	nuclear mRNA splicing, via spliceosome (GO:0000398)	DNA binding (GO:0003677)	chromosome, telomeric region (GO:0000781)
3187	HNRNPH1	heterogeneous nuclear ribonucleoprotein H1 (H)	nuclear mRNA splicing, via spliceosome (GO:0000398)	poly(U) binding (GO:0008266)	nucleus (GO:0005634)
3190	HNRNPK	heterogeneous nuclear ribonucleoprotein K	nuclear mRNA splicing, via spliceosome (GO:0000398)	DNA binding (GO:0003677)	nucleus (GO:0005634)
3191	HNRNPL	heterogeneous nuclear ribonucleoprotein L	nuclear mRNA splicing, via spliceosome (GO:0000398)	RNA binding (GO:0003723)	nucleus (GO:0005634)
3305	HSPA1L	heat shock 70kDa protein 1-like	response to unfolded protein (GO:0006986)	ATP binding (GO:0005524)	
3306	HSPA2	heat shock 70kDa protein 2	male meiosis (GO:0007140)	ATP binding (GO:0005524)	cell surface (GO:0009986)
3311	HSPA7	heat shock 70kDa protein 7 (HSP70B)	response to unfolded protein (GO:0006986)	ATP binding (GO:0005524)	cellular_component (GO:0005575)
3312	HSPA8	heat shock 70kDa protein 8	protein folding (GO:0006457)	ATPase activity, coupled (GO:0042623)	melanosome (GO:0042470)
3313	HSPA9	heat shock 70kDa protein 9 (mortalin)	anti-apoptosis (GO:0006916)	ATP binding (GO:0005524)	mitochondrion (GO:0005739)
3315	HSPB1	heat shock 27kDa protein 1	anti-apoptosis (GO:0006916)	identical protein binding (GO:0042802)	nucleus (GO:0005634)
3320	HSP90AA1	heat shock protein 90kDa alpha (cytosolic), class A member 1	positive regulation of nitric oxide biosynthetic process (GO:0045429)	ATP binding (GO:0005524)	melanosome (GO:0042470)
3326	HSP90AB1	heat shock protein 90kDa alpha (cytosolic), class B member 1	positive regulation of nitric oxide biosynthetic process (GO:0045429)	ATP binding (GO:0005524)	melanosome (GO:0042470)
3329	HSPD1	heat shock 60kDa protein 1 (chaperonin)	protein import into mitochondrial matrix (GO:0030150)	ATP binding (GO:0005524)	mitochondrial matrix (GO:0005759)
3371	TNC	tenascin C (hexabrachion)	signal transduction (GO:0007165)	receptor binding (GO:0005102)	proteinaceous extracellular matrix (GO:0005578)
3848	KRT1	keratin 1 (epidermolytic hyperkeratosis)	fibrinolysis (GO:0042730)	receptor activity (GO:0004872)	cytoskeleton (GO:0005856)
3856	KRT8	keratin 8	cytoskeleton organization and biogenesis (GO:0007010)	protein binding (GO:0005515)	intermediate filament (GO:0005882)
3921	RPSA	ribosomal protein SA	translational elongation (GO:0006414)	structural constituent of ribosome (GO:0003735)	cytosolic small ribosomal subunit (GO:0022627)
3958	LGALS3	lectin, galactoside-binding, soluble, 3		IgE binding (GO:0019863)	nucleus (GO:0005634)
4082	MARCKS	myristoylated alanine-rich protein kinase C substrate	cell motility (GO:0006928)	actin filament binding (GO:0051015)	actin cytoskeleton (GO:0015629)
4267	CD99	CD99 molecule	cell adhesion (GO:0007155)	protein binding (GO:0005515)	integral to plasma membrane (GO:0005887)
4637	MYL6	myosin, light chain 6, alkali, smooth muscle and non-muscle	muscle filament sliding (GO:0030049)	actin-dependent ATPase activity (GO:0030898)	unconventional myosin complex (GO:0016461)
4676	NAP1L4	nucleosome assembly protein 1-like 4	nucleosome assembly (GO:0006334)	unfolded protein binding (GO:0051082)	nucleus (GO:0005634)
4691	NCL	nucleolin	angiogenesis (GO:0001525)	DNA binding (GO:0003677)	nucleus (GO:0005634)
4830	NME1	non-metastatic cells 1, protein (NM23A) expressed in	GTP biosynthetic process (GO:0006183)	ATP binding (GO:0005524)	nucleus (GO:0005634)
4841	NONO	non-POU domain containing, octamer-binding	mRNA processing (GO:0006397)	DNA binding (GO:0003677)	nucleus (GO:0005634)
4914	NTRK1	neurotrophic tyrosine kinase, receptor, type 1	activation of adenylate cyclase activity (GO:0007190)	transmembrane receptor protein tyrosine kinase activity (GO:0004714)	integral to plasma membrane (GO:0005887)
4924	NUCB1	nucleobindin 1		calcium ion binding (GO:0005509)	ER-Golgi intermediate compartment (GO:0005793)

4925	NUCB2	nucleobindin 2		calcium ion binding (GO:0005509)	ER-Golgi intermediate compartment (GO:0005793)
5034	P4HB	procollagen-proline, 2-oxoglutarate 4-dioxygenase (proline 4-hydroxylase), beta polypeptide	peptidyl-proline hydroxylation to 4-hydroxy-L-proline (GO:0018401)	procollagen-proline 4-dioxygenase activity (GO:0004656)	melanosome (GO:0042470)
5052	PRDX1	peroxiredoxin 1	skeletal development (GO:0001501)	peroxiredoxin activity (GO:0051920)	melanosome (GO:0042470)
5223	PGAM1	phosphoglycerate mutase 1 (brain)	glycolysis (GO:0006096)	bisphosphoglycerate 2-phosphatase activity (GO:0004083)	cytosol (GO:0005829)
5230	PGK1	phosphoglycerate kinase 1	glycolysis (GO:0006096)	ATP binding (GO:0005524)	cytoplasm (GO:0005737)
5232	PGK2	phosphoglycerate kinase 2	glycolysis (GO:0006096)	ATP binding (GO:0005524)	cytosol (GO:0005829)
5339	PLEC1	plectin 1, intermediate filament binding protein 500kDa	cytoskeletal anchoring at plasma membrane (GO:0007016)	actin binding (GO:0003779)	cytoskeleton (GO:0005856)
5478	PPIA	peptidylprolyl isomerase A (cyclophilin A)	provirus integration (GO:0019047)	peptidyl-prolyl cis-trans isomerase activity (GO:0003755)	nucleus (GO:0005634)
5479	PPIB	peptidylprolyl isomerase B (cyclophilin B)	protein folding (GO:0006457)	peptidyl-prolyl cis-trans isomerase activity (GO:0003755)	melanosome (GO:0042470)
5589	PRKCSH	protein kinase C substrate 80K-H	protein kinase cascade (GO:0007243)	calcium ion binding (GO:0005509)	endoplasmic reticulum (GO:0005783)
5686	PSMA5	proteasome (prosome, macropain) subunit, alpha type, 5	anaphase-promoting complex-dependent proteasomal ubiquitin-dependent protein catabolic process (GO:0031145)	threonine endopeptidase activity (GO:0004298)	nucleus (GO:0005634)
5713	PSMD7	proteasome (prosome, macropain) 26S subunit, non-ATPase, 7	anaphase-promoting complex-dependent proteasomal ubiquitin-dependent protein catabolic process (GO:0031145)	protein binding (GO:0005515)	cytosol (GO:0005829)
5725	PTBP1	polypyrimidine tract binding protein 1	nuclear mRNA splicing, via spliceosome (GO:0000398)	poly-pyrimidine tract binding (GO:0008187)	nucleus (GO:0005634)
6125	RPL5	ribosomal protein L5	translational elongation (GO:0006414)	5S rRNA binding (GO:0008097)	cytosolic large ribosomal subunit (GO:0022625)
6128	RPL6	ribosomal protein L6	regulation of transcription, DNA-dependent (GO:0006355)	DNA binding (GO:0003677)	cytosolic large ribosomal subunit (GO:0022625)
6147	RPL23A	ribosomal protein L23a	translational elongation (GO:0006414)	rRNA binding (GO:0019843)	cytosolic large ribosomal subunit (GO:0022625)
6176	RPLP1	ribosomal protein, large, P1	translational elongation (GO:0006414)	RNA binding (GO:0003723)	cytosolic large ribosomal subunit (GO:0022625)
6206	RPS12	ribosomal protein S12	translational elongation (GO:0006414)	RNA binding (GO:0003723)	cytosolic small ribosomal subunit (GO:0022627)
6233	RPS27A	ribosomal protein S27a	protein modification process (GO:0006464)	zinc ion binding (GO:0008270)	ribosome (GO:0005840)
6238	RRBP1	ribosome binding protein 1 homolog 180kDa (dog)	intracellular protein transport across a membrane (GO:0065002)	receptor activity (GO:0004872)	integral to endoplasmic reticulum membrane (GO:0030176)
6281	S100A10	S100 calcium binding protein A10	signal transduction (GO:0007165)	calcium ion binding (GO:0005509)	
6421	SFPQ	splicing factor proline/glutamine-rich (polypyrimidine tract binding protein associated)	mRNA processing (GO:0006397)	DNA binding (GO:0003677)	nucleus (GO:0005634)
6648	SOD2	superoxide dismutase 2, mitochondrial	response to superoxide (GO:0000303)	manganese ion binding (GO:0030145)	mitochondrial matrix (GO:0005759)
6709	SPTAN1	spectrin, alpha, non-erythrocytic 1 (alpha-fodrin)	barbed-end actin filament capping (GO:0051016)	actin binding (GO:0003779)	cytosol (GO:0005829)
6711	SPTBN1	spectrin, beta, non-erythrocytic 1	barbed-end actin filament capping (GO:0051016)	actin binding (GO:0003779)	nucleolus (GO:0005730)
6876	TAGLN	transgelin	muscle development (GO:0007517)	actin binding (GO:0003779)	cytoplasm (GO:0005737)
7086	TKT	transketolase (Wernicke-Korsakoff syndrome)	metabolic process (GO:0008152)	transketolase activity (GO:0004802)	cytosol (GO:0005829)
7170	TPM3	tropomyosin 3	regulation of muscle contraction (GO:0006937)	actin binding (GO:0003779)	cytoskeleton (GO:0005856)
7171	TPM4	tropomyosin 4	cell motility (GO:0006928)	actin binding (GO:0003779)	cytoskeleton (GO:0005856)
7184	HSP90B1	heat shock protein 90kDa beta (Grp94), member 1	anti-apoptosis (GO:0006916)	ATP binding (GO:0005524)	melanosome (GO:0042470)

7273	TTN	titin	regulation of Rho protein signal transduction (GO:0035023)	protein serine/threonine kinase activity (GO:0004674)	condensed nuclear chromosome (GO:0000794)
7307	U2AF1	U2 small nuclear RNA auxiliary factor 1	nuclear mRNA splicing, via spliceosome (GO:0000398)	zinc ion binding (GO:0008270)	Cajal body (GO:0015030)
7381	UQCRB	ubiquinol-cytochrome c reductase binding protein	aerobic respiration (GO:0009060)	ubiquinol-cytochrome-c reductase activity (GO:0008121)	mitochondrion (GO:0005739)
7415	VCP	valosin-containing protein	caspase activation (GO:0006919)	ATPase activity (GO:0016887)	microsome (GO:0005792)
7416	VDAC1	voltage-dependent anion channel 1	apoptotic program (GO:0008632)	voltage-gated anion channel activity (GO:0008308)	mitochondrial outer membrane (GO:0005741)
7417	VDAC2	voltage-dependent anion channel 2	anion transport (GO:0006820)	voltage-gated anion channel activity (GO:0008308)	mitochondrial outer membrane (GO:0005741)
7520	XRCC5	X-ray repair complementing defective repair in Chinese hamster cells 5 (double-strand-break rejoining; Ku autoantigen, 80kDa)	double-strand break repair via nonhomologous end joining (GO:0006303)	ATP binding (GO:0005524)	nucleus (GO:0005634)
7529	YWHAB	tyrosine 3-monooxygenase/tryptophan 5-monooxygenase activation protein, beta polypeptide	activation of pro-apoptotic gene products (GO:0008633)	monooxygenase activity (GO:0004497)	melanosome (GO:0042470)
7532	YWHAG	tyrosine 3-monooxygenase/tryptophan 5-monooxygenase activation protein, gamma polypeptide	negative regulation of protein kinase activity (GO:0006469)	protein kinase C binding (GO:0005080)	cytoplasm (GO:0005737)
7534	YWHAZ	tyrosine 3-monooxygenase/tryptophan 5-monooxygenase activation protein, zeta polypeptide	anti-apoptosis (GO:0006916)	transcription factor binding (GO:0008134)	melanosome (GO:0042470)
8335	HIST1H2AB	histone cluster 1, H2ab	nucleosome assembly (GO:0006334)	DNA binding (GO:0003677)	nucleus (GO:0005634)
8339	HIST1H2BG	histone cluster 1, H2bg			
8343	HIST1H2BF	histone cluster 1, H2bf			
8344	HIST1H2BE	histone cluster 1, H2be			
8346	HIST1H2BI	histone cluster 1, H2bi			
8347	HIST1H2BC	histone cluster 1, H2bc	nucleosome assembly (GO:0006334)	DNA binding (GO:0003677)	nucleus (GO:0005634)
8348	HIST1H2BO	histone cluster 1, H2bo	nucleosome assembly (GO:0006334)	DNA binding (GO:0003677)	nucleus (GO:0005634)
8411	EEA1	early endosome antigen 1	vesicle fusion (GO:0006906)	phosphatidylinositol binding (GO:0005545)	early endosome membrane (GO:0031901)
8546	AP3B1	adaptor-related protein complex 3, beta 1 subunit	endocytosis (GO:0006897)	protein binding (GO:0005515)	Golgi apparatus (GO:0005794)
8570	KHSRP	KH-type splicing regulatory protein	mRNA processing (GO:0006397)	RNA splicing factor activity, transesterification mechanism (GO:0031202)	nucleus (GO:0005634)
8826	IQGAP1	IQ motif containing GTPase activating protein 1	regulation of small GTPase mediated signal transduction (GO:0051056)	Ras GTPase activator activity (GO:0005099)	actin filament (GO:0005884)
8880	FUBP1	far upstream element (FUSE) binding protein 1	transcription from RNA polymerase II promoter (GO:0006366)	single-stranded DNA binding (GO:0003697)	nucleus (GO:0005634)
9217	VAPB	VAMP (vesicle-associated membrane protein)-associated protein B and C	endoplasmic reticulum unfolded protein response (GO:0030968)	beta-tubulin binding (GO:0048487)	endoplasmic reticulum (GO:0005783)
9218	VAPA	VAMP (vesicle-associated membrane protein)-associated protein A, 33kDa	positive regulation of I-kappaB kinase/NF-kappaB cascade (GO:0043123)	protein heterodimerization activity (GO:0046982)	tight junction (GO:0005923)
9991	ROD1	ROD1 regulator of differentiation 1 (S. pombe)	mRNA processing (GO:0006397)	RNA binding (GO:0003723)	nucleus (GO:0005634)
10092	ARPC5	actin related protein 2/3 complex, subunit 5, 16kDa	actin cytoskeleton organization and biogenesis (GO:0030036)	actin binding (GO:0003779)	cytoplasm (GO:0005737)
10146	G3BP1	GTPase activating protein (SH3 domain) binding protein 1	Ras protein signal transduction (GO:0007265)	ATP binding (GO:0005524)	nucleus (GO:0005634)
10151	HNRNPA3P1	heterogeneous nuclear ribonucleoprotein A3 pseudogene 1			
10236	HNRNPR	heterogeneous nuclear ribonucleoprotein R	nuclear mRNA splicing, via spliceosome (GO:0000398)	RNA binding (GO:0003723)	nucleus (GO:0005634)
10250	SRRM1	serine/arginine repetitive matrix 1	nuclear mRNA splicing, via spliceosome (GO:0000398)	RNA splicing factor activity, transesterification mechanism (GO:0031202)	nuclear speck (GO:0016607)

10382	TUBB4	tubulin, beta 4	microtubule-based movement (GO:0007018)	GTPase activity (GO:0003924)	cytoskeleton (GO:0005856)
10424	PGRMC2	progesterone receptor membrane component 2		steroid hormone receptor activity (GO:0003707)	integral to membrane (GO:0016021)
10487	CAP1	CAP, adenylate cyclase-associated protein 1 (yeast)	activation of adenylate cyclase activity (GO:0007190)	actin binding (GO:0003779)	plasma membrane (GO:0005886)
10493	VAT1	vesicle amine transport protein 1 homolog (T. californica)	cell growth (GO:0016049)	zinc ion binding (GO:0008270)	synaptic vesicle (GO:0008021)
10540	DCTN2	dynactin 2 (p50)	microtubule-based process (GO:0007017)	protein binding (GO:0005515)	centrosome (GO:0005813)
10549	PRDX4	peroxiredoxin 4	I-kappaB phosphorylation (GO:0007252)	thioredoxin peroxidase activity (GO:0008379)	cytoplasm (GO:0005737)
10581	IFITM2	interferon induced transmembrane protein 2 (1-8D)	immune response (GO:0006955)	protein binding (GO:0005515)	integral to membrane (GO:0016021)
10726	NUDC	nuclear distribution gene C homolog (A. nidulans)	mitosis (GO:0007067)	protein binding (GO:0005515)	nucleus (GO:0005634)
10857	PGRMC1	progesterone receptor membrane component 1		transition metal ion binding (GO:0046914)	microsome (GO:0005792)
10935	PRDX3	peroxiredoxin 3	positive regulation of NF-kappaB transcription factor activity (GO:0051092)	alkyl hydroperoxide reductase activity (GO:0008785)	mitochondrion (GO:0005739)
10959	TMED2	transmembrane emp24 domain trafficking protein 2	protein transport (GO:0015031)	protein binding (GO:0005515)	zymogen granule membrane (GO:0042589)
10963	STIP1	stress-induced-phosphoprotein 1 (Hsp70/Hsp90-organizing protein)	response to stress (GO:0006950)	binding (GO:0005488)	nucleus (GO:0005634)
10970	CKAP4	cytoskeleton-associated protein 4			integral to membrane (GO:0016021)
10971	YWHAQ	tyrosine 3-monooxygenase/tryptophan 5-monooxygenase activation protein, theta polypeptide	negative regulation of transcription, DNA-dependent (GO:0045892)	protein kinase C inhibitor activity (GO:0008426)	cytoplasm (GO:0005737)
11034	DSTN	destrin (actin depolymerizing factor)	actin polymerization and/or depolymerization (GO:0008154)	actin binding (GO:0003779)	actin cytoskeleton (GO:0015629)
11052	CPSF6	cleavage and polyadenylation specific factor 6, 68kDa	mRNA processing (GO:0006397)	RNA binding (GO:0003723)	paraspeckles (GO:0042382)
11171	STRAP	serine/threonine kinase receptor associated protein	mRNA processing (GO:0006397)	protein binding (GO:0005515)	nucleus (GO:0005634)
11328	FKBP9	FK506 binding protein 9, 63 kDa	protein folding (GO:0006457)	peptidyl-prolyl cis-trans isomerase activity (GO:0003755)	endoplasmic reticulum (GO:0005783)
11335	CBX3	chromobox homolog 3 (HP1 gamma homolog, Drosophila)	chromatin remodeling (GO:0006338)	protein domain specific binding (GO:0019904)	nuclear centromeric heterochromatin (GO:0031618)
22948	CCT5	chaperonin containing TCP1, subunit 5 (epsilon)	protein folding (GO:0006457)	ATP binding (GO:0005524)	cytoplasm (GO:0005737)
23193	GANAB	glucosidase, alpha; neutral AB	carbohydrate metabolic process (GO:0005975)	glucan 1,3-alpha-glucosidase activity (GO:0033919)	melanosome (GO:0042470)
23673	STX12	syntaxin 12	cholesterol efflux (GO:0033344)	SNAP receptor activity (GO:0005484)	phagocytic vesicle (GO:0045335)
26237					
26355	FAM162A	family with sequence similarity 162, member A			integral to membrane (GO:0016021)
26509	FER1L3	fer-1-like 3, myoferlin (C. elegans)	muscle contraction (GO:0006936)		nucleus (GO:0005634)
29978	UBQLN2	ubiquilin 2	protein modification process (GO:0006464)	binding (GO:0005488)	nucleus (GO:0005634)
29979	UBQLN1	ubiquilin 1	protein modification process (GO:0006464)	kinase binding (GO:0019900)	nucleus (GO:0005634)
50809	HP1BP3	heterochromatin protein 1, binding protein 3	nucleosome assembly (GO:0006334)	DNA binding (GO:0003677)	nucleus (GO:0005634)
51060	TXNDC12	thioredoxin domain containing 12 (endoplasmic reticulum)	cell redox homeostasis (GO:0045454)	protein-disulfide reductase (glutathione) activity (GO:0019153)	endoplasmic reticulum (GO:0005783)
51087	YBX2	Y box binding protein 2	transcription from RNA polymerase II promoter (GO:0006366)	DNA binding (GO:0003677)	nucleus (GO:0005634)
51132	RNF12	ring finger protein 12	regulation of transcription, DNA-dependent (GO:0006355)	transcription corepressor activity (GO:0003714)	transcriptional repressor complex (GO:0017053)
54344	DPM3	dolichyl-phosphate mannosyltransferase polypeptide 3	protein amino acid C-linked glycosylation via 2-alpha-mannosyl-L-tryptophan	dolichyl-phosphate beta-D-mannosyltransferase activity (GO:0004582)	integral to endoplasmic reticulum membrane (GO:0030176)

			(GO:0018406)		
55752	11-Sep	septin 11	protein heterooligomerization (GO:0051291)	GTP binding (GO:0005525)	stress fiber (GO:0001725)
55970	GNG12	guanine nucleotide binding protein (G protein), gamma 12	G-protein coupled receptor protein signaling pathway (GO:0007186)	signal transducer activity (GO:0004871)	heterotrimeric G-protein complex (GO:0005834)
56254	RNF20	ring finger protein 20	chromatin modification (GO:0016568)	zinc ion binding (GO:0008270)	nucleus (GO:0005634)
56969	RPL23AP13	ribosomal protein L23a pseudogene 13		nucleotide binding (GO:0000166)	ribosome (GO:0005840)
57142	RTN4	reticulon 4	negative regulation of axon extension (GO:0030517)	protein binding (GO:0005515)	integral to endoplasmic reticulum membrane (GO:0030176)
57153	SLC44A2	solute carrier family 44, member 2	positive regulation of I-kappaB kinase/NF-kappaB cascade (GO:0043123)	choline transmembrane transporter activity (GO:0015220)	integral to membrane (GO:0016021)
65992	C20orf116	chromosome 20 open reading frame 116		protein binding (GO:0005515)	extracellular region (GO:0005576)
80184	CEP290	centrosomal protein 290kDa	eye photoreceptor cell development (GO:0042462)	microtubule minus-end binding (GO:0051011)	centrosome (GO:0005813)
81567	TXNDC5	thioredoxin domain containing 5	anti-apoptosis (GO:0006916)	isomerase activity (GO:0016853)	endoplasmic reticulum (GO:0005783)
81873	ARPC5L	actin related protein 2/3 complex, subunit 5-like	regulation of actin filament polymerization (GO:0030833)	actin binding (GO:0003779)	cytoskeleton (GO:0005856)
90462	ZNF605	zinc finger protein 605	regulation of transcription, DNA-dependent (GO:0006355)	zinc ion binding (GO:0008270)	nucleus (GO:0005634)
92689	FAM114A1	family with sequence similarity 114, member A1			cytoplasm (GO:0005737)
113146	AHNAK2	AHNAK nucleoprotein 2	keratinization (GO:0031424)	protein binding (GO:0005515)	nucleus (GO:0005634)
114799	ESCO1	establishment of cohesion 1 homolog 1 (S. cerevisiae)	DNA repair (GO:0006281)	zinc ion binding (GO:0008270)	nucleus (GO:0005634)
114990	VASN	vasorin		protein binding (GO:0005515)	integral to membrane (GO:0016021)
126961	HIST2H3C	histone cluster 2, H3c			
140465	MYL6B	myosin, light chain 6B, alkali, smooth muscle and non-muscle	muscle filament sliding (GO:0030049)	calcium ion binding (GO:0005509)	muscle myosin complex (GO:0005859)
140576	S100A16	S100 calcium binding protein A16		calcium ion binding (GO:0005509)	
158358	KIAA2026	KIAA2026			
167227	DCP2	DCP2 decapping enzyme homolog (S. cerevisiae)	nuclear-transcribed mRNA catabolic process, nonsense-mediated decay (GO:0000184)	manganese ion binding (GO:0030145)	nucleus (GO:0005634)
222068	TMED4	transmembrane emp24 protein transport domain containing 4	positive regulation of I-kappaB kinase/NF-kappaB cascade (GO:0043123)	signal transducer activity (GO:0004871)	integral to membrane (GO:0016021)
287023			mRNA processing (GO:0006397)	single-stranded DNA binding (GO:0003697)	nucleus (GO:0005634)
343069	HNRNPCL1	heterogeneous nuclear ribonucleoprotein C-like 1		RNA binding (GO:0003723)	nucleus (GO:0005634)
345651	ACTBL2	actin, beta-like 2		ATP binding (GO:0005524)	cytoskeleton (GO:0005856)
347701	LOC347701	calgizzarin-like			
360132	FKBP9L	FK506 binding protein 9-like	protein folding (GO:0006457)	calcium ion binding (GO:0005509)	endoplasmic reticulum (GO:0005783)
375775	PNPLA7	patatin-like phospholipase domain containing 7	lipid metabolic process (GO:0006629)	hydrolase activity (GO:0016787)	integral to membrane (GO:0016021)
440055					
440686	HIST2H3PS2	histone cluster 2, H3, pseudogene 2	nucleosome assembly (GO:0006334)	DNA binding (GO:0003677)	nucleus (GO:0005634)
440915	FKSG30	kappa-actin		ATP binding (GO:0005524)	cytoskeleton (GO:0005856)
441531	PGAM4	phosphoglycerate mutase family member 4	glycolysis (GO:0006096)	bisphosphoglycerate 2-phosphatase activity (GO:0004083)	
641455	P704P	prostate-specific P704P		protein binding (GO:0005515)	

642461	LOC642461	similar to Isoleucyl-tRNA synthetase, mitochondrial precursor (Isoleucine--tRNA ligase) (IleRS)			
646821	LOC646821	similar to beta-actin		protein binding (GO:0005515)	
653852	LOC653852	similar to Filamin-C (Gamma-filamin) (Filamin-2) (Protein FLNc) (Actin-binding-like protein) (ABP-L) (ABP-280-like protein)			
850981	SMD2	Core Sm protein Sm D2; part of heteroheptameric complex (with Smb1p, Smd1p, Smd3p, Sme1p, Smx3p, and Smx2p) that is part of the spliceosomal U1, U2, U4, and U5 snRNPs; homolog of human Sm D2	nuclear mRNA splicing, via spliceosome (GO:0000398)	RNA splicing factor activity, transesterification mechanism (GO:0031202)	nucleus (GO:0005634)
30	ACAA1	acetyl-Coenzyme A acyltransferase 1 (peroxisomal 3-oxoacyl-Coenzyme A thiolase)	fatty acid metabolic process (GO:0006631)	acetyl-CoA C-acyltransferase activity (GO:0003988)	peroxisome (GO:0005777)
38	ACAT1	acetyl-Coenzyme A acetyltransferase 1 (acetooacyl Coenzyme A thiolase)	metabolic process (GO:0008152)	acetyl-CoA C-acetyltransferase activity (GO:0003985)	mitochondrial matrix (GO:0005759)
47	ACLY	ATP citrate lyase	ATP catabolic process (GO:0006200)	succinate-CoA ligase (ADP-forming) activity (GO:0004775)	cytosol (GO:0005829)
59	ACTA2	actin, alpha 2, smooth muscle, aorta		ATP binding (GO:0005524)	cytoskeleton (GO:0005856)
60	ACTB	actin, beta	sensory perception of sound (GO:0007605)	ATP binding (GO:0005524)	NuA4 histone acetyltransferase complex (GO:0035267)
71	ACTG1	actin, gamma 1	sensory perception of sound (GO:0007605)	ATP binding (GO:0005524)	cytoskeleton (GO:0005856)
72	ACTG2	actin, gamma 2, smooth muscle, enteric		ATP binding (GO:0005524)	cytoskeleton (GO:0005856)
160	AP2A1	adaptor-related protein complex 2, alpha 1 subunit	regulation of defense response to virus by virus (GO:0050690)	protein binding (GO:0005515)	clathrin coat of trans-Golgi network vesicle (GO:0030130)
163	AP2B1	adaptor-related protein complex 2, beta 1 subunit	regulation of defense response to virus by virus (GO:0050690)	protein binding (GO:0005515)	cytosol (GO:0005829)
205	AK3L1	adenylate kinase 3-like 1	nucleobase, nucleoside, nucleotide and nucleic acid metabolic process (GO:0006139)	ATP binding (GO:0005524)	mitochondrial matrix (GO:0005759)
238	ALK	anaplastic lymphoma receptor tyrosine kinase	protein amino acid N-linked glycosylation (GO:0006487)	transmembrane receptor protein tyrosine kinase activity (GO:0004714)	integral to plasma membrane (GO:0005887)
293	SLC25A6	solute carrier family 25 (mitochondrial carrier; adenine nucleotide translocator), member 6	apoptosis (GO:0006915)	ATP:ADP antiporter activity (GO:0005471)	mitochondrion (GO:0005739)
308	ANXA5	annexin A5	anti-apoptosis (GO:0006916)	phospholipase inhibitor activity (GO:0004859)	cytoplasm (GO:0005737)
372	ARCN1	archain 1	COPI coating of Golgi vesicle (GO:0048205)	protein binding (GO:0005515)	COPI vesicle coat (GO:0030126)
498	ATP5A1	ATP synthase, H+ transporting, mitochondrial F1 complex, alpha subunit 1, cardiac muscle	ATP synthesis coupled proton transport (GO:0015986)	hydrogen ion transporting ATP synthase activity, rotational mechanism (GO:0046933)	mitochondrial matrix (GO:0005759)
509	ATP5C1	ATP synthase, H+ transporting, mitochondrial F1 complex, gamma polypeptide 1	ATP synthesis coupled proton transport (GO:0015986)	hydrogen ion transporting ATP synthase activity, rotational mechanism (GO:0046933)	mitochondrial matrix (GO:0005759)
633	BGN	biglycan		extracellular matrix structural constituent (GO:0005201)	transport vesicle (GO:0030133)
800	CALD1	caldesmon 1	muscle contraction (GO:0006936)	actin binding (GO:0003779)	cytoskeleton (GO:0005856)
976	CD97	CD97 molecule	neuropeptide signaling pathway (GO:0007218)	G-protein coupled receptor activity (GO:0004930)	integral to plasma membrane (GO:0005887)
1213	CLTC	clathrin, heavy chain (Hc)	intracellular protein transport (GO:0006886)	protein binding (GO:0005515)	clathrin coat of trans-Golgi network vesicle (GO:0030130)
1282	COL4A1	collagen, type IV, alpha 1	phosphate transport (GO:0006817)	extracellular matrix structural constituent (GO:0005201)	cytoplasm (GO:0005737)
1289	COL5A1	collagen, type V, alpha 1	phosphate transport (GO:0006817)	heparin binding (GO:0008201)	collagen type V (GO:0005588)
1303	COL12A1	collagen, type XII, alpha 1	phosphate transport (GO:0006817)	extracellular matrix structural constituent conferring tensile strength (GO:0030020)	collagen type XII (GO:0005595)
1314	COPA	coatamer protein complex, subunit alpha	COPI coating of Golgi vesicle (GO:0048205)	hormone activity (GO:0005179)	microsome (GO:0005792)
1329	COX5B	cytochrome c oxidase subunit Vb	respiratory gaseous exchange (GO:0007585)	zinc ion binding (GO:0008270)	mitochondrial inner membrane (GO:0005743)

1495	CTNNA1	catenin (cadherin-associated protein), alpha 1, 102kDa	apical junction assembly (GO:0043297)	vinculin binding (GO:0017166)	actin cytoskeleton (GO:0015629)
1508	CTSB	cathepsin B	proteolysis (GO:0006508)	cysteine-type endopeptidase activity (GO:0004197)	lysosome (GO:0005764)
1778	DYNC1H1	dynein, cytoplasmic 1, heavy chain 1	mitotic spindle organization and biogenesis (GO:0007052)	ATPase activity, coupled (GO:0042623)	cytoplasmic dynein complex (GO:0005868)
1832	DSP	desmoplakin	peptide cross-linking (GO:0018149)	protein binding, bridging (GO:0030674)	cell-cell adherens junction (GO:0005913)
1937	EEF1G	eukaryotic translation elongation factor 1 gamma	translational elongation (GO:0006414)	translation elongation factor activity (GO:0003746)	cytosol (GO:0005829)
1938	EEF2	eukaryotic translation elongation factor 2	translational elongation (GO:0006414)	GTPase activity (GO:0003924)	cytoplasm (GO:0005737)
1973	EIF4A1	eukaryotic translation initiation factor 4A, isoform 1	translation (GO:0006412)	ATP binding (GO:0005524)	cytosol (GO:0005829)
2025	ENO1P	enolase 1, (alpha) pseudogene	glycolysis (GO:0006096)	phosphopyruvate hydratase activity (GO:0004634)	phosphopyruvate hydratase complex (GO:0000015)
2058	EPRS	glutamyl-prolyl-tRNA synthetase	glutamyl-tRNA aminoacylation (GO:0006424)	glutamate-tRNA ligase activity (GO:0004818)	soluble fraction (GO:0005625)
2194	FASN	fatty acid synthase	fatty acid biosynthetic process (GO:0006633)	oleoyl-(acyl-carrier-protein) hydrolase activity (GO:0004320)	melanosome (GO:0042470)
2199	FBLN2	fibulin 2		calcium ion binding (GO:0005509)	proteinaceous extracellular matrix (GO:0005578)
2539	G6PD	glucose-6-phosphate dehydrogenase	glucose 6-phosphate utilization (GO:0006010)	glucose-6-phosphate dehydrogenase activity (GO:0004345)	cytosol (GO:0005829)
2617	GARS	glycyl-tRNA synthetase	glycyl-tRNA aminoacylation (GO:0006426)	glycine-tRNA ligase activity (GO:0004820)	soluble fraction (GO:0005625)
2673	GFPT1	glutamine-fructose-6-phosphate transaminase 1	fructose 6-phosphate metabolic process (GO:0006002)	glutamine-fructose-6-phosphate transaminase (isomerizing) activity (GO:0004360)	cytoplasm (GO:0005737)
2876	GPX1	glutathione peroxidase 1	anti-apoptosis (GO:0006916)	SH3 domain binding (GO:0017124)	mitochondrion (GO:0005739)
3008	HIST1H1E	histone cluster 1, H1e	nucleosome assembly (GO:0006334)	DNA binding (GO:0003677)	nucleus (GO:0005634)
3009	HIST1H1B	histone cluster 1, H1b	nucleosome assembly (GO:0006334)	DNA binding (GO:0003677)	nucleus (GO:0005634)
3030	HADHA	hydroxyacyl-Coenzyme A dehydrogenase/3-ketoacyl-Coenzyme A thiolase/enoyl-Coenzyme A hydratase (trifunctional protein), alpha subunit	fatty acid beta-oxidation (GO:0006635)	acetyl-CoA C-acetyltransferase activity (GO:0003985)	mitochondrion (GO:0005739)
3032	HADHB	hydroxyacyl-Coenzyme A dehydrogenase/3-ketoacyl-Coenzyme A thiolase/enoyl-Coenzyme A hydratase (trifunctional protein), beta subunit	fatty acid beta-oxidation (GO:0006635)	acetyl-CoA C-acyltransferase activity (GO:0003988)	mitochondrial matrix (GO:0005759)
3151	HMGN2	high-mobility group nucleosomal binding domain 2	establishment and/or maintenance of chromatin architecture (GO:0006325)	DNA binding (GO:0003677)	chromatin (GO:0000785)
3159	HMGA1	high mobility group AT-hook 1	nucleosome disassembly (GO:0006337)	ligand-dependent nuclear receptor transcription coactivator activity (GO:0030374)	chromatin (GO:0000785)
3182	HNRNPAB	heterogeneous nuclear ribonucleoprotein A/B	positive regulation of gene-specific transcription (GO:0043193)	transcription factor activity (GO:0003700)	nucleus (GO:0005634)
3418	IDH2	isocitrate dehydrogenase 2 (NADP+), mitochondrial	tricarboxylic acid cycle (GO:0006099)	isocitrate dehydrogenase (NADP+) activity (GO:0004450)	mitochondrion (GO:0005739)
3615	IMPDH2	IMP (inosine monophosphate) dehydrogenase 2	GMP biosynthetic process (GO:0006177)	IMP dehydrogenase activity (GO:0003938)	cytosol (GO:0005829)
3799	KIF5B	kinesin family member 5B	vesicle transport along microtubule (GO:0047496)	ATP binding (GO:0005524)	kinesin complex (GO:0005871)
3895	KTN1	kinectin 1 (kinesin receptor)	microtubule-based movement (GO:0007018)	receptor activity (GO:0004872)	integral to plasma membrane (GO:0005887)
3915	LAMC1	laminin, gamma 1 (formerly LAMB2)	positive regulation of epithelial cell proliferation (GO:0050679)	extracellular matrix structural constituent (GO:0005201)	laminin-1 complex (GO:0005606)
3939	LDHA	lactate dehydrogenase A	anaerobic glycolysis (GO:0019642)	L-lactate dehydrogenase activity (GO:0004459)	cytosol (GO:0005829)
4017	LOXL2	lysyl oxidase-like 2	protein modification process (GO:0006464)	protein-lysine 6-oxidase activity (GO:0004720)	extracellular space (GO:0005615)

4191	MDH2	malate dehydrogenase 2, NAD (mitochondrial)	glycolysis (GO:0006096)	L-malate dehydrogenase activity (GO:0030060)	mitochondrial matrix (GO:0005759)
4430	MYO1B	myosin IB		ATP binding (GO:0005524)	myosin complex (GO:0016459)
4628	MYH10	myosin, heavy chain 10, non-muscle	regulation of cell shape (GO:0008360)	actin-dependent ATPase activity (GO:0030898)	stress fiber (GO:0001725)
4629	MYH11	myosin, heavy chain 11, smooth muscle	muscle thick filament assembly (GO:0030241)	ATP binding (GO:0005524)	striated muscle thick filament (GO:0005863)
4632	MYL1	myosin, light chain 1, alkali; skeletal, fast	muscle filament sliding (GO:0030049)	calcium ion binding (GO:0005509)	muscle myosin complex (GO:0005859)
4701	NDUFA7	NADH dehydrogenase (ubiquinone) 1 alpha subcomplex, 7, 14.5kDa	mitochondrial electron transport, NADH to ubiquinone (GO:0006120)	NADH dehydrogenase (ubiquinone) activity (GO:0008137)	mitochondrion (GO:0005739)
4735	2-Sep	septin 2	cell cycle (GO:0007049)	GTP binding (GO:0005525)	nucleus (GO:0005634)
4904	YBX1	Y box binding protein 1	nuclear mRNA splicing, via spliceosome (GO:0000398)	double-stranded DNA binding (GO:0003690)	nucleus (GO:0005634)
4907	NT5E	5'-nucleotidase, ecto (CD73)	nucleotide catabolic process (GO:0009166)	5'-nucleotidase activity (GO:0008253)	anchored to membrane (GO:0031225)
5033	P4HA1	procollagen-proline, 2-oxoglutarate 4-dioxygenase (proline 4-hydroxylase), alpha polypeptide I	protein metabolic process (GO:0019538)	procollagen-proline 4-dioxygenase activity (GO:0004656)	endoplasmic reticulum (GO:0005783)
5106	PCK2	phosphoenolpyruvate carboxykinase 2 (mitochondrial)	gluconeogenesis (GO:0006094)	phosphoenolpyruvate carboxykinase (GTP) activity (GO:0004613)	mitochondrion (GO:0005739)
5236	PGM1	phosphoglucomutase 1	glucose metabolic process (GO:0006006)	phosphoglucomutase activity (GO:0004614)	cytosol (GO:0005829)
5250	SLC25A3	solute carrier family 25 (mitochondrial carrier; phosphate carrier), member 3	generation of precursor metabolites and energy (GO:0006091)	phosphate carrier activity (GO:0015320)	mitochondrial inner membrane (GO:0005743)
5270	SERPINE2	serpin peptidase inhibitor, clade E (nexin, plasminogen activator inhibitor type 1), member 2	regulation of proteolysis (GO:0030162)	serine-type endopeptidase inhibitor activity (GO:0004867)	extracellular region (GO:0005576)
5591	PRKDC	protein kinase, DNA-activated, catalytic polypeptide	double-strand break repair via nonhomologous end joining (GO:0006303)	DNA-dependent protein kinase activity (GO:0004677)	nucleus (GO:0005634)
5596	MAPK4	mitogen-activated protein kinase 4	protein amino acid phosphorylation (GO:0006468)	MAP kinase activity (GO:0004707)	
5866	RAB3IL1	RAB3A interacting protein (rabin3)-like 1		guanyl-nucleotide exchange factor activity (GO:0005085)	
5954	RCN1	reticulocalbin 1, EF-hand calcium binding domain		calcium ion binding (GO:0005509)	endoplasmic reticulum (GO:0005783)
5965	RECQL	RecQ protein-like (DNA helicase Q1-like)	DNA repair (GO:0006281)	ATP binding (GO:0005524)	nucleus (GO:0005634)
6124	RPL4	ribosomal protein L4	translational elongation (GO:0006414)	RNA binding (GO:0003723)	cytosolic large ribosomal subunit (GO:0022625)
6133	RPL9	ribosomal protein L9	translational elongation (GO:0006414)	RNA binding (GO:0003723)	cytosol (GO:0005829)
6134	RPL10	ribosomal protein L10	translational elongation (GO:0006414)	structural constituent of ribosome (GO:0003735)	cytosolic large ribosomal subunit (GO:0022625)
6135	RPL11	ribosomal protein L11	translational elongation (GO:0006414)	rRNA binding (GO:0019843)	cytosolic large ribosomal subunit (GO:0022625)
6138	RPL15	ribosomal protein L15	translational elongation (GO:0006414)	RNA binding (GO:0003723)	cytosol (GO:0005829)
6139	RPL17	ribosomal protein L17	positive regulation of I-kappaB kinase/NF-kappaB cascade (GO:0043123)	RNA binding (GO:0003723)	cytosol (GO:0005829)
6141	RPL18	ribosomal protein L18	translational elongation (GO:0006414)	RNA binding (GO:0003723)	cytosolic large ribosomal subunit (GO:0022625)
6146	RPL22	ribosomal protein L22	translational elongation (GO:0006414)	heparin binding (GO:0008201)	cytosolic large ribosomal subunit (GO:0022625)
6156	RPL30	ribosomal protein L30	translational elongation (GO:0006414)	RNA binding (GO:0003723)	cytosolic large ribosomal subunit (GO:0022625)
6157	RPL27A	ribosomal protein L27a	translational elongation (GO:0006414)	RNA binding (GO:0003723)	cytosolic large ribosomal subunit (GO:0022625)
6159	RPL29	ribosomal protein L29	translational elongation (GO:0006414)	heparin binding (GO:0008201)	cytosolic large ribosomal subunit (GO:0022625)
6175	RPLP0	ribosomal protein, large, P0	translational elongation (GO:0006414)	RNA binding (GO:0003723)	cytosolic large ribosomal subunit (GO:0022625)

6181	RPLP2	ribosomal protein, large, P2	translational elongation (GO:0006414)	RNA binding (GO:0003723)	cytosolic large ribosomal subunit (GO:0022625)
6185	RPN2	ribophorin II	protein amino acid N-linked glycosylation via asparagine (GO:0018279)	dolichyl-diphosphooligosaccharide-protein glycotransferase activity (GO:0004579)	endoplasmic reticulum (GO:0005783)
6187	RPS2	ribosomal protein S2	translational elongation (GO:0006414)	RNA binding (GO:0003723)	cytosolic small ribosomal subunit (GO:0022627)
6191	RPS4X	ribosomal protein S4, X-linked	translational elongation (GO:0006414)	rRNA binding (GO:0019843)	cytosolic small ribosomal subunit (GO:0022627)
6201	RPS7	ribosomal protein S7	translational elongation (GO:0006414)	RNA binding (GO:0003723)	cytosolic small ribosomal subunit (GO:0022627)
6207	RPS13	ribosomal protein S13	translational elongation (GO:0006414)	RNA binding (GO:0003723)	cytosolic small ribosomal subunit (GO:0022627)
6209	RPS15	ribosomal protein S15	translational elongation (GO:0006414)	structural constituent of ribosome (GO:0003735)	cytosolic small ribosomal subunit (GO:0022627)
6427	SFRS2	splicing factor, arginine/serine-rich 2	nuclear mRNA splicing, via spliceosome (GO:0000398)	transcription corepressor activity (GO:0003714)	PML body (GO:0016605)
6520	SLC3A2	solute carrier family 3 (activators of dibasic and neutral amino acid transport), member 2	calcium ion transport (GO:0006816)	calcium:sodium antiporter activity (GO:0005432)	melanosome (GO:0042470)
7045	TGFB1	transforming growth factor, beta-induced, 68kDa	visual perception (GO:0007601)	integrin binding (GO:0005178)	proteinaceous extracellular matrix (GO:0005578)
7058	THBS2	thrombospondin 2	cell adhesion (GO:0007155)	heparin binding (GO:0008201)	platelet alpha granule lumen (GO:0031093)
7094	TLN1	talin 1	cytoskeletal anchoring at plasma membrane (GO:0007016)	actin binding (GO:0003779)	focal adhesion (GO:0005925)
7120	TMSL6	thymosin-like 6 (pseudogene)			
7168	TPM1	tropomyosin 1 (alpha)	regulation of muscle contraction (GO:0006937)	actin binding (GO:0003779)	sarcomere (GO:0030017)
7169	TPM2	tropomyosin 2 (beta)	regulation of ATPase activity (GO:0043462)	actin binding (GO:0003779)	cytoskeleton (GO:0005856)
7203	CCT3	chaperonin containing TCP1, subunit 3 (gamma)	protein folding (GO:0006457)	ATP binding (GO:0005524)	cytoskeleton (GO:0005856)
7278	TUBA3C	tubulin, alpha 3c	microtubule-based movement (GO:0007018)	GTPase activity (GO:0003924)	microtubule (GO:0005874)
7284	TUFM	Tu translation elongation factor, mitochondrial	translational elongation (GO:0006414)	GTPase activity (GO:0003924)	mitochondrion (GO:0005739)
7385	UQCRC2	ubiquinol-cytochrome c reductase core protein II	proteolysis (GO:0006508)	metalloendopeptidase activity (GO:0004222)	mitochondrion (GO:0005739)
7408	VASP	vasodilator-stimulated phosphoprotein	cell motility (GO:0006928)	actin binding (GO:0003779)	actin cytoskeleton (GO:0015629)
7414	VCL	vinculin	lamellipodium biogenesis (GO:0030032)	actin binding (GO:0003779)	focal adhesion (GO:0005925)
7791	ZYX	zyxin	signal transduction (GO:0007165)	zinc ion binding (GO:0008270)	focal adhesion (GO:0005925)
8294	HIST1H4I	histone cluster 1, H4i			
8301	PICALM	phosphatidylinositol binding clathrin assembly protein	receptor-mediated endocytosis (GO:0006898)	phosphatidylinositol binding (GO:0005545)	Golgi apparatus (GO:0005794)
8407	TAGLN2	transgelin 2	muscle development (GO:0007517)	protein binding (GO:0005515)	
8802	SUCLG1	succinate-CoA ligase, alpha subunit	tricarboxylic acid cycle (GO:0006099)	succinate-CoA ligase (ADP-forming) activity (GO:0004775)	mitochondrial matrix (GO:0005759)
8815	BANF1	barrier to autointegration factor 1	provirus integration (GO:0019047)	DNA binding (GO:0003677)	nucleus (GO:0005634)
8968	HIST1H3F	histone cluster 1, H3f	nucleosome assembly (GO:0006334)	DNA binding (GO:0003677)	nucleus (GO:0005634)
8974	P4HA2	procollagen-proline, 2-oxoglutarate 4-dioxygenase (proline 4-hydroxylase), alpha polypeptide II	protein metabolic process (GO:0019538)	procollagen-proline 4-dioxygenase activity (GO:0004656)	endoplasmic reticulum (GO:0005783)
9260	PDLIM7	PDZ and LIM domain 7 (enigma)	receptor-mediated endocytosis (GO:0006898)	zinc ion binding (GO:0008270)	cytoskeleton (GO:0005856)
9551	ATP5J2	ATP synthase, H ⁺ transporting, mitochondrial F0 complex, subunit F2	ATP biosynthetic process (GO:0006754)	hydrogen ion transmembrane transporter activity (GO:0015078)	mitochondrion (GO:0005739)
9601	PDIA4	protein disulfide isomerase family A, member 4	protein secretion (GO:0009306)	protein disulfide isomerase activity (GO:0003756)	melanosome (GO:0042470)

9689	BZW1	basic leucine zipper and W2 domains 1	regulation of transcription, DNA-dependent (GO:0006355)	binding (GO:0005488)	cytoplasm (GO:0005737)
9948	WDR1	WD repeat domain 1	sensory perception of sound (GO:0007605)	actin binding (GO:0003779)	cytoskeleton (GO:0005856)
10095	ARPC1B	actin related protein 2/3 complex, subunit 1B, 41kDa	cell motility (GO:0006928)	actin binding (GO:0003779)	cytoplasm (GO:0005737)
10097	ACTR2	ARP2 actin-related protein 2 homolog (yeast)	cell motility (GO:0006928)	ATP binding (GO:0005524)	cytoplasm (GO:0005737)
10105	PPIF	peptidylprolyl isomerase F (cyclophilin F)	protein folding (GO:0006457)	peptidyl-prolyl cis-trans isomerase activity (GO:0003755)	mitochondrial matrix (GO:0005759)
10109	ARPC2	actin related protein 2/3 complex, subunit 2, 34kDa	regulation of actin filament polymerization (GO:0030833)	actin binding (GO:0003779)	cytoskeleton (GO:0005856)
10130	PDIA6	protein disulfide isomerase family A, member 6	protein folding (GO:0006457)	protein disulfide isomerase activity (GO:0003756)	melanosome (GO:0042470)
10226	M6PRBP1	mannose-6-phosphate receptor binding protein 1	vesicle-mediated transport (GO:0016192)		endosome (GO:0005768)
10376	TUBA1B	tubulin, alpha 1b	microtubule-based movement (GO:0007018)	GTPase activity (GO:0003924)	microtubule (GO:0005874)
10383	TUBB2C	tubulin, beta 2C	microtubule-based movement (GO:0007018)	GTPase activity (GO:0003924)	cytoskeleton (GO:0005856)
10399	GNB2L1	guanine nucleotide binding protein (G protein), beta polypeptide 2-like 1		receptor binding (GO:0005102)	cytoplasm (GO:0005737)
10409	BASP1	brain abundant, membrane attached signal protein 1			cytoskeleton (GO:0005856)
10492	SYNCRIP	synaptotagmin binding, cytoplasmic RNA interacting protein	mRNA processing (GO:0006397)	RNA binding (GO:0003723)	microsome (GO:0005792)
10514	MYBBP1A	MYB binding protein (P160) 1a	regulation of transcription, DNA-dependent (GO:0006355)	DNA-directed DNA polymerase activity (GO:0003887)	nucleus (GO:0005634)
10525	HYOU1	hypoxia up-regulated 1	response to stress (GO:0006950)	ATP binding (GO:0005524)	endoplasmic reticulum (GO:0005783)
10575	CCT4	chaperonin containing TCP1, subunit 4 (delta)	protein folding (GO:0006457)	ATP binding (GO:0005524)	melanosome (GO:0042470)
10594	PRPF8	PRP8 pre-mRNA processing factor 8 homolog (S. cerevisiae)	nuclear mRNA splicing, via spliceosome (GO:0000398)	RNA splicing factor activity, transesterification mechanism (GO:0031202)	nuclear speck (GO:0016607)
10631	POSTN	periostin, osteoblast specific factor	skeletal development (GO:0001501)	heparin binding (GO:0008201)	proteinaceous extracellular matrix (GO:0005578)
10694	CCT8	chaperonin containing TCP1, subunit 8 (theta)	protein folding (GO:0006457)	ATPase activity, coupled (GO:0042623)	cytoplasm (GO:0005737)
10787	NCKAP1	NCK-associated protein 1	apoptosis (GO:0006915)	protein binding (GO:0005515)	integral to membrane (GO:0016021)
10979	FERMT2	fermitin family homolog 2 (Drosophila)	regulation of cell shape (GO:0008360)	protein binding (GO:0005515)	stress fiber (GO:0001725)
10985	GCN1L1	GCN1 general control of amino-acid synthesis 1-like 1 (yeast)	regulation of translation (GO:0006417)	translation factor activity, nucleic acid binding (GO:0008135)	cytoplasm (GO:0005737)
10989	IMMT	inner membrane protein, mitochondrial (mitofilin)		protein binding (GO:0005515)	mitochondrial inner membrane (GO:0005743)
11098	PRSS23	protease, serine, 23	proteolysis (GO:0006508)	serine-type endopeptidase activity (GO:0004252)	nucleus (GO:0005634)
11117	EMILIN1	elastin microfibril interfacier 1	phosphate transport (GO:0006817)	extracellular matrix structural constituent (GO:0005201)	cytoplasm (GO:0005737)
11316	COPE	coatamer protein complex, subunit epsilon	COPI coating of Golgi vesicle (GO:0048205)	protein binding (GO:0005515)	COPI vesicle coat (GO:0030126)
22872	SEC31A	SEC31 homolog A (S. cerevisiae)	ER to Golgi vesicle-mediated transport (GO:0006888)	protein binding (GO:0005515)	COPII vesicle coat (GO:0030127)
22874	PLEKHA6	pleckstrin homology domain containing, family A member 6			
22995	CEP152	centrosomal protein 152kDa			centrosome (GO:0005813)
23451	SF3B1	splicing factor 3b, subunit 1, 155kDa	nuclear mRNA splicing, via spliceosome (GO:0000398)	RNA splicing factor activity, transesterification mechanism (GO:0031202)	nuclear speck (GO:0016607)
23474	ETHE1	ethylmalonic encephalopathy 1		zinc ion binding (GO:0008270)	mitochondrial matrix (GO:0005759)

23603	CORO1C	coronin, actin binding protein, 1C	phagocytosis (GO:0006909)	actin binding (GO:0003779)	actin cytoskeleton (GO:0015629)
25796	PGLS	6-phosphogluconolactonase	pentose-phosphate shunt (GO:0006098)	6-phosphogluconolactonase activity (GO:0017057)	
28298	Rpl32	ribosomal protein L32	translation (GO:0006412)	structural constituent of ribosome (GO:0003735)	cytosolic large ribosomal subunit (GO:0022625)
28972	SPCS1	signal peptidase complex subunit 1 homolog (S. cerevisiae)	proteolysis (GO:0006508)		integral to endoplasmic reticulum membrane (GO:0030176)
29956	LASS2	LAG1 homolog, ceramide synthase 2	regulation of transcription, DNA-dependent (GO:0006355)	transcription factor activity (GO:0003700)	nucleus (GO:0005634)
29995	LMCD1	LIM and cysteine-rich domains 1		zinc ion binding (GO:0008270)	cellular_component (GO:0005575)
30846	EHD2	EH-domain containing 2		GTPase activity (GO:0003924)	nucleus (GO:0005634)
30968	STOML2	stomatin (EPB72)-like 2		receptor binding (GO:0005102)	cytoskeleton (GO:0005856)
55226	NAT10	N-acetyltransferase 10	metabolic process (GO:0008152)	N-acetyltransferase activity (GO:0008080)	nucleus (GO:0005634)
55324	ABCF3	ATP-binding cassette, sub-family F (GCN20), member 3		ATPase activity (GO:0016887)	
55379	LRRC59	leucine rich repeat containing 59		protein binding (GO:0005515)	microsome (GO:0005792)
57455	REXO1	REX1, RNA exonuclease 1 homolog (S. cerevisiae)	regulation of transcription, DNA-dependent (GO:0006355)	exonuclease activity (GO:0004527)	chromatin (GO:0000785)
58477	SRPRB	signal recognition particle receptor, B subunit		GTP binding (GO:0005525)	endoplasmic reticulum (GO:0005783)
63905	MANBAL	mannosidase, beta A, lysosomal-like			integral to membrane (GO:0016021)
64098	PARVG	parvin, gamma	cell-matrix adhesion (GO:0007160)	actin binding (GO:0003779)	cytoskeleton (GO:0005856)
64307	Rpl24	ribosomal protein L24	translation (GO:0006412)	structural constituent of ribosome (GO:0003735)	ribosome (GO:0005840)
79068	FTO	fat mass and obesity associated	determination of left/right symmetry (GO:0007368)		
79664	NARG2	NMDA receptor regulated 2			nucleus (GO:0005634)
79709	GLT25D1	glycosyltransferase 25 domain containing 1	lipopolysaccharide biosynthetic process (GO:0009103)	transferase activity, transferring glycosyl groups (GO:0016757)	endoplasmic reticulum (GO:0005783)
81876	RAB1B	RAB1B, member RAS oncogene family	regulation of transcription, DNA-dependent (GO:0006355)	ATP binding (GO:0005524)	Golgi apparatus (GO:0005794)
84617	TUBB6	tubulin, beta 6	microtubule-based movement (GO:0007018)	GTPase activity (GO:0003924)	microtubule (GO:0005874)
84790	TUBA1C	tubulin, alpha 1c	microtubule-based movement (GO:0007018)	GTPase activity (GO:0003924)	microtubule (GO:0005874)
85443	DCLK3	doublecortin-like kinase 3	protein amino acid phosphorylation (GO:0006468)	protein serine/threonine kinase activity (GO:0004674)	nucleus (GO:0005634)
92755	LOC92755	hypothetical gene LOC92755			
94081	SFXN1	sideroflexin 1	iron ion transport (GO:0006826)	iron ion binding (GO:0005506)	mitochondrion (GO:0005739)
94239	H2AFV	H2A histone family, member V	nucleosome assembly (GO:0006334)	DNA binding (GO:0003677)	nucleus (GO:0005634)
112464	PRKCDBP	protein kinase C, delta binding protein	negative regulation of cell cycle (GO:0045786)		
167681	PRSS35	protease, serine, 35	proteolysis (GO:0006508)	serine-type endopeptidase activity (GO:0004252)	extracellular region (GO:0005576)
203068	TUBB	tubulin, beta	microtubule-based movement (GO:0007018)	GTPase activity (GO:0003924)	cytoskeleton (GO:0005856)
347733	TUBB2B	tubulin, beta 2B	microtubule-based movement (GO:0007018)	GTPase activity (GO:0003924)	microtubule (GO:0005874)
388474	LOC388474	similar to ribosomal protein L7a	translation (GO:0006412)	structural constituent of ribosome (GO:0003735)	ribosome (GO:0005840)
392447	hCG_1644323	hCG1644323	translation (GO:0006412)	structural constituent of ribosome (GO:0003735)	ribosome (GO:0005840)

402221	LOC402221	actin pseudogene		protein binding (GO:0005515)	
554313	HIST2H4B	histone cluster 2, H4b	nucleosome assembly (GO:0006334)	DNA binding (GO:0003677)	nucleus (GO:0005634)
562774			collagen catabolic process (GO:0030574)	oxidoreductase activity, acting on single donors with incorporation of molecular oxygen, incorporation of two atoms of oxygen (GO:0016702)	
641293	LOC641293	ribosomal protein L21 pseudogene	translation (GO:0006412)	structural constituent of ribosome (GO:0003735)	ribosome (GO:0005840)

Appendix C

Protocols used for background subtraction from fluorescence images acquired using CoolSnap EZ camera (Photometrics, Tucson, AZ) mounted on a Nikon Eclipse TE 2000-S inverted microscope (Nikon, Melville, NY)

Acquiring images

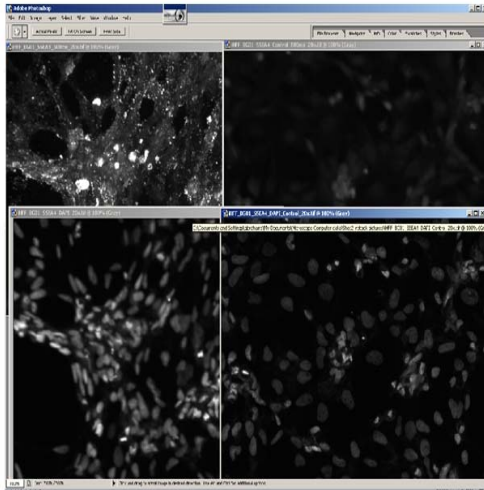
- Start → Program → NIS Elements F → nis_f.exe
- Be sure that the ‘Live’ button is clicked in the Camera section within the left hand side panel
- Focus the microscope on your sample → Click on ‘Autoexposure’ → Note the autoexposure value → Click on “Capture”
- Save the image (top panel - ‘save as’) as a TIFF file.
- Now acquire an image of your control at the same autoexposure value as your sample image.....***NOTE this step is important to be able to compare the two images and subtract your background.***

Photoshop steps

File → Open → open both your sample and the control image.

NOTE: if you want to overlay DAPI along with your stain, you will have to open 4 images:

- a) Stain_sample
- b) Stain_control
- c) DAPI_sample...same precise spot,
- d) DAPI_control...not necessarily the same spot as your stain_control image (just a reference)

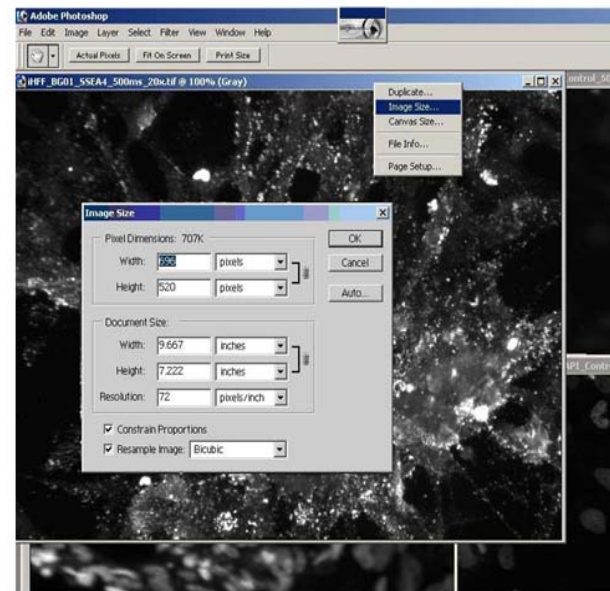



Things to note:

The images should be at a 100% ...the title bar of the image will read xxxyyy.tif@100%(Gray) All the images should be the same size.

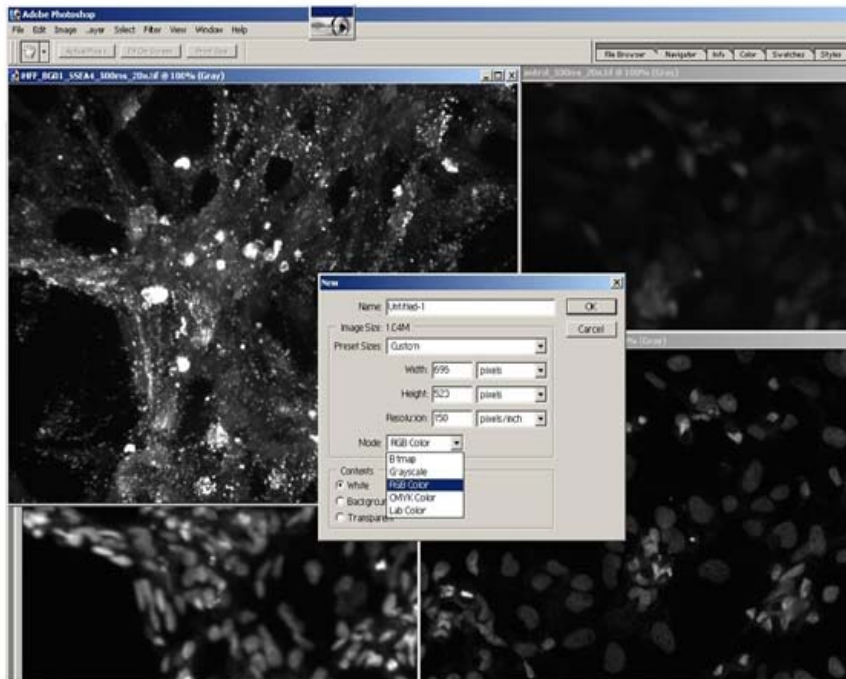
Right Click on the title bar  Image size, *Note image size*.

Preferred - Width - 696 pixels , Height - 520 pixels



Open a new image--- File  New

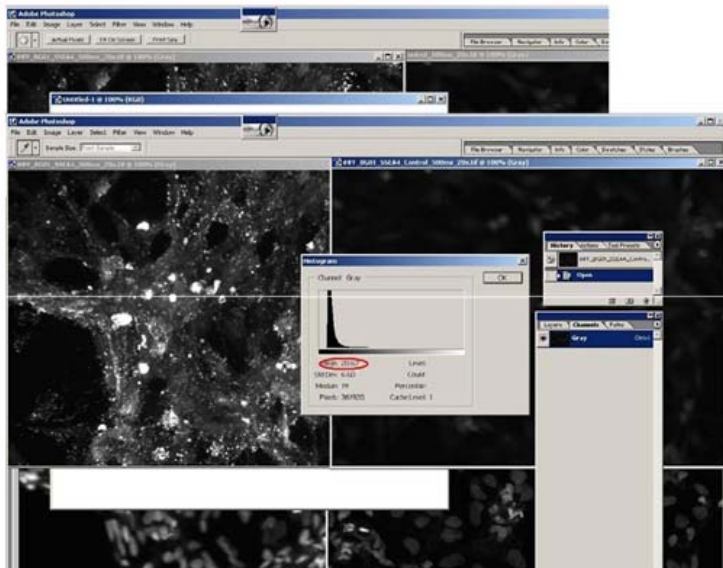
Within the 'New' Window, make sure that the Width and Height match with your image size and in Mode - RGB color must be selected



Background subtraction

Click on your **control** image

Go to image on the menu-bar and click on histogram. Note the value of the mean intensity, click OK. In older versions of photoshop the way to get the histogram is by Windows ⇨ Histogram



Click on your sample image

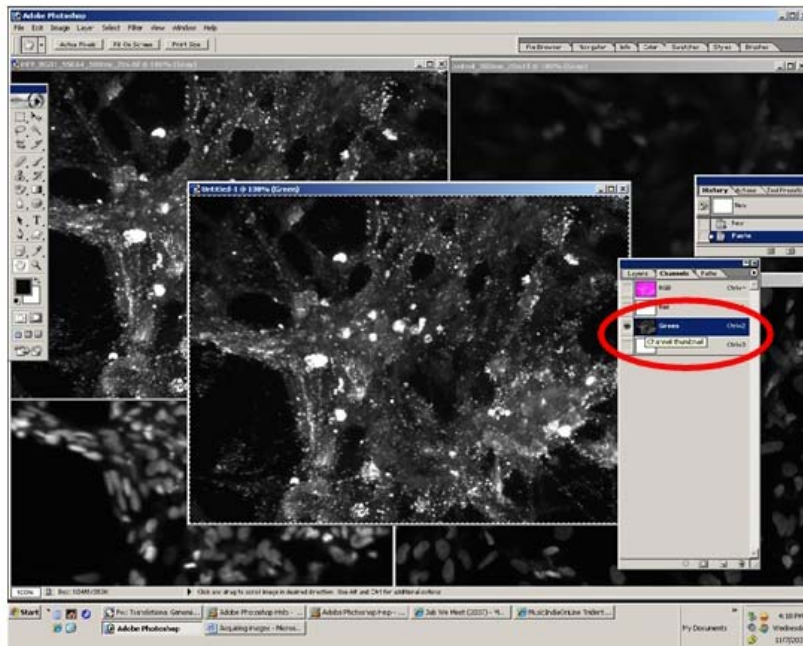
Go to Image ⇨ Adjustments ⇨ Levels

In the 'Levels' window, within the Input levels boxes, enter the mean noted in the control image.

There will be a reduction in the background of the sample image.

Now copy the content of the background subtracted image (Select the image by Ctrl+A followed by copy Ctrl+C)

Click on the window of the new image, click on the appropriate channel and paste the image in image window. For eg select channel Green for FITC. Your image *will not* show up green, it will when you select RGB



Similarly subtract background for DAPI and copy the image and select the blue channel of the new image and paste the blue image

Unselect the RGB as well the RED channel so as to view the colours of the stains

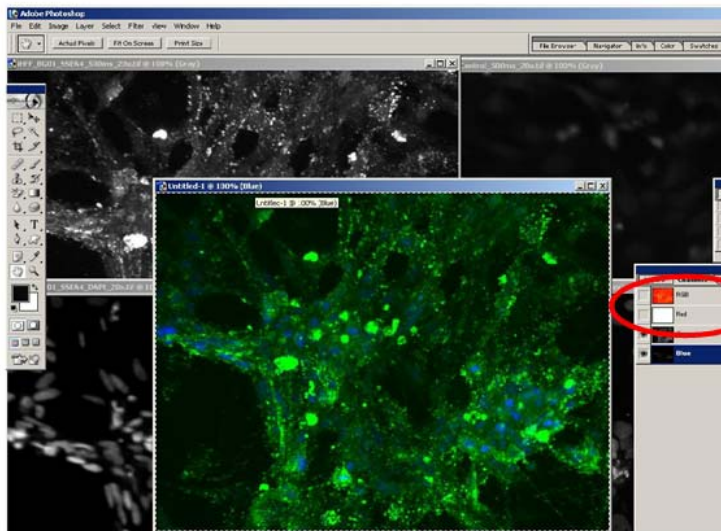
Before saving your final image do not forget to delete the red (unused channel)

Select the red channel

Go to Image → Adjustments → Levels

Set output values as 0 to 0

Save.



Appendix D

- A) Preliminary results for microwell studies
- B) Representative image for quantification of positive expression of pluripotent markers SSEA3 and SSEA4 using cytospin
- C) Representative images of hPSCs cultured on lyophilized acellular substrates

A) Preliminary results for microwell studies

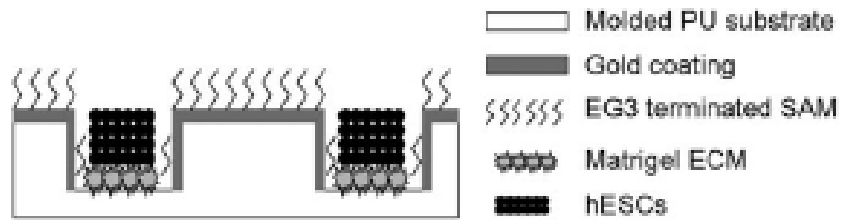


Figure 1: Schematic of the microwell slide fabrication [72]

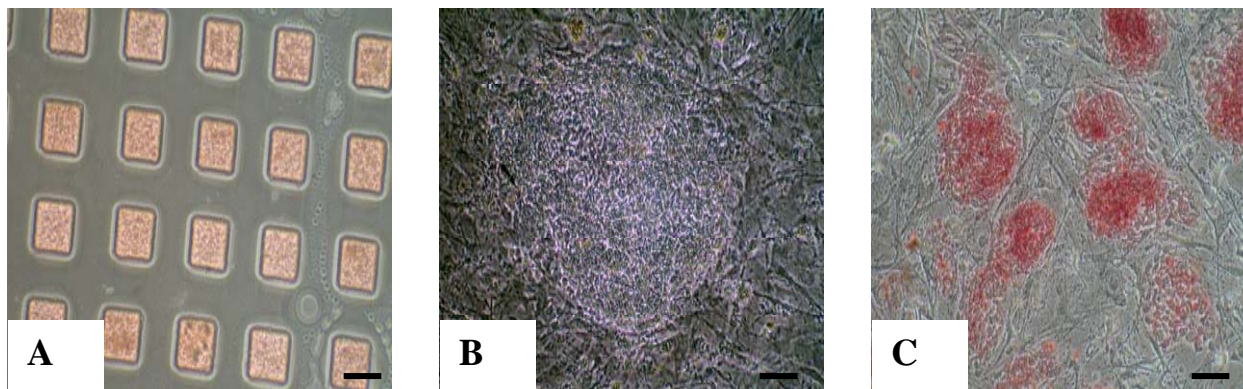


Figure 2: Representative images of hPSCs grown in the microwell with regular media changes (A), cells collected from the media on Day 40 were plated on MEF formed colonies (B) and stained positive for alkaline phosphatase (C), Scale bar = 100 μ m.

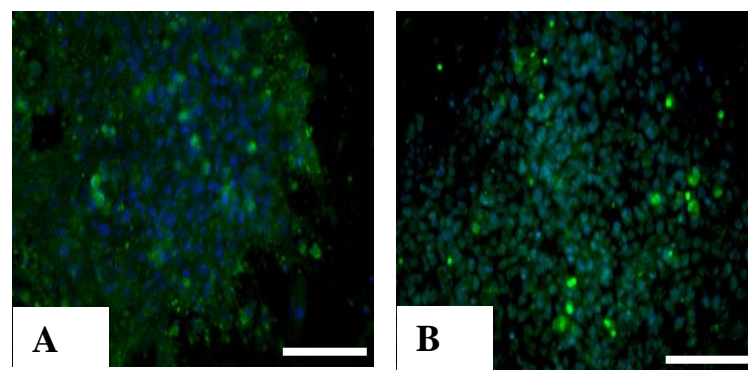


Figure 3: Representative images of hPSCs grown in the microwell, collected on Day 40 and plated on MEFs formed colonies that stained positive for SSEA4 (A) and OCT4 (B), Scale bar = 100 μ m

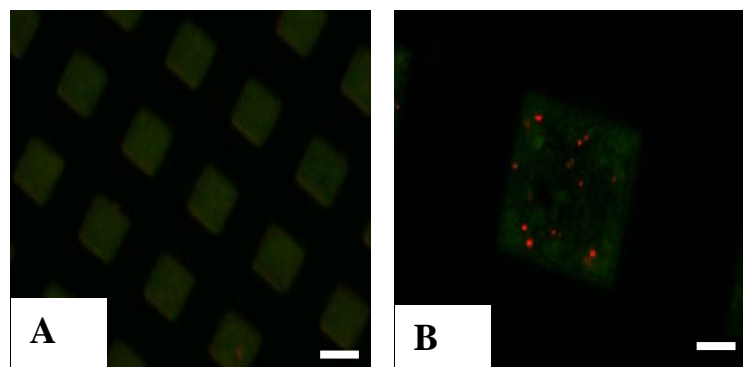


Figure 4: Live dead assay was performed on cells in 100 and 300 μ m microwell slide, Scale bar = 100 μ m
Green dye stains for live cells, Red dye stains for dead cells

B) Representative image for quantification of positive expression of pluripotent markers SSEA3 and SSEA4 using cytospin

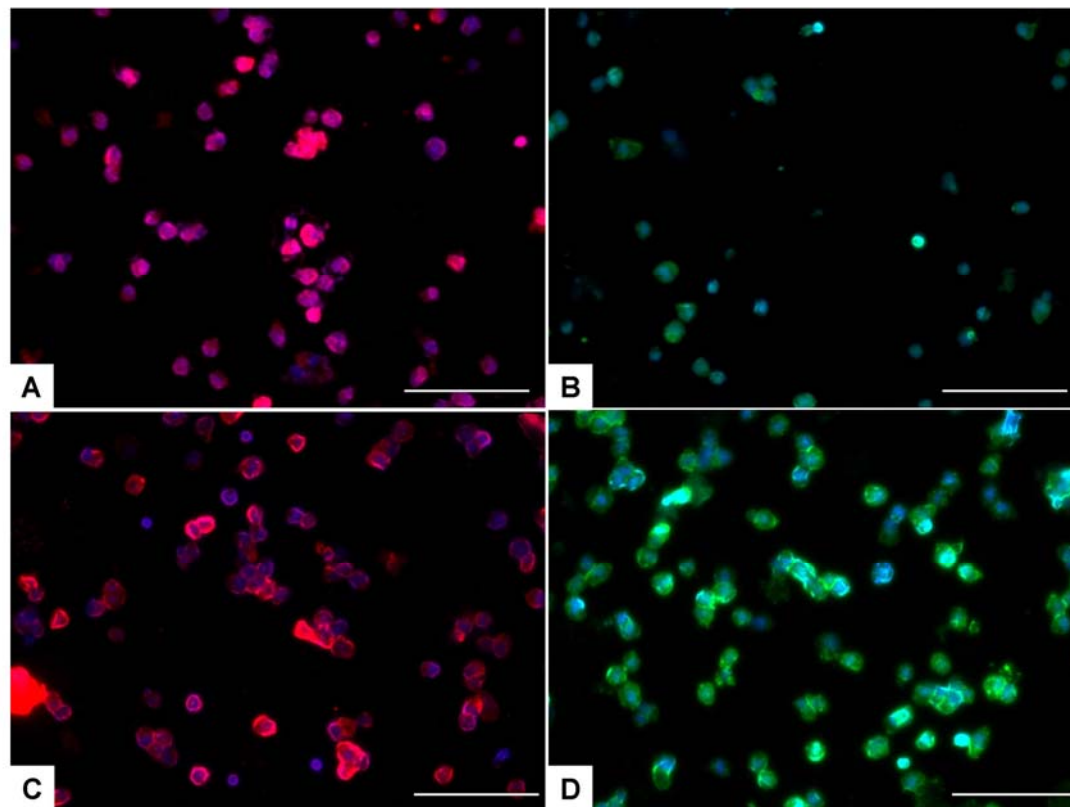


Figure 1: Representative images of hPSCs, BG01v (A,B) and WA09 (C,D) stained for pluripotent markers SSEA3 (A, C) and SSEA4 (B,D) for quantification of marker expression. Scale bar = 100μm

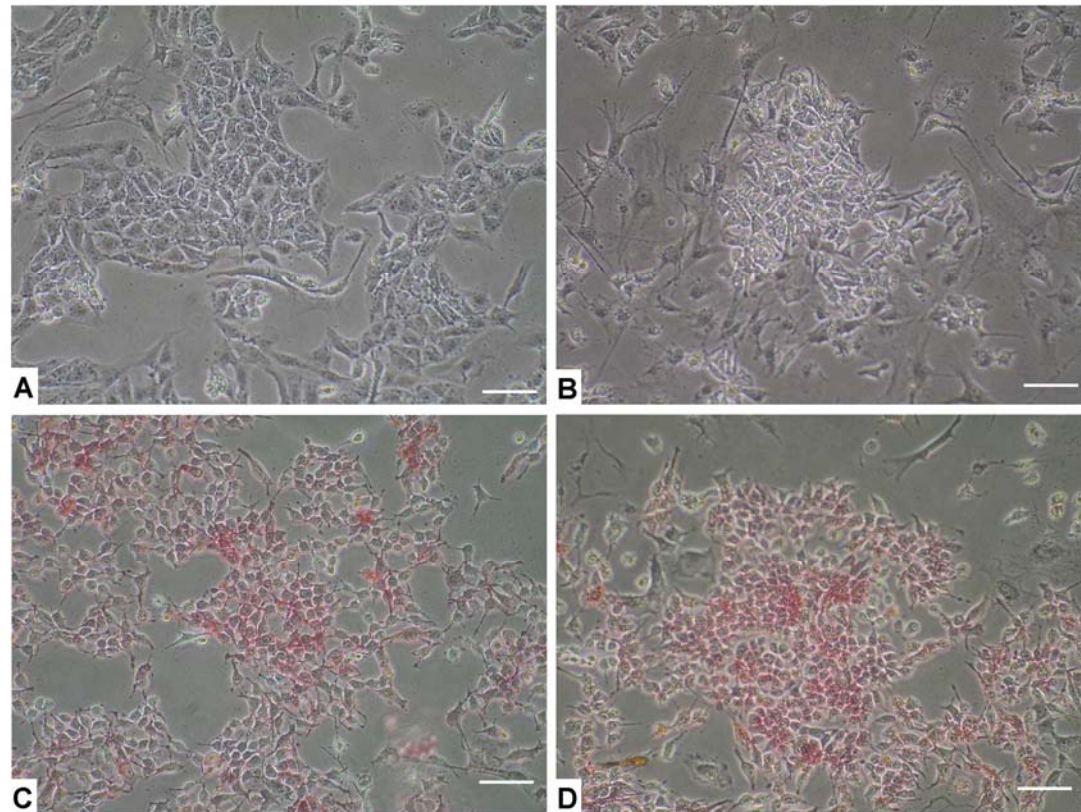
C) Representative images of hPSCs cultured on lyophilized acellular substrates

Figure 1: Representative images of hPSCs, BG01v (A,C) and WA09 (B,D) stained for pluripotent markers alkaline phosphatase (C,D). Scale bar = 100 μ m

VITA

Sheena Abraham was born in Kuwait in 1980 and completed her undergraduate studies in Chemical Engineering at the University of Mumbai, India. She received her Masters degree in Chemical Engineering from Virginia Commonwealth University with Dr. Anthony Guiseppi and continued with her studies to pursue a Ph.D. at the Rao Laboratory. She has published multiple articles in scientific journals based on her masters and doctoral research. She currently resides in California. She wishes to pursue research in stem cell biology and engineering.